

Alma Mater Studiorum – Università di Bologna

DOTTORATO DI RICERCA IN
Ingegneria Chimica dell’Ambiente e della Sicurezza

Ciclo XXII

Settore/i scientifico-disciplinare/i di afferenza: ING-IND/24-25

**METODI PER L’ANALISI DELLA SOSTENIBILITA’: VALUTAZIONE DI
FILIERE ENERGETICHE PER LA VALORIZZAZIONE DI BIOMASSE**

-
**METHODS FOR SUSTAINABILITY ASSESSMENT: ANALYSIS OF
ENERGY SUPPLY CHAINS FOR BIOMASS VALORISATION**

Presentata da: Ing. Mauro Cordella

Coordinatore Dottorato:

Prof. Ing. Giulio Cesare Sarti

Relatore:

Prof. Ing. Francesco Santarelli

Correlatore:

Prof. Ing. Valerio Cozzani

Esame finale anno 2010

TABLE OF CONTENTS

Introduction	1
Ch. 1: World energy scenarios and sustainable energy supply	3
1.1 The hunger of energy of the World	3
1.2 The need for a sustainable energy supply	4
1.3. The biomass potential	5
Ch. 2: Energy from biomass	7
2.1 Biomass and bio-energy	7
2.2 Combustion, gasification, pyrolysis and digestion for power and heat	8
2.2.1 <i>Combustion</i>	10
2.2.2 <i>Gasification</i>	13
2.2.3 <i>Pyrolysis</i>	18
2.2.4. <i>Digestion</i>	24
2.3 Production of transportation fuels via gasification, fermentation and extraction	25
2.3.1. <i>Methanol, Hydrogen and Hydrocarbons via Gasification</i>	26
2.3.2 <i>Fermentation Production of Ethanol</i>	27
2.4 The bio-refinery concept	29
2.5 The bio-energy market	30
Ch. 3: The agro-industrial concept of bio-energy supply chain	32
3.1 The bio-energy supply chain	32
3.2 From a process-specific to a system view	34
Ch. 4: Methods for the sustainability assessment of a process	36
4.1 General introduction	36
4.2 Economic assessment	37
4.2.1 <i>Discount Cash Flow (DCF) analysis</i>	37
4.2.2 <i>Net Present Value (NPV)</i>	38
4.2.3 <i>Alternative investment performance criteria</i>	39
4.2.4 <i>Methods for the engineering estimation of the costs</i>	40
4.2.5 <i>Costs data localisation and actualisation</i>	42
4.3 Life cycle assessment	42
4.3.1 <i>Introduction</i>	42
4.3.2 <i>Goal and scope definition</i>	42
4.3.3 <i>Life cycle inventory</i>	44
4.3.4 <i>Life cycle impact assessment</i>	44
4.3.5 <i>Life Cycle Interpretation</i>	47
4.4 Assessment of the inherent hazards due to substances	47
4.4.1 <i>Introduction</i>	47
4.4.2 <i>Collection of hazard data</i>	48
4.4.3 <i>Hazard assessment of a single compound</i>	48

4.4.4 Hazard assessment of a mixture of compound	51
4.4.5 Family compounds-based assessment	51
Ch. 5 Experimental analysis on the slow pyrolysis process	52
5.1 General introduction	52
5.2 Experimental pyrolysis in fixed bed reactors	53
5.2.1 Introduction	53
5.2.2 Materials and methods	53
5.2.3 Results and discussion	56
5.2.4 Conclusions	58
5.3 Thermo-gravimetric analysis of the char samples	59
5.3.1 Introduction	59
5.3.2 Materials and methods	59
5.3.3 Results and discussion	60
5.3.4 Conclusions	62
5.4 Study of the pyro-oil stability	63
5.4.1 Introduction	63
5.4.2 Materials and methods	67
5.4.3 Results and discussion	74
5.4.4 Conclusions	114
5.5 Assessment of the hazards due to the pyro-oil compounds	116
5.5.1 Introduction	116
5.5.2 Materials and methods	116
5.5.3 Results and discussion	119
5.5.4 Conclusions	130
Ch. 6: Economical assessment of an energy supply chain based on biomass slow pyrolysis	131
6.1 Introduction	131
6.2 Description of the economic model	132
6.2.1 General methodological assumptions	133
6.2.2 Biomass production	133
6.2.3 Transport of the biomass to the pyrolysis plant	134
6.2.4 Biomass pyrolysis	136
6.2.5 Transport of the pyrolysis products	143
6.2.6 Co-combustion of the pyrolysis products with coal	143
6.3 Results and discussion	144
6.3.1 Costs analysis	144
6.3.2 Electricity Surcharge Indicator	147
6.3.3 Market saturation analysis	149
6.3.4 Sensitivity analysis	150
6.3.5 Analysis of the performances of different public support systems	151
6.3.6 Conclusions	154
Ch. 7: LCA of alternative bio-energy supply chains	155
7.1 Goal and scope definition	155

7.2 Key Performance Indicators	156
7.2.1 <i>Non-renewable Cumulative Energy Demand</i>	157
7.2.2 <i>Carbon footprint</i>	157
7.2.3 <i>Land Occupation</i>	157
7.3 Supply chain modelling	157
7.3.1 <i>Production of the biomass</i>	158
7.3.2 <i>Transport of the biomass to concentration points</i>	160
7.3.3 <i>Potential application of a densification process</i>	161
7.3.4 <i>Transport of the bio-fuel to the power plant</i>	163
7.3.5 <i>Power generation</i>	164
7.3.6 <i>Power supply chain based on coal</i>	166
7.4 Results and discussion	166
7.4.1 <i>Assessment of power supply chains based on different biomass species</i>	166
7.4.2 <i>Gravity analysis</i>	168
7.4.3 <i>Comparison with the coal based power supply chain</i>	169
7.4.4 <i>Comparison with power supply chains based on direct biomass combustion</i>	170
7.4.5 <i>Comparison between different typologies of power plant and different densification processes</i>	176
7.5 Conclusions	178
Conclusions	180
List of references	183
Appendix A: List of abbreviations	197
Appendix B: List of publications	200

INTRODUCTION

World energy scenarios point out an increasing energy demand which strongly collides with environmental, economic and geo-politic limits of fossil fuels, the source of energy most commonly used by mankind. The need of producing energy in a sustainable way has brought in the course of time to the development of several “green” technologies based on renewable sources of energy. Biomass can be an interesting and topical opportunity inside the renewable energy market, in particular due to its wide availability and to the know-how on the biomass-to-energy conversion processes, which allows the production of carbon neutral bio-fuels (Chapter 1).

Sustainability of bio-energy systems is however to be addressed with reference to several issues. Extensive amounts of territory are for instance required as a consequence of the low energy density of the biomass and they could result in direct competition between food vs. non food destination of the feedstock or indirect competition for the land use. Bio-energy should be techno-economically feasible, environmental compatible and inherently safe. Fossil fuels substitution with biomass should also increase energy and carbon efficiencies effectively.

Bio-energy can be produced through direct combustion of the original feedstock or through preliminary conversion of the biomass into solid, liquid and gaseous fuels. Pyrolysis-based densification processes appear a promising route for the exploitation of the energy content of biomass. Pyrolysis is the chemical decomposition of material through application of heat in absence of oxygen. During pyrolysis processes, biomass is converted into a liquid fraction (i.e. bio-oil), a solid residue (i.e. char), and several gaseous compounds (e.g. carbon dioxide, carbon monoxide, hydrogen and light hydrocarbons). The heating value of the pyrolysis products can be exploited in energy production. Liquid and solid fractions are in particular interesting energy vectors because of their higher energy densities in comparison with the original biomass. Several pyrolysis concepts have been developed in the course of time; slow pyrolysis is a simple and effective technique (it is based on fixed bed reactors) which could be easily implemented also on a local basis. Slow pyrolysis allows the production of similar amounts of liquid, solid and gaseous products. Oil and char slurries can be transported and converted to energy; gas could instead supply the heat needed in the process. Slow pyrolysis can be thus considered an auto-thermal process (Chapter 2).

Energy production from biomass is possible after a sequence of stages which are mutually dependent and interconnected. Different stakeholders are involved in the bio-energy supply chain: farmers, logistic companies, industrial operators (Chapter 3). It is thus apparent that an integrated perspective and cross-disciplinary competences are necessary in order to link the agricultural dimension of the bio-energy system with the industrial market and to yield, with the support of specific analytical tools applied in a life cycle perspective, a consistent discussion of economical, environmental and societal aspects (Chapter 4).

The aim of the present work is the definition and analysis of potential power supply chains based on the biomass slow pyrolysis process and the addressing of aspects related to their sustainability. In order to avoid direct competition with the food market, that is the case of crops conventionally used in the production of bio-fuels (e.g. bio-ethanol from corn or bio-diesel from palm fruits), only lignocellulosic feedstock is considered in this study (i.e. corn stalks, poplar, sorghum and switchgrass).

The following sustainability aspects were addressed in the thesis:

- inherent hazards associated with the pyrolysis products and practical limitations in their energy use on the basis of experimental process investigation (Chapter 5);
- economical feasibility of the pyrolysis process implementation in a power supply chain (Chapter 6);
- life cycle assessment (LCA) of energy consumptions, greenhouse gases (GHG) emissions and land occupation associated with alternative bio-power supply chains (Chapter 7).

The assessment is complicated by the lack of robust industrial and commercial references about biomass slow pyrolysis. Pyrolysis is indeed a process which is mainly investigated on a lab/pilot scale, also because of current inherent limitations concerning with the quality of the pyrolysis products (e.g. bio-oil instability).

Two groups of activities were performed in order to achieve the goals outlined:

- A first group (G1) was based on the experimental investigation of the slow pyrolysis process. Biomass specific products yields, to be used in the supply chain analysis, were collected and liquid and solid products of pyrolysis characterised with reference to their inherent hazards and to the storage stability problem (Chapter 5).
- The modelling of bio-power supply chains and the analysis, development and application of tools for the sustainability assessment of these systems (Chapters 4, 5, 6, 7) was instead the object of a second group of activities (G2).

CHAPTER 1

WORLD ENERGY SCENARIOS AND SUSTAINABLE ENERGY SUPPLY

1.1 The hunger of energy of the World

There is no doubt that energy is fundamental for our development. The World energy demand in 2006 amounted to about 490 EJ, mainly filled by fossil fuels (i.e. oil, coal, natural gas) as apparent on figure 1.1 [IEA, 2008].

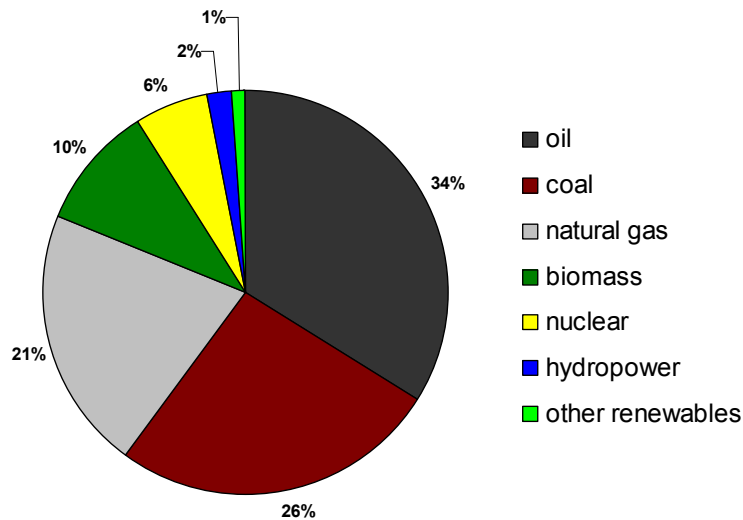


Fig. 1.1 – World primary energy demand by fuel in 2006 [IEA, 2008]

Total world consumption of marketed energy is projected to increase by 44 percent from 2006 to 2030, with larger demand in the non-OECD economies (see figure 1.2) [EIA, 2009].

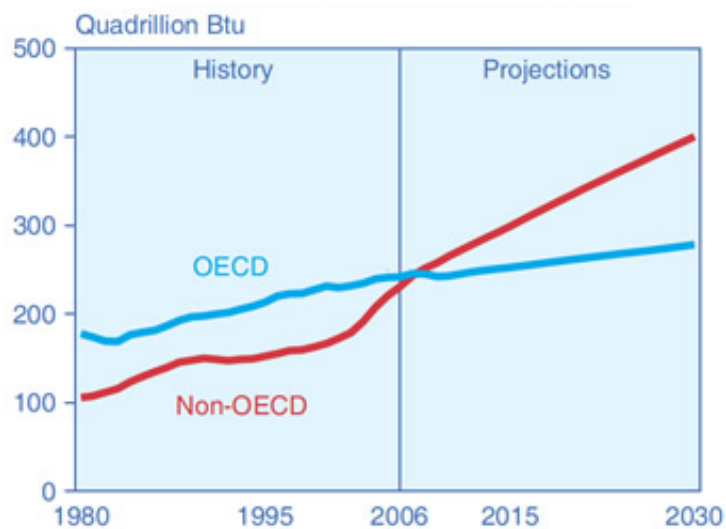


Fig. 1.2 - World marketed energy consumption in OECD and non OECD countries [EIA, 2009]

The increasing hunger of energy is worsened by the strong dependence on fossil fuels. Environmental, economical and geo-political are indeed associated with the conventional sources of energy.

Fossil fuels are a non-renewable source of energy because geological times are required for their generation. As a direct consequence, fossil fuels combustion processes are considered the main cause of CO₂ concentration increase in atmosphere, which is supposed to be responsible for global warming and climate change [IPPC].

Moreover, costs of fossil fuels are variable (but relatively high) over time, in part due to uncertain forecasts on the global reserves and to political reasons. In particular, easy-accessible reserves could decrease dramatically with the current (and future) consumption rates. As a result, fuels extraction should become more expensive in future [Gagnon et al., 2009].

In addition, access to fossil fuels can be also cause of social, political and, sometimes, armed conflicts worldwide since oil and gas tend to be concentrated in politically unstable areas (e.g. Iraqi and Nigeria) [Klare, 2004].

1.2 The need for a sustainable energy supply

It is apparent from the energy scenario outlined in paragraph 1.1 that a sustainable supply of energy is more and more necessary in our society. As a result, there is a general trend to search for energy alternatives based on locally available renewable resources and at the same time pursuing increased energy efficiency throughout the economy [Silveira, 2005]. Renewable energy and energy efficiency are sometimes said to be the “twin pillars” of sustainable energy policy. Efficiency can slow down energy demand growth so that rising clean energy supplies can make deep cuts in fossil fuel use. Unless clean energy supplies are implemented widely, slowing demand growth will only begin to reduce total emissions.

Renewable energy sources can be either produced continuously or within a moderate time frame through natural energy flows, including solar energy (heat and electricity), bio-energy (i.e. energy from biomass), wind power, hydropower, and geothermal power [EPRI and U.S. Department of Energy, 1997; Teske et al., 2007]. Renewable energy sources are expected to grow quickly in the near future and to play a key role in the global energy mix.

Many countries have already adopted the goal of enhancing the role of renewable sources in their energy supplies. The European Union for instance has set ambitious targets, i.e. to achieve a 20 % share of energy from renewable sources in the Community's gross final consumption of energy and a 10 % share of energy from renewable sources in each Member State's transport energy consumption by 2020. The improvement of energy efficiency is another key objective of the Community, and the aim is to achieve a 20 % improvement in energy efficiency by 2020 [Directive 2009/28/EC of the European Parliament and of the Council of 23 April 2009].

The exploitation of renewable energy sources can help the European Union to meet many of its environmental and energy policy goals, including its obligation to reduce greenhouse gases under the Kyoto Protocol [Directive 2003/87/EC Of the European Parliament and of the Council of 13 October 2003] and the aim of securing its energy supply [Commission Green Paper of 29 November 2000].

1.3. The biomass potential

Since the beginning of civilization, biomass has been a major source of energy throughout the World. Biomass is the primary source of energy for more than one third of the World's population [Karekezi and Kithyoma, 2006; United Nations Department of Economic and Social Affairs / Population Division, 2009] and the primary source of energy in the developing countries. In the past decade, the number of countries exploiting biomass opportunities for the provision of energy has increased rapidly, and has helped make biomass an attractive and promising option in comparison to other renewable energy sources. According to [World Bank, 2009] the global use of biomass for energy increases continuously and has doubled in the last 40 years.

The principal factors which drive the growing interest in bio-energy are:

1. concerns about energy security and sustainable energy supply;
2. availability of the biomass worldwide;
3. know-how on the biomass-to-energy conversion technologies;
4. carbon neutrality during the combustion stage;
5. possibility to easily transport and utilise biomass based fuels even aloof from the production site (this is a unique characteristic among renewables);
6. potential creation of opportunities for regional development.

Unfortunately, many potential investors in bio-energy projects do not have a solid understanding of all the technical, social and environmental issues involved [Sims et al., 2006].

Biomass resources are currently available from a wide range of sources: wood, agricultural sources and wastes. Biomass can be used in several fields: heat, power, liquid bio-fuels and bio-based products (see figure 1.3) [AEBIOM].

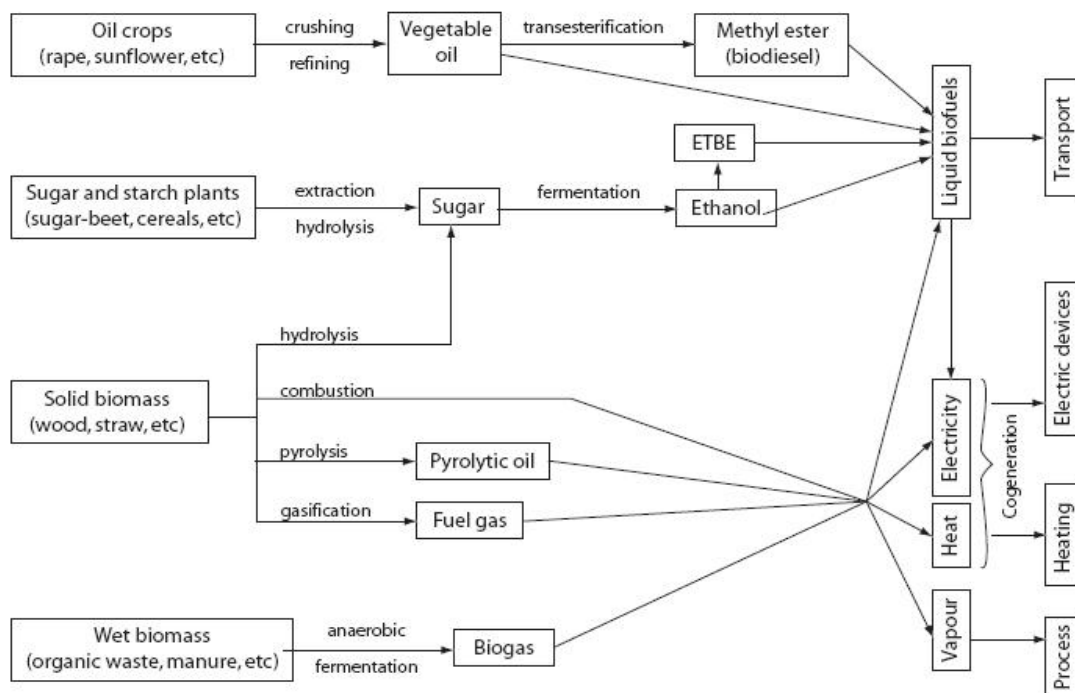


Fig. 1.3 – Main biomass to energy routes [AEBIOM]

Because of its widespread non-commercial use in developing countries, biomass is by far the world greatest source of renewable energy (roughly 10% of the global energy demand in 2006). Approximately two-thirds of biomass is used for cooking and heating in developing countries. The remaining energy use of biomass takes place in industrialised countries where biomass is utilised both in industrial applications within the heat, power, and road transportation sectors and for heating purposes in the private sector [Heinimöa and Jungingerb].

Currently, biomass is the largest renewable energy source in the European Union (EU), comprising two-thirds of all the renewable sources consumed and nearly 4% of the total primary energy supply. Relative use of biomass energy in the EU varies widely among nations (for example, it constitutes about 1% of total primary energy consumption in Italy and the United Kingdom, about 10% of consumption in Denmark and Portugal, and about 20% and 16% of consumption in Finland and Sweden, respectively). In most cases, however, biomass occupies the dominant position in each member country's renewable portfolio for primary energy. About 90% of bio-energy in the EU is used for heating applications, while the remainder is used for electricity generation, transportation fuel, and chemical applications. According to the International Energy Agency, almost 65000 GWh of electricity was generated in the EU with biomass in 2003, which comprised 14.5% of the electricity generated using renewable resources, second only to hydropower [Green Power Market Development Group].

The current standing stock of wood, with a total energy content corresponding to 2011 EJ, is a large reservoir of bio-energy [Smeets et al., 2004]. The overall annual primary production of biomass is equivalent to the 4500 EJ [World Energy council, 2004]. About 5% of this energy, i.e. 225 EJ, would have covered almost 50% of the world's total primary energy demand in 2006. Nevertheless, the energy potential of biomass depends to a great extent on the availability and destination of lands. The amount of land currently devoted to energy crops all around the World (about 0.025 Gha) is approximately equal to 0.19% of the World land surface and to 1.7% of the global agricultural lands. [Ladanai and Vinterbäck, 2009].

There are many scenarios which predicts the future energy potential of biomass; a detailed analysis and comparison is given for instance in [Berndes et al., 2003]. Published estimates to 2050 ranged from below 100 EJ/yr to above 400 EJ/yr in 2050, with a significant contribution due to energy crops. Several studies report that also algal biomass can, in principle, be effectively used as a renewable source for energy production [e.g. Beer et al., 2009].

CHAPTER 2

ENERGY FROM BIOMASS

2.1 Biomass and bio-energy

Biomass is the biodegradable fraction of products, waste and residues from agriculture (including vegetal and animal substances), forestry and related industries, as well as the biodegradable fraction of industrial and municipal waste [Directive 2001/77/EC of the European Parliament and of the Council]. Within this definition, biomass for energy can include a wide range of materials, such as [Biomass Energy Centre]:

- Virgin wood, from forestry, arboricultural activities or from wood processing;
- Energy crops: high yield crops grown specifically for energy applications;
- Agricultural residues: residues from agriculture harvesting or processing;
- Food waste, from food and drink manufacture, preparation and processing, and post-consumer waste;
- Industrial waste and co-products from manufacturing and industrial processes.

Biomass is a carbon based material and it is composed of a mixture of organic molecules containing hydrogen, usually including atoms of oxygen, often nitrogen and also small quantities of other atoms (e.g. alkali, alkaline earth and heavy metals) [Biomass Energy Centre]. The structural and chemical composition of biomass is highly variable and it is a key factor in energy production.

The term “biomass” usually refers to vegetal biomass, which is composed primarily of carbohydrate polymers (e.g. starch, cellulose, and hemicellulose) and phenolic polymers (i.e. lignin). Lower concentrations of various other compounds, such as proteins, acids, salts, and minerals, are also present [Lee et al., 2007]. Ligno-cellulosic material is in particular attractive because it is abundant and usually not in direct competition with the food market.

Ligno-cellulose is the term used to describe the three-dimensional polymeric composites formed by plants as structural material (see figure 2.1). It consists of variable amounts of cellulose, hemicellulose, and lignin [Lee et al., 2007]:

- Cellulose (30–50% of total feedstock dry matter) is a glucose polymer linked by β -1,4 glycosidic bonds. The basic building block of this linear polymer is cellubiose, a glucose-glucose dimer (dimer: two simpler molecules—monomers—combined to form a polymer). Hydrolysis of cellulose (i.e. saccharification) results in individual glucose monomers.
- Hemicellulose (20–40% of total feedstock dry matter) is a short, highly branched polymer of five-carbon (C5) and six-carbon (C6) sugars. Specifically, hemicellulose contains xylose and arabinose (C5 sugars) and galactose, glucose, and mannose (C6 sugars). Hemicellulose is more readily hydrolyzed compared to cellulose because of its branched, amorphous nature. A major product of hemicellulose hydrolysis is the C5 sugar xylose.
- Lignin (15–25% of total feedstock dry matter), a polyphenolic structural constituent of plants, is the largest non-carbohydrate fraction of lignocellulose.

Ash and other compounds are also present in biomass feedstock [Lee et al., 2007]:

- Ash (3–10% of total feedstock dry matter) is the residue remaining after ignition (dry oxidation at $575 \pm 25^\circ\text{C}$) of biomass. It is composed of minerals such as silicon, aluminium, calcium, magnesium, potassium, and sodium;
- Other compounds are known as extractives and include resins, fats and fatty acids, phenols, phytosterols, salts, minerals, and other compounds.

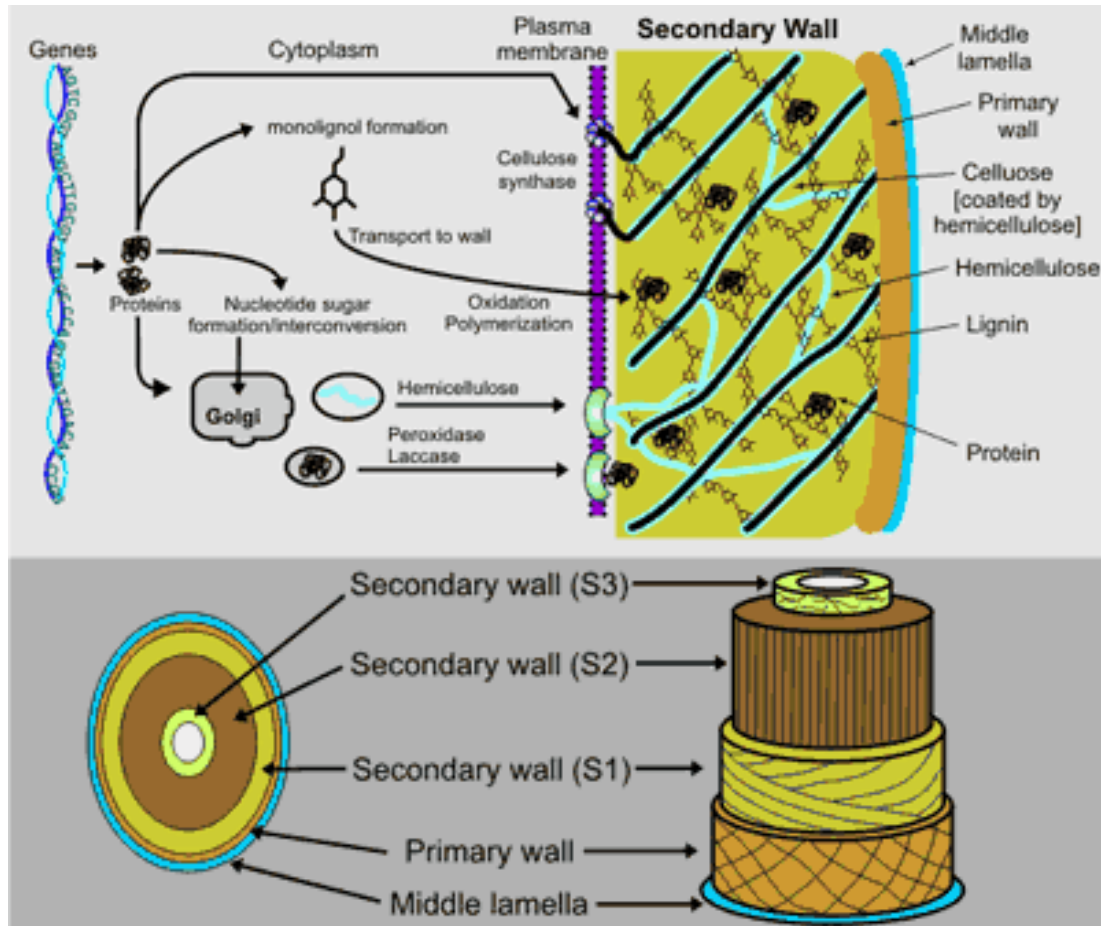


Fig. 2.1 – Structural composition of vegetable biomass material

The energy which is derived from biomass is generally indicated as bio-energy. The biomass can be transformed into bio-fuels for transport, bio-heat or bioelectricity and used for energy purposes through various transformation processes [AEBIOM]. The main conversion routes that are used or still under development for the production of energy from biomass are illustrated on figure 2.2 [Faaij, 2006].

2.2 Combustion, gasification, pyrolysis and digestion for power and heat

Several options allow the production of heat (domestic, industrial), electricity or combined heat and power (CHP), as apparent on figure 2.2. Table 2.1 summarizes some key performance figures with respect to typically capacity ranges and efficiency of different power and heat options. Costs and some summarizing remarks on the status of each technology is instead discussed in table 2.2.

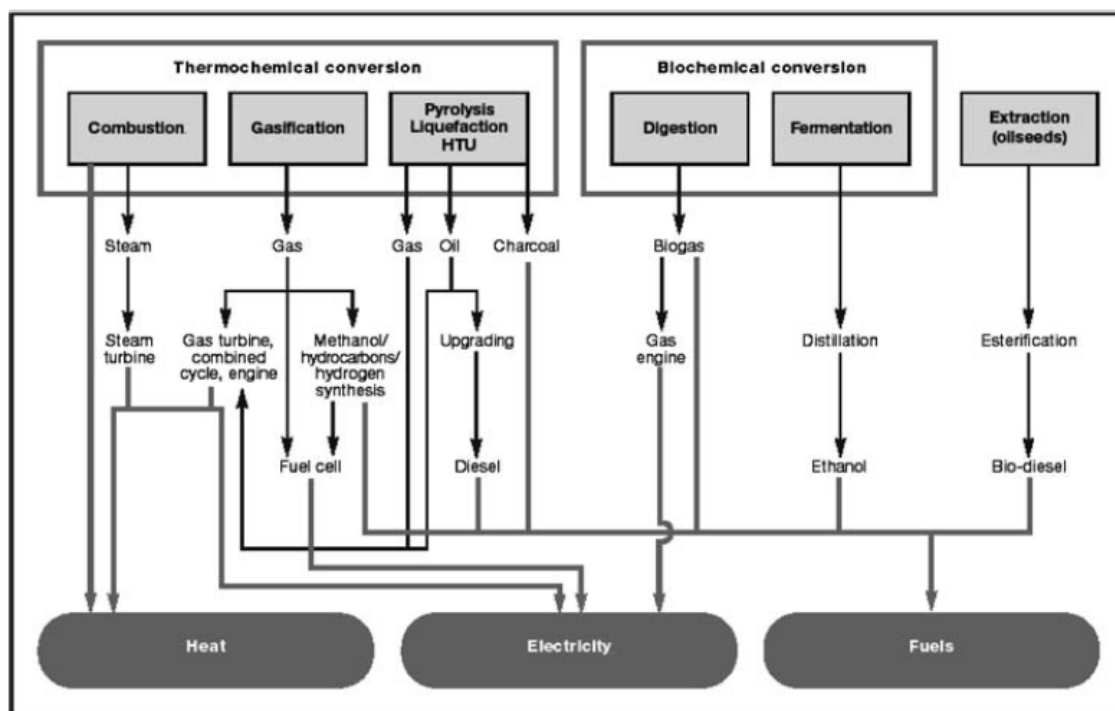


Fig. 2.2 - Main conversion options for biomass to secondary energy carriers

Tab. 2.1 – Indicative capacity range and efficiency of different conversion routes of biomass to power and heat [Faaij, 2006]

Conversion option		Typical capacity range	Net efficiency (LHV basis)
Biogas production	Anaerobic digestion	Up to several MWe	10-15% (electrical)
	Landfill gas	Generally several 100's kWe	Gas engine efficiency
Combustion	Heat	Domestic: 5-50 kWth Industrial: 1-5 MWth	From very low (classic fireplaces) up to 70-90% for modern furnaces
	CHP	0.1-1 MWe	60-90% (overall)
	Stand alone power	1-10 MWe	80-100% (overall)
	Co-combustion	20-100's MWe Typically 5-20 MWe at existing coal fired stations. Higher for new multifuel power plants	20-40% (electrical) 30-40% (electrical)
Gasification	Heat	Usually smaller capacity range around 100's kWth	80-90% (overall)
	CHP gas engine	0.1-1 MWe	15-30%
	BGCC	30-100 MWe	40-50% (or higher; electrical efficiency)
Pyrolysis	Bio-oil/Char	Generally smaller capacities are proposed of several 100's kWth	60-70% heat content of bio-oil/feedstock

Tab. 2.2 – Indicative costs and status of different conversion routes of biomass to power and heat [Faaij, 2006]

Conversion option		Investment cost ranges	Status and deployment in Europe
<i>Biogas Production</i>	<i>Anaerobic digestion</i>		<ul style="list-style-type: none"> - Well established technology - Widely applied for homogeneous wet organic waste streams and waste water. - To a lesser extent used for heterogeneous wet wastes such as organic domestic wastes.
	<i>Landfill gas</i>		<ul style="list-style-type: none"> - Very attractive GHG mitigation option. - Widely applied in EU and in general part of waste treatment policies of most countries.
<i>Combustion</i>	<i>Heat</i>	100 €/kWth 300-700 €/kWth (for larger furnaces)	<ul style="list-style-type: none"> - Classic firewood use still widely deployed in Europe, but decreasing. - Replacement by modern heating systems (i.e. automated, flue gas cleaning, pellet firing) in e.g. Austria, Sweden, Germany ongoing for years.
	<i>CHP</i>		<ul style="list-style-type: none"> - Widely deployed in Scandinavia countries, Austria, Germany and to a lesser extent France. - In general increasing scale and increasing electrical efficiency over time.
	<i>Stand alone power</i>	2500-1600 €/kWe	<ul style="list-style-type: none"> - Well established technology, especially deployed in Scandinavia; - Various advanced concepts using Fluid Bed technology giving high efficiency, low costs and high flexibility commercially deployed. - Mass burning or waste incineration goes with much higher capital costs and lower efficiency; - Widely applied in EU (e.g. the Netherlands and Germany)
	<i>Co-combustion</i>	250 €/kWe + cost of existing power station	<ul style="list-style-type: none"> - Widely deployed in many EU countries. - Interest for larger biomass co-firing shares and utilisation of more advanced options (e.g. feeding fuel gas from gasifiers) is growing in more recent years.
<i>Gasification</i>	<i>Heat</i>	Several 100's €/kWth (depending on capacity)	<ul style="list-style-type: none"> - Commercially available and deployed; - Total contribution to energy production in the EU is very limited.
	<i>CHP gas engine</i>	3000-1000 €/kWth	<ul style="list-style-type: none"> - Various systems on the market. - Deployment limited due to relatively high costs, critical operational demands and fuel quality.
	<i>BGCC</i>	5000-3500 €/kWth (demo) 2000-1000 €/kWth (longer term, larger scale)	<ul style="list-style-type: none"> - Demonstration phase at 5–10MWe range obtained. - Rapid development in the nineties has stalled in recent years. - First generation concepts are capital intensive.
<i>Pyrolysis</i>	<i>Bio-oil/Char</i>		<ul style="list-style-type: none"> - Not commercially available; - Mostly considered a pre-treatment option for longer distance transport.

2.2.1 Combustion

Heat and/or power are widely provided from high temperature gases obtained through oxidation of biomass and related materials with air, i.e. combustion. A great range of equipments can be used, e.g. stoves, furnaces, boilers, steam turbines, turbo-generators. It is possible to burn any type of biomass but in practice combustion is feasible only for biomass with a moisture content <50%, unless the biomass is pre-dried. High moisture content biomass is better suited to biological conversion processes. The scale of combustion plant ranges from very small scale (e.g. for domestic heating) up to large-scale industrial plants in the range 100 MWe and more. Co-combustion of biomass in coal-fired power plants is an especially attractive option because of the high conversion efficiency of these plants. Direct combustion is the main process adopted worldwide for the utilisation of the biomass energy content [Demirbas, 2001].

Domestic heating

A classic application of biomass combustion is heat production for domestic applications. This is still a major market for biomass in countries like Austria, France, Germany and Sweden. Use of wood in open fireplaces and small furnaces in houses is generally poorly documented, but estimated contributions to meet heat demand are considerable in the countries mentioned. Traditional use of wood generally has a low efficiency (sometimes as low as 10%) and generally goes with considerable emissions e.g. of dust and soot. Technology development has led to the application of strongly improved heating systems, which are for example automated, have catalytic gas cleaning and make use of standardized fuel (such as pellets). The efficiency benefit compared to open fireplaces is considerable: open fireplaces may even have a negative efficiency over the year (due to heat losses through the chimney), while advanced domestic heaters can obtain efficiencies of 70–90% with strongly reduced emissions. The application of such systems is widespread in Scandinavia, Austria and Germany. In Sweden in particular, a significant market has been developed for biomass pellets, which are fired in automated firing systems. [Van Loo and Koppejan, 2002].

District heating and CHP

The application of biomass fired power production coupled with district heating is widely applied in Scandinavian countries and in Austria. In Scandinavia, the scale of CHP systems, originally retrofits of existing coal-fired boilers to biomass fired CHP, shows an increasing trend over time, with apparent advantages because of higher electrical efficiencies and lower costs. Various technical concepts were developed also to deal with the difficult combustion characteristics of some biomass feedstock. For instance, straw is rich in alkali and chlorine compounds which can cause corrosion problems and slag production [Van Loo and Koppejan, 2002]. Austria, another leader country in deploying biomass fired CHP focused on smaller scale systems (i.e. on a village level basis), generally combined with local fuel supply systems. Cogeneration is viable where there is a local demand for both heat and electricity. CHP is economically attractive in these countries due to the presence of cold climates. Involvement of local communities has proven to be an other significant element of success. Energy costs of those systems are usually somewhat higher. Local

societal support is generally strong though, especially due to the employment and expenditures that benefit the local community [Faaij, 2006].

Large-scale combustion

Large-scale combustion of biomass for the production of electricity (plus heat and process steam) is applied commercially worldwide. Many plant configurations have been developed and deployed over time. Power is usually generated using superheated steam in a Rankine cycle (see figure 2.3). Basic combustion concepts include also pile burning, various types of grate firing (stationary, moving, vibrating), suspension firing and fluidized bed concepts [Faaij, 2006].

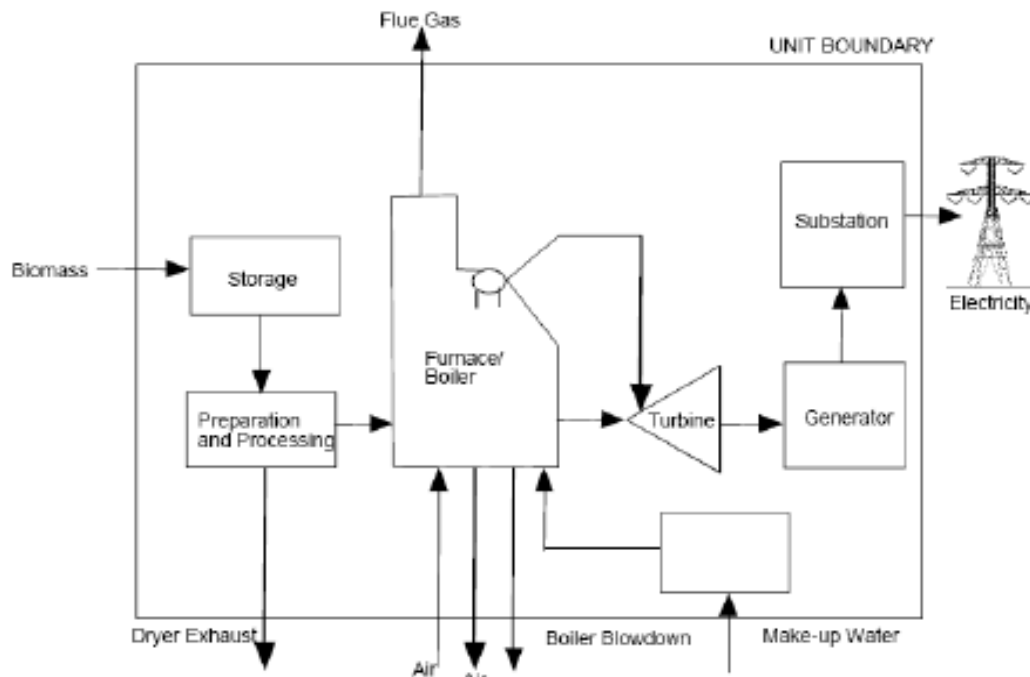


Fig. 2.3 – Flow-sheet of a typical thermo-electric plant

Plants for waste incineration have large capacities (i.e. around 1 Mt capacity per plant per year), moving grate boilers (which allow mass burning of material with very diverse properties), low steam pressures and temperatures (to avoid corrosion) and extensive flue gas cleaning. Typical electrical efficiencies are between 15 to over 20% and more efficient designs (reaching about 30% electrical efficiency) are now commissioned [Faaij, 2006].

Typical capacities for stand-alone biomass combustion plants (typically using wood, such as forest residues, as fuel) range between 20–50 MWe, with related electrical efficiencies in the 25–30% range. Such plants are only economically viable when fuels are available at low costs or when a carbon tax or a feed-in tariff for renewable electricity is in place. The application of fluid bed technology and advanced gas cleaning allows for efficient production of electricity (and heat) from biomass. On a scale of about 50–80 MWe, electrical efficiencies of 30–40% are possible [Van den Broek et al., 1996; Van Loo and Koppejan, 2002]. Large biomass power generation systems can have comparable efficiencies to those of fossil fuel systems, but this comes at a higher cost due to the moisture content of biomass [Demirbas, 2001].

Bubbling Fluidized Bed (BFB) and Circulating Fluidized Bed (CFB) boilers with high fuel flexibility, lower specific investment costs and high efficiency are currently deployed in Finland. One of the latest plants realized has a capacity of 500MWth and is co-fired with a portfolio of biomass fuels, partly supplied by water transport [Faaij, 2006].

Co-combustion

Co-combustion of biomass, in particular in coal-fired power plants is the single largest growing conversion route for biomass in many EU countries (e.g. Spain, Germany, and the Netherlands). The advantages of co-firing are apparent: the overall electrical efficiency is high (usually around 40%) due to economies of scale of the existing plant and investments costs are low to negligible when high quality fuels as pellets are used. Also, directly avoided emissions are high due to direct replacement of coal. Combined with the fact that many coal-fired power plants in operation are fully depreciated, this makes co-firing usually a very attractive GHG mitigation option. In addition, biomass firing leads to lowering sulphur and other emissions. Biomass firing is also a route to avoid the need of additional flue gas cleaning equipment otherwise needed for 100% coal firing. Generally, relatively low co-firing shares are deployed with very limited consequences for boiler performance and maintenance. Because many plants are already equipped with some co-firing capacities, interest for higher co-firing shares (e.g. up to 40%) is rising. Technical consequences, e.g. for feeding lines and boiler performance, are however more severe and current development efforts focus on these issues [Van Loo and Koppejan, 2002]. Power plants capable of firing natural gas or coal with various biomass streams are built in Denmark with the benefit of gaining economies of scale as well as reduced fuel supply risks [Faaij, 2006].

2.2.2 Gasification

Gasification is a process which converts carbonaceous materials at temperatures higher than 1000 °C and with a controlled amount of oxygen (i.e. partial oxidation) and/or steam. The resulting gas mixture is called synthesis gas or syngas and it is also a fuel gas. Modes and products of gasification are reported in table 2.3 [Bridgwater, 2003].

Tab. 2.3 – Modes and products of biomass gasification [Bridgwater, 2003]

Gasification System	Gasification products
<i>Partial oxidation with air</i>	- Main products are: CO, CO ₂ , H ₂ , CH ₄ , N ₂ , tar (LHV: 5 MJ/m ³). - Utilisation problems can arise in combustion, particularly in gas turbines.
<i>Partial oxidation with oxygen</i>	- Main products are: CO, CO ₂ , H ₂ , CH ₄ , tar (LHV: 10–12 MJ/m ³). - The cost of providing and using oxygen is compensated by a better quality fuel gas. The trade-off is finely balanced.
<i>Steam gasification</i>	- Main products are: CO, CO ₂ , H ₂ , CH ₄ , tar (LHV: 15–20 MJ/m ³). - The gas heating value is maximised due to a higher methane and higher hydrocarbon gas content, but at the expense of lower overall efficiency due to loss of carbon.

Gas is more versatile than the original solid biomass and it can be burnt to produce process heat and steam, or used in gas turbines to produce electricity. High conversion efficiencies are in particular achievable with Biomass Integrated

Gasification/Combined Cycle (BGCC), when waste gases from the gas turbine are recovered to produce steam to be used in a steam turbine (i.e. from 35% for small applications up to 50% for the largest installations) [Bridgwater, 2003].

Devolatilization is the first step of gasification, occurring at 350-800 °C as a consequence of the heating up of the biomass. Gas, vaporised tars and a solid char residue are produced at those temperatures. The relative yields of gas, liquid and char depend mostly on the rate of heating and the final temperature [Higman and Van der Burgt, 2003].

Volatile materials and char react with an oxidant agent, usually air, to give CO, CO₂, H₂ and less amounts of hydrocarbons. In a combustion environment, where there is an overall excess of oxygen, the combustion of the volatiles is complete. In a gasification environment this is not necessarily the case, especially where the biomass has a high volatiles content. The slowest reactions in gasification, and therefore those that govern the overall conversion rate of the gasification process, are the heterogeneous reactions, which involve the solid carbon of the char [Higman and Van der Burgt, 2003].

On the whole, the chemical reactions occurring in gasification [Higman and Van der Burgt, 2003] can be represented by:

- combustion reactions,
 - $C + \frac{1}{2} O_2 \rightarrow CO$ - 111 MJ/kmol (2.1)
 - $CO + \frac{1}{2} O_2 \rightarrow CO_2$ - 283 MJ/kmol (2.2)
 - $H_2 + \frac{1}{2} O_2 \rightarrow H_2O$ - 242 MJ/kmol (2.3)
- the Boudouard reaction,
 - $C + CO_2 = 2 CO$ + 172 MJ/kmol (2.4)
- the water gas reaction,
 - $C + H_2O = CO + H_2$ + 131 MJ/kmol (2.5)
- and the methanation reaction,
 - $C + 2 H_2 = CH_4$ - 75 MJ/kmol (2-6)

Reactions 2.1, 2.2, and 2.3 are reactions with free oxygen and are all complete under gasification conditions. Equilibrium syngas composition is essentially due to the three heterogeneous (i.e., gas and solid phase) reactions 2.4, 2.5 and 2.6. In general, gasification concerns with situations where also the carbon conversion is essentially complete. Equations 2.4, 2.5 and 2-6 can thus be reduced into the following two homogeneous gas reactions:

- CO shift reaction:
 - $CO + H_2O = CO_2 + H_2$ - 41 MJ/kmol (2.7)
- and the steam methane reforming reaction:
 - $CH_4 + H_2O = CO_2 + 3 H_2$ + 206 MJ/kmol (2.8)

Reactions 2.1, 2.4, 2.5, and 2.6 describe the four ways in which a carbonaceous or hydrocarbon fuel can be gasified. Most gasification processes rely on a balance between reactions 2.1 (partial oxidation) and 2.5 (water gas reaction). Gasification temperatures are so high that no other hydrocarbons than methane can be thermodynamically present in any appreciable quantity [Higman and Van der Burgt, 2003].

The gas composition is influenced by many other factors such as feed composition, water content, reaction temperature, and the extent of oxidation of the pyrolysis products [Bridgwater, 2003].

The gas is very costly to store or transport so it has to be used immediately. Hot-gas efficiencies for the gasifier (total energy in raw product gas divided by energy in feed)

can be as high as 95–97% for close-coupled turbine and boiler applications [Bridgwater, 2003].

The fuel gas quality requirements, for turbines in particular, are very high. Nevertheless, not all the tar produced in the devolatilization step is completely converted due to physical or geometrical limitations of the reactor and to chemical limitations of the reactions involved. As a consequence, syngas results to be contaminated by tar, which is to be removed by thermal, catalytic or physical processes. This aspect of tar cracking or removal in gas clean-up is one of the most important technical barriers which limits the implementation of gasification technologies [Bridgwater, 2003].

A number of reactor configurations (see figure 2.4) have been developed and tested, with advantages and disadvantages as summarised in table 2.4 [Bridgwater, 2003].

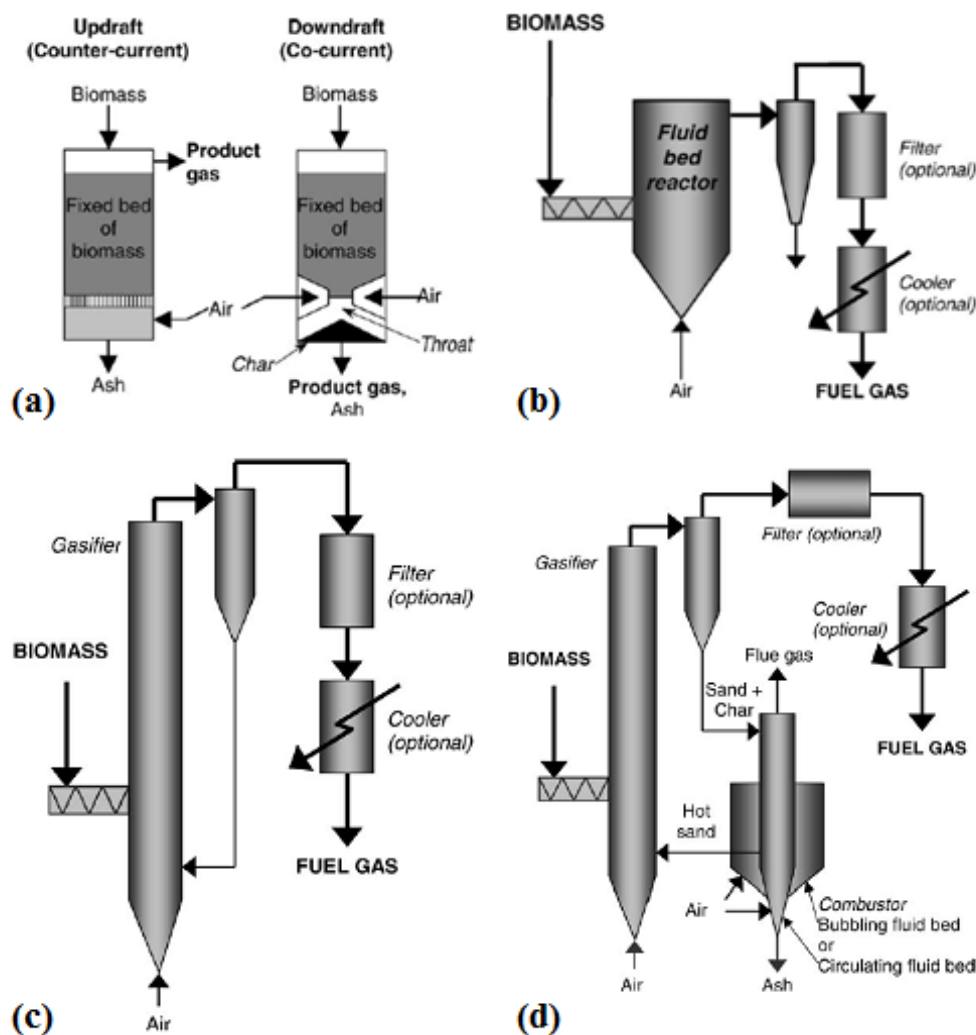


Fig. 2.4 – Some of the reactor configurations used in biomass gasification [Bridgwater, 2003]: (a) Fixed bed gasifiers; (b) Fluid bed gasifier; (c) Circulating fluid bed gasifier; (d) Twin fluid bed gasifier with char combustor

Tab. 2.4 - Gasifier reactor types and main characteristics [Bridgwater, 2003]

Reactor type and main characteristics

Downdraft-fixed bed reactor

- Solid moves slowly down a vertical shaft and air is introduced and reacts at a throat that supports the biomass;
- Solid and product gas move downward in co-current mode;
- The technology is simple, reliable and proven for fuels that are relatively uniform in size and have a low content of fines (below 5 mm);
- A relatively clean gas is produced with low tar and usually with high carbon conversion;
- There is limited scale-up potential to about 500 kg/h feed rate;
- There is a maximum feed moisture content of around 35% wet basis.

Updraft-fixed bed reactor

- Solid moves down a vertical shaft and contacts a counter-current upward moving product gas stream;
- The technology is simple, reliable and proven for fuels that are relatively uniform in size and have a low content of fines (below 5 mm);
- The product gas is very dirty with high levels of tars, although tar crackers have been developed;
- Scale up limited to around 4 dry t/h feed rate;
- There is high thermal efficiency and high carbon conversion;
- Intolerant of high proportion of fines in feed;
- The gas exit temperature is low;
- Good turn-down capability.

Bubbling fluid bed

- Good temperature control & high reaction rates;
- Higher particulates in the product gas and moderate tar levels in product gas;
- Good scale-up potential to 10–15 dry t/h with high specific capacity and easily started and stopped;
- Greater tolerance to particle size range;
- Good temperature control;
- Tar cracking catalyst can be added to bed;
- Limited turn-down capability;
- There is some carbon loss with ash.

Circulating Fluid Bed

- All the features of bubbling beds;
- Large minimum size for viability, above around 15 t/h dry feed rate;
- High cost at low capacity;
- In-bed catalytic processing not easy.

Entrained flow

- Inherently simple reactor design, but only potentially viable above around 20 dry t/h feed rate and with good scale-up potential;
- Costly feed preparation needed for woody biomass;
- Carbon loss with ash;
- Little experience with biomass available.

Twin fluid bed

- Complex process with two close-coupled reactors with difficult scale-up and high cost;
- The gasifier is usually a circulating fluid bed, while the char combustor can be either a bubbling bed or a second circulating fluid bed;
- Complexity requires capacities of >10 t/h for viability;
- MHV gas produced with air and without requiring oxygen;
- Low carbon conversion to gas as carbon in char is lost to reheat sand for recycling;
- High tar levels in gas;
- Tar cracking catalyst can be added to bed.

Continued on next page

Tab. 2.4 (Continued)

Other reactors

- Moving bed with mechanical transport of solid; usually lower temperature processes. Includes: Multiple hearth; Horizontal moving bed; Sloping hearth; Screw/auger kiln;
- Rotary kiln: good gas–solid contact; careful design needed to avoid solid carry over
- Multi-stage reactors with pyrolysis and gasification separated for improved process control and better quality gas
- Cyclonic and vortex reactors: high particle velocities give high reaction rates

Use of oxygen

- Gives better quality gas;
- High cost of providing oxygen and high cost of meeting extra process requirements;
- No evidence that benefits exceed costs.

High pressure gasification

- Significant efficiency and cost advantage in IGCC applications, but large sizes are needed;
- Significant additional costs for pressure with smaller savings from reduced vessel and piping sizes.

Small scale gasification

A key concept pursued for a long period of time was the use of agricultural residues close to the production source, thus minimizing the transport distances. A wide array of concepts for gasifiers, gas cleaning and system integration for such concepts was proposed and tested in a wide variety of conditions. Small scale gasification usually involves downdraft or updraft, fixed bed gasifiers with capacities of less than a 100 kWth up to a few MWth [Faaij, 2006].

Heat production using small gasifiers is commercially established (e.g. in Finland) even if it is in strong competition with combustion. Despite investments and large number of demonstration units, the concept of small-scale gasification has never taken off [Faaij, 2006].

Small (fixed bed) gasifiers coupled with diesel/gas engines (typically 100– 200 kW_e systems with an approximate, modest, electrical efficiency of 15– 25%) are also commercially available on the market. However, their deployment is limited by the critical demands for fuel quality (preferably standardized and hence more expensive fuel, such as pellets) and the careful operation required for effective gas cleaning [Faaij, 2006].

Techno-economic performances could be improved with fuel cells and micro-turbines but such systems need further development and will depend on cheap and reliable fuel cells and major advances in small scale gas cleaning [Faaij, 2006].

Larger scale (CFB) biomass gasification

Larger gasifiers (i.e. over several 10's MWth capacity) are generally associated with Circulating Fluidized Bed concepts and with a higher fuel flexibility [Faaij, 2006].

Atmospheric pressure circulating fluidized bed (A-CFB) gasifiers are used for the production of syngas and process heat (e.g. in Italy, Austria, Sweden and Germany), but not in very large numbers. Biomass Integrated Gasification/Combined Cycle (BG/CC) systems combine flexibility with a high electrical efficiency. Electrical efficiencies around 40% (LHV basis) are possible on a scale of about 30MWe. The promise of this technology, allowing for high electrical efficiency at modest scales combined with modest capital costs, resulted in a variety of research and demonstration initiatives. Furthermore, BG/CC concepts can achieve low emission to

air levels, because the fuel gas needs severe cleaning prior to combustion in order to meet gas turbine specifications [Faaij, 2006].

Demonstration projects were launched in various countries and for various gasification concepts. However, the realization of the demonstration projects proved to be difficult due to high capital costs. Moreover, various technological issues (e.g. concerning pre-treatment and tar removal) still need to be solved. As a consequence, several demonstration units were put out of operation recently. Co-firing and other combustion technologies (which also develops over time) are generally favoured by the risk-averse energy sector. This has led to the stalled development of a technology which shows the potential of producing power from biomass at competitive market price when the scale is larger than 100 MWe [Faaij, 2006].

Gasification for co-firing

Syngas can be also co-fired in existing (coal-fired) power plants, avoiding the consumption of solid fuel and allowing for better control of the combustion process. Successful deployment of (A)CFB gasifiers is recently shown in co-firing schemes [Van Loo and Koppejan, 2002]. An other interesting alternative application for gas produced from biomass gasification is co-firing in natural gas fired combined cycles. In this way, economies of scale are utilised resulting in low cost and (very) high overall efficiencies (currently up to 60% for NG fired combined cycles). Furthermore, a secure fuel supply would be possible since one can vary the share of fuel gas and natural gas fired. This option has not been demonstrated anywhere in the world, but research efforts are increasing and it could prove to be of major importance on short term [Faaij, 2006].

2.2.3 Pyrolysis

Pyrolysis is always the first step of combustion and gasification, where it is followed by total or partial oxidation of the primary products. Pyrolysis is the thermal degradation of biomass in complete absence of oxidizing agents. In a typical pyrolysis process the biomass is cut to a specific size, dried and then fed to a reactor, in which heat is applied by means of electrical resistances or heat exchangers (e.g. gas or sand). Air can sometimes be used to burn that part of biomass necessary to supply heat to the process. Relatively low temperatures are employed, from 500 to 800 °C, if compared to 800-1000 °C and higher temperatures applied in gasification [Nan et al., 1994].

Biomass is made of complex chemical products (mainly cellulose, hemicellulose, lignin). During pyrolysis, biomass particles are decomposed in two gaseous pseudo-species, i.e. non-condensable light products and condensable liquid products (a.k.a crude bio-oil, pyro-oil, tar), and a solid residue (char). Primary liquid of pyrolysis can be also transformed into gas and char by secondary reactions pathways [Mousquès et al., 2001; Zaror et al., 1985].

The relative proportions of the pyrolysis products depends very much on the pyrolysis method, the characteristics of the biomass and the reaction parameters. The biomass pyrolysis is attractive because solid biomass and wastes, which are difficult and costly to manage, can be readily converted into liquid and solid products. A system of cyclones and condensers allows to recover these products. In pilot plants, the pyro-gas is usually flared but in a commercial process it would be used to drive the process or used in drying or power generation, as represented on figure 2.5.

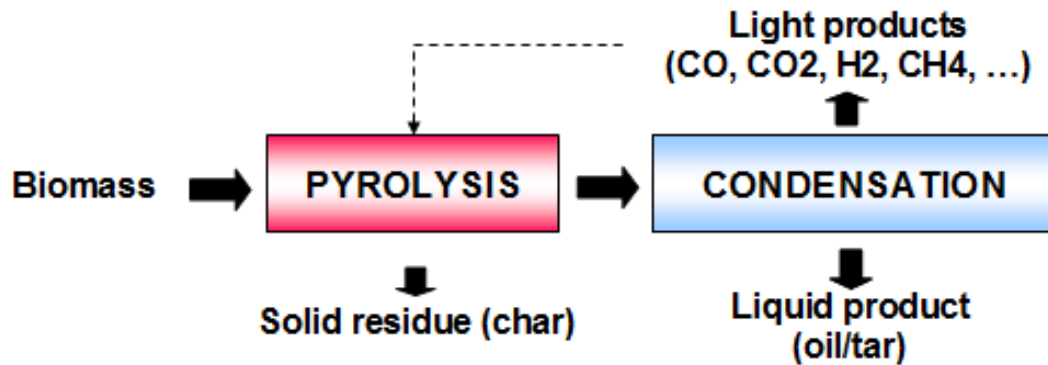


Fig. 2.5 – Overview of the pyrolysis process

Liquid products and charcoal-oil slurries present much higher energy density (see table 2.5) with consequent benefits for transport and storage processes. Bulk and energy densities are fundamental factors in transport. Oil and char mixtures have a clear advantage on raw biomass and this difference can be significant for long distances. Storage is important because of seasonal variations in production and demand. Moreover, raw biomass deteriorates during storage due to biological degradation processes while char is very stable and do not biologically degrade [Nan et al., 1994].

Generally, liquid products are easier to control in the combustion process and this is important in retrofitting existing equipment. Current oil fired burners can not be fully fed directly with solid biomass without any modification of the unit. Powered coal burners can easily accept bio-oil, charcoal and char-oil slurry as a partial replacement of the fuel. In power station, the gas turbines can be readily fired with bio-oil and slurry fuels although the alkali ash in the char content of the slurry needs to be treated. Bio-oil contains about 40 weight percent of oxygen and it is corrosive and acidic [Nan et al., 1994]. The oil can be upgraded (e.g. via hydrogenation) in order to reduce the oxygen content. Upgrading however comes with both economic and energy penalties [Faaij, 2006].

Tab. 2.5 - Energy and density characteristics of biomass feedstock and pyrolysis products [Nan et al., 1994]

Feed	Bulk density (kg/m ³)	Heating value (GJ/t _{db})	Energy density (GJ/m ³)
Straw	100	20	2
Woodchips	400	20	8
Pyro-oil	1200	25	30
Charcoal	300	30	9
Char-oil slurry (20/80 % by weight)	1150	23	26

Pyrolysis systems

A list of pyrolysis systems is given in table 2.6. Several processes have been developed, such as conventional, flash or fast pyrolysis, depending on reaction parameters [Nan et al., 1994].

Tab. 2.6 – Foremost biomass pyrolysis systems [Nan et al., 1994]

Technology	Residence time	Heating rate	Temperature (°C)	Max. products
Carbonation	days	very low	400	char
Slow (conventional)	5-30 min	Low	600	oil, gas, char
Fast	0.5-5 s	very high	650	Bio-oil
Flash	< 1 s	High	< 650	Bio-oil
Vacuum	2-30 s	Medium	400	Bio-oil
Hydro-Pyrolysis	< 10s	High	< 500	Bio-oil

The heart of a pyrolysis process is the reactor. Several concepts have been developed (see figure 2.6). A comprehensive survey of pyrolysis processes is shown in table 2.7 [Bridgewater, 2003].

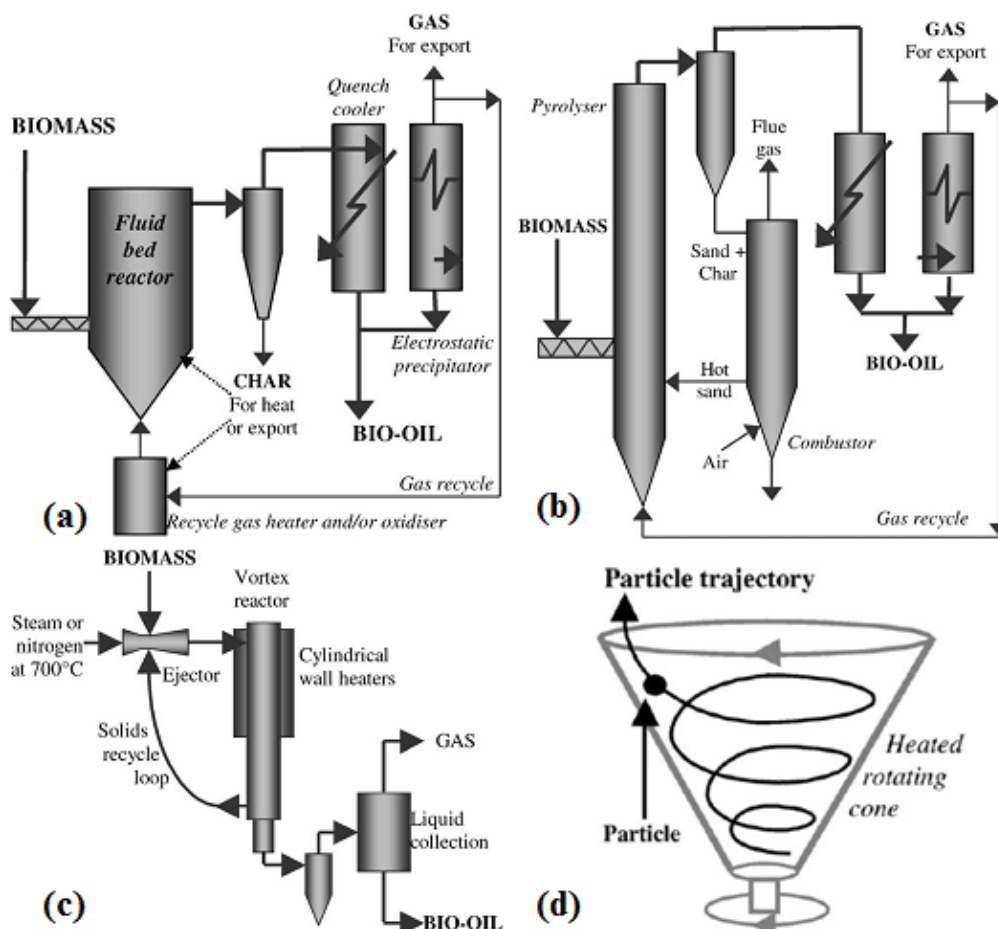


Fig. 2.4 – Some of the reactor configurations used in biomass pyrolysis [Bridgewater, 2003]: (a) Bubbling fluid bed reactor; (b) Circulating fluid bed reactor; (c) Vortex ablative reactor; (d) rotating cone pyrolysis reactor

Tab. 2.7 - Pyrolysis reactor types and characteristics [Bridgewater, 2003]

Reactor type and main characteristics

Fixed bed

- Well-understood technology;
- Simple construction and reliable operation
- Several possible configurations for biomass feeding and heat transfer;
- It can process large particles;
- Used in slow pyrolysis for the production of liquid and solid fuels (potential auto-thermal process if pyro-gas is used to supply the heat required by pyrolysis).

Bubbling fluid beds

- Good temperature control
- Well-understood technology
- Very efficient heat transfer to biomass particles; heat transfer at large scale is to be considered carefully due to scale-up limitations
- Small biomass particle sizes are needed (less than 2-3 mm) in order to achieve high biomass heating rates;
- Good and consistent performance with high liquid yields;
- Residence time of solids and vapours is controlled by the fluidising gas flow rate and is higher for char than for vapours;
- Char acts as an effective vapour cracking catalyst at fast pyrolysis reaction temperatures. Rapid and effective char separation is important.

Circulating fluid beds and transported bed

- Good temperature control;
- Well-understood technology;
- Heat transfer at large scale has to be proven;
- Hydrodynamics more complex;
- Suitable for very large throughputs;
- Residence time for char is almost the same as for vapours and gas;
- Higher gas velocities; char separation by cyclone;
- Closely integrated char combustion in a second reactor.

Ablative pyrolysis

- High pressure of particles on hot reactor walls due to centrifugal or mechanical forces;
- High relative motion between particles and reactor walls;
- Reactor wall temperature should be less than 600 °C;
- Large feeding sizes can be used;
- Inert gas is not required, so the processing equipment is smaller (in case of mechanically applied pressure);
- Reaction rates are limited by heat transfer to the reactor, not to the biomass;
- Surface area controls the process surface area so scaling is more costly;
- The process is mechanically driven so the reactor is more complex.

Entrained flow

- Simple technology;
- Poor heat transfer;
- Large plants required and more difficult liquid collection due to high gas flows;
- Lower liquid yield;
- Good scale-up.

Continued on next page

Tab. 2.7 (Continued)

Rotating cone

- Centrifugation drives hot sand and biomass on a rotating heated cone;
- Char and sand drop into a fluid bed surrounding the cone from which they are lifted to a separate fluid bed combustor;
- Char is burned in a secondary bubbling fluid bed combustor. The hot sand is re-circulated to the reactor;
- Carrier gas requirements in the pyrolysis reactor are much less than for fluid bed and transported bed systems, however, gas is needed for char burn-off and for sand transport;
- Complex integrated operation of three subsystems is required: rotating cone pyrolyser, riser for sand recycling, and bubbling bed char combustor.

Vacuum pyrolysis

- Solids residence time is very high;
- It can process larger particles;
- There is less char in the liquid product due to lower gas velocities;
- There is no requirement for a carrier gas;
- Liquid yields of 35–50% on dry feed are typically obtained with higher char yields than fast pyrolysis systems; conversely, the liquid yields are higher than in slow pyrolysis technologies because of fast removal of vapours from the reaction zone;
- The process is relatively complicated mechanically.

Distribution of the pyrolysis products: experimental trends

Pyrolysis has been practised for centuries for production of charcoal. This required relatively slow reaction at very low temperatures to maximize solid yield. More recently, studies have suggested ways of substantially changing the proportions of the gas, liquid and solid products by changing the rate of heating, temperature and residence time [Kandiyoti et al., 2006]. The distribution of the products from the pyrolysis of solid fuels depends on the combined effects of numerous operative parameters. Considering these effects in isolation requires a level of simplification, but can serve as a convenient device for outlining an initially straightforward qualitative picture.

Biomass usually contain up to 35-45 % oxygen in chemical structures. Lignocellulosic material appears thermally more labile than coal. This material begins to decompose at low temperatures (i.e. around 300 °C). Most volatile evolution is usually completed by about 450-500 °C. Depending on heating rate and particle size, the proportion of volatile matter released from biomass may range from 65 to nearly 99 % of the original mass. Flash-heating finely divided wood particles (i.e with a size equal to 100 µm or less), either in inert or in reactive atmospheres gives nearly similar volatile yields, leaving practically no char behind above 550-600 °C. Larger particles of the same wood may give higher char yields, between 10-30 % of the original mass, depending on whether tar vapours are swept away or left to linger in-situ.

The pyrolysis of hemicellulose and cellulose occurs quickly, with the weight loss of hemicellulose mainly at 220–315 °C and that of cellulose at 315–400°C. Lignin is instead more difficult to decompose, as its weight loss happens in a wide temperature range (from 160 to 900 °C) with generation of a high solid residue (about 40% by weight) [Yang et al., 2003]. Synergistic effects are present between the several polymeric components of biomass particles. One likely explanation for synergistic effects relies on the difference between the decomposition temperatures of the biomass main components. When the cellulose in wood begins to decompose, the very fine intermeshing with lignin and with hemicelluloses would provide a heated solid matrix in contact with thermally sensitive cellulose tars. This set of secondary reaction

paths appears to decompose the laevoglucosan, which under has been shown to constitute the predominant primary product in cellulose tar.

When biomass is heated rapidly, the speed of the temperature rise does not allow the completion of the sequence of pyrolytic events. At rates above 100-200 °C/s the sequence of pyrolytic events is shifted up the temperature scale and telescoped into a shorter time interval. Greater heating rates have also been observed to boost volatile yields by as much as 6 – 8 %. This is explained in terms of the greater survival of tars during faster heating. The rapid build-up of internal pressure in volatile bubbles is thought to force the faster ejection of tar precursors, thereby reducing the probability of retrogressive repolymerisation reactions.

The combined effects of heating rate and reactor shape on the “temperature - tar yield” relationship is quite complicated.

When biomass particles are introduced into an already heated fluidised-bed reactor, particle heating rates are high, forcing the release of correspondingly high proportions of tar vapours. However, provided the temperature is sufficiently high, the fluidised-bed configuration allows sufficient residence time for extensive secondary reactions to take place before tar vapours can sequentially exit from the reactor. When separate experiments are performed at a succession of increasing temperatures in fluidised-beds, tar yields initially increase. With increasing temperature, tar cracking reactions begin to affect tar yields. When the increase in tar production is matched by tar cracking reactions, the tar-yield curve traces a maximum and declines with further increases in temperature. For thermally sensitive materials such as cellulose or softwood the tar-yield maximum is observed between 400 and 425 °C.

In fixed bed reactors, the temperature-tar yield relationship again depends on a combination of several factors. In this type of reactor, tars released by solid particles may be destroyed by contact with other solid particles, through cracking and char forming reactions. Due to their thermal inertia, fixed bed reactors cannot be heated at rates much faster than about 10 °C/s. This type of reactor is normally operated by ramping the temperature from ambient. When the reactor is reasonably short, tars that survive secondary processes may exit from the reactor, well before the intended peak experimental temperature is reached. In other words, some tars may exit from the reactor without experiencing temperatures very much higher than those at which they were released, since the heating rate is relatively slow. The overall effect is of tar yields initially rising with temperature and flattening out between 500-600 °C, irrespective of the final temperature reached by the reactor. When using similar materials, peak tar yields reached in fixed beds are usually lower than yields that can be attained in fluidised-bed reactors.

When pyrolysis experiments are performed under reduced pressure, both volatile and tar release tends to increase compared to operation at atmospheric pressure. Furthermore, the increase in tar yields due to operation under “vacuum” are often, somewhat counter-intuitively, a little larger than corresponding increases in the total volatiles. Depending on the nature of the sample, the incremental increase in tar yield could be as much as 5 %. These observations suggest that reduced external pressure allows tar precursors to exit from solid particles more rapidly. The effect is not without its parallel with fast heating, where the rapid build-up of internal pressure tends to force tar precursors to exit from solid particles more rapidly. Experimental data suggest that when the initial external pressure is reduced from atmospheric pressure, intra-particle tar loss through re-condensation (re-polymerisation) reactions of some tar precursors is reduced. Conversely, as the pressure is raised towards atmospheric pressure, some tar precursor material is lost through re-polymerisation

processes giving off gas and char and perhaps some lighter tar. Increasing the external pressure thus acts against internal forces, which tend to drive volatiles out of solid particles. Higher external pressures tend to slow down (i) the flow and diffusion of volatiles towards the external surfaces of particles, and, (ii) the diffusion from external particle surfaces to the surrounding bulk gas. When the external pressure of inert gas is raised above atmospheric pressure, volatile and tar yields initially tend to diminish rapidly, up to about 5 bars. With increasing pressure, this trend slows down and appears to level off above 40 bars. Compared with atmospheric pressure results, the overall decline in total volatiles may be as much as 10-12 %. The effect can be explained in terms of the partial suppression of volatile release by the physical effect of increasing external pressure.

Volatile yields tend to diminish with increasing particle size, again providing indications of the extent of intra-particle volatile loss during pyrolysis. However, the effect is difficult to evaluate quantitatively at higher heating rates, as the propagation of the temperature front towards the centre of a large particle is limited by the thermal conductivity of the intervening mass. The high rates of heating imposed at the boundary would not be “seen” by the mass of sample inside large particles. Instead, the temperature front would advance at a rate modulated by the thermal conductivity of the mass of sample.

Industrial applications

Up to now, pyrolysis is less well developed than gasification. Major attention was especially caused in the past by the potential deployment of this technology on small scale in rural areas and as feedstock for the chemical industry. Reducing transport costs because of the higher energy density of bio-oil compared to untreated biomass was used as another key argument. Although considerable experience was gained over time, still few successful demonstration units were realized. Actual market implementation is so far in its infancy. Pyrolysis now receives increasing attention as a pre-treatment step for long distance transport of bio-oil and char, which can be used in further energy conversion (e.g. efficient power generation or entrained flow) gasification for syngas production) [Faaij, 2006].

2.2.4. Digestion

Biogas

Anaerobic digestion of biomass has been demonstrated and applied commercially with success in a multitude of situations and for a variety of feedstock such as organic domestic waste, organic industrial wastes, manure, sludge, etc. Digestion is particularly suited for wet biomass materials, but it has a low overall electrical efficiency when the gas produced is fed to fuel gas engine driven generators (typically 10–15%). Biomass to gas conversions strongly depending on the feedstock; highest conversions are roughly equal to 35%. Digestion has been deployed for a long time in the food and beverage industry to process waste water with high loads of organic matter [Faaij, 2006].

Landfill gas utilisation

A specific source of biogas is landfill. The production of methane rich landfill gas from landfill sites makes a significant contribution to atmospheric methane emissions. In many situations the collection of landfill gas and production of electricity by converting this gas in gas engines is profitable and the application of such systems has become widespread. The benefits are obvious: useful energy carriers are produced from gas that would otherwise contribute to increase methane in the atmosphere (which has stronger GHG impact than the CO₂ emitted from the power) [Faaij, 2006].

2.3 Production of transportation fuels via gasification, fermentation and extraction

As follows from figure 2.2, three main routes based on gasification can be followed to produce transportation fuels from biomass. Gasification can be indeed used to produce syngas that can be converted to methanol, Fischer-Tropsch liquids, Di-Methyl-Ether (DME) and hydrogen [Faaij, 2006].

Production of ethanol can take place via direct fermentation of sugar and starch rich biomass, the most utilized route for production of biofuels, or this can be preceded by hydrolysis processes to convert ligno-cellulosic biomass to sugars first. Finally, biofuels can be produced via extraction from oil seeds (vegetal oil from e.g. rapeseed or palm), which can be esterificated to produce biodiesel [Faaij, 2006].

The characteristics of these fuels differ widely as reported on table 2.8.

Tab. 2.8 - Main properties of bio-fuels for the transport sector [Faaij, 2006].

Fuel	Density at 15 °C (kg/L)	HHV (MJ/kg)	Other aspects
Hydrogen	0.07	142	Lighter than air, low explosion limits
Methanol	0.8	23	Toxic in direct contact; octane number: 88.6 (gasoline: 85)
DME	0.66	28.2	Vapour pressure: 5.1 bar at 20 °C
Fischer-Tropsch	0.75	46-48	Very comparable to diesel and gasoline; zero sulphur, no aromatic compounds
gasoline			
Ethanol	0.79	30	Octane number: 89.7 (gasoline: 85)
Diesel from bio-oil	0.85	47	When fully de-oxygenated
Bio-diesel	0.88	42	Cetane number: 58 (diesel 47.5)
Gasoline	0.75	46	Depending on refining process, contains sulphur and aromatic compounds
Diesel	0.85	46	Depending on refining process, contains sulphur and aromatic compounds

Hydrogen, being a very light gas, requires very extensive infrastructure. All the other fuels considered, except DME, are liquids and can be stored and distributed with relatively conventional infrastructure. Ethanol and especially methanol have a lower energy density than gasoline so for the same amount of energy in a vehicle more weight has to be taken on board. Other aspects concern with the toxicity and the environmental impacts of the fuels due to leakages or calamities. Gasoline and diesel partly contain aromatic compounds, with present carcinogenic properties. Methanol is not carcinogenic but is a more dangerous liquid than gasoline when it comes into contact with humans. Measures need to be taken to reduce exposure risks compared to gasoline and diesel, such as closed filling systems (e.g. as applied for LPG). This will

result in (somewhat) higher (investment) costs. Fischer-Tropsch liquids and ethanol are barely toxic and with negligible content of sulphur and aromatic compounds, in comparison with gasoline and diesel. In addition, the existing infrastructure for gasoline and diesel can be used [Faaij, 2006].

2.3.1. Methanol, Hydrogen and Hydrocarbons via Gasification

Methanol, hydrogen and Fischer-Tropsch diesel can be produced from biomass via gasification. All these routes need very clean syngas before the secondary energy carrier is produced. Relatively conventional gas processing methods are used. DME and SNG (Synthetic Natural Gas) can also be produced from syngas. Several routes involving conventional, commercial, or advanced technologies under development, are possible. Figure 2.7 pictures a generic conversion flowsheet for this category of processes [Faaij, 2006].

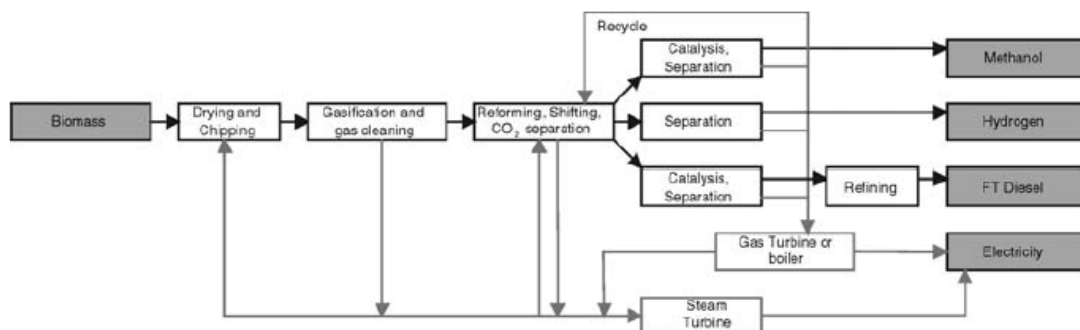


Fig. 2.7 – Generic flowsheet for MeOH, H₂ or FT diesel production via gasification of biomass

A train of processes to convert biomass to required gas specifications precedes the methanol or FT reactor, or the hydrogen separation equipment. The gasifier produces syngas, a mixture of CO and H₂, and few other compounds. The syngas then undergoes a series of chemical reactions. The equipment downstream of the gasifier for the conversion to H₂, methanol or FT diesel is the same which is used to obtain these products from natural gas, except for the gas cleaning train. A gas turbine or a boiler and a steam turbine optionally employ the unconverted gas fractions for electricity co-production [Faaij, 2006].

Commercial bio-fuels production is still on a development stage. Interest on biomass derived syngas for the production of transport fuels (such as methanol) is strongly related to the oil price. Pressurized gasification for methanol production from biomass was tested and developed in France and Sweden. A large-scale CFB gasifier was installed in Finland for producing syngas for an ammonia factory (which was shut down). Also noteworthy is the installed gasification capacity (entrained flow) at Schwarze Pumpe (former East Germany) for producing methanol from waste streams, which is a major industrial experience with this technology. Low energy prices worsened the position of advanced gasification technologies for large-scale applications. In Germany, the company Choren demonstrates FT-diesel production via biomass gasification. Although this seems a viable development, given the techno-economic potential of such concepts, technological challenges remain and are likely to be more complex than for BGCC concepts because gas cleaning needs to be more

severe in order to protect downstream catalytic gas processing equipment [Faaij, 2006].

Once clean syngas is available, known process technology for producing methanol, FT-liquids, DME and hydrogen can be applied. The main development challenges are gas cleaning, scale-up of processes and process integration. More recent technological concepts, such as liquid phase methanol production and Fischer-Tropsch synthesis (combined with electricity generation), and new gas cleaning and separation technology offer potentially lower production costs and higher overall efficiencies on the longer term. More research, demonstration and development activities over a prolonged period of time are however needed to reach such a situation [Faaij, 2006].

Overall energy efficiencies of relatively conventional production facilities, could be close to 60% (on a scale of about 400MWth input). Deployment on large scale (e.g. over 1000 MWth) is required in order to achieve the greatest benefits from economies of scale, which are inherent to this type of installations [Faaij, 2006].

Flexible production of fuels may be obtained through co-gasification of biomass with coal and natural gas. Organizing large-scale biomass supplies may be indeed difficult on short term, making a co-feeding strategy, e.g. with coal, attractive on short term. When equipped with CO₂ capture facilities, the input share of fossil fuel can still become carbon neutral. When more biomass would be utilized, negative emissions could be obtained. Also, existing large-scale gasification technology (entrained flow) can be used, because such gasification processes are developed and deployed for coal and heavy oil residues [Faaij, 2006].

Biomass feedstock could be supplied also as crude bio-oil/bio-slurry from pyrolysis. or treated via torrefaction, which basically means 'roasting' of the biomass reducing the moisture content and facilitating grinding and further pelletizing. Such densification steps reduce long distance transport costs and facilitate feeding to pressurized gasification systems. This is a concept that deserves further study and development efforts [Faaij, 2006].

2.3.2 Fermentation Production of Ethanol

Ethanol from sugar and starch

Production of ethanol via fermentation of sugars is a classic conversion route, which is applied for sugar cane, maize and cereals on a large scale, especially in Brazil, the United States and France. Sweden and Spain have more modest production levels of ethanol [Faaij, 2006].

Ethanol is generally mixed with gasoline, which, at low percentages, can be done without adaptations to the current vehicle fleet. Ethanol has the advantage that it lowers NO_x and dust emissions to some extent, if compared with straight gasoline.

The US and European programmes are particularly promoting the conversion of surpluses from food crops to useful products. Ethanol production from food crops like maize and cereals is however not economically competitive with gasoline and diesel and no major cost reduction will be likely achieved on longer term [Faaij, 2006].

Ethanol production from sugar cane, however, has established a strong position in Brazil and increasingly in other countries in tropical regions (such as India, China and various countries in Sub-Saharan Africa). Production costs of ethanol in Brazil have steadily declined over the past few decades and have reached a point where ethanol is competitive with production costs of gasoline. As a result, bio-ethanol is no longer financially supported in Brazil and competes openly with gasoline. Large scale

production facilities, better use of bagasse and trash residues from sugar cane production (e.g. with advanced gasification based power generation or hydrolysis techniques) and further improvements in cropping systems offer further perspectives for sugar cane based ethanol production. The key limitations for sugar cane production are climatic and the required availability of good quality soils. Lignocellulosic feedstock production is more flexible in respect to this [Faaij, 2006].

Ethanol from (ligno)-cellulosic biomass

Hydrolysis of cellulosic (e.g. straw) and ligno-cellulosic (woody) biomass can open the way towards low cost and efficient production of ethanol from these abundant types of biomass. The conversion is more difficult than for sugar and starch because sugars need first to be produced from lignocellulosic materials via hydrolysis [Faaij, 2006].

Lignocellulosic biomass requires pretreatment by mechanical and physical actions (e.g. steam) to clean and size the biomass, and destroy its cell structure to make it more accessible to further chemical or biological treatment. Also, the lignin part of the biomass is removed, and the hemicellulose is hydrolysed (saccharified) to monomeric and oligomeric sugars. The cellulose can then be hydrolysed to glucose. The sugars are fermented to ethanol, which is to be purified and dehydrated [Faaij, 2006].

Two pathways are possible towards future processes: a continuing consolidation of hydrolysis-fermentation reactions in fewer reactor vessels and with fewer micro organisms, or an optimisation of separate reactions. As only the cellulose and hemicellulose can be used in the process, the lignin is used for power production (see figure 2.8) [Faaij, 2006].

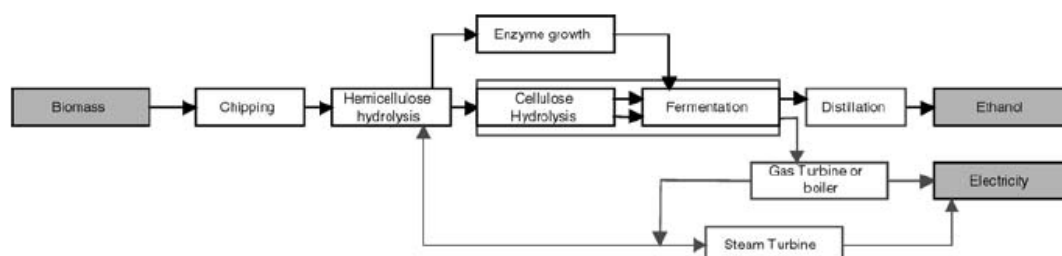


Figure 2.8 Ethanol production by hydrolysis fermentation [Faaij, 2006]

Acid treatment is an available process which is so far relatively expensive and inefficient. Enzymatic treatment is commercially unproven but various test facilities have been built in North America and Sweden. It is relatively uncertain how fast attractive performance levels can be achieved. Assuming, however, that mentioned issues are solved and that ethanol production is combined with efficient electricity production from unconverted wood fractions (lignin, in particular), ethanol costs could come close to current gasoline prices. Overall system energy efficiencies (fuel + power and heat output) could be up to about 70% (LHV) [Faaij, 2006].

For the agricultural sector and agro-food industry this technology is interesting already to boost the competitiveness of existing production facilities (e.g. by converting available crop and process residues), which provides drivers for both industry and agriculture in order to support this technology [Faaij, 2006].

Extraction and production of esters from oilseeds

Oilseeds, like rapeseed, can be extracted and converted to esters and are well suited to replace diesel. Rapeseed production and subsequent esterification and distribution is an established technology in Europe. Significant quantities of Rapeseed Methyl Ester (RME) are produced in the EU (concentrated in Germany, France and to a lesser extent in Austria and Italy). RME, however, requires substantial subsidies to compete with diesel, also on the longer term. Subsidies in Europe generally consist of a combination of farm subsidies (e.g. for producing non-food crops) and tax exemption of the fuel itself [Faaij, 2006].

Key drivers for the implementation of RME schemes are rural employment and the flexible nature of the crop because it can easily replace conventional food crops. Energy balances of RME fuel chains are less favourable when compared to perennial crops and net energy production per hectare is lower. Energy balances and economic performance can be improved to some extent, particularly by using straw for efficient heat and power production [Faaij, 2006].

2.4 The bio-refinery concept

A bio-refinery is a facility that integrates biomass conversion processes and equipment to produce fuels, power, and chemicals from biomass. The bio-refinery concept is analogous to today's petroleum refineries, which produce multiple fuels and products from petroleum. Industrial bio-refineries have been identified as the most promising route to the creation of a new domestic bio-based industry.

By producing multiple products, a bio-refinery can take advantage of the differences in biomass components and intermediates and maximize the value derived from the biomass feedstock. A bio-refinery might, for example, produce one or several low-volume, but high-value, chemical products and a low-value, but high-volume liquid transportation fuel, while generating electricity and process heat for its own use and perhaps enough for sale of electricity. The high-value products enhance profitability, the high-volume fuel helps meet national energy needs, and the power production reduces costs and avoids greenhouse-gas emissions.

The bio-refinery concept may be built on two different "platforms" in order to promote different product slates, as represented on figure 2.9.

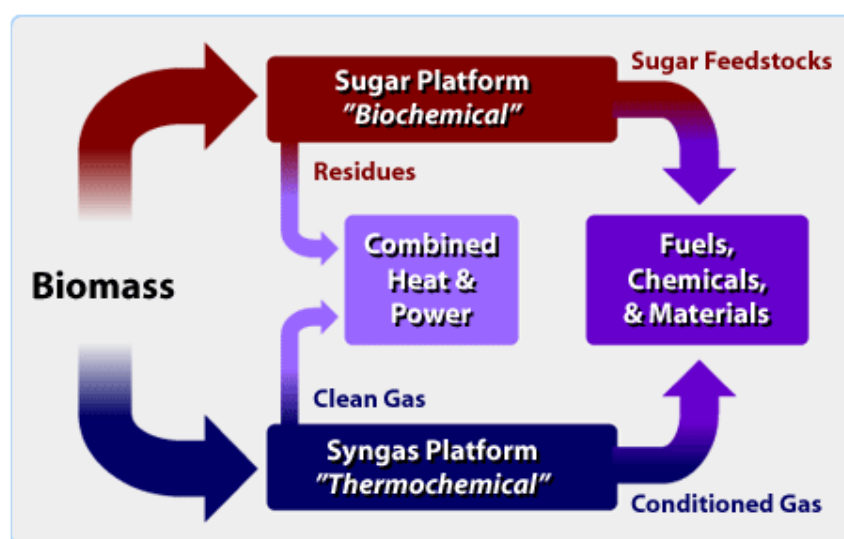


Fig. 2.9 – The bio-refinery concept

2.5 The bio-energy market

Absolutely crucial for the success of bio-energy systems is their economic performance. Biomass is a competitive alternative in many situations, but this is generally observed where cheap, or even negative costs biomass residues or wastes are available. Further development and optimisation of conversion technologies, biomass production, as well as the total bio-energy systems, are required in order to improve the competitiveness of large scale bio-energy use (especially from dedicated biomass crops). Table 2.9, table 2.10 and table 2.11 give a global overview of the main markets on short and longer term for biomass use for energy [Faaij, 2006].

Tab. 2.9 – General overview of biomass markets for heat production on shorter (i.e. 5) and longer (i.e. > 20) years [Faaij, 2006]

Biomass feedstock Category	Heat	
	Short term; Roughly stabilizing market	Long term
Organic wastes	<ul style="list-style-type: none"> ➤ Undesirable for domestic purposes (emissions); ➤ Industrial use attractive; ➤ In general competitive. 	<ul style="list-style-type: none"> ➤ Especially attractive in industrial setting and CHP (advanced combustion and gasification for fuel gas)
Residues: – Forestry; – Agriculture	<ul style="list-style-type: none"> ➤ Major market in developing countries; ➤ Stabilizing market in industrialized countries. 	<ul style="list-style-type: none"> ➤ Especially attractive in industrial setting and CHP. ➤ Advanced heating systems (domestic) possible but not on global scale
Energy crops: – oil seeds; – sugar/starch; – sugar cane; – perennials	N.A.	<ul style="list-style-type: none"> ➤ Unlikely market due to high costs feedstock for lower value energy carrier; ➤ Possible niches for pellet or bio-char (“charcoal”) ➤ Production in specific contexts

Tab. 2.10 – General overview of biomass markets for electricity production on shorter (i.e. 5) and longer (i.e. > 20) year [Faaij, 2006]

Biomass feedstock Category	Electricity	
	Short term; Strong growth market worldwide	Long term; Growth may stabilize due to competition of alternative options
Organic wastes	<ul style="list-style-type: none"> ➤ Economics strongly affected by tipping fees and emission standards. 	<ul style="list-style-type: none"> ➤ Similar range; ➤ Improvements in efficiency and environmental performance, in particular through IGCC technology at large scale.
Residues: – Forestry; – Agriculture	<ul style="list-style-type: none"> ➤ Major variable is supply costs of biomass; ➤ Lower costs also in CHP operation and industrial setting depending on heat demand. 	<ul style="list-style-type: none"> ➤ Major variable is supply costs of biomass
Energy crops: – oil seeds; – sugar/starch; – sugar cane; – perennials	<ul style="list-style-type: none"> ➤ High costs for small scale power generation with high quality feedstock (wood); ➤ Lower costs for large scale (i.e. >100MWth); state-of-the art: combustion (wood, grasses) and co-combustion. 	<ul style="list-style-type: none"> ➤ Low costs especially possible with advanced co-firing schemes and BGCC technology over 100–200 MWe.

Tab. 2.11 – General overview of biomass markets for transport fuel production on shorter (i.e. 5) and longer (i.e. > 20) year [Faaij, 2006]

Biomass feedstock Category	Transport fuels	
	Short term; Growing market, but dependent on policies and financial support.	Long term; Potential key market for (cultivated) biomass
Organic wastes	N.A.	➤ In particular possible via gasification routes
Residues: – Forestry; – Agriculture	➤ Only for surpluses of food crops	➤ Low costs obtainable with lignocellulosic advanced hydrolysis techniques and large scale gasification (i.e. < 1000 MWth) for MeOH/H ₂ /FT, as well as improved sugar cane production and subsequent ethanol production in optimized distilleries.
Energy crops: – oil seeds; – sugar/starch; – sugar cane; – perennials	<ul style="list-style-type: none"> ➤ Lower figures for ethanol from sugar cane; ➤ Higher for biodiesel (RME) and sugar and starch crops in Europe and North America. 	➤ Low costs obtainable with lignocellulosic advanced hydrolysis techniques and large scale gasification (i.e. < 1000 MWth) for MeOH/H ₂ /FT, as well as improved sugar cane production and subsequent ethanol production in optimized distilleries.

CHAPTER 3

THE AGRO-INDUSTRIAL CONCEPT OF BIO-ENERGY SUPPLY CHAIN

3.1 The bio-energy supply chain

Because of a robust know-how on the biomass-to-energy carriers conversion processes [Bridgwater, 2003; Faaij, 2006; Goyal et al., 2008; IEA, 2007; Mitchell et al., 1995], the bio-energy industry is expanding rapidly around the globe, also in response to climate change and rising oil prices [Allen et al., 1998].

The production of energy from biomass consists of a series of sequential stages, as represented on figure 3.1, which are mutually dependent and interconnected. Steps required before the biomass-to-energy conversion can include: ground preparation and planting, cultivation, harvest, handling, storage, in-field/forest/road transportation, mechanical and chemical processes. A bio-energy supply chain is thus a network of different activities aimed at the production of energy from biomass. The combination of these activities can be varied in order to meet the need of a given conversion technology and cost structure. In particular, with reference to the final destination of the feedstock, supply chains can be based on different processes, e.g. pyrolysis or pelletizing in power production and starch fermentation or Fischer-Tropsch synthesis [Spath and Dalton, 2003] in the production of transport fuels.

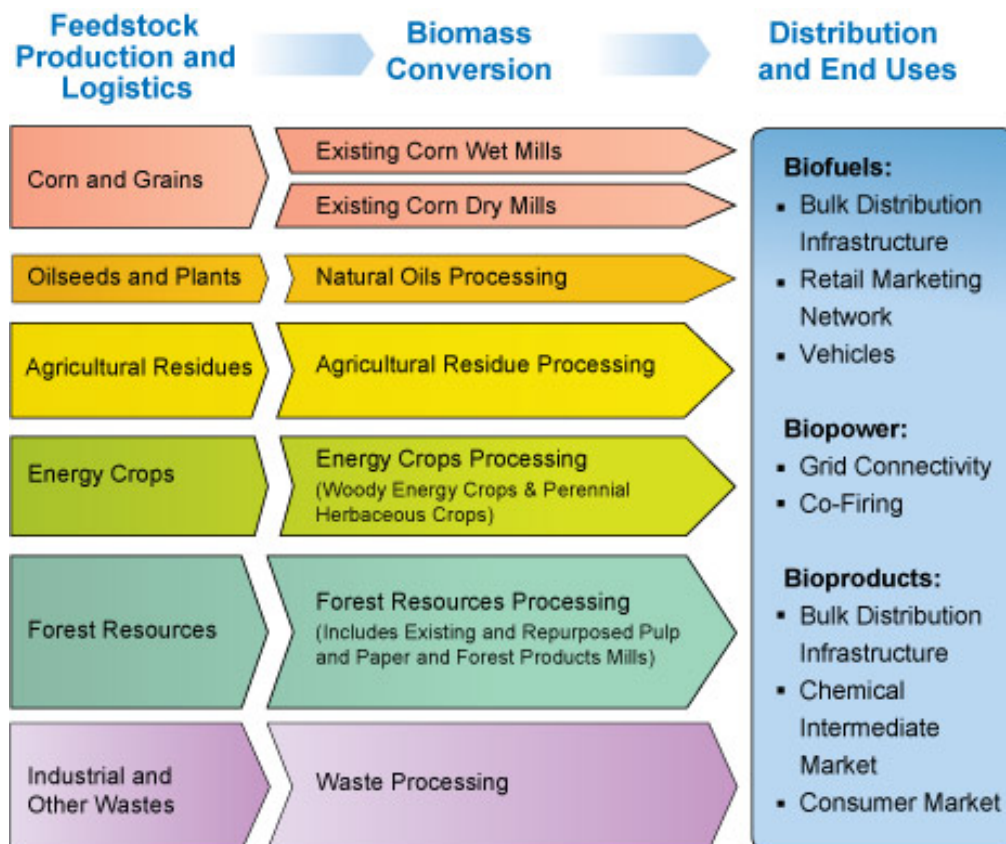


Fig. 3.1 – Alternative bio-energy supply chains

The following groups of activities can be generally identified in bio-energy supply chain:

1. Biomass production;
2. Biomass conditioning;
3. Biomass processing;
4. Logistics;
5. Final conversion to energy.

Biomass production is the stage in which the feedstock is grown and harvested. Forest residues, herbaceous biomass fuel, short rotation crops (SRC) are typical production systems. A wide range of specific activities can be planned depending on the kind of biomass materials and on the local conditions (e.g. clear felling, thinning and comminution for forest residues; fertilising, cutting and further baling or chopping for herbaceous biomass fuel; cutting, bundling and comminution for SRC) [Van Loo and Koppejan, 2008].

Biomass conditioning includes all the activities required in order to improve the feedstock quality to desired process specifications (e.g. removal of the impurities, screening, reduction of the particle size, drying).

Several processes can be applied to the biomass material preliminarily to the energy conversion. The biomass processing is aimed at the chemical-physical modification of the feedstock. For instance, this can involve a densification process before power generation in order to increase the energy density of the fuel (e.g. pyrolysis or pelletizing). Other processes are also inherently required in some biomass destinations, e.g. starch fermentation or Fischer-Tropsch process in the production of transport fuels [Spath and Dalton, 2003]).

Storage, handling and transport of the biomass/bio-products are included among the logistic activities. Biomass logistics depends on the scale of the system and on the territorial location of farms/forests and conversion facilities. Biomass is usually handled and transported from the field/forest to some collection points. Many types of biomass are harvested at a specific time of year but they are required on a year round basis. The storage points can be located on the farm/forest or further on the supply chain. Dry matter losses, heat development, change in moisture and growth of fungi and bacteria can occur during storage due to biological and biochemical degradation [Van Loo and Koppejan, 2008]. Transport processes can involve different vehicle types (e.g. trucks, rails, ships) depending on the scale of the supply chain and the infrastructures available in the territory. Heavy goods vehicles are often necessary.

Finally, the final stage of the supply chain includes all the activities required in order to convert biomass based fuels to energy.

The activities that take place in the biomass fuel supply chains are highly interconnected. It is easy to understand how upstream decisions affect later activities in the chain. For instance, trees grown on farmland on a short rotation coppice basis can either be harvested as whole sticks or immediately processed into wood chips. Different harvesting machinery is required for each of these harvesting systems. However, this is only the first of the consequences in the supply chain. While sticks can be stored directly on the fields without experiencing decomposition, chips need to be stored on a hard standing and in a covered environment because decomposition is to be prevented. Sticks and chips require very different transport systems in terms of both handling (i.e. loading and unloading vehicles) and load capacities [Allen et al., 1998]. The harvest system thus fundamentally affects the storage, handling and transport requirements in the supply chain. Similarly, the process technologies at the other end of the chain can influence the upstream activities because the biomass is to

be supplied at the correct time, in the correct quantity, and in the desired shape, size and quality [Allen et al., 1998].

3.2 From a process-specific to a system view

It is apparent that bio-energy systems are strongly related to site-specific conditions. Great attention should thus be paid on the territory. The scale of a supply chain should be based on the availability of territory, which also affects the logistic connection between production of biomass and energy conversion and, more in general, the efficiency and the effectiveness of the system.

The optimal scale of a bio-energy project varies depending on the spatial distribution and on the demand of the biomass resources. While small-scale local projects can minimise transport distances and may deliver higher social benefits, large scale feedstock production, and industrial-scale bio-energy plants can yield higher efficiencies than small-scale projects but they require expansive land demands due to the low energy density of the biomass. It is thus fundamental to evaluate the trade-offs existing between different alternative options [Dale et al., 2009].

Biomass supply chains involve different stakeholders, including: farmers, forest owners, agricultural and forestry contractors, transport and distribution companies, fuel suppliers and industrial operators [Allen et al., 1998]. An approach focusing on a single aspect of the supply chain is not sufficient in order to avoid the public concerns on the economical, environmental and social impacts (i.e. the sustainability [IUCN, 2006]) of bio-energy systems. An integrated perspective is thus necessary in order to link the agricultural dimension of bio-energy system with the industrial market (see figure 3.2).

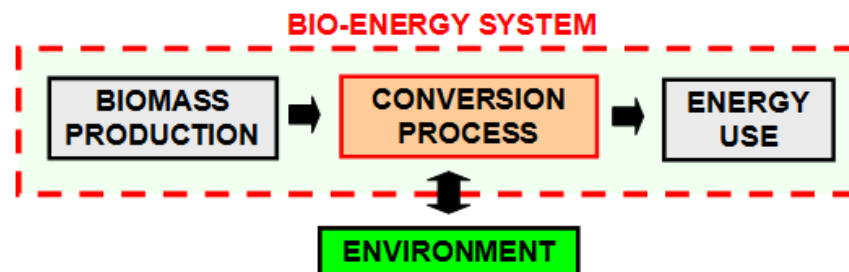


Fig. 3.2 – System view of energy production from biomass

The advantages of an integrated approach is that it can allow the full consideration of the system effects present in the supply chains as well as dynamic interactions in space and time. The complexity of bio-energy issues, indeed, can be fully understood only with a system view which takes into account for both direct and indirect impacts across the energy economy (e.g. agriculture is both an energy producer and a consumer and bio-fuels both displace and use fossil energy). Furthermore, trade-offs in technological, economic and environmental feasibility can often emerge only at the systems level [Dale et al., 2009].

Nevertheless, a regional perspective is still needed [Dale et al., 2009] in order to:

- Understand how regional variation can affect the production, distribution, and use of bio-fuels;
- Evaluate how bio-energy production systems may evolve differently in each region on the basis of the biomass feedstock potential, the bio-energy outputs (e.g., fuels, electricity, heat, etc.), the level of investment in fossil fuels

needed, the demand for bio-fuels and bio-energy and the competition with conventional energy systems and other biomass/land destination (e.g. food);

- Provide better estimates of the effects due to logistics (i.e. transportation and distribution of biomass feedstock and bio-fuels).

The system approach is to be coupled with specific assessment tools in order to address sustainability issues to all the supply chain stakeholders. Some of these tools will be presented in the next chapter, however it is now anticipated that most of them are based on a life cycle perspective.

CHAPTER 4

METHODS FOR THE SUSTAINABILITY ASSESSMENT OF A BIO-ENERGY SUPPLY CHAIN

4.1 General introduction

Chapter 1 highlighted that great attention is nowadays paid on renewable sources of energy as a consequence of the increasing worldwide need of sustainable energy supply. Biomass is in particular considered one of the most important renewable energy source for the coming decades [Van den Broek, 2000].

Sustainable development has been defined by the World Commission on Environment and Development (WCED) as “a development that ensures the needs of the present generation without compromising the ability of future generations to meet their own needs”. Sustainable development is generally seen as a multidimensional concept in which economical growth, environmental protection and social progress are pursued [IUCN, 2006].

Regarding with the economical dimension, the objectives of sustainable development are [Van den Broek, 2000]:

- the achievement of personal welfare by efficient allocation of resources; the meeting of basic human needs and the elimination of poverty (individual level);
- the attainment of a competitive market position (company level);
- the conservation of a healthy economy (national and international level).

The environmental dimension of sustainable development aims at the preservation of healthy condition for humans, animals and plants. Protecting biodiversity and avoiding unacceptable environmental risks play an important role in this respect [Van den Broek, 2000].

The societal dimension of sustainable development is focused at the human well-being. This includes an equitable distribution of the incomes, the public participation at various levels in society and the safety and quality of life at a local and an international level [Van den Broek, 2000]. Inherent safety is of particular concern in engineering sciences [Kletz, 1998].

Several issues related to sustainability are to be considered in the investigation of bio-energy systems.

Some of the traditional biomass uses, mainly cooking and heating in developing countries, are not sustainable. One of the reasons for this is that, according to several authorities, an intensive biomass exploitation may contribute to desertification and other forms of land degradation. Unsustainable harvesting of biomass may also contribute to a decline of the worldwide carbon pool stored in forests which would affect climate change. Another problem of traditional bio-energy use for cooking is the negative impact on indoor air quality, mainly caused by inefficient and incomplete combustion combined with a lack of adequate flue gas removal from the house. Firewood collection for own fuel consumption can instead demand huge time investments in developing countries, often to women, thereby limiting their ability to find paid employment elsewhere [Van den Broek, 2000].

Large portions of territory are moreover demanded by bio-energy systems, particularly at large scale production. This can result in direct competition between food vs. non food destination of the feedstock or indirect competition for the land use.

Criticism is therefore levelled against biomass by some authors [see for all Pimentel et al., 2009] due to the risk of diverting agricultural production away from food crops, especially in developing countries.

A positive contribution to sustainable development can be however obtained with modern uses of biomass (e.g. production of electricity, steam and bio-fuels) when balanced land management policies are implemented on the territory. Biomass is indeed a source of CO₂ neutral energy, which can reduce greenhouse gases emissions to the atmosphere when it replaces fossil energy carriers. Moreover, sustainable cultivation of energy crops has the potential to improve degraded land, e.g. adding additional carbon to the soil and reducing the risk of erosion. Another important contribution to sustainable development is the potential creation of new employment opportunities in rural areas in developing countries [Van den Broek, 2000].

The following aspects concerning with the sustainability of bio-energy systems were in particular addressed in the present work:

- the economical feasibility of pyrolysis based power supply chains;
- the insight of the inherent hazards due to the biomass pyrolysis products;
- the environmental compatibility of alternative bio-power supply chains (with reference to energy demand, climate change land occupation).

Life cycle thinking [Fava, 2002] and availability of specific analytical methods become necessary elements in order to perform a consistent “3-D” sustainability assessment (i.e. including economic, environmental and societal issues). The economic and the environmental assessment were performed resorting to conventional methodologies, i.e. Net Present Value (NPV) and Life Cycle Assessment (LCA). A specific approach was instead developed in order to investigate the inherent hazards associated with the biomass pyrolysis products. Details on the tools which will be used in the present work are described in this chapter; a wider set of instruments which can be used in the sustainability assessment of bio-energy systems can be found, for example, in [Dewulf, J. and Van Langenhove, H., 2006].

4.2 Economic assessment

4.2.1 Discount Cash Flow (DCF) analysis

The financial and economic analysis of investment projects is typically carried out using a Discounted Cash Flow (DCF) analysis [Herbohn and Harrison, 2002]. DCF is an evaluation method based on a time series of cash flows, both incoming and outgoing, related to a capital investment. The term cash flow refers to any movement of money to or away from an investor (i.e. an individual, a firm, an industry or a government). Projects require payments in the form of capital outlays and annual operating costs (i.e. cash outflows, negative sign) and they yield receipts or revenues (i.e. cash inflows, positive sign).

For each year, the difference between cash outflows and cash inflows is known as the net cash flow for that year. Each net cash flow is discounted back to its Present Value (PV) according to equation 4.1:

$$PV = \frac{R_t}{(1+i)^t} \quad (4.1)$$

Where,

- t is the time of the cash flow;

- i is the discount rate (or interest rate);
- R_t is the net cash flow (the cash inflow minus the cash outflow) at time t .

The rate used to discount future cash flows to their present values is a key variable of this process and it can be obtained from equation 4.2 [Bertocchi, 2008]:

$$i = (i_i + 1) \cdot (i_r + 1) - 1 \quad (4.2)$$

Where,

- i_i is the inflation rate;
- i_r is the rate of return, expressing the minimum profit to be gained with the investment.

Fixed or variable discount rates and other discounting criteria can be also used [Herbohn and Harrison, 2002].

Cash flows can be assessed before or after taxes and they are composed of a variable number of voices. A possible classification of the cash flows is given in the following [Bertocchi, 2008]:

- sales, i.e. the total money collected for goods and services provided;
- fixed expenses, i.e. costs which do not vary with changes in production activity level or sales volume (e.g. rent, insurance, dues and subscriptions, equipment leases, payments on loans, depreciation, management salaries, and advertising);
- variable expenses, i.e. costs which respond directly and proportionately to changes in activity level or volume (e.g. raw materials, hourly wages and commissions, utilities, inventory, office supplies, and packaging, mailing, and shipping costs)
- total expenses, i.e. the sum of fixed and variable expenses;
- cash income, i.e. the difference between sales and total expenses;
- fiscal depreciation, i.e. the depreciation charges related to the acquisition, production, construction, assembly, installation or improvement of fixed assets which can be recovered from a fiscal standpoint.
- fiscal pre-tax income, i.e. the difference between cash income and fiscal depreciation;
- tax burden: the financial charge on the fiscal pre-tax income (if positive);
- net cash income, i.e. the difference between fiscal pre-tax incomes and tax burdens.
- investment, i.e. expenses due to immobilised capital, and circulating capital and residual cash income after the life span of the assets.

4.2.2 Net Present Value (NPV)

DCF analysis can be used for the derivation of investment performance criteria, such as the Net Present Value (NPV) [Herbohn and Harrison, 2002].

NPV is a central tool in discounted cash flow (DCF) analysis, and is a standard method for using the time value of money to appraise long-term projects. Used for capital budgeting, and widely throughout economics, it is the sum of the discounted annual cash flows. NPV is an indicator of how much value an investment or project is able to yield. A project is considered profitable when the NPV is positive. The project can then bear the cost of capital (i.e. the interest rate) and still leave a surplus or profit.

4.2.3 Alternative investment performance criteria

Other performance criteria can be obtained from DCF analysis [Herbohn and Harrison, 2002].

Net Future Value (NFV)

The Net Future Value (NFV) is similar to the NPV with the difference that the cash flows are compounded forward to their value at the end of the project life-span. Once the NPV is known, the NFV can be obtained indirectly by compounding forward the NPV by the number of years of the project life.

Internal rate of return (IRR)

The internal rate of return (IRR) is the interest rate such that the discounted sum of net cash flows is zero. If the interest rate were equal to the IRR, the net present value would be exactly zero. The IRR is the highest interest rate which the project can support and still break even. A project is judged to be worthwhile in economic terms if the internal rate of return is greater than the cost of capital. If this is the case, the project could have supported a higher rate of interest than was actually experienced, and still made a positive payoff. From a practical viewpoint, the IRR may not exist or it may not be unique.

Benefit-to-cost ratios

Different benefit-cost ratio concepts have been developed, such as the gross and the net B/C ratios, defined respectively as

- Gross B/C ratio = $PV \text{ of benefits} / (PV \text{ of capital costs} + PV \text{ of operating costs})$;
- Net B/C ratio = $(PV \text{ of benefits} - PV \text{ of operating costs}) / PV \text{ of capital costs}$

A project is judged to be worthwhile in economic terms if it has a B/C ratio is greater than unity, i.e. if the present value of benefits exceeds the present value of costs (in gross or net terms).

The payback period

The payback period (PP) is the number of years requested by the projects in order to break even, i.e. the number of years for which discounted annual net cash flows must be summed before the sum becomes constantly positive. The payback period indicates the number of years until the investment in a project is recovered. It is a useful criterion for short planning horizons but it does not take account of all the net cash flows for years beyond the payback period.

The peak deficit

This is a measure of the greatest money amount that the project requires. Peak deficit is a useful measure in terms of financing a project, since it indicates the total amount of finance that will be required.

4.2.4 Methods for the engineering estimation of the costs

Immobilised capital

Immobilised capital, or fixed-capital, is usually regarded as the capital needed to provide all the depreciable facilities. It is sometimes divided into two classes by defining battery limits and auxiliary facilities for the project. The boundary of the battery limits includes all the manufacturing equipment but excludes administrative offices, storage areas, utilities, and other essential and nonessential auxiliary facilities [Perry and Green, 1997].

Fixed-capital investment can be estimated through a multiple-factor methods, e.g. Miller [Perry and Green, 1997]. All the contributions to the fixed-capital are added together to give an overall factor. This factor can be used to multiply the total cost of the equipments in order to obtain a forecast of the total fixed-capital investment, either for grass-roots or for battery-limit plants. The costs can be divided into four areas:

1. Cost of plant within battery limits;
2. Cost of auxiliaries;
3. Cost of engineering and field expenses;
4. Cost of contractor's fees plus contingency allowance.

Cost of the single equipments is to be evaluated through other methods, e.g. Chilton [Perry and Green, 1997]. Rapid capital-cost estimates can be made according to Chilton using capacity-ratio exponents based on existing cost data of a company or drawn from published correlations. If the cost of a piece of equipment or plant of size or capacity q_1 is C_1 , then the cost of a similar piece of equipment or plant of size or capacity q_2 can be calculated from the equation 4.3:

$$C_2 = C_1 \cdot (q_2 / q_1)^n \quad (4.3)$$

where the value of the exponent n depends on the type of equipment or plant. For process plants, capacity is expressed in terms of annual production capacity in metric tons per year. Care must be taken in determining whether the cost of the equipment has been expressed as free on board (FOB), delivered (DEL), or installed (INST). In many cases the cost must be correlated in terms of parameters related to capacity such as surface area for heat exchangers or power for grinding equipment.

Direct product costs

Direct manufacturing costs include raw materials, operating labour, utilities, and some miscellaneous items.

The cost of raw materials is normally the largest item of expense in the manufacturing cost of a product. The quantities of raw materials consumed can be calculated from material balances. Material costs are conveniently presented in tables published in various trade journals, however, quotations from suppliers should be used whenever possible.

The cost of operating labour is the second largest item of expense in the manufacturing cost. Labour requirements for a process can be estimated from an intelligent study of the equipment flow sheet, paying careful attention to the various primary process steps such as fractionation, filtration, etc. The hourly wage rate should be that currently paid in the company. Once the number of persons required

per shift has been estimated for a particular production rate, the annual labour cost and the labour cost per unit of production can be estimated. H. E. Wessel made a study of the operating-labour requirements in the United States chemical industry and presented the data as a plot of labour-hours per ton per processing step versus plant capacity in tons per day. These data can be represented by equation 4.4:

$$\log_{10} Y = 0.783 \log_{10} c + 1.252 + B \quad (4.4)$$

where:

- Y is the operating-labour-hours per ton per processing step;
- c is plant capacity, tons per day;
- B is a constant having values of 0.132 when multiple units are used to increase capacity or when the process is completely batch, of 0 for the average chemical-processing plant, and of -0.167 for large, highly automated plants or plants concerned with fluid processing.

Wessel's data for the United States chemical industry refer to the short ton equal to 2000 lb, or 907.2 kg. Labour requirements are higher in countries with lower productivities. The approximate cost of supervision for operating labour is equivalent to 10 percent of the labour cost for simple operations and 25 percent for complex operations.

Utilities include steam, cooling water, process water, electricity, fuel, compressed air, and refrigeration. The consumption of utilities can be estimated from the material and energy balances for the process, together with the equipment flow sheet. The current cost per unit for each utility is usually well known in a company. Thus, the annual cost for utilities and the utilities cost per unit of production can be estimated. The latter is normally much smaller than the raw-materials and labour costs. However, a great deal more work is involved in calculating the utilities cost than for any other item in the manufacturing cost. Unfortunately, there are no satisfactory shortcut methods for doing this. When the utilities cost is relatively small, it may be possible to make an intelligent guess on the basis of known costs for similar processes in the company. Alternatively, published data for the consumption of utilities per unit of production for various processes may be used.

Estimation of the miscellaneous direct costs, i.e. the costs of maintenance and repairs, operating supplies, royalties, and patents, are best based on company records for similar processes. A rough average value for the annual cost of maintenance is 6 percent of the capital cost of the plant. This percentage can vary from 2 to 10 percent, depending on the severity of plant operation. Approximately half of the maintenance costs are for materials and half for labour. Royalty and patents costs are in the order of 1 to 5 percent of the sales price of the product [Perry and Green, 1997].

Indirect product costs

Indirect manufacturing costs include the cost of payroll overhead, control laboratory, general plant overhead, packaging, and storage facilities and their estimation is best based on company records for similar processes. Payroll overhead includes the cost of pensions, holidays, sick pay, etc., and is normally between 15 and 20 percent of the operating-labour cost. Laboratory work is required for product quality control, and its cost is approximately 10 to 20 percent of the operating-labour cost. Plant overhead includes the cost of medical, safety, recreational, effluent-disposal, and warehousing facilities, etc. In general, the larger the plant, the lower the overhead per unit of

production. Plant overhead costs can vary between 15 and 150 percent of the operating-labour cost. Packaging costs depend on the physical and chemical nature of the product as well as on its use and value (e.g. the cost of packaging is as high as one-third of the selling price for soaps and pharmaceuticals) [Perry and Green, 1997].

4.2.5 Costs data localisation and actualisation

Cost indices (e.g. Marshall & Swift Equipment Cost Index [Peters et al., 2003], ISTAT data [ISTAT], OECD Comparative Price Levels [OECD]) should be used in order to refer the costs data to a geographical and temporal context of analysis. If C_r is the cost at a reference year in a reference geographical area, the updated cost C_u will be expressed according to equation 4.5:

$$C_u = \frac{I_u}{I_r} \cdot C_r \quad (4.5)$$

Where,

- I_r is the index score for the reference year and the reference geographical area;
- I_u is the index score for the geographical and temporal context of analysis.

4.3 Life cycle assessment

4.3.1 Introduction

The Life Cycle Assessment (LCA), a.k.a life cycle analysis or eco-balance, is a methodology to evaluate the environmental burdens associated with a product, process, or activity. It is based on the identification and on the quantification of energy and materials used (i.e. inputs) and wastes released to the environment (i.e. outputs). The assessment should include the entire life cycle of the product, process or activity, i.e. from cradle-to-grave, encompassing: extraction and processing of raw materials; manufacturing, transportation and distribution; use, re-use, maintenance; recycling, and final disposal [SETAC].

The methodology is fully described in the ISO 14000 environmental management standards [ISO 14040, 2006; ISO 14044, 2006] and it is composed of four main phases, represented on figure 4.1:

1. Goal and scope definition;
2. Life Cycle Inventory (LCI);
3. Life Cycle Impact Assessment (LCIA);
4. Life Cycle Interpretation.

4.3.2 Goal and scope definition

The goal and scope definition [Cordella, 2006] is a fundamental phase in a LCA study because it defines: the purposes of the study; the system whose environmental performances are investigated; the pieces of information which are needed; how accurate the results must be and how the results should be interpreted and used. The system description in particular requires the definition of:

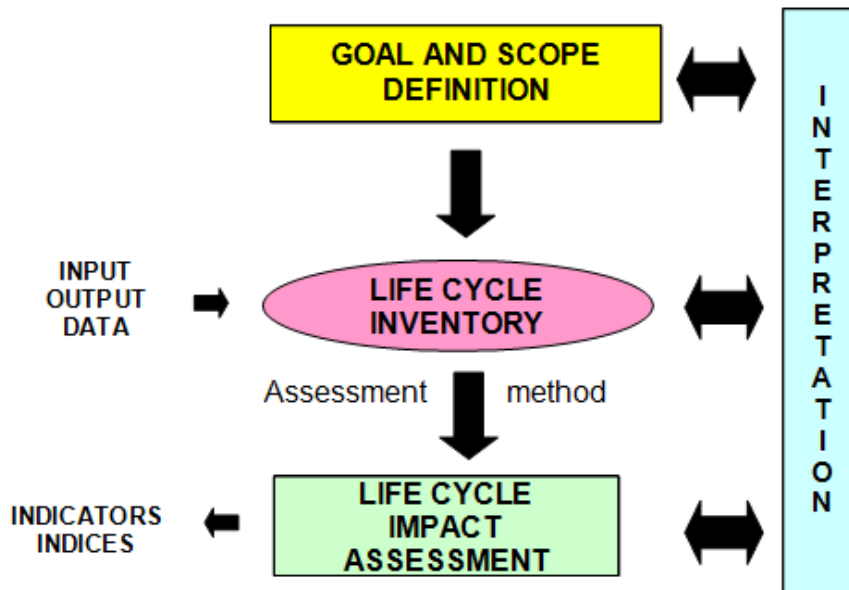


Fig. 4.1 – LCA phases according to the ISO standards.

- The Functional Unit, a calculation basis which appropriately describes the function of the product or process being studied. Careful selection of the FU to measure and display the LCA results will improve the accuracy of the study and the usefulness of the results;
- The system boundary, which determines the unit processes included in the study, in accordance with the goal of the study. It is generally impossible to include all the elements of a life cycle due to its complexity, so that engineering rules are often used to set-up cut-off bases. Presence of two or more products may also occur in some systems. In that case an allocation procedure or the extension of the system function is required, if the specific impacts associated with one product cannot be identified. Physical, economical or environmental criteria can be used as allocation basis according to ISO standards. With reference to the capital goods, three levels of detail can be pursued [Goedkoop et al., 2007]:
 1. I order analysis, in which only materials and transports are included;
 2. II order analysis, in which all the processes of the life cycle are included apart from the capital goods;
 3. III order analysis, in which also the capital goods are included (usually with I order modelling).

Based on the extension of the boundary it is possible to distinguish between:

- Cradle-to-grave analysis, i.e. from manufacture to disposal phase;
- Cradle-to-gate analysis, i.e. from manufacture to the production site;
- Cradle-to-cradle analysis, i.e. a specific kind of cradle-to-grave assessment, where the end-of-life disposal step for the product is a recycling process;
- Gate-to-gate: a partial LCA looking at only one process in the entire production chain.

Data quality is one of the main uncertainty in a LCA study. Quality of the information available should be stated in order to understand the validity of the results of the assessment, together with methodological choices, operational hypotheses and limitations.

The goal and scope phase finally includes a description of the impact categories that are included in the assessment and the method applied for the quantification of the potential environmental impacts.

4.3.3 Life cycle inventory

The Life Cycle Inventory is the most sensitive stage of a LCA study, the one in which the input/output flows are quantified. The more complicated the system analysed, the more difficult the inventory definition is.

The life cycle is modelled according to the following steps:

1. the flow chart of the processes is drawn. The flow chart links all the processes and the material and energy streams involved in the life cycle;
2. the data required for the analysis are collected and processed. This is usually the most resource expensive task. Depending on the source, it is possible to classify:
 - primary data (or foreground data), directly collected on site;
 - secondary data (or background data), obtained from literature, database, technical handbooks, other studies, engineering calculations, estimates, laboratory tests, environmental statistics, average figures.

Data are referred to the Functional Unit of the system;

3. the system boundary is refined, if necessary.

At the end of the modelling, a list is yielded containing the amounts of wastes released into the environment and the materials and energy consumed for the production of the functional unit.

4.3.4 Life cycle impact assessment

The Life Cycle Impact Assessment (LCIA) is aimed at the evaluation of the environmental impacts due to the LCI voices. The choice of the impact categories and of the assessment methods depend on the goal and scope of the analysis. LCIA is composed of several steps:

1. Classification;
2. Characterisation;
3. Normalisation;
4. Grouping
5. Weighting.

Classification and characterisation are based on scientific data and are mandatory; normalisation and weighting voluntary due to a higher level of subjectivity.

Classification

Impact categories are identified and the LCI data assigned to the categories. The inclusion of one or more impact categories in the assessment is a complex task, inherently connected with the goal of the analysis. A limited set of independent impact categories should be moreover selected. A list with some of the impact categories which are used in LCA is given on table 4.1.

Characterisation

Impact characterization [EPA, 2006] uses science-based conversion factors, called characterization factors, to convert and combine the LCI results into representative

indicators of impacts to human and ecological health. Characterization factors also are commonly referred to as equivalency factors. Characterization provides a way to directly compare the LCI results within each impact category. In other words, characterization factors translate different inventory inputs into directly comparable impact indicators.

Tab. 4.1 – Some impact categories which can be used in LCA [EPA, 2006]

Impact Category	Scale	Examples of LCI Data	Ex. of characterization factor (Description)
Global Warming	Global	Carbon Dioxide (CO ₂) Nitrogen Dioxide (NO ₂) Methane (CH ₄) Chlorofluorocarbons (CFCs) Hydrochlorofluorocarbons (HCFCs) Methyl Bromide (CH ₃ Br)	Global Warming Potential (Converts LCI data to carbon dioxide equivalents)
Stratospheric Ozone Depletion	Global	Chlorofluorocarbons (CFCs) Hydrochlorofluorocarbons (HCFCs) Halons Methyl Bromide (CH ₃ Br)	Ozone Depleting Potential (Converts LCI data to CFC-11 equivalents)
Acidification	Regional Local	Sulfur Oxides (SO _x) Nitrogen Oxides (NO _x) Hydrochloric Acid (HCL) Hydroflouric Acid (HF) Ammonia (NH ₄)	Acidification Potential (Converts LCI data to hydrogen ion equivalents)
Eutrophication	Local	Phosphate (PO ₄) Nitrogen Oxide (NO) Nitrogen Dioxide (NO ₂) Nitrates Ammonia (NH ₄)	Eutrophication Potential (Converts LCI data to phosphate ion equivalents)
Photochemical Smog	Local	Non-methane hydrocarbon (NMHC)	Photochemical Oxident Creation Potential (Converts LCI data to ethane equivalents)
Terrestrial Toxicity	Local	Toxic chemicals with a reported lethal concentration to rodents	LC50 (Converts LC50 data to equivalents; uses multi-media modeling, exposure pathways)
Aquatic Toxicity	Local	Toxic chemicals with a reported lethal concentration to fish	
Human Health	Global Regional Local	Total releases to air, water, and soil.	
Resource Depletion	Global Regional Local	Quantity of minerals used Quantity of fossil fuels used	Resource Depletion Potential (Converts LCI data to a ratio of quantity of resource used versus quantity of resource left in reserve)
Land Use	Global Regional Local	Quantity disposed of in a landfill or other land modifications	Land Availability (Converts mass of solid waste into volume using an estimated density)
Water Use	Regional Local	Water used or consumed	Water Shortage Potential (Converts LCI data to a ratio of quantity of water used versus quantity of resource left in reserve)

Impact indicators are typically characterized using the following equation 4.6:

$$\text{Inventory Data} \times \text{Characterization Factor} = \text{Impact Indicators} \quad (4.6)$$

A spatial and temporal scale is associated with every impact category (see tab. 4.1), so that data scale should be tracked.

Two main categories of indicators can be generally used: midpoint indicators and endpoint indicators, according to the intensity in the modelling of the cause-effect chain (i.e. fate analysis, exposure analysis, effect analysis, damage analysis) [Bare et al., 2000]. Midpoint modelling is on the middle of the environmental mechanism chain and it aims to quantify environmental impacts on the basis of equivalence factors between the items present in the LCI. A deeper modelling characterizes endpoint indicators, which are thus closer to the representation of the physical effects on society. Perception and interpretation of endpoints indicators is easier but at the expense of an increase in uncertainty. A graphical representation of the midpoint-endpoint concept is given on figure 4.2.

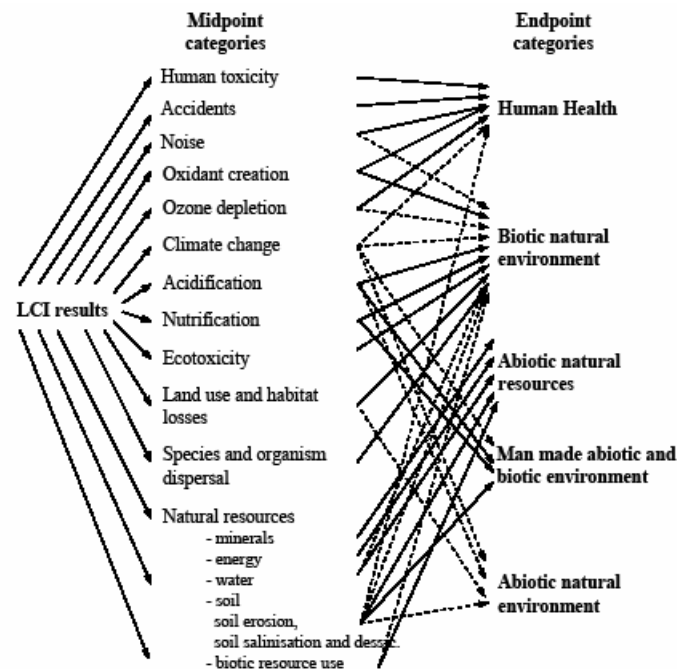


Fig. 4.2 – Midpoint and endpoint indicators [UNEP]

Normalisation

Normalization [EPA, 2006] provides a basis for comparing different types of environmental impact categories. This procedure divides the indicator results by a selected reference value. There are numerous methods of selecting a reference value, including:

- The total emissions or resource use for a given area that may be global, regional or local;
- The total emissions or resource use for a given area on a per capita basis;
- The ratio of one alternative to another (i.e., the baseline);
- The highest value among all options.

The goal and scope of the LCA may influence the choice of an appropriate reference value.

Grouping

Grouping [EPA, 2006] assigns impact categories into one or more sets to better facilitate the interpretation of the results into specific areas of concern. Typically, grouping involves sorting or ranking indicators.

Weighting

The weighting step (also referred to as valuation) [EPA, 2006] of an LCIA assigns weights or relative values to the different impact categories based on their perceived importance or relevance. Normalised indicators can also be aggregated into one or more indices. Weighting is important because the impact categories should also reflect study goals and stakeholder values. Because weighting is not a scientific process, it is vital that the weighting methodology is clearly explained and documented. Although weighting is widely used in LCAs, the weighting stage is the least developed of the impact assessment steps and also is the one most likely to be challenged for integrity. In general, weighting includes the following activities:

- Identifying the underlying values of stakeholders;
- Determining weights to place on impacts;
- Applying weights to impact indicators.

Weighted data could possibly be combined across impact categories, but the weighting procedure must be explicitly documented. The un-weighted data should be shown together with the weighted results to ensure a clear understanding of the assigned weights

4.3.5 Life Cycle Interpretation

Interpretation completes a LCA study. Several investigations can be performed in order to understand better the results of the study, such as [Cordella, 2006]:

- contribution (or gravity) analysis, aimed at the identification of the most critical processes/LCI data and the further selection of solutions for the improvement of the environmental performances;
- sensitivity analysis, aimed at the analysis of the significance of preliminary assumptions on the final results;
- uncertainty analysis, aimed at the assessment of the data uncertainty on the final results;
- comparative analysis, aimed at the comparison between two or more options.

4.4 Assessment of the inherent hazards due to substances

4.4.1 Introduction

Inherent hazards can be associated with production, storage, delivery and use of chemicals due to the presence of flammable, explosive and toxic substances [Cozzani and Zanelli, 1997; Cozzani and Zanelli, 1999; Cozzani et al., 1998; Lees, 1996]. The actual understanding of the hazards related to chemical compounds should be a core issue in sustainability assessment and it would be also consistent with the European REACH system [Regolamento CE n. 1907/2006 del Parlamento Europeo e del Consiglio], aimed at the improvement of the protection of human health and the

environment through a better and earlier identification of the inherent properties of chemical substances.

A multistage procedure originally developed in order to address the analysis of the consequences due to the possible release of decomposition products in accidental conditions [Cordella et al., 2009] was extended to the analysis of fossil and renewable liquid fuels [Cordella et al., 2008a] and it can be adapted and applied to the more general assessment of the inherent hazards due to chemical substances.

The assessment is based on the inherent properties of substances and it is aimed at the identification and quantification of the possible hazards for humans (i.e. acute toxicity, chronic toxicity, carcinogenicity), ecosystems (i.e. ecotoxicity) and things (i.e. fire). A metric of parameters allows the definition of an overall Hazard Footprint and of a set of Hazard Indices related to specific endpoints.

4.4.2 Collection of hazard data

Different groups of properties allow a substance to be classified as potentially hazardous, with reference to different endpoints.

Thirteen parameters are used in order to represent the hazard profile of a chemical; these may be grouped in five categories of properties, as shown in table 4.2.

The properties listed in table 4.2 have to be quantified in order to perform the hazard assessment. Information can be collected from several sources: scientific literature [Lewis, 1992], databases [ESIS; RTECS; SCORECARD; SIRI; TOXNET], material safety data sheets [Chemexper] and predictive models (e.g. group contribution methods and structure activity relationships as those reported by [Allen and Shonnard, 2002]) if no experimental data is available.

Tab. 4.2 – Hazard parameters and properties of the assessment methodology

Group of properties	Parameter (properties of concern)
1. Toxicological	1a Acute toxicity (LC ₅₀ inh. rat, LD ₅₀ oral rat; LD ₅₀ dermal rat)
	1b Ecotoxicity (LC ₅₀ fishes, EC ₅₀ daphnia, LD ₅₀ avian species)
	1c Chronic toxicity (RfC; RfD)
	1d Carcinogenicity (CSF)
2. Dispersion and environmental fate	2a Molecular weight (MW)
	2b Henry's law constant (H)
	2c Boiling point (B _p)
	2d Solubility in water (S _w)
3. Uptake by organisms	3a Octanol-water partition coeff. (K _{OW})
4. Environmental Persistence	4a Overall persistence time (T ₀)
	5a Vapour relative density ($\rho_{\text{vap}}/\rho_{\text{air}}$)
5. Flammability	5b Flammability (F _p)
	5c Ignition energy (A _p)

4.4.3 Hazard assessment of a single compound

When information on a substance are available, thirteen scores are assigned to the properties quantified. Score assignment is based on data provided by ranking systems proposed by the legislation or available in technical and scientific literature [Allen &

Shonnard, 2002; European Commission, 2001; Mackay, 2001; Presidenza del Consiglio dei Ministri della Repubblica Italiana, 1989]. Ranking criteria are reported in table 4.3.

Tab. 4.3 – Ranking criteria used in the parameter score assignment

Property	Parameters	SCORE			
		0	1	2	3
1a	LC ₅₀ (4h), inhalation rat (mg/l)	>20	2-20	0.5-2	< 0.5
	Risk Phrases, inhalation [European Commission, 2001]	-	R20	R23	R26
	LD ₅₀ , ingestion, rat (mg/kg)	>2000	200-2000	25-200	< 25
	Risk Phrases, ingestion [European Commission, 2001]	-	R22	R25	R28
	LD ₅₀ , dermal, rabbit (mg/kg)	>2000	400-2000	50-400	< 50
	Risk Phrases, contact with skin [European Commission, 2001]	-	R21	R24	R27
1b	LC ₅₀ (96h), fish (mg/l)	>100	10-100	1-10	<1
	LC ₅₀ (48h), daphnia (mg/l)	>100	10-100	1-10	<1
	EC ₅₀ (72h), algae (mg/l)	>100	10-100	1-10	<1
	LD ₅₀ , avian species (mg/kg)	>1000	100-1000	10-100	<10
1c	RfD (mg/kg·d)	-	>0.1	0.001-0.1	<0.001
	RfC (mg/m ³)	-	>0.35	0.0035-0.35	<0.0035
	Qualitative data [SCORECARD]	-	1	-	-
1d	CSF (mg/kg·d) ⁻¹	-	<1	1-10 ³	>10 ³
	Qualitative data [SCORECARD, SIRI]	-	1	-	-
2a	MW (kg/kmol)	-	100-300	<100	>300
2b	H (atm·m ³ /mol)	-	10 ⁻⁶ -10 ⁻²	>10 ⁻²	<10 ⁻⁶
2c	B _p (°C)	-	50-150	<50	>150
2d	S (mg/l)	-	1-10 ³	>10 ³	<1
3a	K _{OW} (Log K _{OW})	-	3.5-4.3	>4.3	<3.5
4a	T _O (h)	-	100-1000	>1000	<100
5a	ρ _v /ρ _{air}	-	< 0.8	0.8 – 1.2	> 1.2
5b	F _p (°C)	> 55	21 – 55	0 – 21	< 0
5c	A _p (°C)	-	> 500	300 – 500	< 300

As shown in the table, the property score is an integer ranging from 0 to 3. A higher score corresponds to more hazardous properties. The 0 value may be assigned only to properties for which a negligible hazard can be considered; for all the other properties the lowest score is 1. If more than one parameter contributes to the ranking of a single hazardous property (e.g. this is the case of the toxicological properties), the score assigned to the property is conservatively assumed equal to the highest score corresponding to the single sub-parameters. A Hazard Vector is defined by the scores

calculated by the above procedure and it can be used to yield the Hazard Footprint' of the substance.

Hazard parameters can then be rearranged into five indices:

- the Acute Toxicity Index (ATI);
- the Ecotoxicity Index (ETI);
- the Chronic Toxicity Index (CTI);
- the Carcinogenicity Index (CI);
- the Fire Hazard Index (FHI).

According to equation (4.7), indices are calculated as the product of three factors:

$$I = HF \cdot AF \cdot CF \quad (4.7)$$

where:

- HF is a Hazard Factor, which expresses the inherent hazard due to the substance;
- AF is an Availability Factor, which quantifies the possibility of presence of the substance in the target;
- CF, is a Probability Factor, which represents the probability of contact of the substance with the target.

By the above definition of the impact indices, based on eq. (1), the numerical scores of the indices are comprised between 0 and 27. Specific relations for the calculation of the four impact indices were derived from the general relation given in eq. (1) and are reported in Table 4.4.

Tab. 4.4 – Equations used in the calculation of the Hazard Indices (symbols refer to the parameters listed in table 4.3)

Index	Formula
Acute Toxicity (IAT)	$1a_{inh} \cdot 2a \cdot (2b+2c)/2$
Ecotoxicity (IET)	$\max (1b_{wat} \cdot 2d \cdot 4a; 1b_{air} \cdot 2b \cdot 4a)$
Chronic Toxicity (ICT)	$1c \cdot 3a \cdot 4a$
Carcinogenicity (IC)	$1d \cdot 3a \cdot 4a$
Fire Hazard (FHI)	$5b \cdot 5a \cdot 5c$

A synthetic hazard index is also introduced in order to rank the overall hazard due to a substance, the Overall Hazard Index (OHI), whose calculation procedure is outlined in the following:

1. the five impact indices are normalised with an external benchmark (i.e. Toluene);
2. OHI is taken as the sum of the normalised indices.

OHI thus expresses the inherent hazard due to a substance with reference to Toluene. Indices scores for Toluene are reported in table 4.5, in accordance with the hazard assessment methodology presented.

Tab. 4.5 – Indices scores for Toluene

Index	Score
ATI	6
ETI	8
CTI	4
CI	2
FHI	12
OHI	5

An Impact Vector composed of six indices can be thus obtained, which can be used together with the Hazard Vector in order to describe the Hazard Profile of the substance.

4.4.4 Hazard assessment of a mixture of compound

Hazard and Impact Vectors allow the definition of the hazard profile of a single compound. Since chemicals are often composed of more components, the assessment of the hazards due to a mixture of compounds is also to be addressed. Two tiers of analysis were developed: a differential and an integral assessment.

In the differential assessment, Partial Hazard Profiles (PHP), i.e. referred to single components, are compared in order to screen the most hazardous components. The comparison between different components (and different chemicals) can be performed both arranging parameters and indices into a matrix or resorting to graphic representations [Cordella et al., 2009]. In particular, Hazard Footprints result from the plot of parameter scores in radial graphs and Impact bar charts from the scores of the impact indices.

Nevertheless, an analysis is necessary in order to understand the hazards due to the mixture as a whole. An Integral Hazard Profile (IHP) is obtained as the mass weighted average of the Partial Hazard Profiles of each component. Clear enough, the direct quantification of the mixture properties would allow also a direct definition of the Mixture Hazard Profile.

If the chemical characterization of the mixture of compounds is not complete, a fraction of the mixture would be excluded from the assessment. In this condition, two mixture profiles are proposed:

- a higher IHP (h-IHP), conservatively obtained considering that the compounds identified are representative for all the mixture,
- a lower IHP (l-IHP), considering that inherent hazards due to the unknown materials are negligible.

4.4.5 Family compounds-based assessment

The identification of the substances contained in a mixture to be evaluated is sometimes a resource-consuming procedure often not leading to a complete and detailed characterization [Cordella et al., 2008a; Cordella et al., 2008b]. A streamlined approach based on the identification of macro-categories of compounds and on the assignment of a representative compound to each “family” may be thus followed in order to understand the inherent hazard of bio-oils. Further details about this approach can be found in [Cordella et al., 2008b]. Obviously, the macro-categories approach does not allow a detailed understanding of the hazards due to single components contained in the mixture but it can be useful when the aim is to understand the hazards due to the mixture as a whole.

CHAPTER 5

EXPERIMENTAL ANALYSIS ON THE SLOW PYROLYSIS PROCESS

5.1 General introduction

The assessment of the sustainability of bio-energy supply chains based on a slow pyrolysis densification process cannot be separated by experimental research. Research on biomass pyrolysis is wide with reference both to process aspects and to the characterisation of the pyrolysis products. The understanding of thermal decomposition mechanisms, kinetics and heat of reactions involved with the pyrolysis process was deeply analysed], as well as the effects due to the reactor configurations and the main operative parameters of the process [Bridgewater and Peacocke, 2000; Gomez Diaz, 2006; Kandyioti et al., 2006]. On the other hand, a detailed overview of the chemical physical properties and composition of char and pyro-oil can be also found in literature [Antal & Gronli, 2003; Oasmaa & Peacocke, 2001; Qiang et al., 2009; Strezov et al., 2007].

A series of experimental activities were needed in order to fulfil the goals of the thesis and to collect data needed for further analysis of the supply chain. The following activities were carried out and they will be described in the present section of the thesis:

1. experimental pyrolysis with fixed bed reactors (EA1);
2. thermal gravimetric analysis of the char samples (EA2);
3. study of the pyro-oil stability (EA3);
4. assessment of the hazards due to the pyro-oil compounds (EA4).

It is apparent the importance that these experimental activities cover in the thesis as an integration to the sustainability analysis. EA1 was aimed to the production of solid and liquid samples to be used for further product characterisation and for the gaining of slow pyrolysis yields. Pyrolysis yields, coupled with the outputs coming from EA2, are in particular seen as essential blocks for the definition of desired process conditions inside the supply chain and for further economic and environmental assessments. EA3 and EA4 were instead performed in order to possibly add useful pieces of information in the study of two problems which may create some limitations to the use of pyro-oils: instability and presence of hazardous substances.

5.2 Experimental pyrolysis in fixed bed reactors

5.2.1 Introduction

Pyrolysis is the thermal decomposition of organic material in absence of oxygen. As a consequence the feedstock is converted in a solid residue (i.e. char), a liquid fraction (i.e. pyro-oil), and a light gaseous phase. Yields in pyrolysis products, strongly dependent on process operative conditions and on biomass feedstock, are key parameters for the assessment of the economic and environmental sustainability of the process in a life cycle perspective. The goals of the present activity were:

1. to collect biomass specific slow pyrolysis yields;
2. to produce solid and liquid samples for further analytical characterisation.

Experimental pyrolysis involved: different feedstock (i.e. corn stalks, poplar, sorghum, switchgrass), different peak temperatures, different reactor configuration. This allowed the analysis of the effects due to temperature and biomass feedstock on the pyrolysis yields which are useful to understand the conditions at which the production of specific products can be maximised.

5.2.2 Materials and methods

Feedstock

Four different biomass samples were processed: corn stalks (CS), poplar (PO), sorghum (SO) and switchgrass “alamo” (SW). The biomass feedstock was provided by the Department of Agro-Environmental Science and Technology of the University of Bologna (Italy). The material was farmed and harvested in Ozzano and Cadriano (Bologna, Italy), dried overnight and ground up to a particle size lower than 1 mm. It is important noticing that biomass samples were selected in order to work with species for which environmental and economic information were available. The proximate analysis of the dried biomass samples are reported in table 5.1.

Tab. 5.1 – Proximate analysis of the biomass feedstock

Proximate analysis (d.b.)	CS	PO	SO	SW
Volatile Fraction (%)	77.7	80.1	78.0	82.6
Fixed Carbon (%)	17.0	14.8	17.4	13.9
Ash (%)	5.3	5.1	4.6	3.5

Reactors

Two lab-scale fixed bed reactors were set up in order to process different kinds of biomass under slow pyrolysis conditions.

A Gray King Reactor (GKR) was used in the laboratories of the Imperial College of London. The layout of the experimental set-up is shown in fig. 5.1 and it was adapted by the well-known Gray-King furnace method [British Standard Institution, 19991]. Applications of this method were successfully tested both with coal [British Standard Institution, 19991] and with biomass [Zaror et al., 1985]. Some relevant modifications were nevertheless applied to the original method in order to deal with the nature of the study.

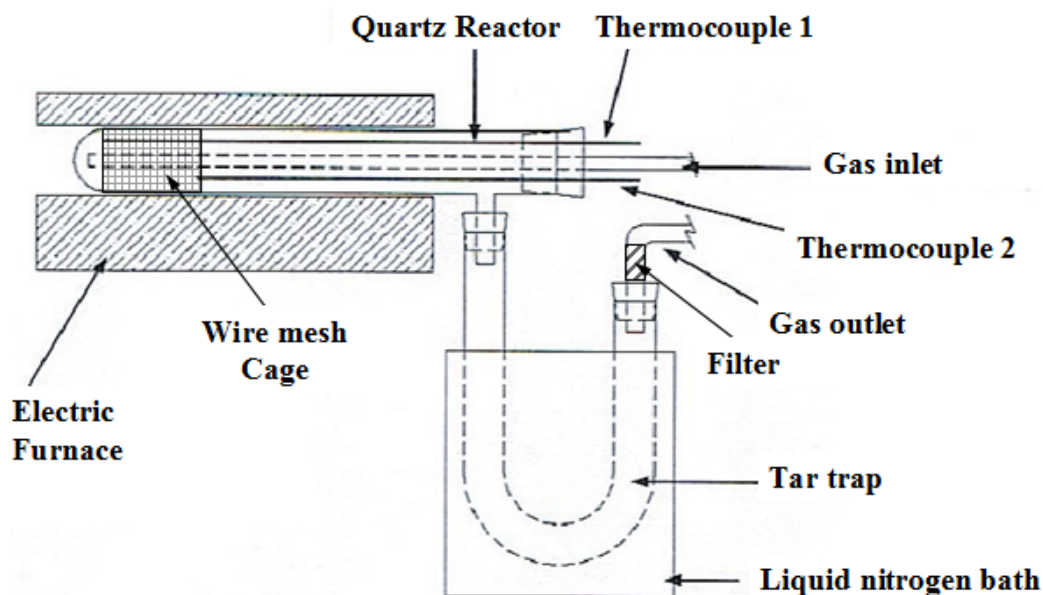


Fig. 5.1 – Layout of the Gray King Reactor (GKR)

Biomass material was placed inside a quartz tube reactor (length: 30 cm, inner diameter: 2 cm) and heated up by means of a furnace to the pyrolysis peak temperature with a heating rate of about 50 °C/min (± 20 °C/min, where lower heating rate were applied to runs performed at lower temperature). A special wire mesh cage was built in order to contain few grams of biomass particles in a fixed position. This artifice allowed more uniform conditions to be established in the biomass bed, located 5 cm from the bottom of the quartz tube (i.e. left side in fig. 5.1). A 6 cm height cage was used, which allowed the pyrolysis of up to 2-3 g of biomass per run, depending on the species processed. Once the peak temperature was achieved, the temperature was kept constant for a holding time of 15 minutes, before the quartz reactor was removed from the furnace. Two thermocouples were used to monitor the temperature inside the biomass bed. Nitrogen gas was used to sweep the volatile products to a trap that was cooled by liquid nitrogen. A gas flow rate equal to 1.2 L/min was applied in each run. The gas flow rate was kept as high as possible, according to the limits imposed by the experimental set-up (i.e. rotameter upper reading and no removal of particles from the biomass bed) in order to minimise the extent of the secondary reactions occurring in the way out (14 cm inside the furnace and 7 cm out of the furnace) from the reactor. An end-of-pipe trap composed by a glass U-tube cooled by liquid nitrogen was used for the pyro-oil collection. High loss of condensable material were instead recorded when an ice-salt mixture bath was tested as cooler. An external cotton-filled filter was also placed in order to trap liquid molecules escaped by the U-tube. The pyrolysis runs were performed at atmospheric pressure.

A Tubular Reactor (TR) consisting of an horizontal tube externally heated by an electrical furnace was also used. The layout of the experimental set-up is shown on figure 5.2.

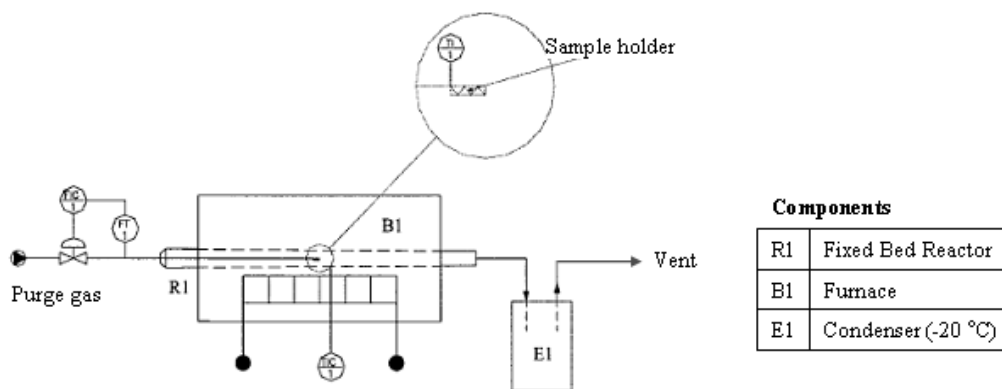


Fig. 5.2 – Layout of the Tubular Reactor (TR)

A sample holder coupled with the tube allowed up to 10 grams of biomass to be charged and moved on the axial direction of the reactor. At the beginning of the pyrolysis runs, the sample holder was charged with several grams of biomass and positioned out of the furnace. Reactor was then heated to the pyrolysis peak temperature and the biomass moved inside the reactor. In such a condition, the sample was heated with a heating rate of about 100 °C/min and held at the peak temperature for 30 min. Temperature inside the biomass bed was monitored by two K-type thermocouples. Experimental runs were performed under pure nitrogen atmosphere. 1.2 L/min of purge gas flow was applied in order to control the reaction environment, to promote the removal of volatile products from the reactor, and to limit the extent of secondary gas-phase reactions. Volatiles were moved to a trap system in which condensable products were collected. The trap system was composed by four glass traps in series, maintained at -20 °C by a sodium chloride brine/ice bath.

Yield in solid product was directly measured weighting the mass of primary char; liquid product yield was indirectly calculated from the difference in weight of trap system and reactor before and after the run. Light products were defined as the material which left the system in a gaseous state. Yields were converted from a wet basis to a dry basis under the assumption that all the moisture of the initial biomass was contained in the liquid product collected from the trap system.

An approximate estimation of the residence time of volatiles in the reactors was performed at different temperatures and it is plotted on figure 5.3. According to these rough data, it is possible that secondary pyrolysis reactions may have occurred in TR with a higher extent even if residence time length and difference between the two reactor configurations decrease significantly as the temperature increases.

Biomass use during the experimental activities was limited by the available amount of sample. A first slot of biomass samples (i.e. CS, SO and SW) were processed in the GKR in order to obtain a trend of the pyrolysis yields as a function of the pyrolysis peak temperature and to produce samples of char for the thermal gravimetric analysis and samples of pyro-oils for the instability study. Biomass samples were dried overnight in a vacuum oven at 35 °C and then stored into a dessicator cabinet before the pyrolysis runs.

Common practice was to register yields at 350, 500 and 650 °C and to carry out additional runs in order to plot the trends of the pyrolysis yields against temperature.

Pyrolysis runs were also performed in the TR at 650 °C for all the biomass samples, which were dried overnight in a oven at 105 °C and then stored into a dessicator

cabinet before the pyrolysis runs. Yields in pyrolysis products were registered and pyro-oils samples from CS, PO and SW collected for the assessment of their inherent hazard.

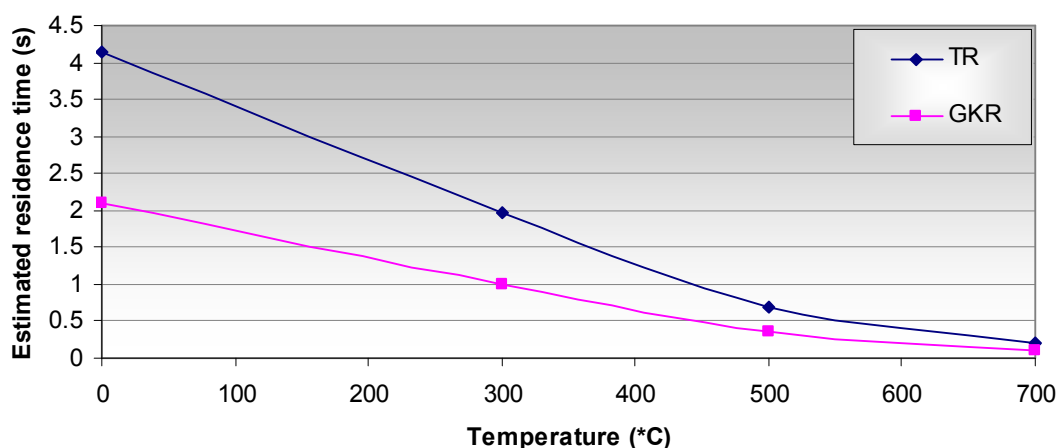


Fig. 5.3 – Approximate estimation of the residence time of volatiles in GKR and in TR at different temperatures

5.2.3 Results and discussion

Pyrolysis yields registered during the runs performed with the GKR are plotted on figure 5.4 and on figure 5.5.

Asymptotic trends were obtained with all the samples investigated: char yield reached a minimum after 500 °C while oil yield appeared to stabilise at lower temperatures, i.e. about 400 °C.

With reference to the char yield, CS and SO show similar trends and values, even if slightly higher yields were registered with CS. SW char yields were sensitively lower at higher temperatures but this trend was reversed when temperatures were lower than 300-350 °C (i.e. a higher yield was registered).

Oil yields appeared to be similar up to 350 °C, then differences between the biomass samples became more and more apparent. The highest yields were registered with SW, while the lowest ones were associated to CS.

At the steady state it was possible to observe that:

- Char yields: CS (>) = SO > SW
- Oil yields: SW > SO > CS
- Char and Oil yields: SW > SO > CS

Not much attention was paid to the yields in light products, whose trends are strongly dependent on the trend in char and oil yields (and to the experimental errors included in their determination). Nevertheless, as a general rule larger amount of light products appeared associated to CS than SO and SW.

Average yields registered at 350, 500 and 650 °C are also shown in table 5.2. The ratio between standard deviation and average yield, i.e. the coefficient of variation, and the number of runs used in the determination of the statistical parameters are reported in round brackets. Char yields resulted to be quite reliable while pyro-oil yields resulted to be affected by a higher level of uncertainty.

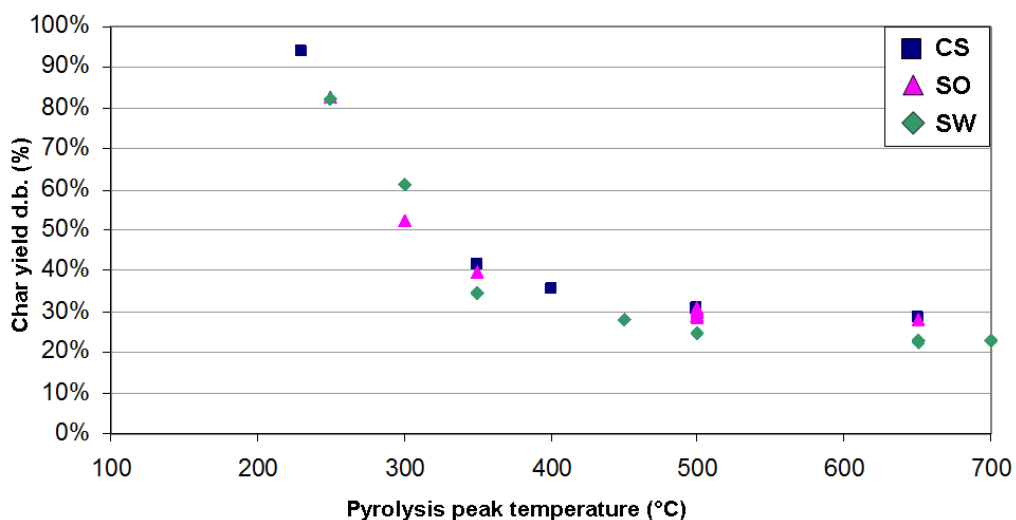


Fig. 5.4 – Char yields (d.b.) registered with the GKR

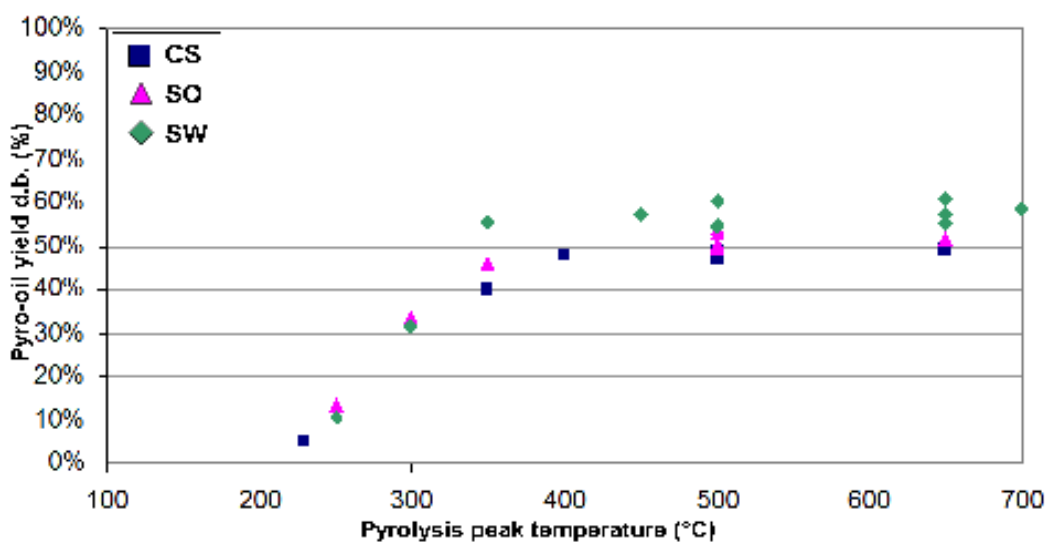


Fig. 5.5 – Pyro-oil yields (d.b.) registered with the GKR

Tab. 5.2 – GKR average yields (d.b.) registered at 350, 500 and 650 °C. In round brackets: coefficient of variation, and number of runs considered

Product	Temperature	CS	SO	SW
Char	350 °C	41.5%	39.7%	34.5%
	500 °C	30.5%	29.8%	24.7%
	650 °C	28.5%	27.8%	22.6%
		(0.7%, 3 runs)	(2.5%, 8 runs)	(0.7%, 3 runs)
Pyro-oil	350 °C	40.1%	46.2%	55.2%
	500 °C	48.2%	52.4%	56.5%
	650 °C	49.4%	51.9%	57.7%
		(2.4%, 3 runs)	(3.4 %, 7 runs)	(6.1%, 3 runs)
				(1.3%, 3 runs)
				(5.0%, 3 runs)

Pyrolysis yields registered at 650 °C can be also compared with the corresponding ones obtained with the TR, as table 5.3 reports.

Tab. 5.3 – Pyrolysis yields (d.b.) registered at 650 °C with GKR and with TR

Product	Biomass	GKR	TR
Char	CS	28.5%	28.7%
	PO	-	26.7%
	SO	27.8%	26.7%
	SW	22.6%	22.8%
Pyro-oil	CS	49.4%	31.6%
	PO	-	33.4%
	SO	51.9%	33.4%
	SW	57.7%	37.1%

Char yields resulted to match strongly between the two sets of runs, while differences in pyro-oil yields were registered, even if the biomass hierarchy was qualitatively confirmed. Mainly due to the different cooling system, a significantly larger amount of pyro-oil was indeed produced in the GKR system (liquid nitrogen cooled), up to 55% more than in the TR (ice-water-salt cooled). It is apparent that this gap is a rough but useful indicator of the range in pyro-oil yields which may be achieved depending on the temperature of the condensation system.

5.2.4 Conclusions

The analysis of the pyrolysis yields showed that some biomass species can be more functional than others to specific applications (e.g. char combustion, bio-slurry combustion or gasification, bio-refining of the pyro-oil). Asymptotic trends moreover suggest that, without considering any additional element, higher temperatures may be not strictly necessary in the char and oil production from slow pyrolysis. Nevertheless, the interpretation of the yields should be coupled also with the results coming from the analysis of the pyrolysis products.

The key importance of the piece of information collected will be more apparent in the next chapters of the thesis, when the economic and environmental assessment of bio-energy supply chains based on the biomass species investigated will be addressed.

5.3 Thermo-gravimetric analysis of the char samples

5.3.1 Introduction

A significant difference in pyrolysis yields resulted from the runs carried out in the experimental reactors as a consequence of the feedstock used. It is apparent that different biomass composition can strongly affect the pyrolysis process in reference to both the yields in char and pyro-oil and the quality of the products obtained, which may create possible limitations to their energy use.

Compositions of original feedstock and solid products of pyrolysis obtained at different peak temperatures were characterised in terms of proximate analysis, i.e. expressing the content as volatile fraction (VF), fixed carbon (FC) and ashes (A). Outcomes of the analysis were coupled with the yields obtained from the experimental activity EA1 and compared with benchmark compositions for the char in order to address the investigated operative parameters of the pyrolysis process (i.e. pyrolysis temperature and biomass feedstock) to an industrial interest. Even if other properties should be examined, proximate analysis outputs can be considered indeed useful indicators for a preliminary screening of the char quality. According to [Antal and Grønli, 2003], for example, volatile fraction in char should be lower than 20-30% in domestic cooking and 10-15% in metallurgic use, with an ash content possibly not higher than 0.5-5%. A good commercial char, moreover, should present also a fixed carbon content higher than 75% [FAO, 1987].

5.3.2 Materials and methods

Feedstock

Samples of CS, SO and SW were analysed with thermogravimetric analysis (TGA). Char produced from the pyrolysis of these samples in the GKR at 350, 500 and 650 °C were also analysed.

Analytical Technique – TGA

Thermo-Gravimetric Analysis (TGA) was applied to 2-3 mg of solid samples (i.e. biomass and char) in order to study their composition in terms of volatile fraction, fixed carbon and ashes (i.e. to obtain their proximate analysis). The instrument used was a Perkin–Elmer Thermogravimetric Analyser Pyris 1 TGA and the thermal program was composed by a ramp (10 °C/min) from 105 °C to 800 °C in an inert atmosphere (nitrogen) followed by an isothermal period at 800 °C in reactive environment (air). The weight loss registered during the initial ramp and combustion at 800 °C were respectively considered corresponding to volatile fraction and fixed carbon. The residual material was instead considered as ash content of the sample. A typical thermal curve obtained during the analysis is shown in figure 5.6.

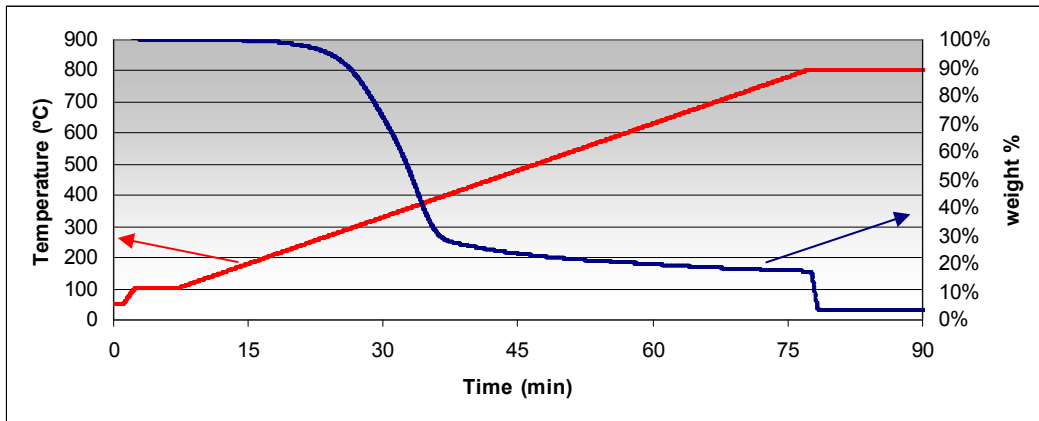


Fig. 5.6 – Example of TGA thermal curve obtained during the study

5.3.3 Results and discussion

The thermal decomposition history of the three raw biomass samples is represented in figure 5.7 and figure 5.8, respectively in terms of dry weight and time-derivative weight loss. Curves are reported as a function of time. Temperatures applied over time are also shown in the graphs.

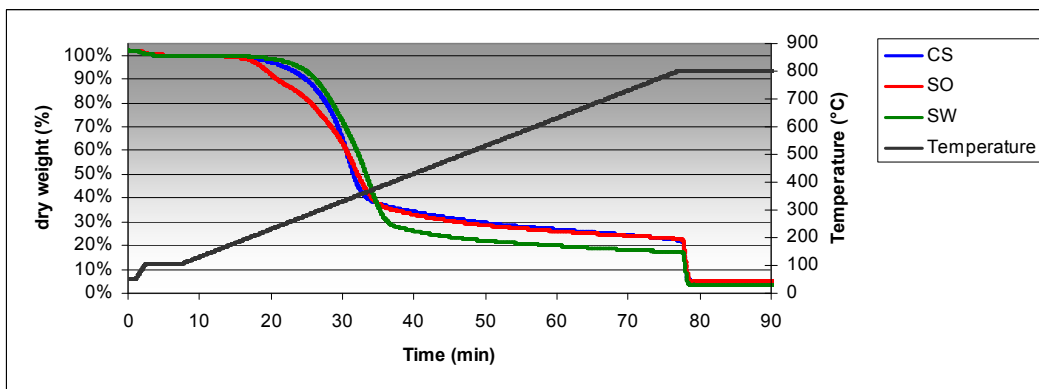


Fig. 5.7 - Weight loss curves (d.b.) for the three raw biomass samples investigated

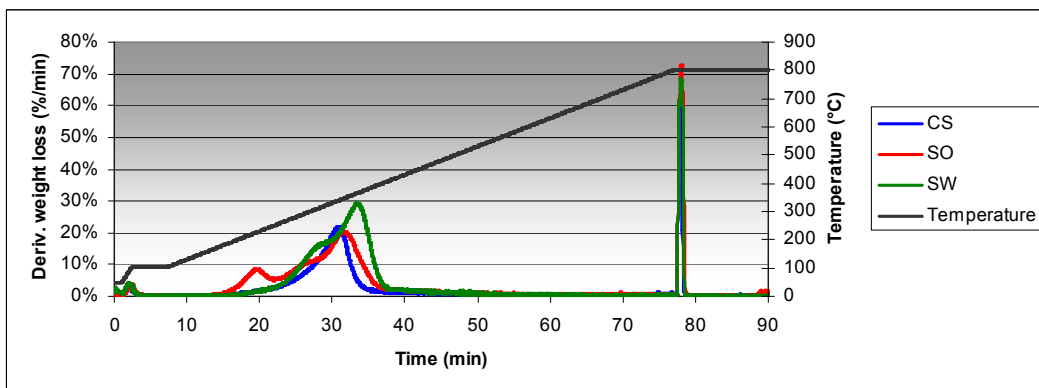


Fig. 5.8 – Time derivative weight loss curves (d.b.) for the three raw biomass samples investigated

From the comparison of the previous figures it is apparent that SW presents a stronger attitude to thermal decomposition, even if this is true only for temperatures higher than 350 °C. CS and SO thermal decomposition histories are similar, and coincident

for temperature higher than 350 °C. These outcomes are strongly consistent with the results obtained with the GKR.

Time-derivative weight loss curves moreover shows significant compositional differences between the three samples, probably due to a different content in macro constituents (i.e. hemicellulose, cellulose, lignin and extractives) and maybe influenced also by a different content in salts and minerals [Gomez Diaz, 2003].

The proximate analysis of the raw biomass samples was also obtained from the thermal decomposition data. Results are reported in table 5.4 on a dry basis. In comparison with CS and SO, whose composition is apparently similar, SW appears to be composed by a larger amount of volatiles, suggesting a larger presence of cellulose. This supports the higher pyro-oil yields registered during the SW experimental pyrolysis.

Proximate analysis was obtained also for chars produced from biomass pyrolysis at 350, 500 and 650 °C. The results are presented in table 5.4 on a dry basis. VF, FC, A and char yields were also plotted against temperature on figure 5.9 and on figure 5.10 for the sake of comparison.

Tab. 5.4 – Proximate analysis of the samples analysed with the TGA

Sample	VF	FC	A
Raw CS	77.7%	17.0%	5.3%
Char from CS at 350 °C	37.7%	50.4%	11.9%
Char from CS at 500 °C	26.5%	58.3%	15.2%
Char from CS at 650 °C	22.3%	60.5%	17.2%
Raw SO	77.1%	18.0%	4.9%
Char from SO at 350 °C	35.2%	54.7%	10.1%
Char from SO at 500 °C	22.2%	63.4%	14.5%
Char from SO at 650 °C	16.3%	68.1%	15.7%
Raw SW	82.6%	13.9%	3.5%
Char from SW at 350 °C	36.7%	56.3%	7.0%
Char from SW at 500 °C	18.8%	70.1%	11.2%
Char from SW at 650 °C	13.7%	73.2%	13.1%

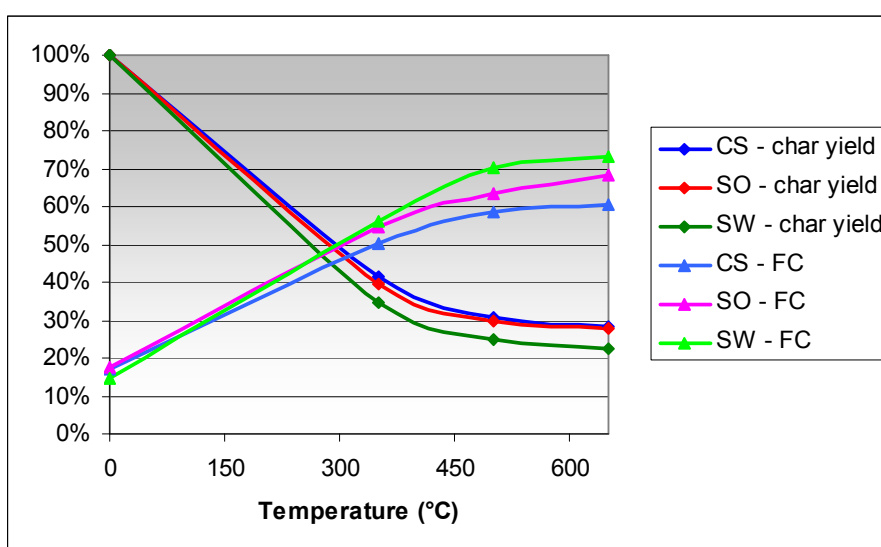


Fig. 5.9 – Yields and FC content over pyrolysis peak temperature for char samples obtained from CS, SO and SW

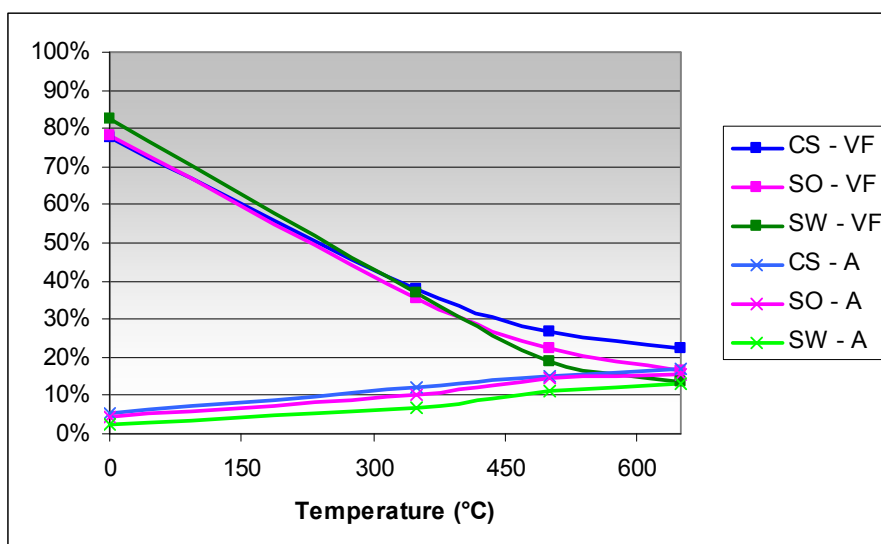


Fig. 5.10 – VF and A content over pyrolysis peak temperature for char samples obtained from CS, SO and SW samples

A partial look to the char yields would recommend the application of lower pyrolysis temperatures in order to produce more char. Nevertheless, the benchmark values reported in the introduction to the paragraph suggest that higher temperatures lead to an improvement of the char quality. FC is indeed the parameter to maximize for energy production.

Char composition seems to stabilise at temperature higher than 500 °C and a significant content of volatile material and ashes is observable in the char analysed.

According to [Antal and Grønli, 2003] and [FAO, 1987] good quality char seems to be produced only from SW at 650 °C, while all the chars produced at 500 650 °C present a VF content lower than 30 %, that is the benchmark for domestic cooking.

5.3.4 Conclusions

Biomass contain a large amount of volatiles and SW resulted to be the sample with the larger content in volatiles, which explains the higher oil yields registered during the experimental pyrolysis runs. CS and SO showed a similar thermal composition and these results are consistent with the pyrolysis yields obtained with GKR.

Low pyrolysis peak temperatures yielded larger amount of char but char quality is improved at higher temperature, when the volatile fraction decreases and the fixed carbon increases, as well as the ash content. A stabilisation in char composition is reached at 500 °C but a good commercial char seems to produced at higher temperatures. Much attention should be however paid to the ash content, since ash content increases as the pyrolysis temperature increases.

From the results exposed, 650 °C was selected as reference temperature for the pyrolysis process and the pyrolysis yields obtained with the TR were considered as key parameters in the modelling performed preliminarily to the environmental and economic assessment of the bio-energy supply chains.

5.4 Study of the pyro-oil stability

5.4.1 Introduction

Pyro-oils are complex mixtures composed by a wide set of molecules derived from depolymerisation and fragmentation reactions of the three main macro-components of the biomass: cellulose, hemicellulose, and lignin [Oasmaa and Czernik, 1999]. Biomass pyrolysis oils, also known as bio-oils or tars, presents quite different physical properties and chemical composition than conventional fossil fuels [Diebold and Czernik, 1997; Oasmaa and Czernik, 1999].

Water is the most abundant single component contained in the bio-oils and it results from the original moisture of the biomass feedstock and from the water generated as a pyrolysis by-product [Oasmaa and Czernik, 1999]. A large amount of oxygenated compounds are also contained in oils derived from biomass [Oasmaa and Czernik, 1999] and distributed in more than 200 compounds [Diebold, 2000], depending on the biomass feedstock processed and on the operative conditions of the pyrolysis process (e.g. reactor configuration, peak temperature, residence time, heating rate profiles). Several classes of oxygenated compounds have been identified in pyro-oils, including alcohols, aldehydes and hydroxyaldehydes, carboxylic acids, esters and ethers, furans, guaiacols, ketones and hydroxyketones, phenols, sugars, syringols and terpenes [Diebold and Czernik, 1997; Oasmaa and Czernik, 1999, Qi et al., 2007]. A list with some of the main compounds detected in pyro-oils is given in table 5.5.

Tab. 5.5 – Main compounds identified in pyro-oils [Diebold, 2000]

Acids	Acetic Formic Hydroxyacetic Propanoic	Guaiacols	Eugenol Isoeugenol Methoxy phenol Methyl guaiacol
Alcohols	Ethanol Ethylene glycol Methanol	Ketons	Acetone Butanone
Aldehydes	Acetaldehyde Acrolein Ethanedial Formaldehyde	Oxygenates (others)	Hydroxyacetaldehyde Hydroxyacetone Methyl cyclopentenolone 4-OH-3-methoxybenzaldehyde
Esthers	Angelicalactone Butyrolactone Methyl formate	Phenol	Ethyl phenol DiOH benzene Dimethyl phenol Methyl phenol Phenol
Furans	Furanone Furfural Furfural alcohol 5-OH-methyl-2-furfural	Syringols	DiOMe phenol Propyl syringol Syringaldehyde

Most of the phenolic compounds are oligomers with a molecular weight ranging from 900 to 2500 g/mol [Oasmaa and Czernik, 1999] and which present ketones and aldehydes groups attached [Qi et al., 2007]. The abundant content in aldehydes and ketones makes bio-oils highly hydrophilic and hydrated, which leads to the water being difficult to be eliminated. At concentrations up to 30 wt%, water is usually miscible with the other components of pyro-oil because of the presence of polar carboxyl and hydroxyl compounds [Oasmaa and Czernik, 1999]. Pyro-oil usually

looks as a continuous phase in which an aqueous solution stabilises a discontinuous phase of pyrolytic lignin macro molecules [Bridgewater, 1999].

Pyrolysis liquids are not stable like conventional petroleum fuels due to their high amount of reactive oxygen-containing compounds and low-boiling volatiles [Oasmaa et al., 2004]. During storage liquids tend to polymerise and to lose volatile material, which can be observed as an increase in: average molecular-weight distribution; water content and viscosity [Boucher et al., 2000; Diebold and Czernik, 1997; Fahmi et al., 2008; Oasmaa et al., 1997; Oasmaa and Kuoppala, 2003; Oasmaa et al., 2004]. Normally, viscosity of the bio-oil decreases with its water content, however, the observed water release during ageing is rather small and its effect is overcompensated by the increase in average molecular weight of the oil. Thus, the rate of viscosity increase, directly related to the average molecular weight, was used as a measure of the ageing rate. The growth of molecular weight is also observed as an increase in the amount of water-insoluble fraction, originally composed of lignin-derived material [Oasmaa and Czernik, 1999, Oasmaa and Kuoppala, 2003]. Changes in co-solubilities and phase separation can also occur during time [Oasmaa and Kuoppala, 2003; Oasmaa et al., 2004].

The process previously described is called ageing, and makes handling, transport, storage and use of the liquid difficult [Oasmaa et al., 1997].

The main physical and chemical changes of pyrolysis liquids due to ageing occurs during the first six months of storage [Oasmaa et al., 2004]. The physical changes includes also an increase in density, flash point and pour point, while the heating value slightly decreases [Oasmaa and Kuoppala, 2003].

The reason for oil instability begins within the pyrolysis reactor during pyrolysis. The biomass is rapidly heated in the absence of oxygen producing unstable free radical volatiles and then quickly condensed to form the oil. The products formed do not reach thermodynamic equilibrium and react with each other until product stability is reached [Fahmi2008].

Main important reactions that occur within bio-oil probably involve [Diebold, 2000]:

1. formation of esters from organic acids reacting with alcohols;
2. formation of esters from organic acids reacting with olefins;
3. formation of hydrates from aldehydes and water;
4. formation of hemiacetals, acetals and water from aldehydes and alcohols;
5. formation of oligomers and resins from aldehydes;
6. formation of resins and water from aldehydes and phenolic compounds;
7. formation of oligomers from aldehydes and proteins;
8. formation of oligomers from organic sulphur;
9. formation of polyolefins from unsaturated compounds;
10. Air oxidation with formation of more acids and reactive peroxides that catalyze the polymerization of unsaturated compounds.

Reactions 1 through 4 can form products in thermodynamic equilibrium with the reactants, which means that a change in temperature or relative amounts of water and other reactive compounds will upset the equilibrium and initiate compositional changes. Reactions 5 through 10 can form resins or polyolefins and may be irreversible under likely bio-oil storage conditions [Diebold, 2000].

Water is formed mainly due to polymerization and condensation reactions [Das et al., 2004; Oasmaa et al., 2004], responsible also for the increase in average molecular mass and viscosity of the liquid [Oasmaa et al., 2004]. Aldehydes seem to be the most unstable fraction contained in bio-oils [Diebold, 2000].

Ageing depends on the bio-oil composition, which is affected by feedstock and pyrolysis conditions [Oasmaa and Kuoppala, 2003], but the storage temperature is the most important control parameter since it affects exponentially the rates of chemical reactions occurring during storage. Ageing is much faster at increased temperatures [Chaala et al., 2004, Garcia-Perez et al., 2002; Oasmaa and Czernik, 1999, Yu et al., 2007], while it is strongly repressed at lower temperatures [Oasmaa et al., 1997]. The extent to which the properties of the pyrolysis bio-oils will change at different temperatures over a certain period of time is very important also for fuel applications [Boucher et al., 2000]. Experiments at high temperatures (e.g. 90 °C) were used to perform accelerated ageing tests, i.e. reducing the amount of time required for the study of the oil stability, and to analyse the effects of preheating on bio-oil for combustion applications [Diebold and Czernik, 1997, Oasmaa and Czernik, 1999].

The organic acids contained in the bio-oils and the presence of residual char particles can act as catalysts for many ageing reactions [Boucher et al. 2000; Das et al., 2004; Diebold and Czernik, 1997].

Ageing reactions change the properties of bio-oils and also their polarity, leading to phase separation as a final consequence [Diebold, 2000]. This phase separation will occur into a light, highly polar aqueous phase and a less polar heavier organic phase. The pyrolytic aqueous phase was found to increase bio-oil rate of ageing and to decrease consequently its stability [Boucher et al., 2000].

Polymerization and polycondensation reactions are favoured by the acidity of the medium [Boucher et al., 2000], while ageing should not be much influenced by the presence of stainless steel and copper containers and of a small amount of air in the headspace above bio-oils of a nearly full, closed container [Oasmaa et al., 1997; Oasmaa and Czernik, 1999].

Pyrolysis oil quality may be modified with a change in process variables such as reactor configuration, heating rate, pyrolysis temperature and residence times [Fahmi et al., 2008]. Several methods of bio-oil upgrading have been proposed [Oasmaa and Czernik, 1999; Qi et al., 2007], including:

- Catalytic cracking of pyrolysis vapors
- Hot-Vapor Filtration
- Steam reforming
- Hydrodeoxygenation
- Emulsification
- Solvent addition.

In particular, solvent addition is a relatively simple method to improve some of the undesired bio-oil characteristics with only minor added costs [Oasmaa and Czernik, 1999]. Polar solvents can be added to improve the homogeneity and to decrease the viscosity and the ageing rate during equipment clean-up, storage and atomization prior to combustion [Diebold and Czernik, 1997; Oasmaa and Czernik, 1999; Oasmaa et al., 1997; Oasmaa et al., 2004; Stamatov et al., 2006]. Quantitative data are reported on the effects of many solvents, such as water, ethanol, methanol, and furfural [Diebold and Czernik, 1997; Doshi et al., 2005; Oasmaa and Czernik, 1999; Yu et al., 2007]. Industrial experience on the upgrading of biomass pyrolysis liquids for use as fuels and as a source of chemicals by reaction with alcohols are known since 1995 [European Patent Office, 2006].

The addition of solvents, especially methanol [Diebold and Czernik, 1997; Oasmaa and Czernik, 1999; Oasmaa et al., 2004], showed a significant effect on the oil stabilization.

From a chemical kinetic perspective, the ageing rate is slowed because the reactants are more dilute (unless the reactions that caused the ageing are effectively zero-order reactions) but the effect of the solvents is greater than would be expected from a physical dilution [Diebold and Czernik, 1997]. The reduction in the viscosity change seems to be primarily due to a stabilizing effect of alcohols on the water insoluble high molecular mass lignin-derived fraction [Oasmaa et al., 2004]. Hemiacetal, acetal, and ester linkages could be important actors in the ageing process of bio-oils. Because they react toward thermodynamic equilibrium, adding a low molecular weight alcohol to a mixture of high molecular weight hemiacetals, acetals, and esters would shift the equilibrium composition to a mixture with a lower molecular weight and viscosity [Diebold, 2000]. This could stabilize bio-oil through four mechanisms: (1) reducing the concentration of reactive aldehydes, by converting more of them to less reactive, relatively low to moderate molecular-weight hemiacetals and acetals; (2) transacetalizing large hemiacetals and acetals to form lower molecular weight hemiacetals and acetals; (3) converting organic acids to low molecular weight esters; and (4) transesterifying large esters to form lower molecular weight esters. The second and fourth mechanisms could be considered like a depolymerisation of the original high molecular weight oligomers of hemiacetals, acetals, and esters [Diebold, 2000]. Alcohols react irreversibly with the reactive sites of the oligomers repressing the ageing process. [Diebold and Czernik, 1997].

Water can also act as a molecular diluent to slow down second-order and higher order reactions. Although the equilibrium formation of esters is favoured thermodynamically, the reaction rates are relatively slow in the absence of catalysts [Diebold and Czernik, 1997].

Adding solvents shortly after producing bio-oil was found to be more effective than adding the same amount of solvent to an oil previously aged. Some ageing reactions indeed are apparently not in thermodynamic equilibrium and they cannot be reversed by adding low molecular weight reactants [Diebold and Czernik 1997; Oasmaa and Czernik, 1999].

In addition to the decrease in viscosity and in the ageing rate, alcohols also lead to other desirable changes such as reduced acidity, improved volatility and heating value, and better miscibility with diesel fuels [Oasmaa and Czernik, 1999].

Considering the simplicity, the low cost of some solvents, especially methanol [Diebold and Czernik, 1997], and their beneficial effects on the bio-oil properties, this method is considered one of the most practical approaches for the bio-oil upgrading [Oasmaa et al., 2004]. The cost of adding a solvent to the bio-oil can be at least partially compensated by the increase in energy content of the mixture [Diebold and Czernik 1997].

Pyrolysis oil quality is dependent on the desired application; however, oil stability is the limiting factor for any application [Fahmi et al. 2008]. Ageing studies up to now mainly focused on bio-oils produced from fast pyrolysis of a wide range of biomass feedstock in experimental, industrial and pilot scale fluidised bed reactors [Diebold, 2000; Oasmaa and Czernik, 1999]. Less studies are present in literature concerning with the analysis of the ageing of bio-oils from slow pyrolysis [Boucher et al., 2000; Das et al., 2004; Garcia-Perez et al., 2002; Stamatov et al., 2006; Yu et al., 2007].

Great attention was paid on the temporal trend of molecular weights, viscosity, water content [Diebold, 2000; Oasmaa and Czernik, 1999], and, with a lower extent, on chemical composition, analysed through GC/GC-MS and FT-IR [Doshi et al., 2005; Fahmi et al., 2008]. Effects on bio-oil stability due to operative parameters such as

storage temperature and solvent addition were much investigated in literature [Diebold, 2000; Oasmaa and Czernik, 1999].

The aim of the present activity was thus to analyse the reactivity of different liquid samples produced from slow pyrolysis of biomass. Reactivity was studied in terms of structural changes during time and several analytical techniques were tested in order to screen their applicability to the study: gel permeation chromatography (GPC); ultra violet fluorescence (UVF); infrared (IR).

The effects due to several operative conditions on the bio-oil stability were investigated (e.g. pyrolysis temperature, storage temperature, solvent addition, biomass feedstock) in order to screen the parameters which can positively affect the production and storage of the oil.

5.4.2 Materials and methods

Production of the bio-oil samples and method of analysis

Bio-oil samples from slow pyrolysis of CS, SO and SW were produced in the GKR. Bio-oil collection was complicated by the presence of the liquid in the U-tube, in the filter and in the retort. A fast and simple procedure was defined in order to collect reliable samples and minimise the influence of the solvent in the further stability study. The liquid product was firstly extracted with a Pasteur pipette from the bottom of the U-tube (see the dashed line drawn on figure GKR inside the tar trap) and collected as pure phase. This single aqueous phase accounted for about the 50% of the total liquid yield and it was labelled as “first oil”.

Some of the material was still sticking on the wall of the U-tube after the first collection and it was collected after the injection of a certain amount of solvent (usually 1 mL of methanol) and 10 minutes in ultrasound bath. This liquid was labelled as “second oil” and it accounted, at the net of the solvent added, for about the 20% of the total liquid yield. The collection of “second oil” with chloroform was also explored. Some samples of “second oil” were dried with nitrogen flow until the weight of the solution was equivalent to the free-solvent liquid weight.

Samples of oil from filter and reactor were also collected with methanol. Nevertheless, it was not possible to obtain a complete collection of the fractions and to know accurately the amount of methanol contained in the oil-methanol solution.

“First oil” produced from 500 °C slow pyrolysis of SO and stored at ambient temperature was considered as a reference case for the stability study. Several liquid samples were obtained from “first oils” as pure phase, or mixed with solvent (i.e. methanol and acetone) or with “second oils” in order to investigate the effects due to:

- different solvent concentrations;
- different pyrolysis peak temperature (350; 500 and 650 °C);
- different storage temperature (5 and 20 °C);
- different feedstock (CS, PO, SW).

Ageing of oil samples was analysed with GPC, UV-F and FT-IR techniques; an overview of the samples analysed in the study is shown in table 5.6. As a general rule, samples were filtered and all sheltered from light.

Standard practice was to repeat the GPC and UV-F runs in the first day of production, as soon as possible (i.e. day 0), and then after 2 days, 1 week, 2 weeks, 1 month. Additional runs were repeated if needed. FT-IR runs were instead programmed for some liquid samples produced from the pyrolysis of SO at 500 °C.

Tab. 5.6 – List of experimental cases analysed during the ageing study

Feedstock	Pyrolysis temp. (°C)	Sample	Solvent (% conc.)	Fridge Storage (5 °C)
CS	500	First oil	-	-
CS	500	Fraction of first oil	Methanol (10%)	-
CS	500	Fraction of first oil	Methanol (25%)	-
CS	500	Fraction of first oil	Acetone (25%)	-
CS	500	Second oil	Methanol (85%)	-
SO	500	First oil	-	Y
SO	500	Fraction of first oil	-	-
SO	500	First oil and second oil	Methanol (10%)	-
SO	500	Fraction of first oil	Methanol (10%)	-
SO	500	First oil and second oil	Methanol (25%)	Y
SO	500	Fraction of first oil	Methanol (25%)	-
SO	500	First oil and second oil	Methanol (50%)	Y
SO	500	Second oil, methanol dried	Negligible	-
SO	500	First and second oil, methanol dried	Negligible	-
SO	500	First and second oil, chloroform dried	Negligible	-
SO	500	Oil from filter and retort dissolved in methanol	Methanol (> 50%)	-
SO	500	Fraction of first oil	Acetone (10%)	-
SO	500	Fraction of first oil	Acetone (25%)	-
SO	350	First oil	-	Y
SO	650	First oil	-	Y
SW	500	Fraction of first oil	-	-
SW	500	Fraction of first oil	Methanol (10%)	-
SW	500	Fraction of first oil	Methanol (25%)	-
SW	500	Fraction of first oil	Acetone (10%)	-
SW	500	Fraction of first oil	Acetone (25%)	-
SW	500	Second oil, methanol dried	Negligible	-

Gel Permeation Chromatography (GPC)

Gel permeation chromatography is a separation technique which separates molecules in solution based on their size or, more correctly, their hydrodynamic volume. It is usually applied to large molecules or macromolecular complexes in order to determine their molecular weight distributions.

GPC is conducted in packed columns filled by porous material. The principle of this technique is showed in figure 5.11. Samples to be analysed are dissolved in an organic solvent and injected into the column after filtration. When an aqueous solution is used to transport the analytes, the technique is known as gel filtration chromatography, while size exclusion chromatography is the general name which refers to these two techniques [Lathe and Ruthven, 1956; Mc Naught and Wilkinson, 1997; Moore, 1964].

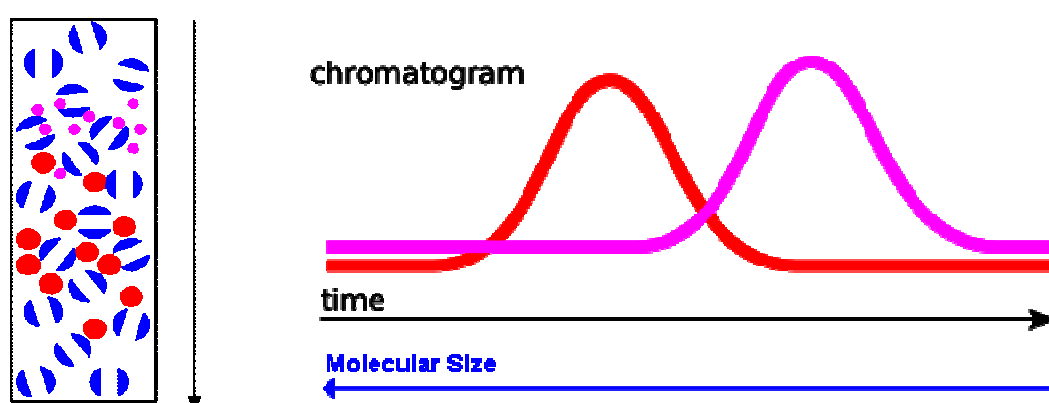


Fig. 5.11 – Principle of the GPC technique

The separation of the components of the mixture takes place into the column. The smaller the analytes entering into the column are, the longer the time spent in the pores of the column is, and thus the retention time. On the contrary, larger analytes spend less time in the pores and are eluted more quickly. There is a limited range of molecular weights that can be separated by a column based on the pore size of the packing material since molecules which are too large or too small can be completely retained or not retained at all from the column.

Gels are used as stationary phase for GPC. The pore size of a gel must be carefully controlled in order to be able to apply the gel to a given separation. Other desirable properties of the gel forming agent are the absence of ionizing groups and, in a given solvent, low affinity for the substances to be separated.

The constant supply of fresh eluent to the column is accomplished by the use of a pump; the eluent (mobile phase) should be a good solvent, should permit high detector response and should wet the packing surface.

Since analytes are usually not visible to the naked eye, a detector is needed. The UV absorption detector is one of the detectors most commonly used. The detector allows the indirect monitoring of the concentration of the analytes eluting with the solvent. The resulting chromatogram is therefore a weight distribution of the polymer as a function of the retention volume [Trathnigg, 1995].

GPC was carried out using a 30 cm long (7.5 mm o.d.) PL-gel Mixed-D column, packed with 5 μm polystyrene–polydivinylbenzene polymer particles. The column, supplied by Polymer Laboratories Ltd (UK), operated at 80 °C. The eluent, 1-methyl-2-pyrrolidinone (NMP), was pumped at a flow rate of 0.5 ml/min with a Knauer

Smartline Pump 100. Detection was carried out using a Knauer Smartline UV detector. Detection of compounds was performed at 270, 300, 350 and 370 nm, where NMP is partially transparent. The chromatograms corresponding to a 270 nm detection wavelength were analysed in the study.

GPC samples were prepared by dissolving one drop of sample in 6 mL of NMP. Samples resulted to be completely soluble in the solvent used. The samples were mixed and filtered prior to the injection in the system (a 30 μ L volume). The resulting chromatograms have been area normalised for ease of interpretation.

Ultraviolet fluorescence (UVF)

Ultraviolet fluorescence spectroscopy is a type of electromagnetic spectroscopy which analyzes fluorescence from a sample. It involves a beam of ultraviolet light, which excites the electrons in the sample molecules leading to the emission of light with different wavelength [Gauglitz and Vo-Dinh, 2003, Lakowicz, 1999; Rendell, 1987; Sharma and Schulman, 1999]

Molecules have various states referred to as energy levels. Fluorescence spectroscopy is primarily concerned with electronic and vibrational states. Generally, the species being examined will have a ground electronic state (a low energy state) of interest, and an excited electronic state of higher energy. Within each of these electronic states are various vibrational states. In fluorescence spectroscopy, the species is first excited, by absorbing a photon, from its ground electronic state to one of the various vibrational states in the excited electronic state. Collisions with other molecules cause the excited molecule to lose vibrational energy until it reaches the lowest vibrational state of the excited electronic state. The molecule then drops down to one of the various vibrational levels of the ground electronic state again, emitting a photon in the process. As molecules may drop down into any of several vibrational levels in the ground state, the emitted photons will have different energies, and thus frequencies. Therefore, by analysing the different wavelengths of light emitted in fluorescent spectroscopy, along with their relative intensities, the structure of the different vibrational levels can be determined.

A schematic representation of a UVF spectrometer is given on figure 5.12.

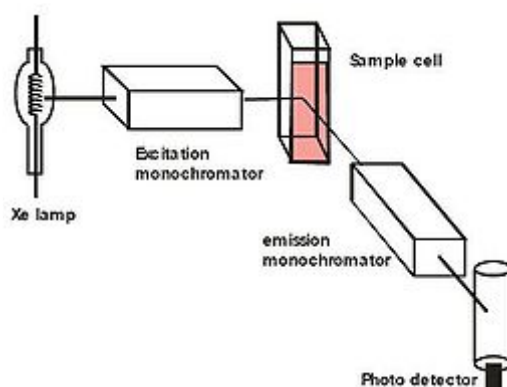


Fig. 5.12 – Schematic configuration of a UVF spectrometer

A light from an excitation source passes through a filter or monochromator, and strikes the sample. The incident light is absorbed by the sample, and some of the molecules in the sample fluoresce. The fluorescent light is emitted in all directions. Some of this fluorescent light passes through a second filter or monochromator and

reaches a detector, which is usually placed at 90° to the incident light beam to minimize the risk of transmitted or reflected incident light reaching the detector. Various light sources may be used as excitation sources, including lasers, photodiodes, and lamps; xenon arcs and mercury-vapor lamps.

As mentioned before, the fluorescence is most often measured at a 90° angle relative to the excitation light in order to avoid interference of the transmitted excitation light.

Three kinds of spectra can be registered with a spectrometer depending on the operative conditions of the instrument:

- Emission spectra, measured keeping the wavelength of the excitation light constant, preferably at a wavelength of high absorption, while the emission monochromator scans the spectrum.
- Excitation spectra, registered keeping the wavelength which passes through the emission filter, or monochromator, constant while the excitation monochromator is scanning. The excitation spectrum generally is identical to the absorption spectrum as the fluorescence intensity is proportional to the absorption.
- Synchronous spectra, obtained keeping the wavelength which passes through the emission filter, or monochromator, at wavelength constantly higher than the excitation wavelength, which is scanned for all the spectrum

In particular, synchronous spectra were registered and analysed since they allow for the identification of the presence and interaction level of poly-condensed aromatic rings [Begon et al., 1998; Begon et al., 2000; Benkhedda and Landais, 1992; Li et al., 1994; Pindoria et al., 1997], as shown in figure 5.13.

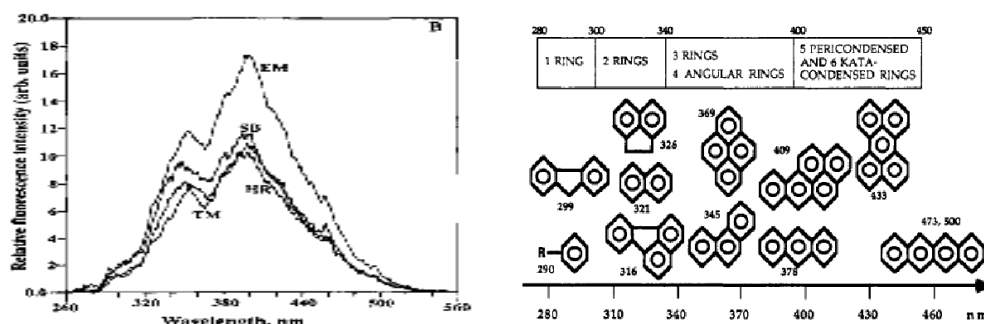


Fig. 5.13 – Typical UVF synchronous spectra and relation between the wavelengths detected and the interaction level of poly-condensed aromatic rings [Benkhedda and Landais, 1992; Li et al., 1994]

At low concentrations the fluorescence intensity will generally be proportional to the concentration of the fluorophore, i.e. of the component of a molecule which causes a molecule to be fluorescent. Several factors can influence and distort the spectra and they are inherent to either instrument and sample analysed.

Correction of instrumental factors is applied in practice only when it is strictly necessary, e.g. in the determinations of quantum yields or when the accurate finding of the wavelength with the highest emission intensity is requested.

Typical distortions due to the sample include photodecomposition, which may decrease the intensity of fluorescence over time, and scattering of light. A further aspect to be considered is the inner filter effects. These include reabsorption, occurring when other molecules or part of a macromolecule absorbs at the wavelengths at which the fluorophore emits radiation. If this is the case, some or all of the photons emitted by the fluorophore may be absorbed again. Another inner filter effect occurs because of high concentrations of absorbing molecules, including the

fluorophore. The result is that the intensity of the excitation light is not constant throughout the solution. As a consequence, only a small percentage of the excitation light reaches the fluorophores that are visible for the detection system. The inner filter effects change the spectrum and intensity of the emitted light and they must therefore be considered when analysing the emission spectrum of fluorescent light. It is usually recommended to work with low concentrations of absorbing material.

Fluorescence spectroscopy is used in, among others, biochemical, medical, and chemical research fields for analyzing organic compounds.

The UV-fluorescence spectra were recorded on a Perkin Elmer LS55 Luminescence Spectrometer. The spectra were recorded from solutions of oil dissolved in 1-methyl-2-pyrrolidinone (NMP) in a quartz cell of 10 mm light pass-length. The data acquisition and the instrument control were carried out by a computer equipped with fluorescence data management software from Perkin Elmer.

Synchronous spectra were recorded with 20 nm difference between excitation and emission over wavelength range 254-800 nm. Standard practice was to increase oil concentration in the quartz cell until the maximum peak of intensity was included in the range 250-300 (arbitrary units). If self absorption occurred (e.g. after few weeks for the pure oil) spectra were registered at lower peak intensities. Spectra have been peak normalised for ease of interpretation. Excitation and emission spectra were also acquired at the peak concentration but not analysed.

Fourier Transform Infrared spectroscopy (FT-IR)

Infrared spectroscopy is the branch of spectroscopy that deals with the infrared region of the electromagnetic spectrum and it can be used to identify compounds or investigate sample composition [Polymer science learning center, 1996; Thermo Nicolet Corporation, 2001].

Infrared spectroscopy is based on the specific frequencies at which molecules rotate or vibrate. The resonant frequencies, corresponding to discrete energy levels (vibrational modes), are related to the strength of the chemical bonds and to the atoms of the chemical compounds. Simple diatomic molecules have only one bond, which may stretch. More complex molecules have many bonds, and vibrations can be conjugated, leading to infrared absorptions at characteristic frequencies that may be related to specific functional groups. A concise summary of absorption regions for organic molecules is given on figure 5.14.

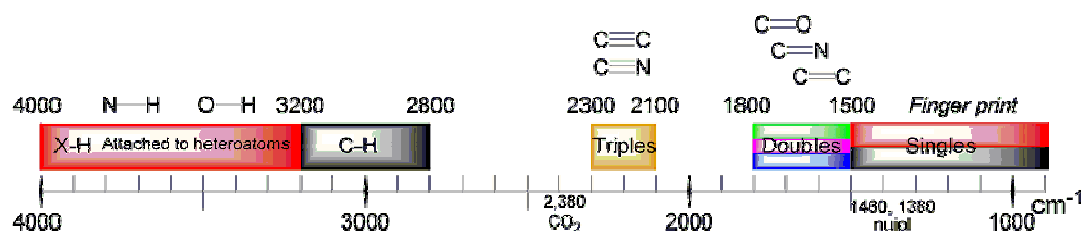


Fig. 5.14 – Summary of absorption regions for organic molecules

The infrared spectrum of a sample is collected by passing a beam of infrared light through a sample. Some of the radiation is absorbed by the sample and some of it is passed through (i.e. transmitted). The resulting spectrum represents the molecular absorption and transmission, creating a molecular fingerprint of the sample. Like a fingerprint, no different molecular structures can produce the same infrared spectrum. Spectra analysis can reveal details about the molecular structure of a compound.

Simple spectra are obtained from samples with few IR active bonds and high levels of purity; more complex molecular structures lead to more absorption bands and more complex spectra.

IR can be applied for the analysis of gaseous, liquid and solid samples. Gaseous samples require little preparation beyond purification, but a sample cell with a long pathlength (typically 5–10 cm) is normally needed, as gases show relatively weak absorbance. Liquid and solid compounds are usually analysed placing a sample film between two plates of a high purity salt (commonly sodium chloride, or common salt, although a number of other salts such as potassium bromide or calcium fluoride are also used), which are transparent to the infrared light.

A typical IR apparatus is shown on figure 5.15. A beam of infrared light is produced and an individual frequency of energy separated by mean of a prism or of a grating. Radiation is passed through the sample and through a reference, if necessary, and then reflected towards a detector which measures the amount of energy which was transmitted. A spectrum which is a plot of intensity vs. frequency results from the detection of the transmitted energy at different frequencies

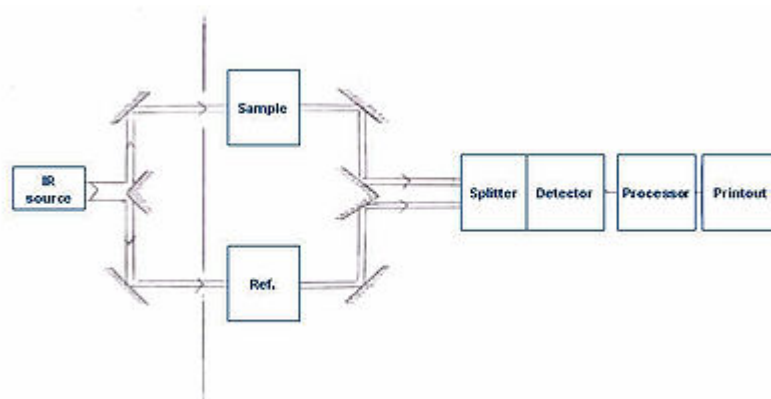


Fig. 5.15 - Typical apparatus used in IR spectrometry

Fourier Transform Infrared (FT-IR) spectrometry was developed in order to speed up the scanning process. The solution employs a very simple optical device called an interferometer. The interferometer produces a unique type of signal which has all of the infrared frequencies “encoded” into it. The signal can be measured very quickly, usually on a time of the order of one second or so. Thus, the time element per sample is reduced to a matter of a few seconds rather than several minutes.

Most interferometers employ a beamsplitter which takes the incoming infrared beam and divides it into two optical beams. One beam reflects off of a flat mirror which is fixed in place. The other beam reflects off of a flat mirror which is on a mechanism which allows this mirror to move a very short distance (typically a few millimeters) away from the beamsplitter. The two beams reflect off of their respective mirrors and are recombined when they meet back at the beamsplitter. Because the path that one beam travels is a fixed length and the other is constantly changing as its mirror moves, the signal which exits the interferometer is the result of these two beams “interfering” with each other. The resulting signal is called an interferogram which has the unique property that every data point (a function of the moving mirror position) which makes up the signal has information about every infrared frequency which comes from the source. This means that as the interferogram is measured, all frequencies are being measured simultaneously. Thus, the use of the interferometer results in extremely fast measurements.

The measured interferogram signal cannot be interpreted directly. A means of “decoding” the individual frequencies is required and this can be accomplished through the well-known Fourier transformation. The transformation is performed by a computer which then presents the user the desired spectral information for analysis. A schematization of the decoding process is shown on figure 5.16 with an example of resulting spectrum.

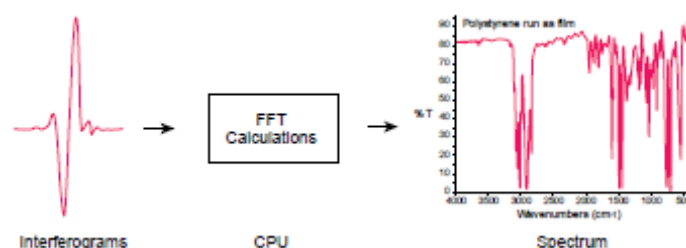


Fig. 5.16 – typical IR spectrum obtained after the FTIR decoding process

Because there is the need of a relative scale for the absorption intensity, a background spectrum must also be measured. This is normally a measurement with no sample in the beam. This can be compared to the measurement with the sample in the beam to determine the “percent transmittance”. This technique results in a spectrum which has all of the instrumental characteristics removed. Thus, all spectral features which are present are strictly due to the sample. A single background measurement can be used for many sample measurements because this spectrum is characteristic of the instrument itself.

Infrared spectra of oils were acquired using a Perkin-Elmer 1760X FT-IR spectrometer. Transmission spectra have been obtained in the range from 4000 to 600 cm^{-1} , scanned at 2 cm^{-1} intervals. Good quality spectra were obtained by co-adding 16 scans and the resultant spectra normalised to the background signal.

5.4.3 Results and discussion

Ageing results are presented in the present section in the following order:

- Pure oil ageing
- Effects due to methanol addition
- Effects due to acetone addition
- Effects due to the pyrolysis temperature
- Effects due to the storage temperature
- Effects due to the biomass feedstock
- Other marginal investigations.

Samples of pure oil produced from SO at 500 °C were initially analysed. The effects of methanol and acetone addition were then examined, as well as the effects of pyrolysis peak temperature and of storage temperature. Further analysis involved samples produced from SW and SO.

Pure oil ageing

GPC chromatograms and synchronous UVF spectra obtained over time with the first oil produced from the pyrolysis of SO at 500 °C and stored at ambient temperature are presented in figure 5.17 and in figure 5.18. It should be remembered that the first oil looked as a single aqueous phase and accounted for about the 50% of the overall liquid yield registered during the pyrolysis runs.

All the chromatograms showed two major peaks, the first near the exclusion limit of the column, corresponding to the largest MW materials contained in the sample, and the other one composed by two shoulders (at 21 and 22 min) corresponding to smaller MW materials 'retained' by the column. A sharp change in the first 5 days of storage was detected, then the signal appeared to be quite stable. The eluted peak intensity was observed to decrease while the excluded part of the chromatogram slightly increased. According to [Begon et al, 1998; Begon et al, 2000], these data may suggest the occurrence of recombination reactions into the oil sample with formation of larger molecules.

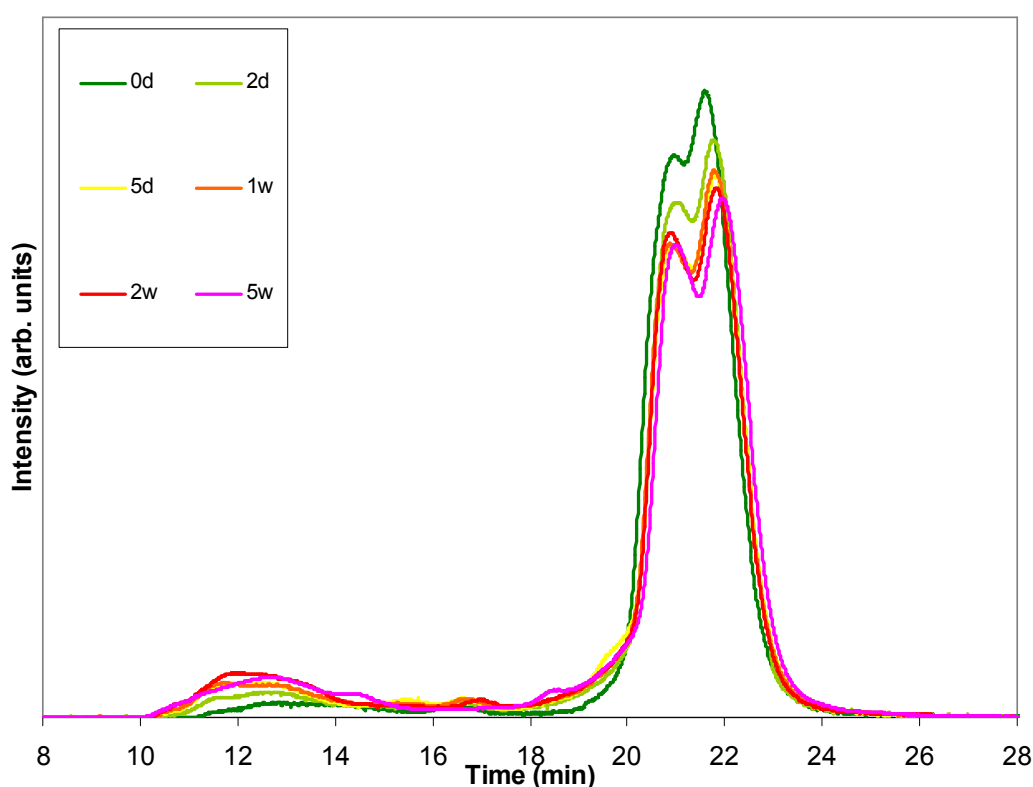


Fig. 5.17 – GPC chromatograms of first oil produced from pyrolysis of SO at 500 °C and stored at ambient temperature

Two peaks were observed in the first day of monitoring: the first one at 310 nm, the second one at 360 nm. Apparent changes in spectra shapes occurred in 5 days, when the relative intensity of the second peak increased, up to the level of the first peak and then more. The formation of an intermediate peak and an increase of the intensity at higher wavelength was also observed during the weeks of monitoring, together with a decrease of the absolute intensities of the main peak. The latter observation suggested to stop the spectra acquisition at lower intensities of the main peak.

Spectra trend may suggest the aggregation of aromatic rings [Begon et al., 2000; Benkhedda and Landais, 1992; Li et al., 1994; Pindoria et al., 1997] and the presence of oxygenated compounds [Pindoria et al., 1997].

Results from UVF seems thus to be consistent with the ones obtained with GPC. The loss of lighter aromatic compounds may also occur and affect the chromatograph and spectrum trends; however, a much more detailed understanding of the existing molecular structures and of the mechanisms of recombination would be requested.

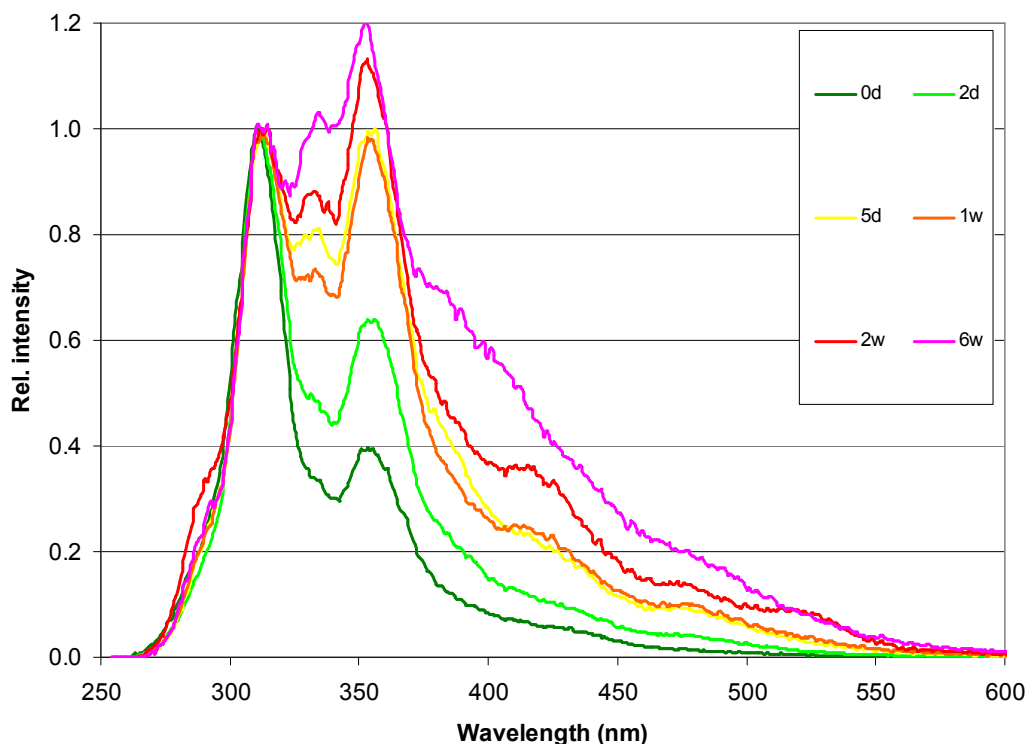


Fig. 5.18 – UVF spectra of first oil produced from pyrolysis of SO at 500 °C and stored at ambient temperature

FT-IR runs were also performed on pure oil samples produced at different time in order to explore the possibility to gain more detailed information about the structural changes occurring during the ageing process. IR spectra are presented in figure 5.19.

The presence of several structural contributions was apparent in the IR spectra as a consequence of the large number of compounds contained in bio-oils (up to 800).

A first wide absorption band was detected in the wavelength number range 2600-3600 cm^{-1} , with a climax around 3200-3300 cm^{-1} . According to several sources [Brossard Perez and Cortez, 1997; Calemma et al., 1995; Coates, 2000; Yang et al., 2007], this band can be related to OH stretching of hydroxyl groups, contained in alcohols, carboxyl acids, phenols and water. Also CH_n stretching of aromatics may affect this region of the spectra [Coates, 2000]. A slight increase over time can be observed for this absorption band if spectra corresponding to fresh and 2 months aged first oils are compared. This may be due to an increase in organic acids and water and it could be in accordance with [Diebold, 2000], which suggested condensation as one of the main reactions occurring during the ageing process with consequent formation of water and longer chains of ethers, esters, olefins and aromatic compounds. Nevertheless, the analysis of the 2 week old first oil sample shows an inverted trend which can be due to lead to two different conclusions:

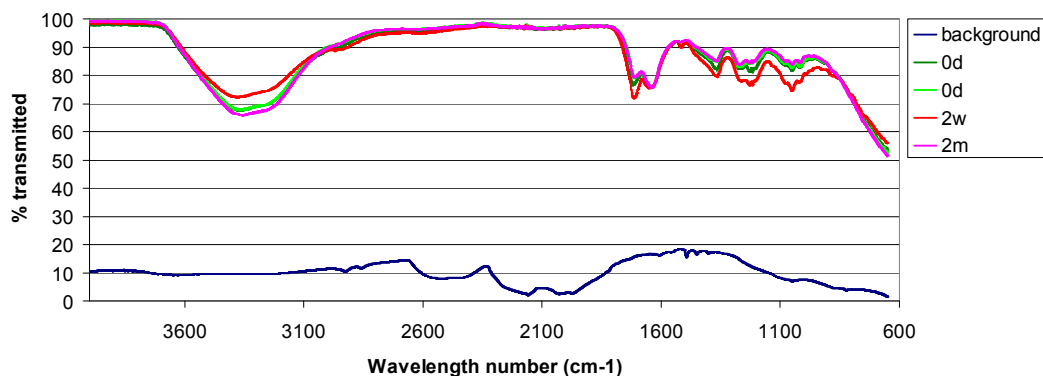


Fig. 5.19 – IR spectra of first oils produced from pyrolysis of SO at 500 °C and stored at ambient temperature

1. the possible presence of a two step ageing mechanism;
2. the unsatisfactory sensitivity of the instrument used and/or the set up of an experimental procedure not appropriate for this kind of study. It should be indeed remarked that IR analysis was performed using samples of bio-oil produced at different times, and not using the same sample of bio-oil at different times as it was done with GPC and UVF.

Scrolling the spectra, other significant absorption bands were found around 1640 and 1710 cm^{-1} , corresponding to C=O and C=C stretching [Coates, 2000; Yang et al., 2007]. C=O may be related to several carbonyl compounds (i.e. ketons, aldehydes, esters, carboxyl acids), while C=C to the presence of olefins and aromatics. Carboxyl groups may be bonded also to aromatic ketons according with [Brossard Perez and Cortez, 1997]. A slight band decrease occurred in the sample analysed after 2 months and it may reveal the possible disappearance of the reactive aldehydes and chetons to polymers and water, as suggested by [Diebold, 2000]. An inverted trend after 2 weeks was found also in this band, which may indicate the possible formation of intermediates as a preliminary step previous to the polymerization reaction ([Diebold, 2000] suggested peroxides).

Further bands were registered at 1220 cm^{-1} , 1240 and 1360 cm^{-1} due to OH and CH bending and C-O-C and C-O stretching [Coates, 2000]. In particular, the band at lower wavelength numbers may correspond to the presence of phenols and aromatic rings, according with [Brossard Perez and Cortez, 1997; Coates, 2000]. Bands at 1010, 1050 and 1070 cm^{-1} , due to OH association and C-O stretching and deformation, may be instead related to the presence of carboxyls and alcohols. The trend found in the previous bands is repeated here. Band corresponding to phenols may be decreased because of group substitution and polymerisation reactions passing through an intermediate state. Nevertheless, the spectra difference may be not so significant.

A strong wide absorption band was finally observable at wavelength numbers lower than 1000 cm^{-1} . These bands should be related to aromatic hydrogen [Coates, 2000] and may confirm the aggregation of aromatic clusters [Munkhtsetseg et al., 2007]. Weak differences can be seen between the different samples: the absorption band slightly decreased after 2 weeks and then increased again over the original state after 2 months. The presence of aromatic compounds and aromatic chains seems to be strong from the beginning of the storage process. Even if the sensitivity of the instrument and/or the accuracy of the experimental procedure could be not good

enough for this application, it is worthy noticing that IR revealed the possible presence of many oxygenated compounds.

Ageing of the second oil, produced and stored under the same conditions, was then analysed with GPC and UVF. Figure 5.20 and figure 5.21 present chromatograms and spectra obtained during the analysis. This sample was obtained from the collection with methanol of the semi-solid phase sticking (roughly the 20% of the total oil) on the walls of the oil trap and dried before the beginning of the analytical series.

Differently from first oil, the main peak of the chromatograms was composed by only one saddle and its intensity decreased with regularity for all the 4 weeks. On the other side, the excluded peak increased its intensity over time. According with the GPC plots, recombination reactions may have occurred also into this sample, leading to formation of larger molecules.

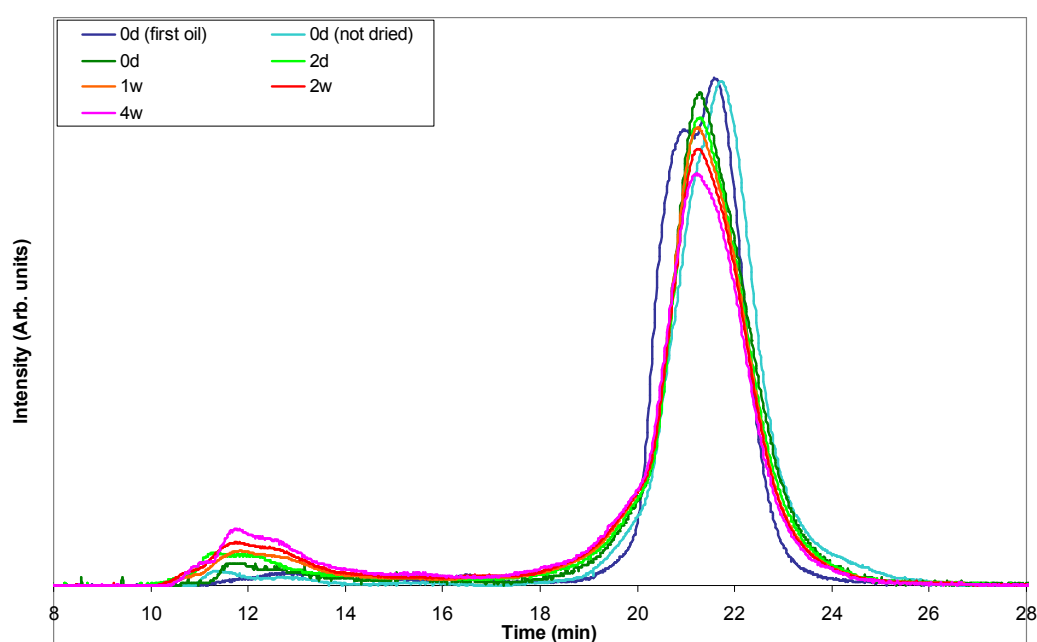


Fig. 5.20 – GPC chromatograms of second oil produced from pyrolysis of SO at 500 °C, methanol dried and stored at ambient temperature

A main peak at 310 nm was again found in the UVF spectra of the sample even if, unlike the first oil, the second peak at 360 nm looks more as a shoulder. High spectra intensities were also registered in the interval between these two limits. No significant shape changes occurred in one month, when only a slight increase of the signal at 360 nm and a slight shift of the first peak toward longer wavelength were detected. According to the spectra obtained, aggregation of aromatic rings may have occurred also in this sample but with minor extent.

The second oil appears thus to contain a larger amount of polymeric material since the beginning of the study but it seems also more stable than first oil, at least during the first month of monitoring.

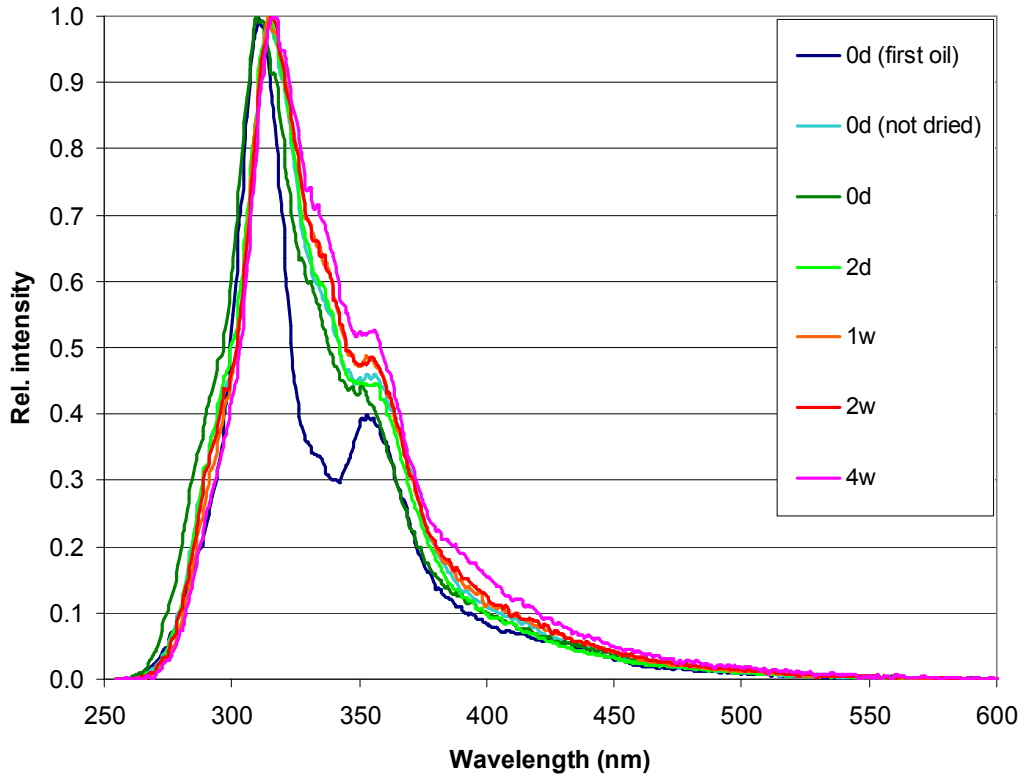


Fig. 5.21 – UVF spectra of second oil produced from pyrolysis of SO at 500 °C, methanol dried and stored at ambient temperature

In order to obtain a more complete picture, first oil and second oil were collected with chloroform, and analysed after chloroform drying. Figure 5.22 and figure 5.23 present chromatograms and spectra obtained over time with GPC and UVF.

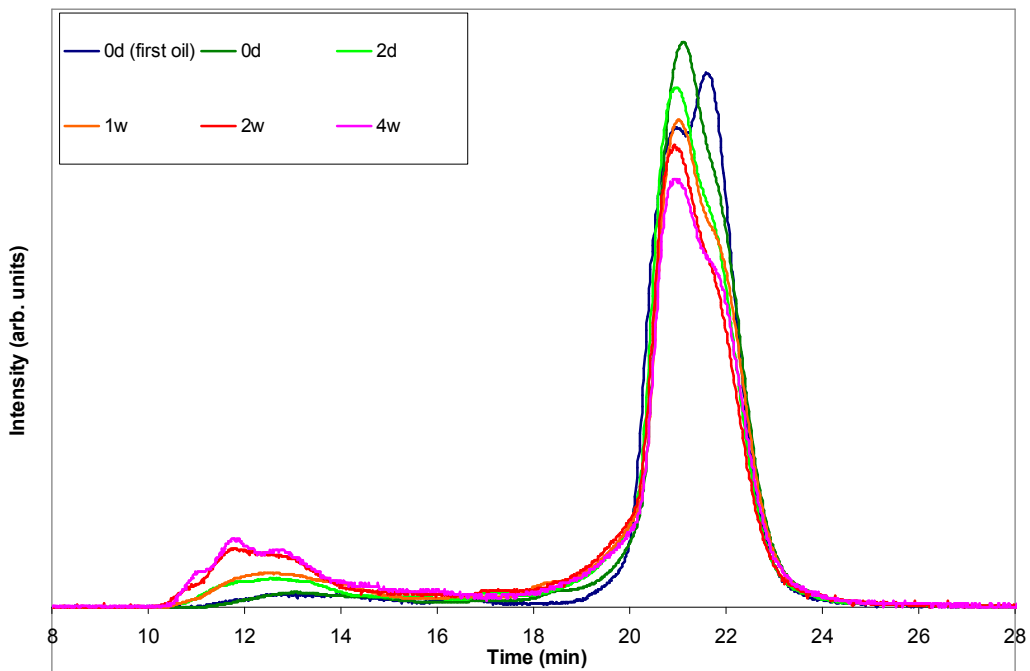


Fig. 5.22 – GPC chromatograms of first and second oil produced from pyrolysis of SO at 500 °C, chloroform dried and stored at ambient temperature

The plot of the chromatograms resulted quite different from the previous ones, looking like a sort of combination between the first and the second oils. The main peak intensity decreased constantly during the 4 weeks of study, while the excluded peak increased significantly in the first 2 weeks and then seemed to stop its growth. The occurrence of recombination reactions into the oil samples is thus suggested also from the GPC runs conducted on the “whole” oil.

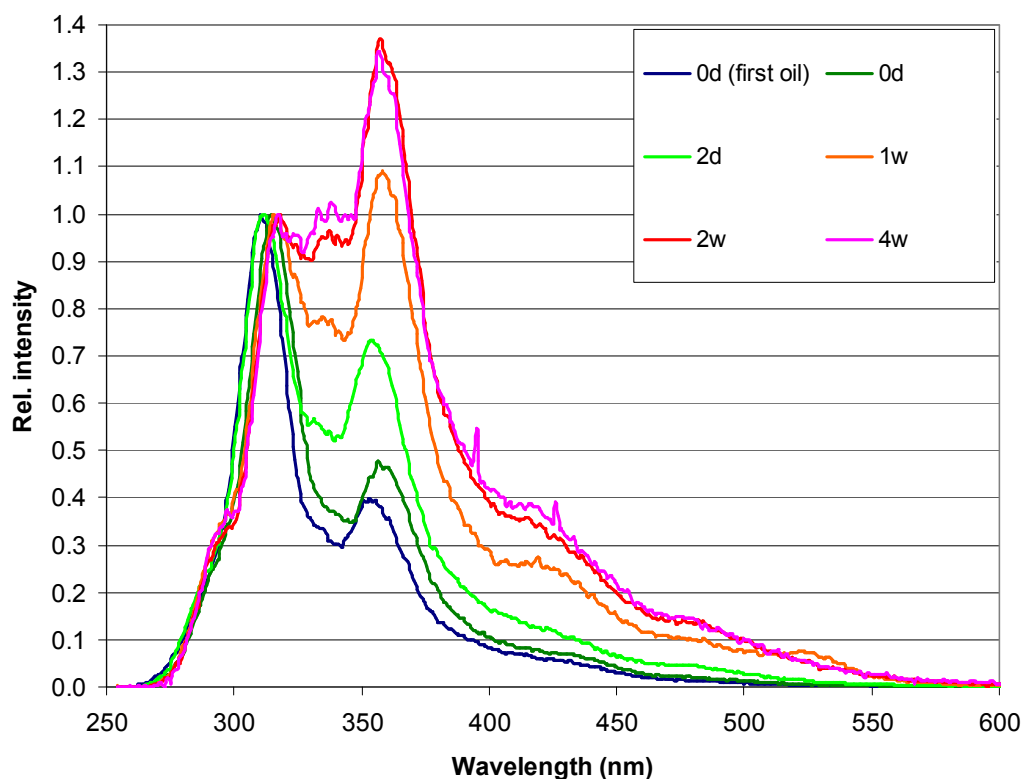


Fig. 5.23 – UVF spectra of first and second oil produced from pyrolysis of SO at 500 °C, chloroform dried and stored at ambient temperature

Like in first oil, two peaks were present in the UVF spectra also from this sample. In the first day of observation, the main peak corresponded at 310 nm while the second one was at 360 nm. Apparent changes in spectra shapes occurred after 7 days, when the relative intensity of the second peak increased over the level of the first peak. The formation of an intermediate peak and an increase of the intensity at higher wavelength was again observed during the weeks of monitoring, together with a decrease of the absolute intensities of the main peak. Spectra trend may suggest the aggregation of aromatic rings and the presence of oxygenated compounds as in the previous cases. Moreover, it is worthy noticing that “whole” oil spectra looks as a combination of the spectra of first and second oils: both the typical shape change occurred in the first oil analysis and the shift toward longer wavelength registered with the second oil are indeed observable.

GPC and UVF runs were then performed on a mixture of first and second oil (5:2 by weight), methanol dried. Figure 5.24 and figure 5.25 present chromatograms and spectra obtained over time on the sample with SEC and UV.

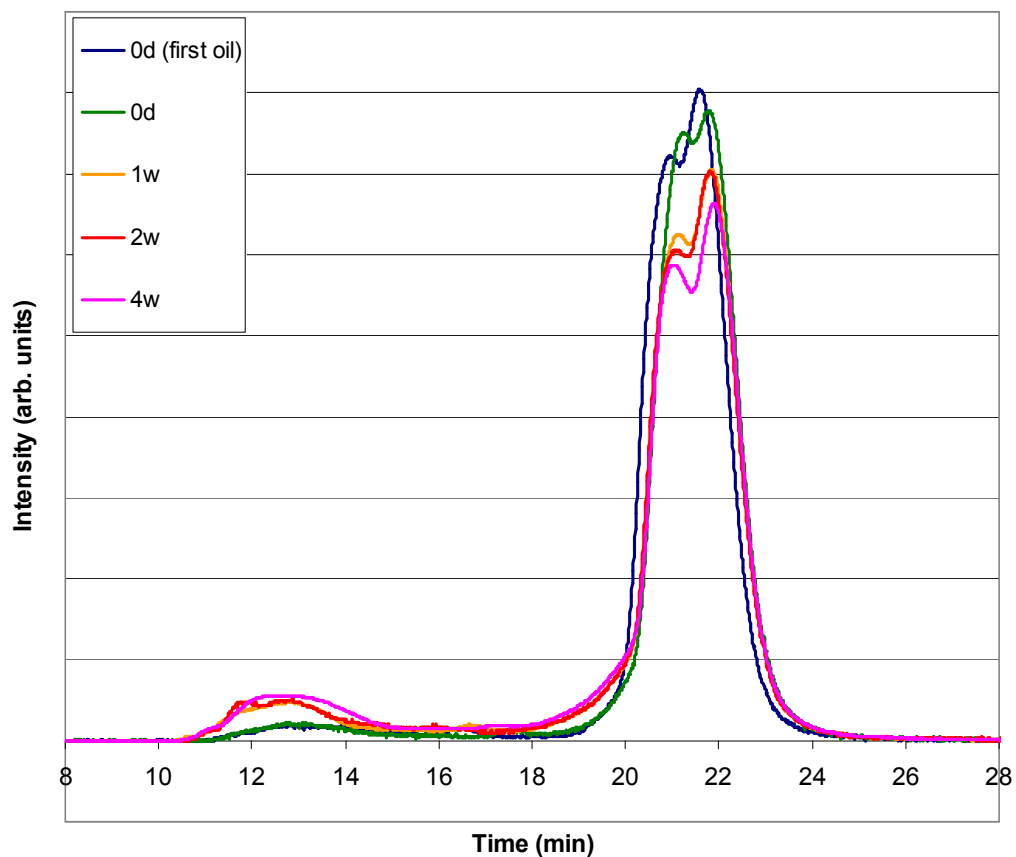


Fig. 5.24 – GPC chromatograms of first and second oil produced from pyrolysis of SO at 500 °C, methanol dried and stored at ambient temperature

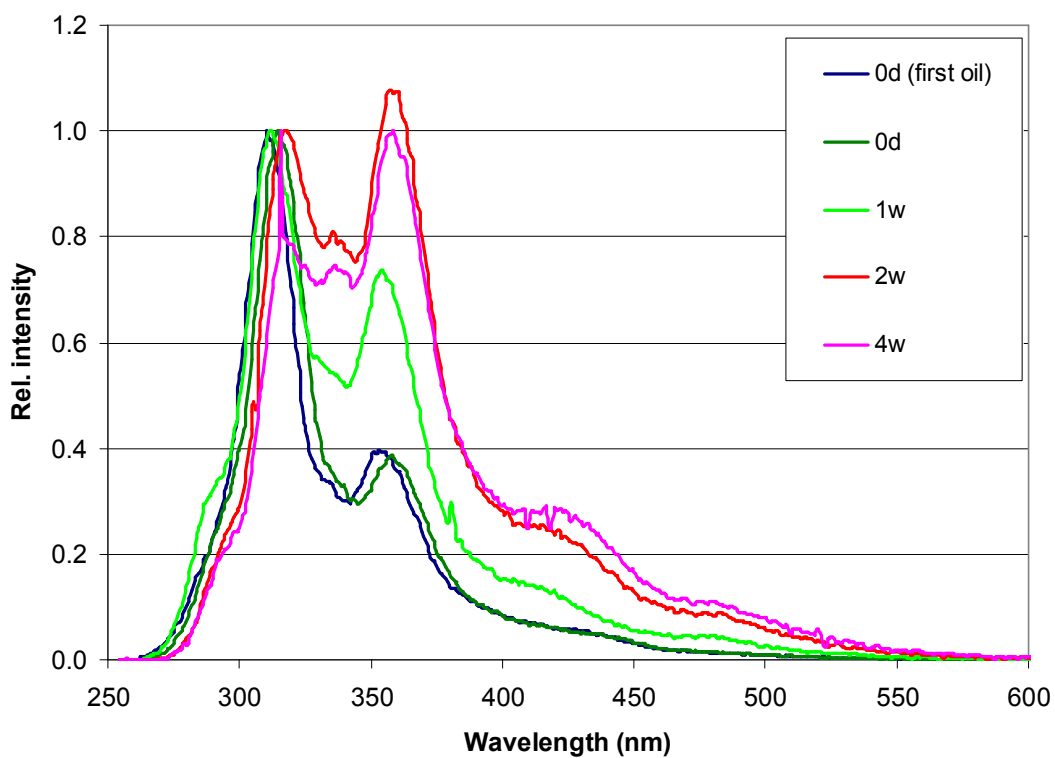


Fig. 5.25 - UVF spectra of first and second oil produced from pyrolysis of SO at 500 °C, methanol dried and stored at ambient temperature

Probably due to a different sample preparation procedure, different shapes were obtained for the GPC chromatograms and a longer time occurred before the main peak of the UVF spectra was inverted. Nevertheless, results appear consistent with the previous ones. The chromatograms indeed show a continuous decrease of the main peak and an increase of the excluded peak with apparent stop after 2 weeks. UVF spectra instead present again an increase of the signal during time at the longer wavelength and a shift of the main peaks toward right.

From the analysis performed it can be evinced that the addition of the second oil, whose structure may be polymeric, should add positive effects on the stabilisation of the bio-oil, at least in the first weeks of storage. On the contrary, high instability seems to be associated with the first oil, composed by an aqueous pure phase.

IR technique was also applied to samples of second oil and mixtures of first and second oils. The resulting IR spectra are shown in figure 5.26.

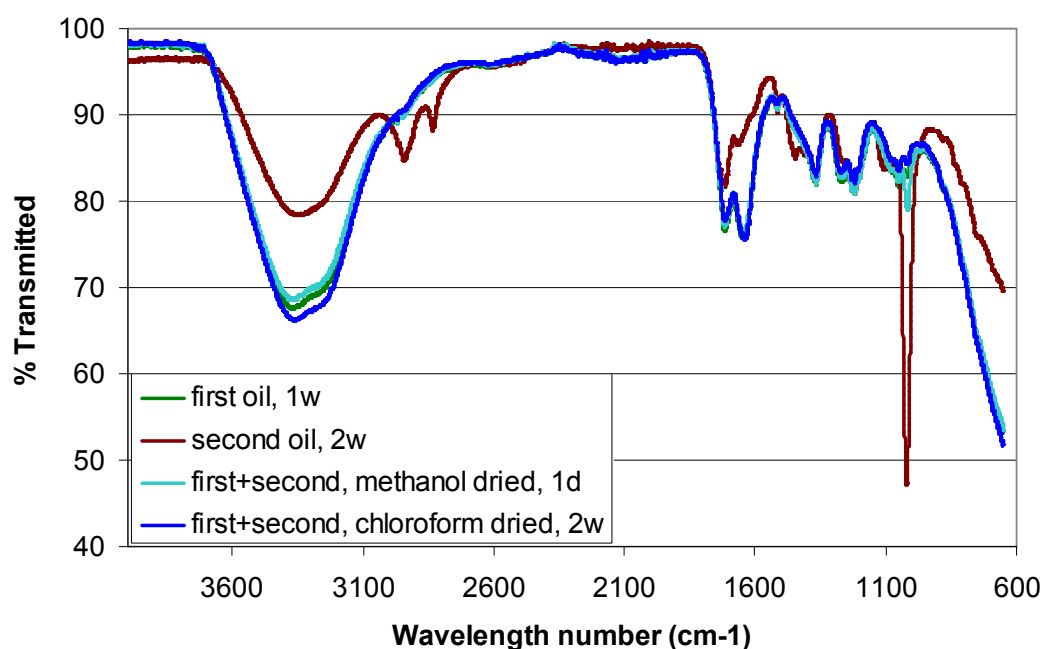


Fig. 5.26 – IR spectra of second oils and mixtures of first and second oils produced from pyrolysis of SO at 500 °C and stored at ambient temperature

Spectra obtained from mixtures of first and second oils appear very similar to the one of the first oil and no apparent differences can be outlined.

It is instead worthy noticing that the second oil spectrum presents some relevant differences. A weaker absorption band was detected in the range of wavelength number 2600-3600 cm^{-1} , with climax around 3200-3300 cm^{-1} , probably due to a lower content of hydroxyls and water. Two peaks were found at 2830 and 2930 cm^{-1} in a region corresponding to aliphatic CH₂ and CH₃ groups [Brossard Perez and Cortez, 1996; Calemma et al., 1995; Munkhtsetseg et al., 2007] and aromatic CH groups [Munkhtsetseg et al., 2007]. The absorption bands at 1640 and 1710 cm^{-1} resulted to be lower, probably due to a lower content of carbonyl compounds, olefins and aromatics. In particular, the lower content in aldehydes and ketons may partially explain the reduced reactivity of the second oil. No significant differences occurred at 1220, 1240 and 1360 cm^{-1} while a strong band was detected at 1030 cm^{-1} , in correspondence with the region of OH association and C-O stretching and

deformation [Coates, 2000]. This may suggest the presence of both phenols, carboxyls and alcohols. A weaker absorption band was finally observed at frequencies lower than 1000 cm^{-1} probably indicating a lower grade of aggregation of the aromatic clusters [Munkhtsetseg et al., 2007]. The last finding would be in disagreement with the hypothesis that the second oil was composed by polymeric material; nevertheless, it is necessary to pay attention to the possible recombination effects due to the solvent used during the oil collection.

Effects due to methanol addition

Figures 5.27 and 5.28 present the GPC chromatograms and the UVF spectra obtained over time with the mixture first oil : second oil : methanol. Methanol content in the mixture was about 10% by weight. Bio-oil was produced from the pyrolysis of SO at $500\text{ }^{\circ}\text{C}$ and stored at ambient temperature.

According with chromatograms, methanol seems to slow down the sample ageing. An asymptote was reached after 2 weeks as in the case of the first oil.

Previous result is supported by UVF spectra since second peak intensity becomes higher than first peak intensity (i.e. corresponding to a relative intensity higher than 1) between 1 and 2 weeks, when 5-7 days resulted needed for the first oil.

Chromatograms and spectra were obtained also with similar samples containing higher amount of methanol. Figure 5.29 and figure 5.30 refer to a 25% methanol content, while figure 5.31 and figure 5.32 to a 50% content.

As a consequence of the higher methanol content, smaller differences were noticeable between chromatograms recorded at different times. A confirmation is given by UVF spectra, which suggest the repression of the sample reactivity due to the methanol addition.

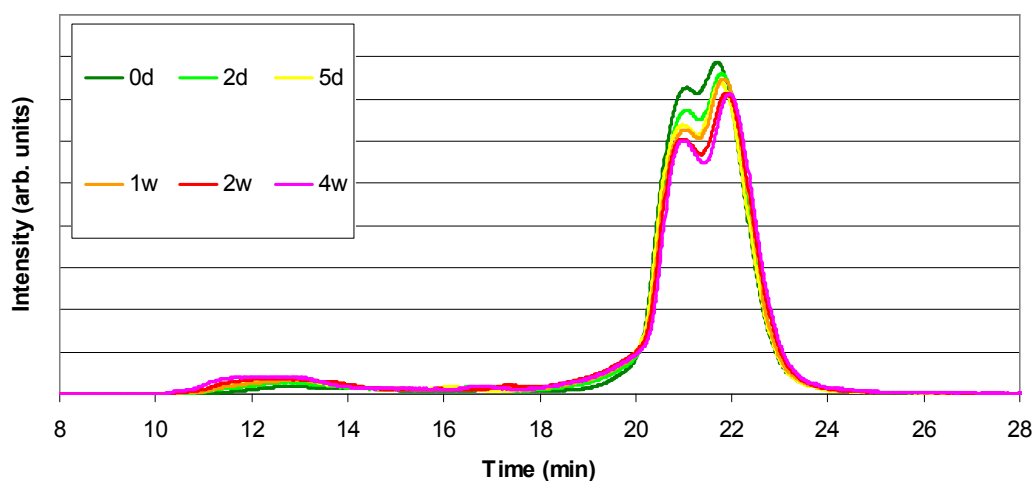


Fig. 5.27 – GPC chromatograms of the mixture first oil : second oil : methanol produced from pyrolysis of SO at $500\text{ }^{\circ}\text{C}$. Methanol content: 10%; storage: ambient temperature

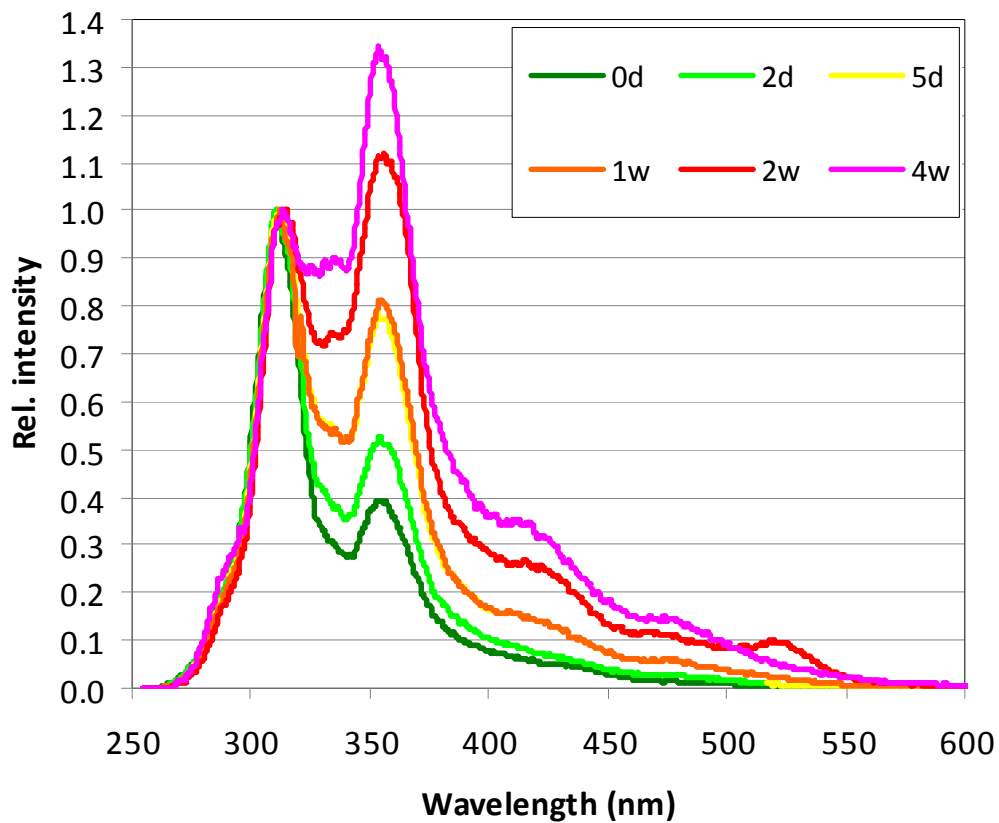


Fig. 5.28 - UVF spectra of the mixture first oil : second oil : methanol produced from pyrolysis of SO at 500 °C. Methanol content: 10%; storage: ambient temperature

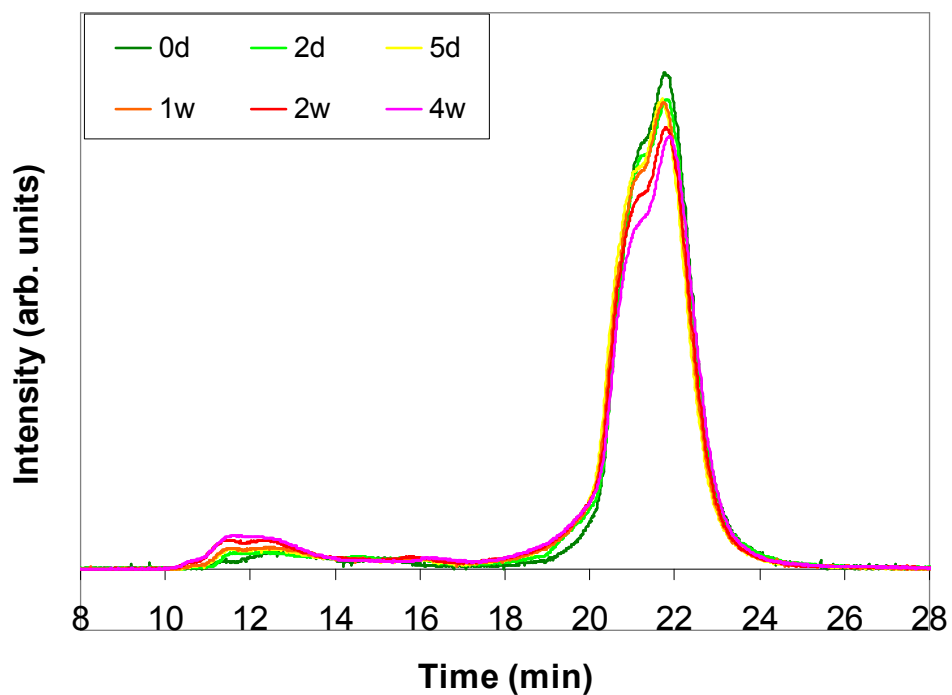


Fig. 5.29 - GPC chromatograms of the mixture first oil : second oil : methanol produced from pyrolysis of SO at 500 °C. Methanol content: 25%; storage: ambient temperature

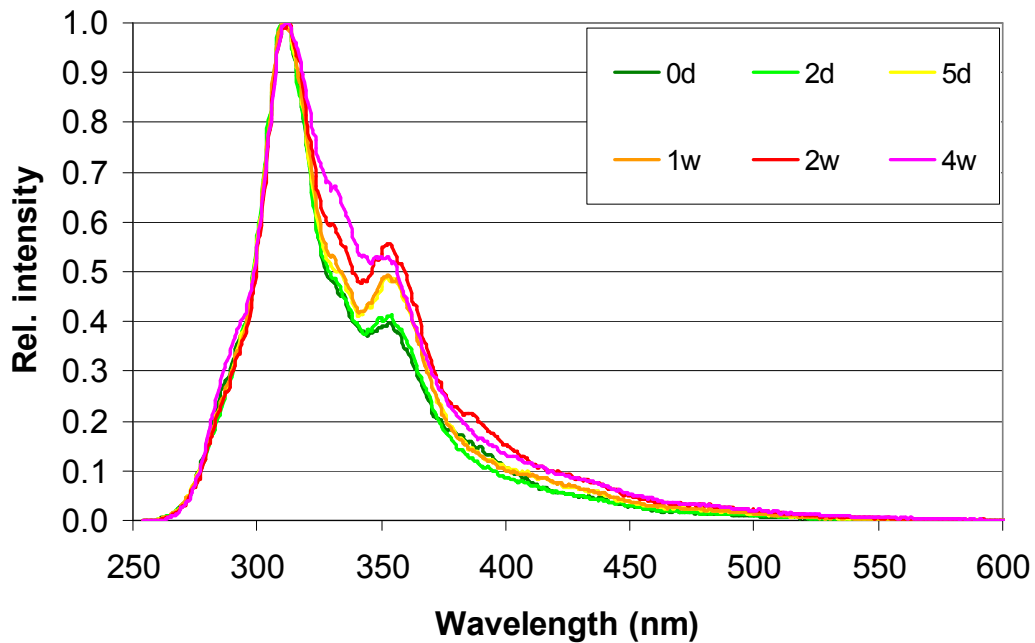


Fig. 5.30- UVF spectra of the mixture first oil : second oil : methanol produced from pyrolysis of SO at 500 °C. Methanol content: 25%; storage: ambient temperature

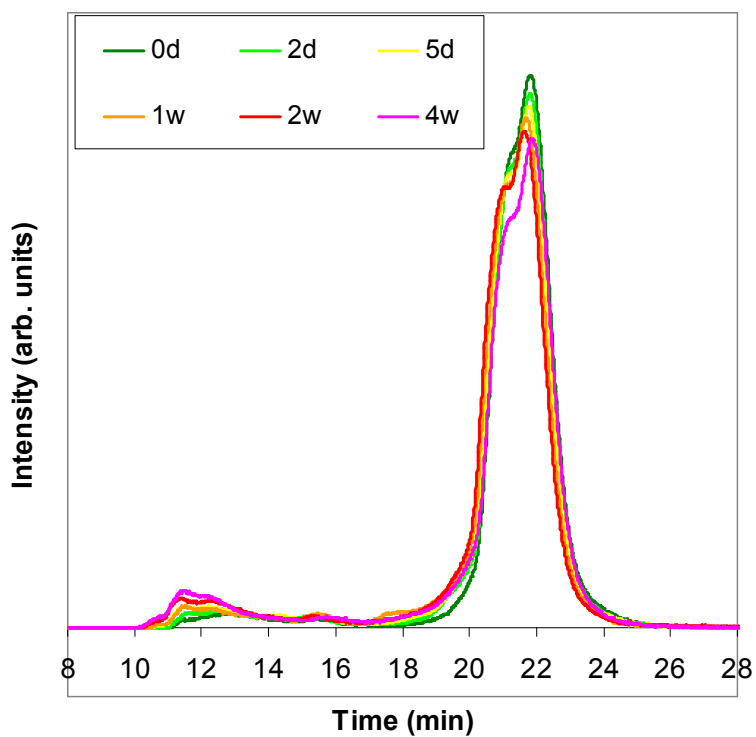


Fig. 5.31 - GPC chromatograms of the mixture first oil : second oil: methanol produced from pyrolysis of SO at 500 °C. Methanol content: 50%; storage: ambient temperature

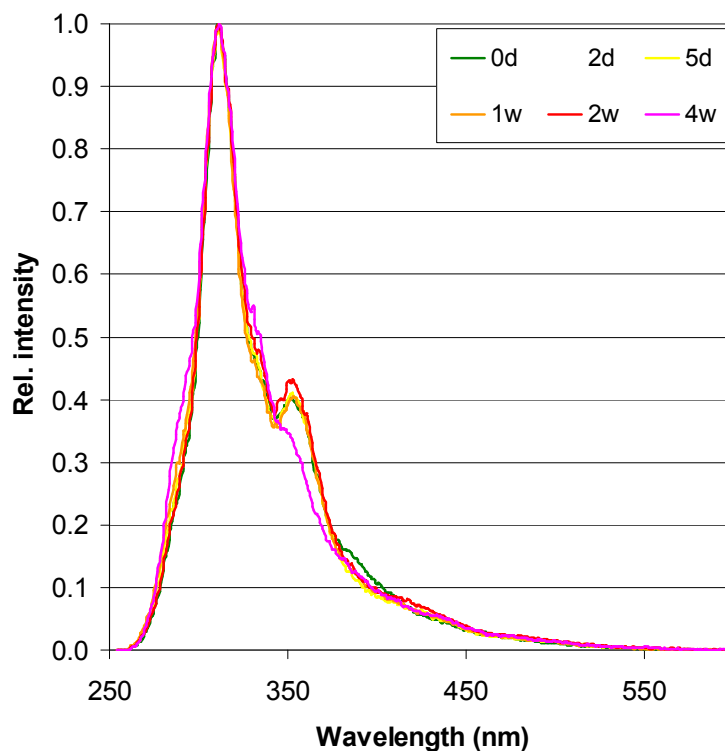


Fig. 5.32 - UVF spectra of the mixture first oil : second oil : methanol produced from pyrolysis of SO at 500 °C. Methanol content: 50%; storage: ambient temperature

GPC and UVF runs were also repeated with samples prepared from the direct addition of methanol to sub-fractions of first oil. Figure 5.33 and figure 5.34 present the chromatograms and spectra obtained over time for the mixture first oil : methanol with the 10% by weight in methanol, while results obtained with the 25% content in methanol are proposed in figure 5.35 and figure 5.36. Oil was produced from the pyrolysis of SO at 500 °C and stored at ambient temperature.

Methanol addition up to concentration of 10% by weight did not appear to slow down significantly the structural changes occurring in the sample. Since second oil was not present in this sample, it is possible that stabilisation effects can be associated with the material stuck on the U-tube after the first oil collection. Nevertheless, analysis may be influenced also by the smaller amount of liquid used for this series which may have increased the occurrence of superficial oxidation.

A higher methanol concentration in the mixture (up to 25% by weight) appeared to slow down the first oil ageing. Also in this case the sample reactivity appeared slightly higher than the one corresponding to the analogous sample containing second oil, supporting the interpretation previously outlined.

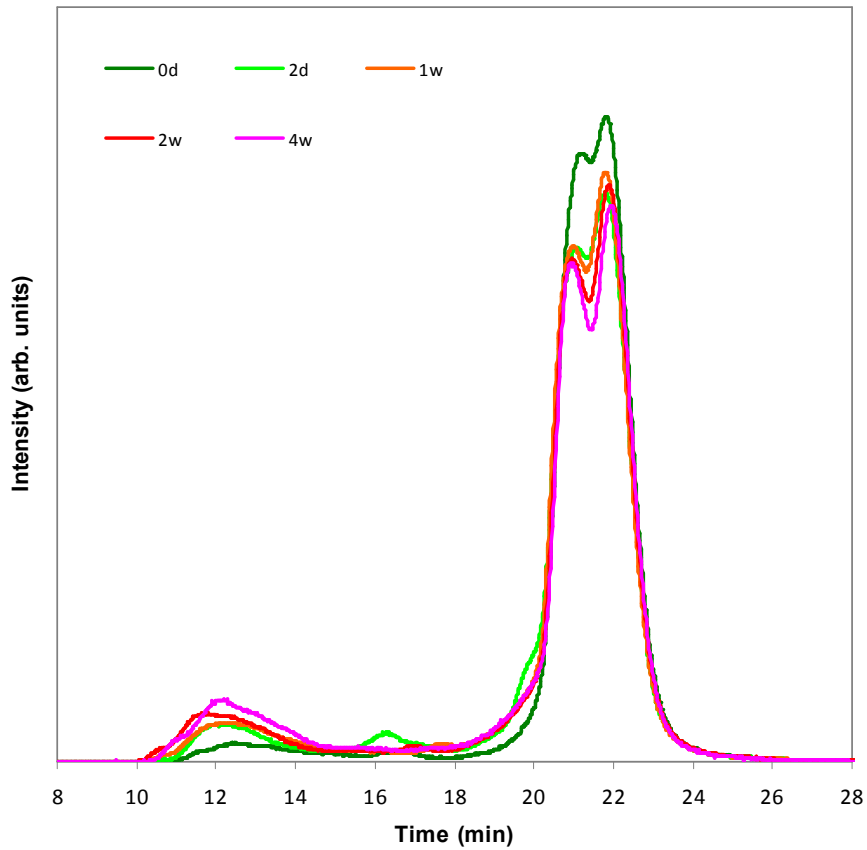


Fig. 5.33 - GPC chromatograms of the mixture first oil : methanol produced from pyrolysis of SO at 500 °C. Methanol content: 10%; storage: ambient temperature

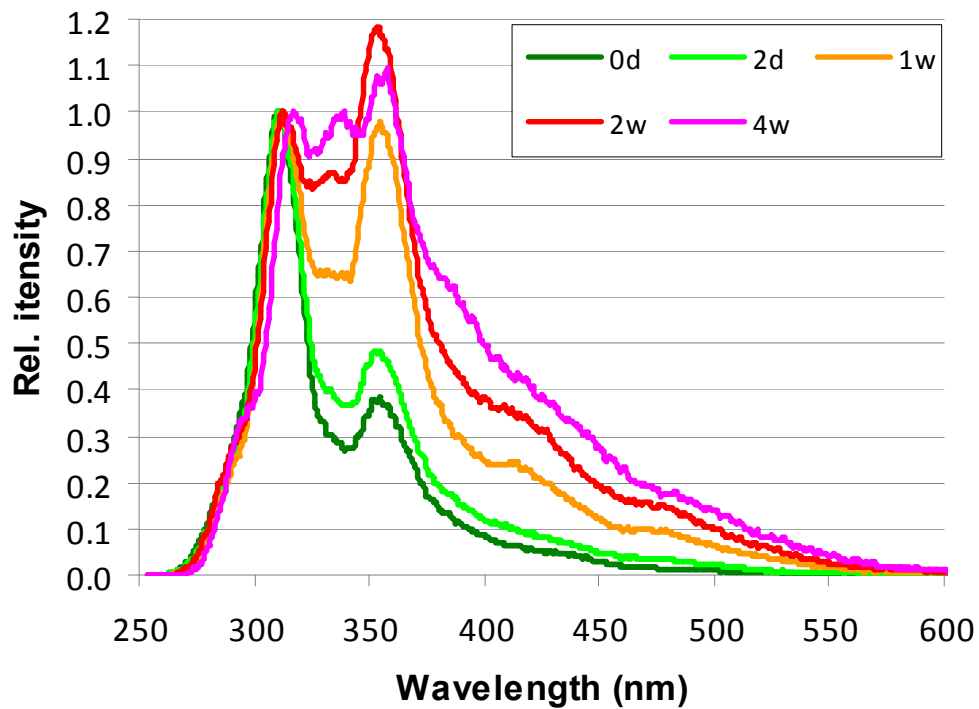


Fig. 5.34 - UVF spectra of the mixture first oil : methanol produced from pyrolysis of SO at 500 °C. Methanol content: 10%; storage: ambient temperature

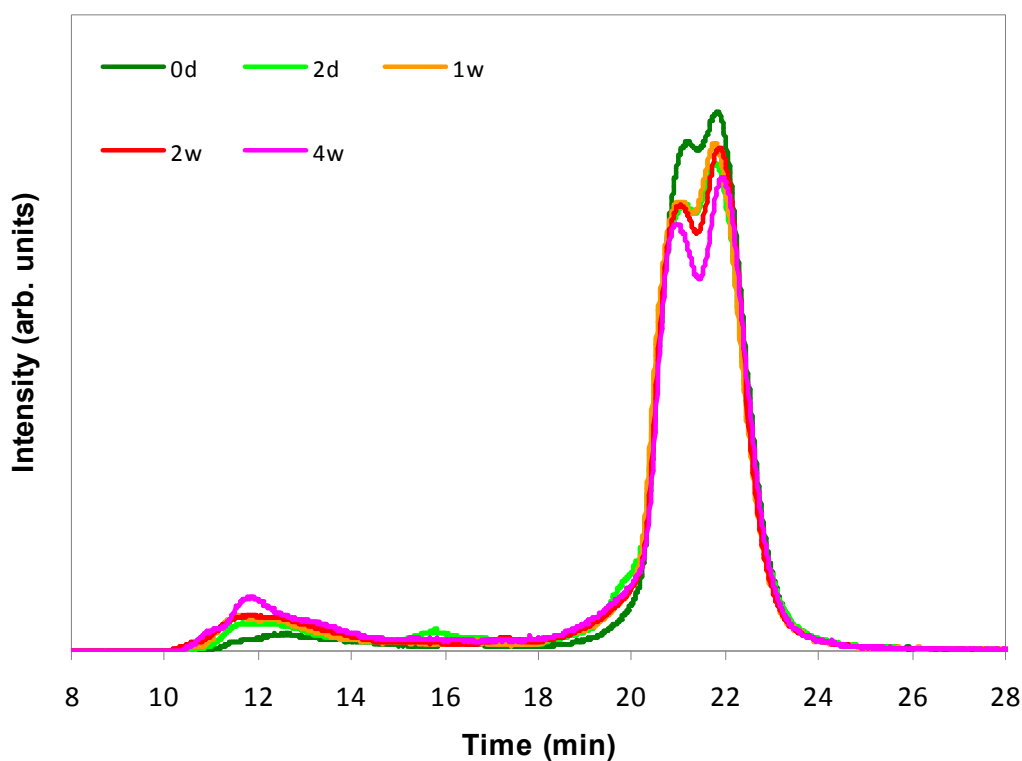


Fig. 5.35 - GPC chromatograms of the mixture first oil : methanol produced from pyrolysis of SO at 500 °C. Methanol content: 25%; storage: ambient temperature

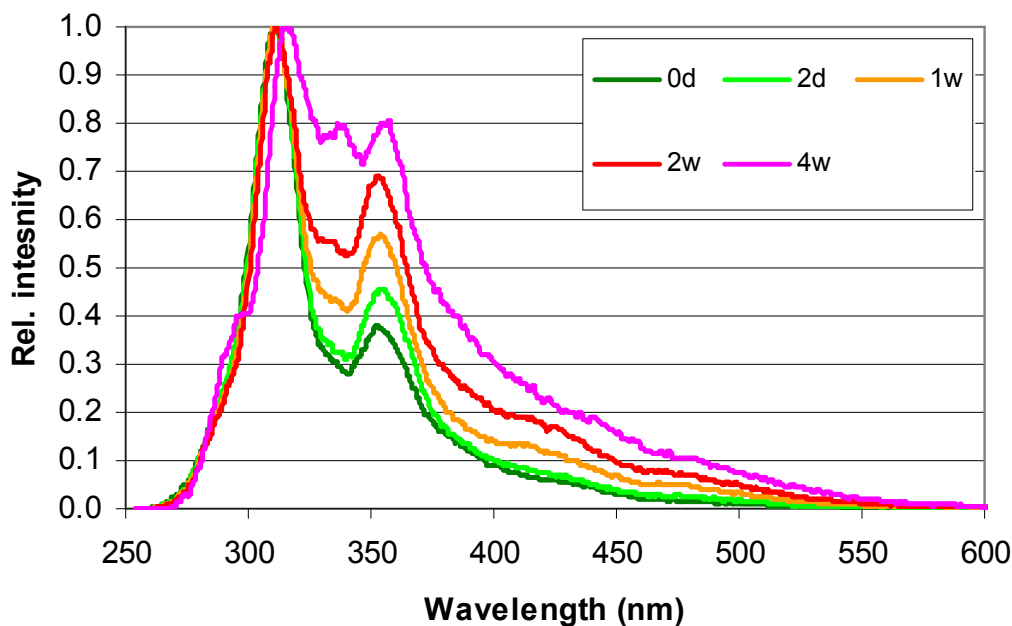


Fig. 5.36 - UVF spectra of the mixture first oil : methanol produced from pyrolysis of SO at 500 °C. Methanol content: 25%; storage: ambient temperature

IR technique was applied to mixtures of first oil, second oil and methanol in order to understand the structural effects due to the solvent addition. IR spectra concerning with samples containing all the three components are shown in figure 5.37. Results from samples of first oil in methanol are reported in figure 5.38.

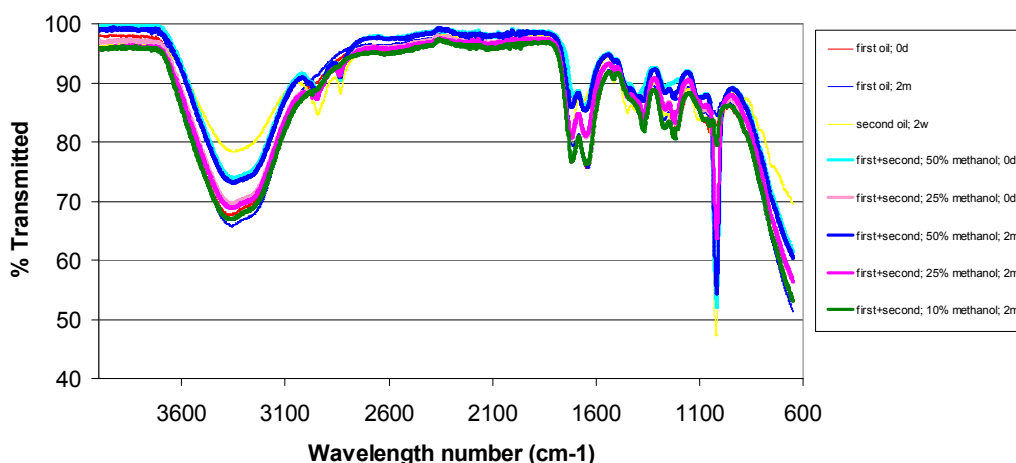


Fig. 5.37 – IR spectra of mixtures of first and second oils with methanol. Oil produced from pyrolysis of SO at 500 °C and stored at ambient temperature

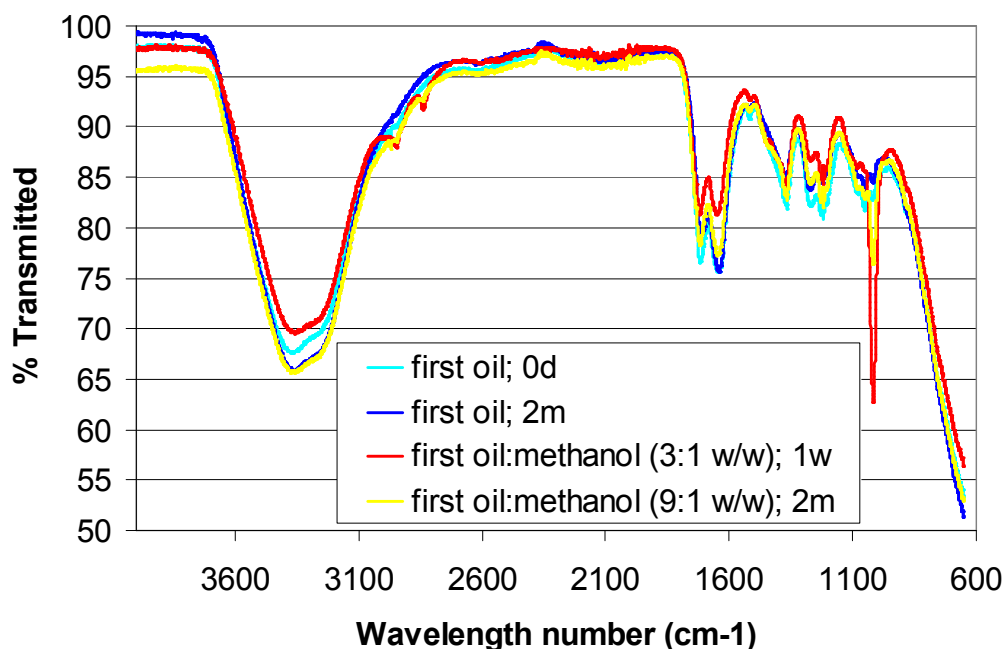


Fig. 5.38 – IR spectra of mixtures of first oils and methanol. Oil produced from pyrolysis of SO at 500 °C and stored at ambient temperature

Samples yielded spectra included between the ones corresponding to second oil (lower absorption bands) and first oil aged (higher absorption bands). In particular, no matter the presence of second oil, addition of methanol seemed to shift the sample spectra toward the spectrum of the second oil. No significant differences were apparent over time, suggesting the occurrence of instantaneous reactions. In comparison with the first oil aged, a lower content of hydroxyls (i.e. alcohols) and water resulted from the analysis of the bands at 2600-3600 cm⁻¹. Even absorption bands at 1220, 1240, 1360, 1640 and 1710 cm⁻¹ generally resulted lower, probably due to a lower content of carbonyl compounds, olefins and aromatics. A strong band was instead detected at 1030 cm⁻¹ and this effect was as more significant as the methanol concentration increased. This band may suggest the presence of phenols, carboxyls and alcohols. A weak absorption band was finally observed for frequencies lower than

1000 cm^{-1} indicating a lower grade of aggregation of the aromatic clusters [Munkhtsetseg et al., 2007]. The last findings may be consistent with the ageing mechanism proposed by [Diebold, 2000]. Accordingly, the effect of the solvent addition is stronger than the effects due only to a simple dilution. Methanol is supposed to shift the equilibrium composition to a mixture with lower molecular weight and viscosity, thus at the expense of polymerization reactions.

Effects due to acetone addition

First oil was used also to obtain batch samples with different concentration of acetone (10% / 25%). Results obtained with GPC and UVF are shown in figure 5.39 and in figure 5.40, referred to a 10% content in acetone, and in figure 5.41 and in figure 5.42, for the sample with the 25% of acetone.

Chromatograms and spectra of the sample containing a 10% by weight in acetone, revealed the occurrence of recombination reactions, even if the ageing process seemed to be slower in comparison both with first oil and with the equivalent sample containing a 10% by weight in methanol.

A stronger stability was found for the mixture first oil : acetone at the 25% by weight in acetone, as suggested by chromatograms and spectra obtained with this sample. In comparison with methanol, acetone would seem to contrast ageing with the same or a little stronger, effectiveness.

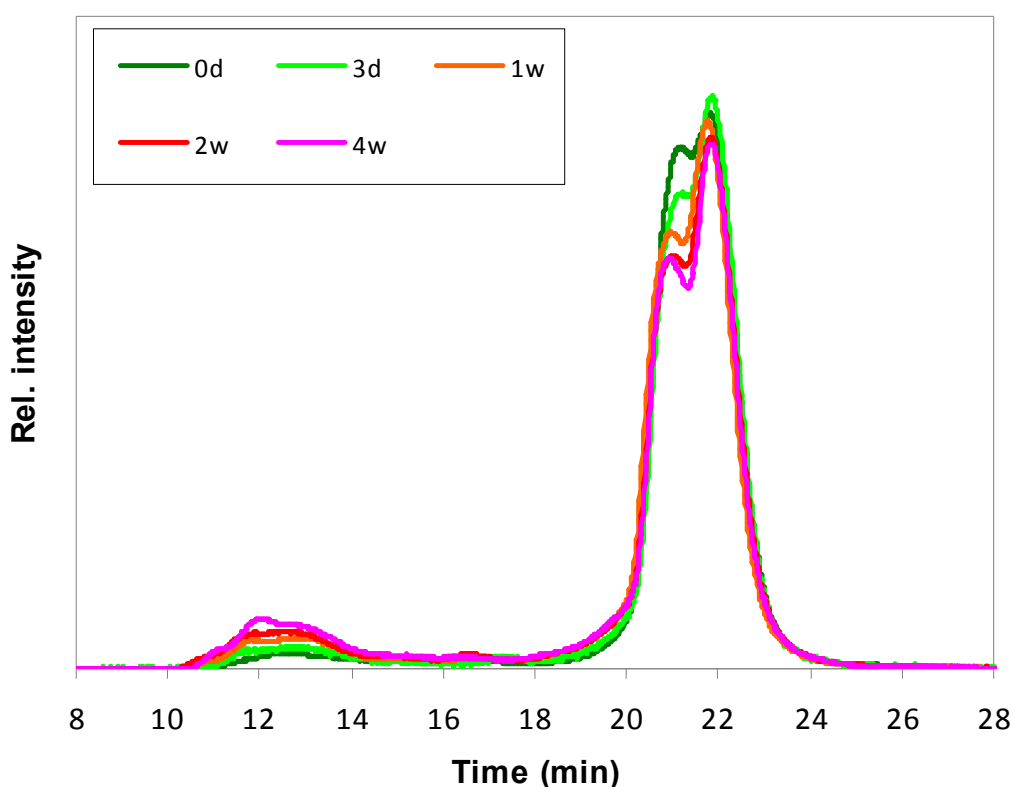


Fig. 5.39 – GPC chromatograms of the mixture first oil : second oil : acetone produced from pyrolysis of SO at 500 °C. Methanol content: 10%; storage: ambient temperature

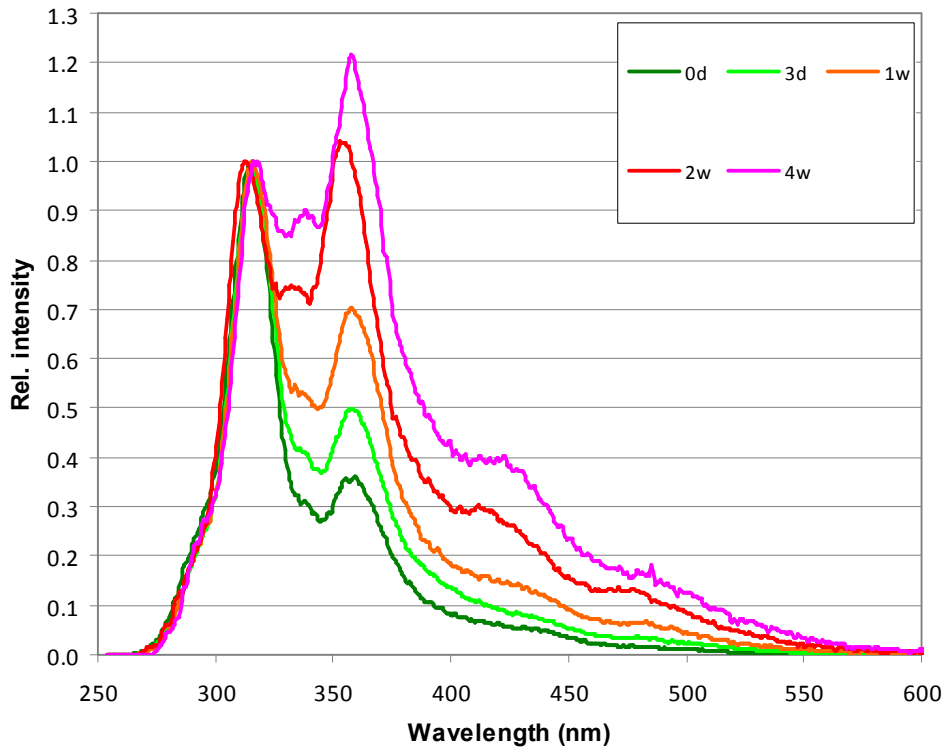


Fig. 5.40 – UVF spectra of the mixture first oil : second oil: acetone produced from pyrolysis of SO at 500 °C. Methanol content: 10%; storage: ambient temperature

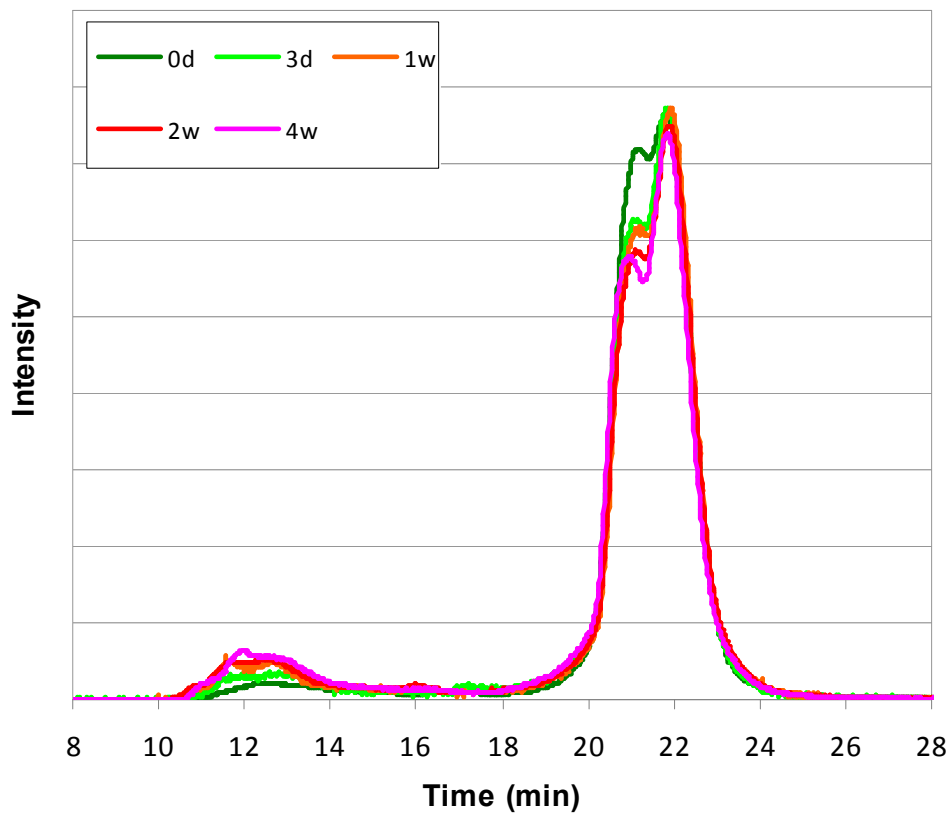


Fig. 5.41 – GPC chromatograms of the mixture first oil : second oil: acetone produced from pyrolysis of SO at 500 °C. Methanol content: 25%; storage: ambient temperature

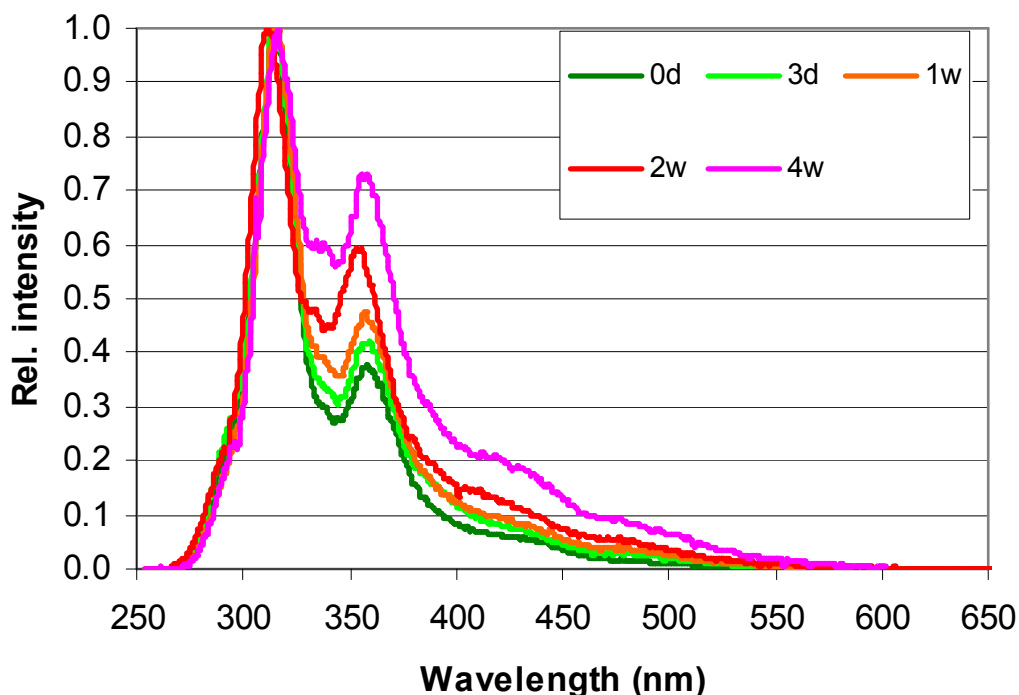


Fig. 5.42 – UVF spectra of the mixture first oil : second oil: acetone produced from pyrolysis of SO at 500 °C. Methanol content: 25%; storage: ambient temperature

IR analysis was also performed on these samples, whose resulting spectra are plotted on figure 5.43 with the aim to collect, potentially, some useful indications on the action mechanism of acetone.

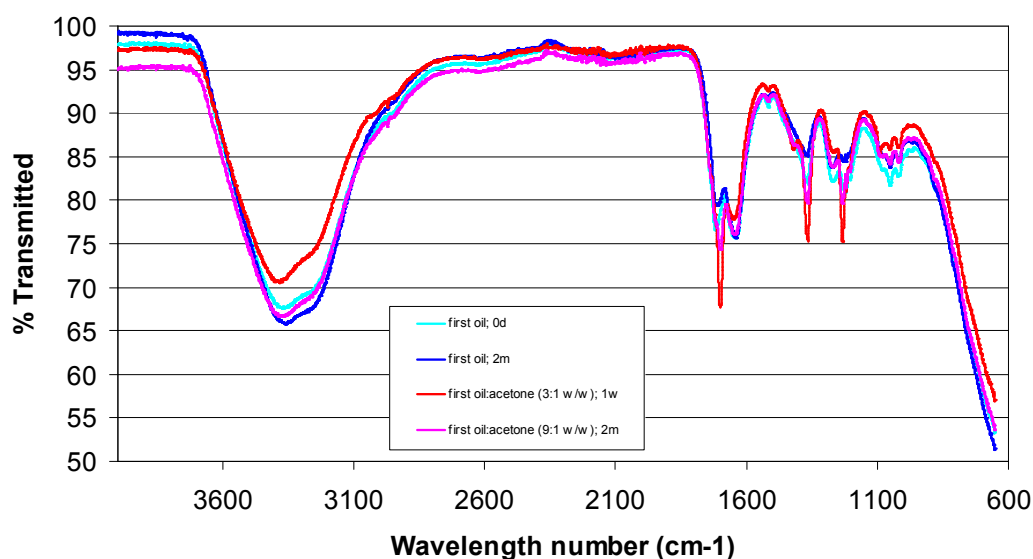


Fig. 5.43 – IR spectra of mixtures of first oils and acetone. Oil produced from pyrolysis of SO at 500 °C and stored at ambient temperature

In comparison with IR spectra obtained previously, some peculiarities seems to characterise spectra from samples containing acetone. First of all, a weaker absorption band was detected at 2600-3600 cm⁻¹, suggesting a lower content of hydroxyls (i.e. alcohols) and water. Moreover, absorption bands at 1220, 1240, 1360, 1640 and 1710

cm^{-1} resulted to be much higher, probably due to a higher content of carbonyl compounds, olefins and aromatics. The strong band detected at 1030 cm^{-1} in the samples containing methanol was instead absent, maybe due to a limited presence of phenols, carboxyls and alcohols. These effects resulted to be more relevant at higher acetone concentrations and may be more consistent with the ageing mechanism proposed by [Diebold, 2000] than the results obtained previously with methanol. IR results, indeed, suggest that a lower content of aldehydes and esters may be present in the oil mixtures.

Effects due to the pyrolysis peak temperature

The effects due to pyrolysis peak temperatures on the stability of the first oil were investigated with GPC and UVF. First oil samples were collected from pyrolysis of SO at 350, 500 and 650 °C and the resulting chromatograms and spectra compared at different time. First oil were stored at ambient temperature. Figure 5.44 and figure 5.45 refer to the fresh oil sample. The analysis after 1, 2, and 3 weeks of storage is instead proposed in figures 5.46 and 5.47; in figures 5.48 and 5.49; in figures 5.50 and figure 5.51.

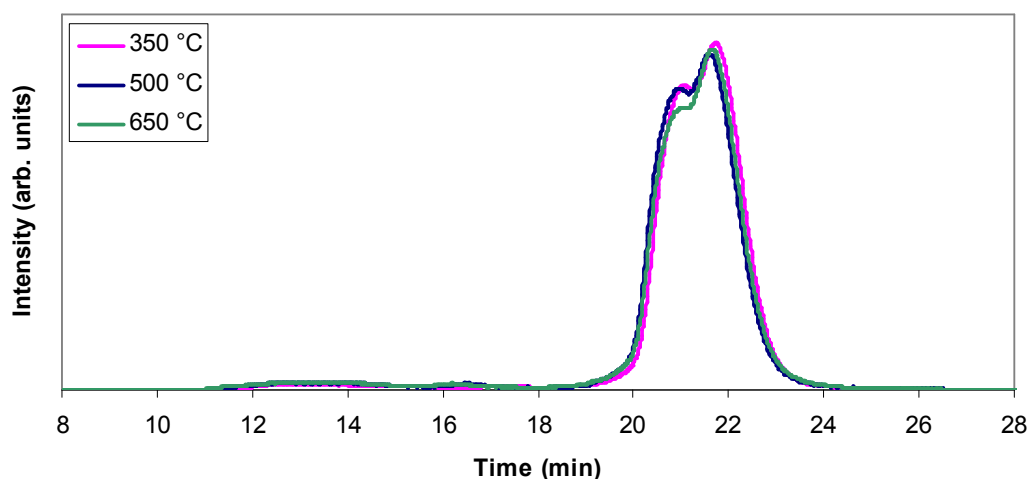


Fig. 5.44 – First oil produced at different pyrolysis temperature: GPC chromatograms of the fresh samples

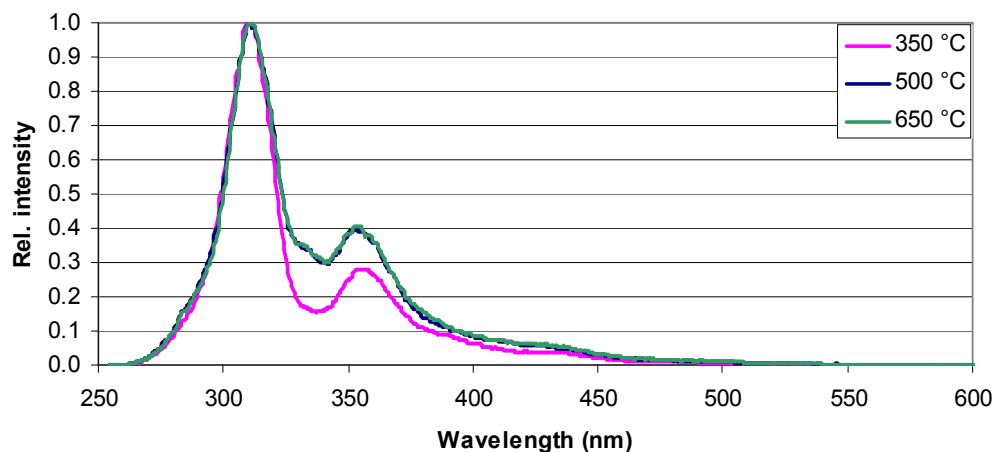


Fig. 5.45 – First oil produced at different pyrolysis temperature: UVF spectra of the fresh samples

No matter the pyrolysis peak temperature, chromatograms are practically coincident. A different spectrum was instead obtained with first oil produced at 350 °C, maybe suggesting a minor extent of polymeric clusters present in that sample.

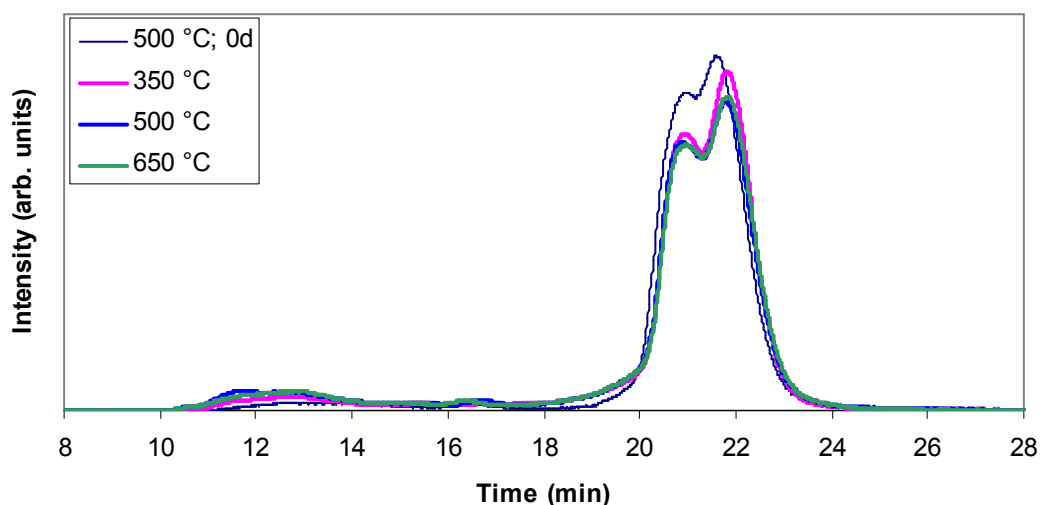


Fig. 5.46 – First oil produced at different pyrolysis temperature: GPC chromatograms after 1 week of storage

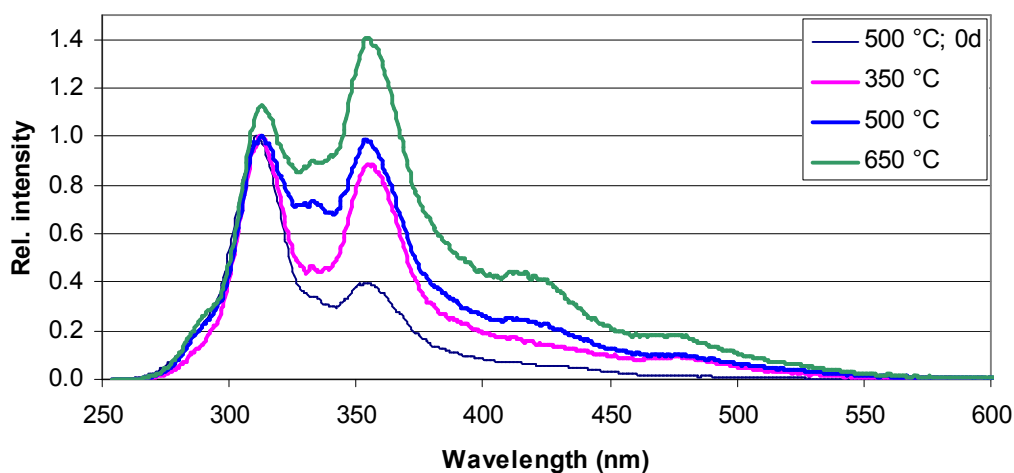


Fig. 5.47 – First oil produced at different pyrolysis temperature: UVF spectra after 1 week of storage

Reactivity in the first week of storage was high in all the samples analysed. Quite similar chromatograms resulted, while UVF spectra strongly suggest that reactivity may increase as pyrolysis peak temperature increases.

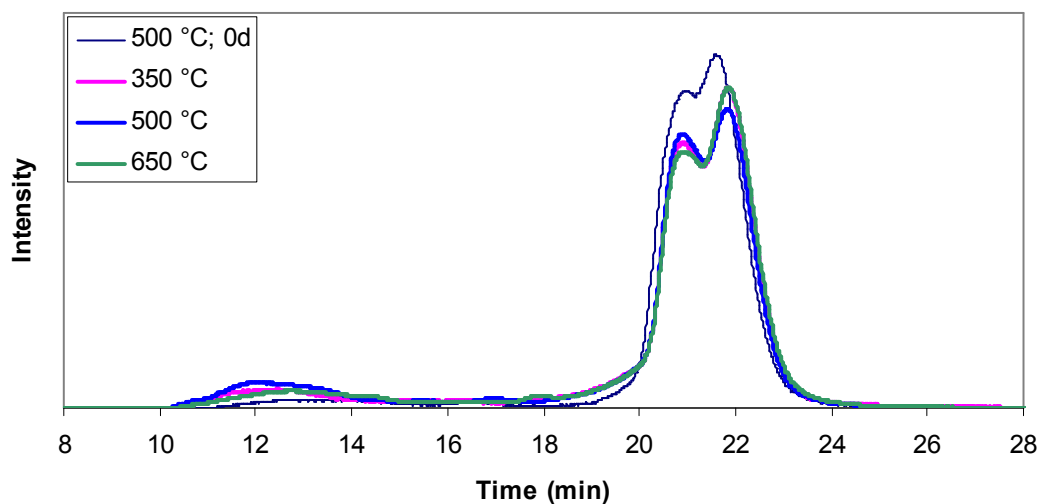


Fig. 5.48 – First oil produced at different pyrolysis temperature: GPC chromatograms after 2 weeks of storage

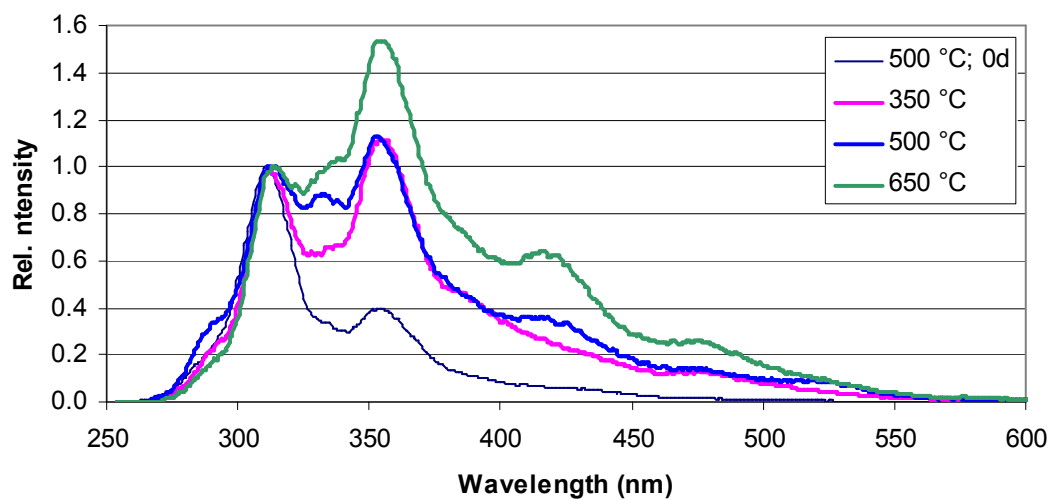


Fig.. 5.49 – First oil produced at different pyrolysis temperature: UVF spectra after 2 weeks of storage

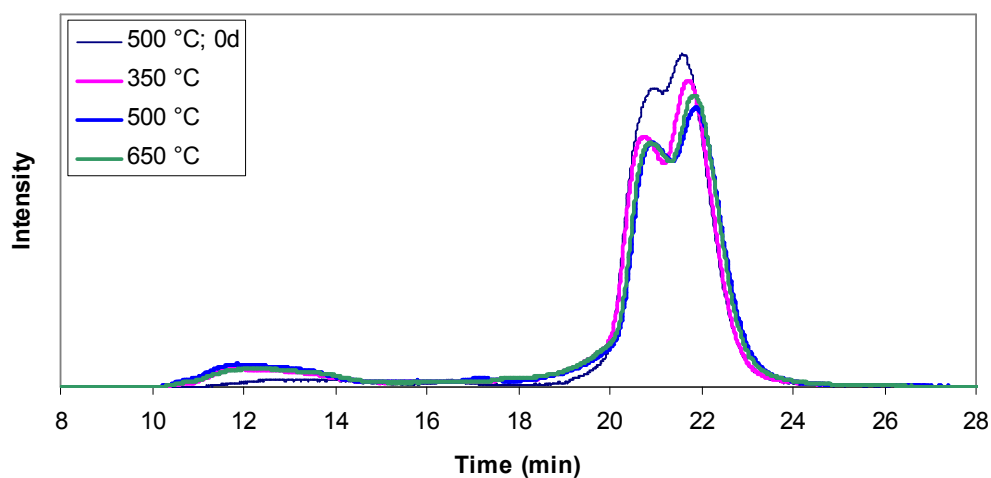


Fig. 5.50 – First oil produced at different pyrolysis temperature: GPC chromatograms after 4 weeks of storage

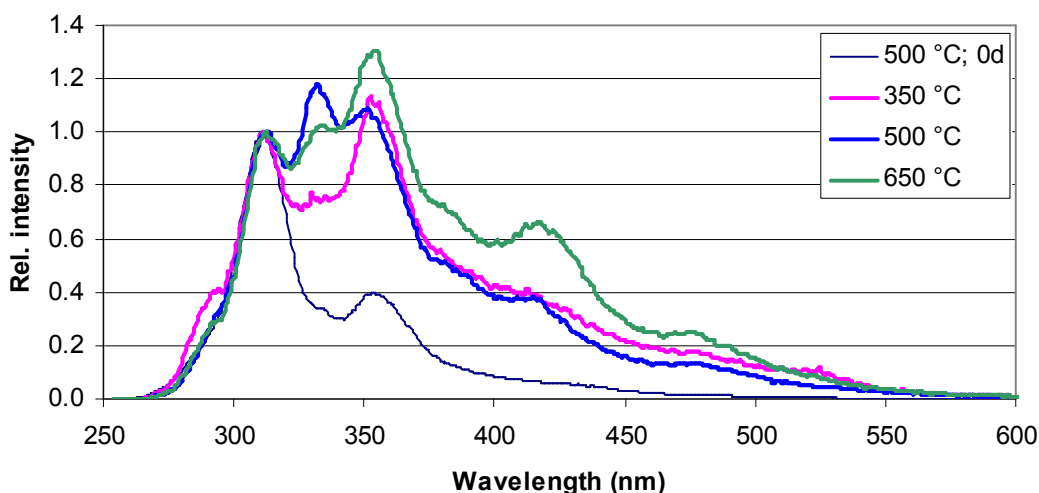


Fig. 5.51 – First oil produced at different pyrolysis temperature: UVF spectra after 4 weeks of storage

GPC and UVF data after 2 and 4 weeks show that recombination reactions occurred with intensity in all the first oil samples, even if samples obtained at higher temperature seems to be affected by a stronger structural recombination. UVF spectra reveal a delay in the peak switching in the sample produced from pyrolysis at 350 °C. Chromatograms are instead more similar and suggest a quick loss of light compounds and a constant increase of high molecular weight material. This trend seemed to slow down with time and after 2 weeks no significant differences were apparent.

Effects due to the storage temperature

The effects due to the storage temperature were investigated with GPC and UVF on some oil samples. The following samples were stored in fridge (about 5 °C) and monitored over time:

- first oil from pyrolysis of SO at 500 °C (see figure 5.52 and figure 5.53);
- first oil and second oil from pyrolysis of SO at 500 °C mixed with methanol (25% by weight of the final solution) (see figure 5.54 and figure 5.55);
- first oil and second oil from pyrolysis of SO at 500 °C mixed with methanol (50% by weight of the final solution) (see figure 5.56 and figure 5.57);
- first oil from pyrolysis of SO at 350 °C (see figure 5.58 and figure 5.59);
- first oil from pyrolysis of SO at 650 °C (see figure 5.60 and figure 5.61).

Data obtained from GPC and UVF show that low storage temperatures stopped the ageing process in all the samples. It is however worthy observing that the sample of first oil produced from pyrolysis at 650 °C resulted to react slightly after 4 weeks. If no anomalies were present, this may support the hypothesis that bio-oils produced at higher pyrolysis temperatures have higher reactivity.

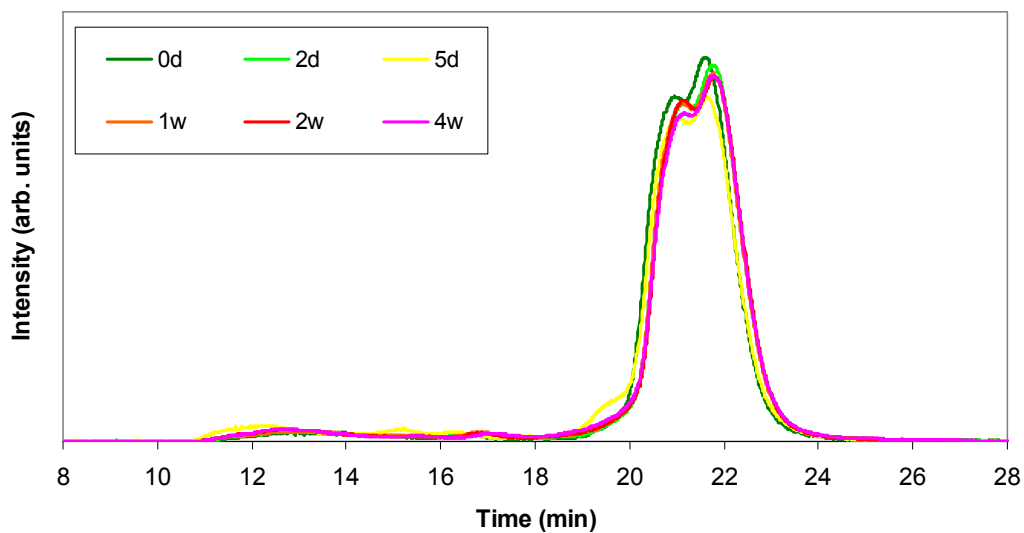


Fig. 5.52 – GPC chromatograms obtained with first oil produced from pyrolysis at 500 °C and stored at 5 °C

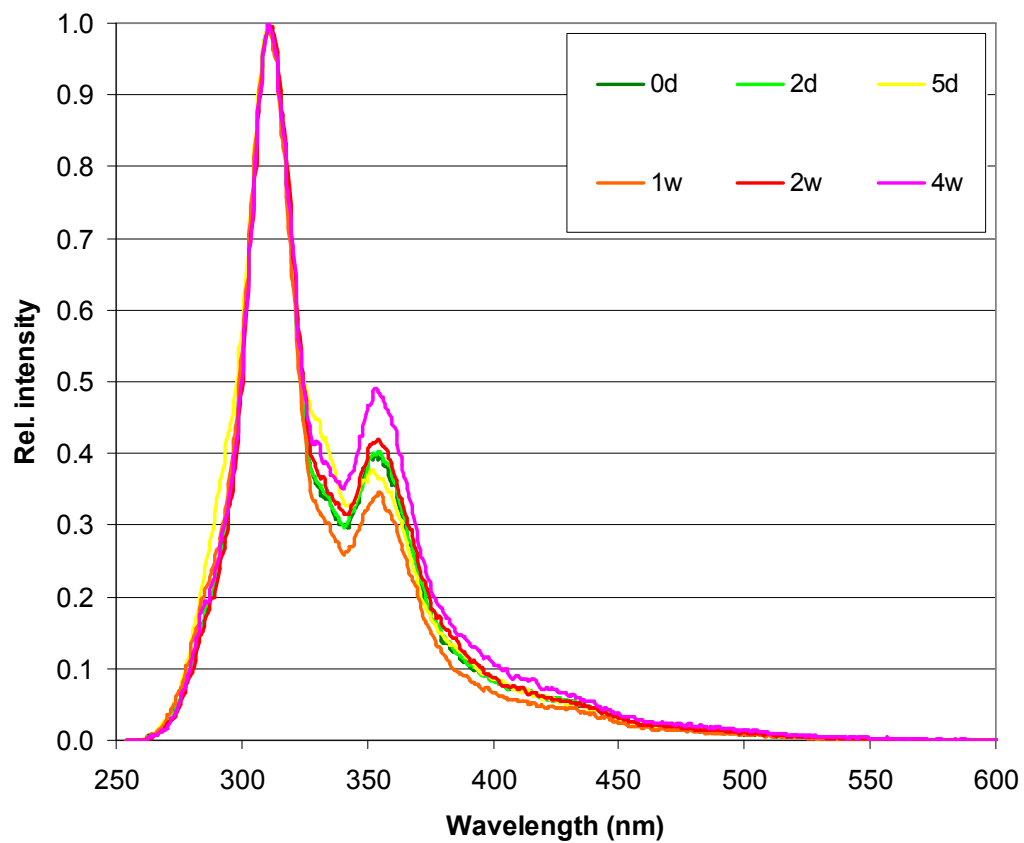


Fig. 5.53 – UVF spectra obtained with first oil produced from pyrolysis at 500 °C and stored at 5 °C

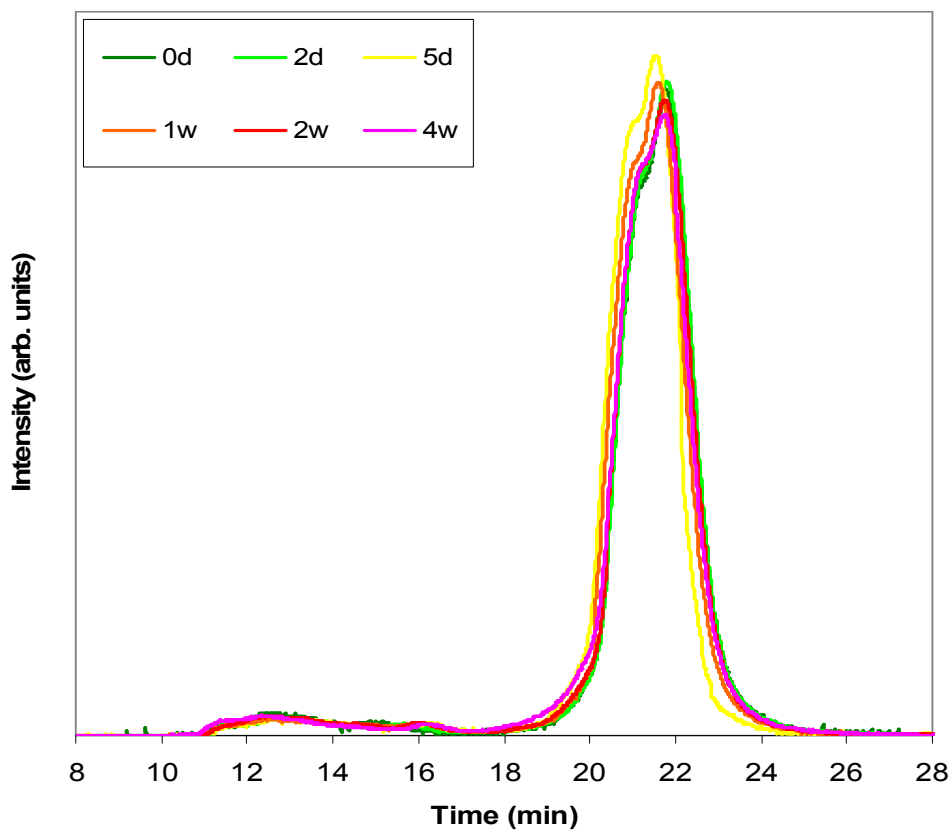


Fig.5.54 – GPC chromatograms obtained with the first oil and second oil from pyrolysis of SO at 500 °C mixed with methanol (25% by weight of the final solution)

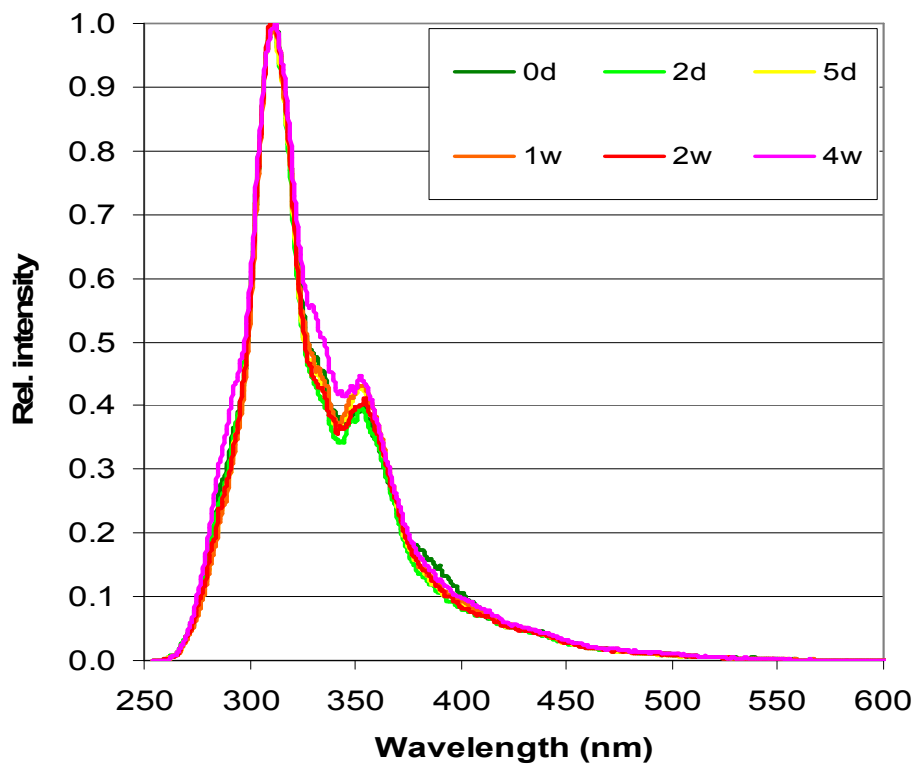


Fig. 5.55 – UVF spectra obtained with the first oil and second oil from pyrolysis of SO at 500 °C mixed with methanol (25% by weight of the final solution)

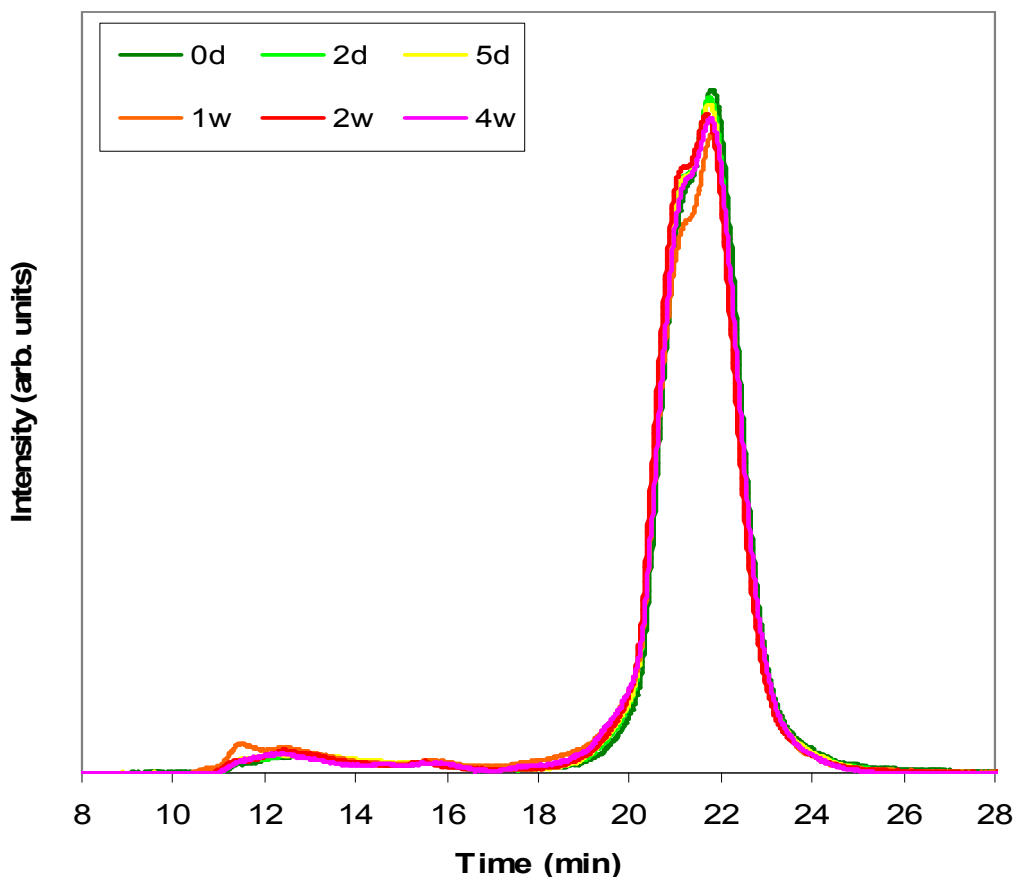


Fig. 5.56 – GPC chromatograms obtained with the first oil and second oil from pyrolysis of SO at 500 °C mixed with methanol (50% by weight of the final solution)

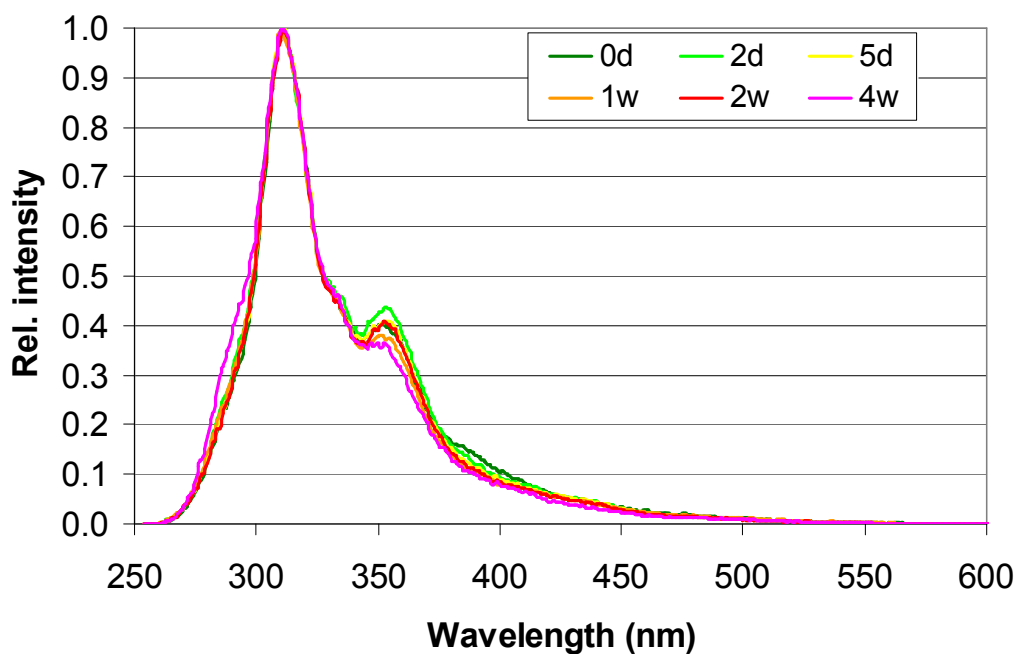


Fig. 5.57 – UVF spectra obtained with the first oil and second oil from pyrolysis of SO at 500 °C mixed with methanol (25% by weight of the final solution)

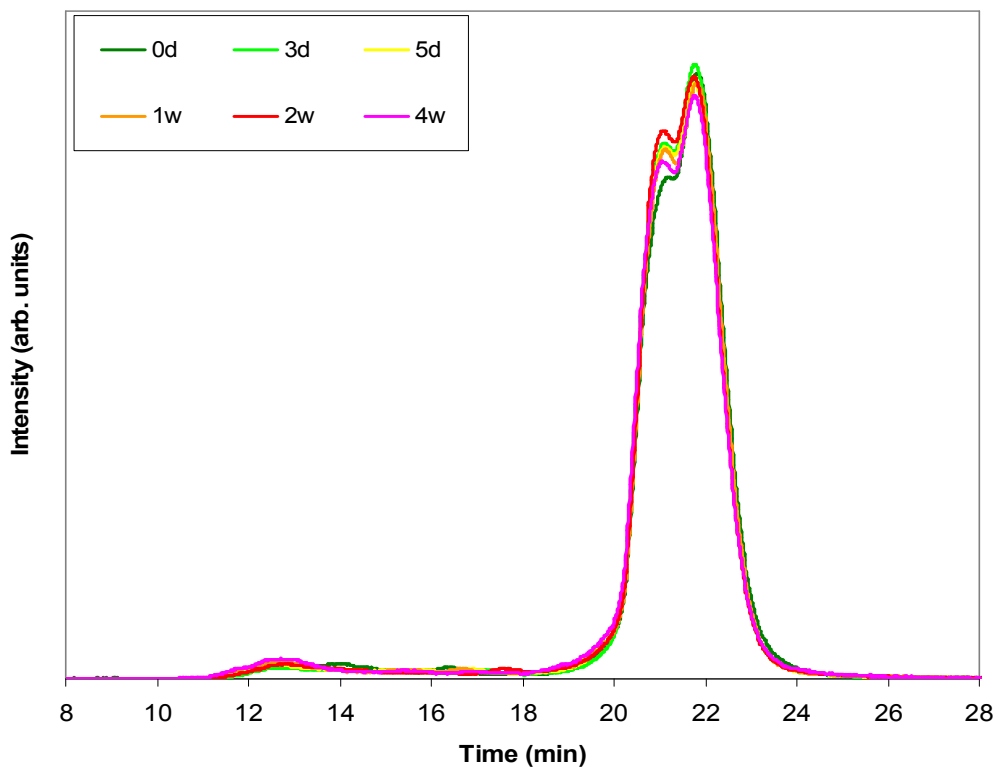


Fig. 5.58 – GPC chromatograms obtained with first oil produced from pyrolysis at 350 °C and stored at 5 °C

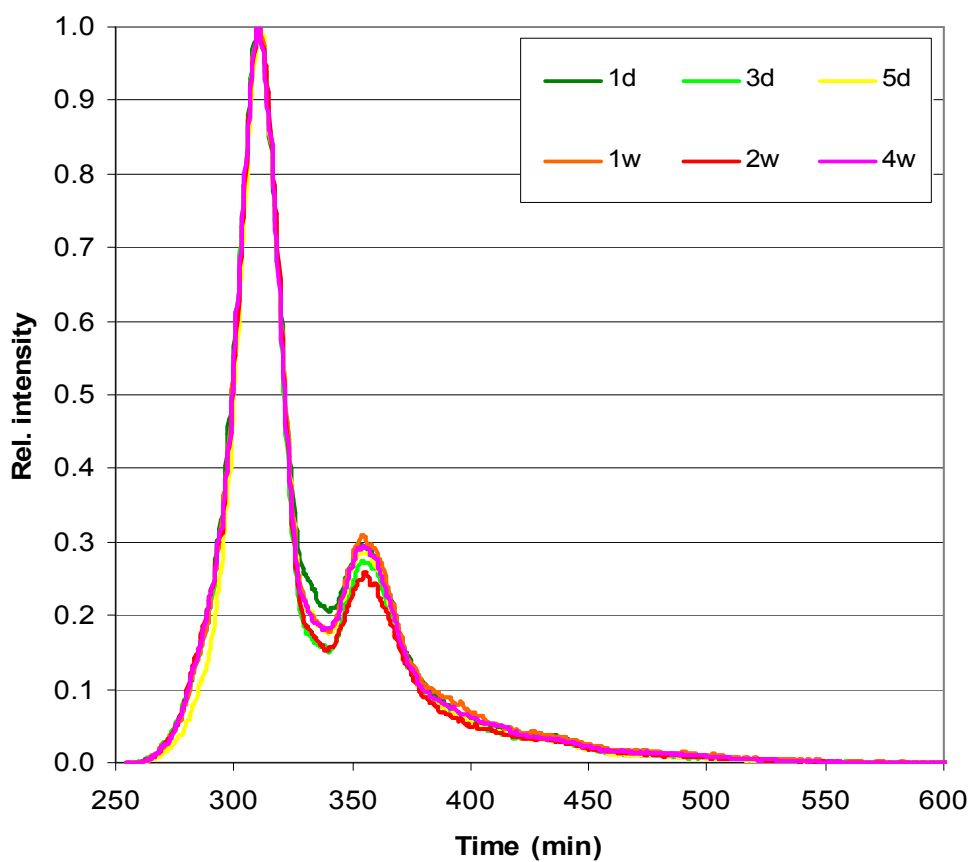


Fig. 5.59 – UVF spectra obtained with first oil produced from pyrolysis at 350 °C and stored at 5 °C

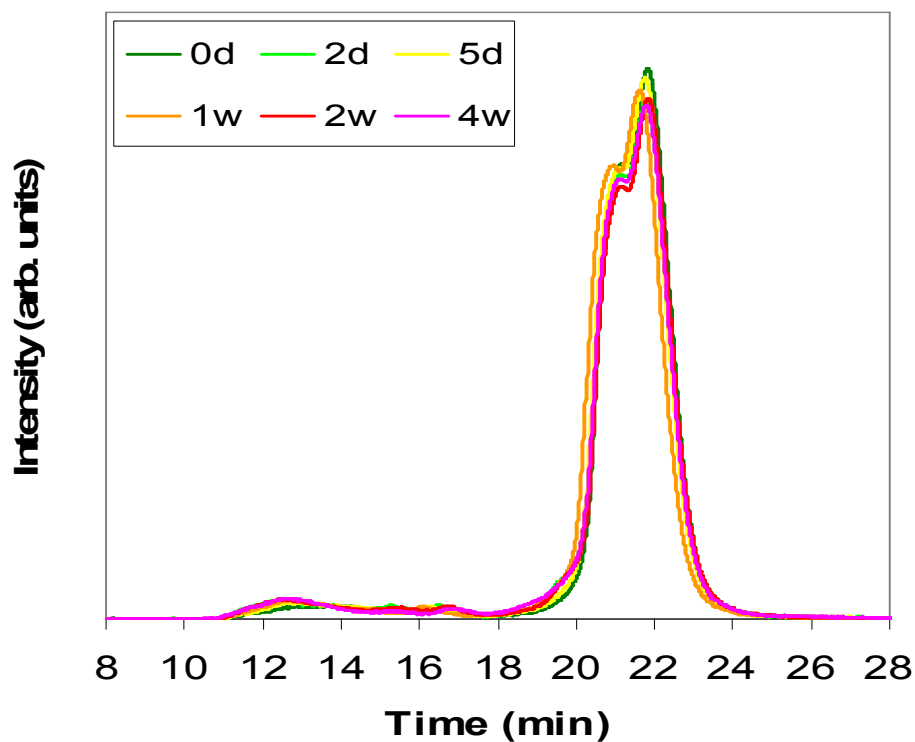


Fig. 5.60 – GPC chromatograms obtained with first oil produced from pyrolysis at 650 °C and stored at 5 °C

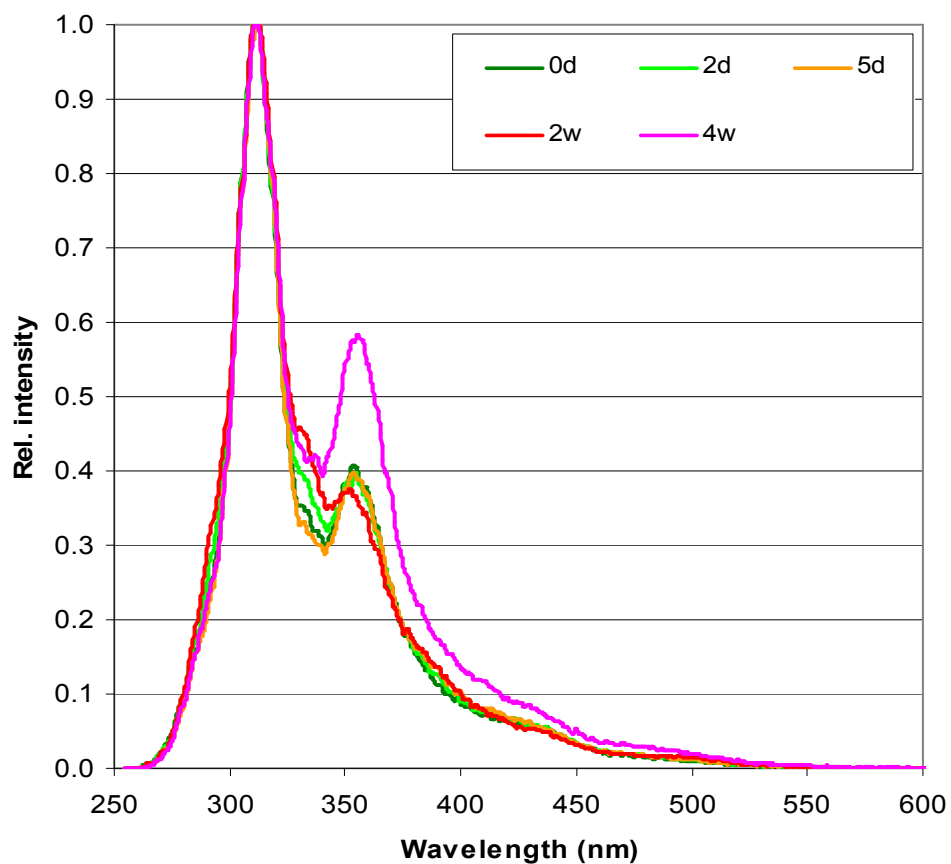


Fig. 5.61 – UVF spectra obtained with first oil produced from pyrolysis at 650 °C and stored at 5 °C

Effects due to the biomass feedstock

GPC and UVF analysis was performed on oil samples produced from pyrolysis of SW and CS at 500 °C. Batch samples were obtained from oils with methanol and acetone in different concentrations. This was necessary in order to understand if the results obtained with SO were repeatable or not with a different feedstock.

Results of the analysis on first oil from SW are reported in figure 5.62 and in figure 5.63. Further analysis considered second oil from SW (figure 5.64 and figure 5.65) and then first oil from SW mixed with methanol (figures 5.66, 5.67, 5.68, 5.69) and with acetone (figures 5.70, 5.71, 5.72, 5.73) to 10% and 25% of solvent concentration.

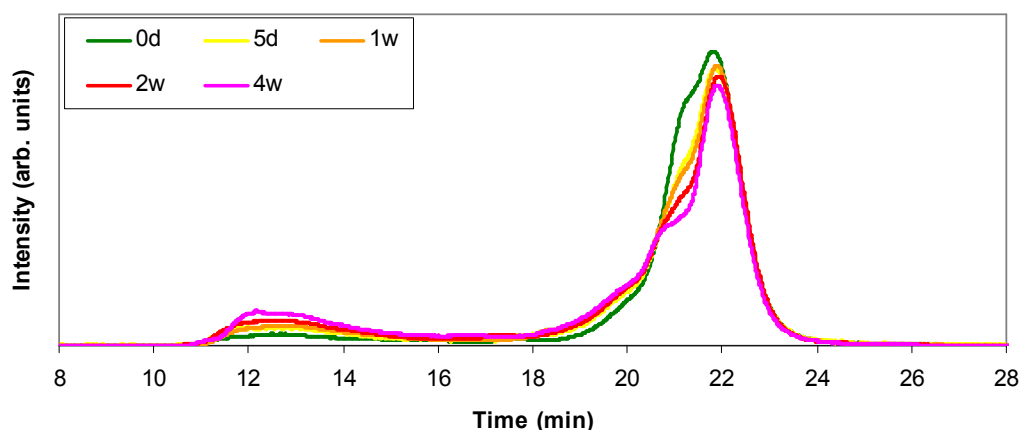


Fig. 5.62 – GPC chromatograms of first oil from SW. Pyrolysis temperature: 500 °C; storage: ambient temperature

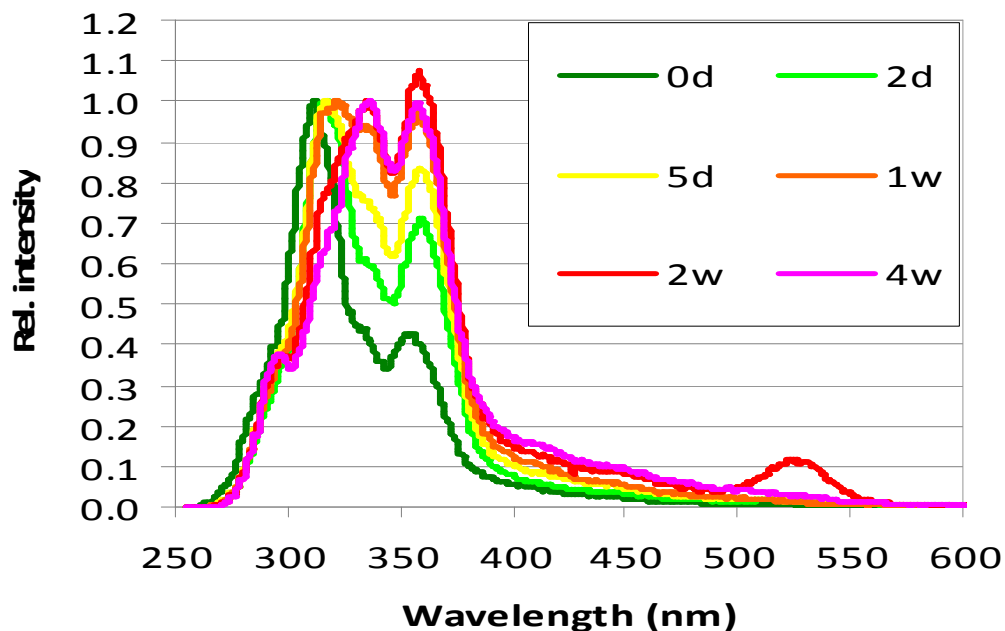


Fig. 5.63 – UVF spectra of first oil from SW. Pyrolysis temperature: 500 °C; storage: ambient temperature

Chromatograms and spectra of first oil from SW reveal a great extent of recombination reactions. Excluded and main peaks of the GPC chromatograms respectively increase and decrease with time. The occurrence of polymerisation is

evidenced also by the UVF spectra, in which the second peak increases its intensity while the first peak shifts towards right, i.e. towards higher wavelengths.. Apparent structural differences are moreover present in comparison with first oil from SO, probably as a consequence of the different biomass composition.

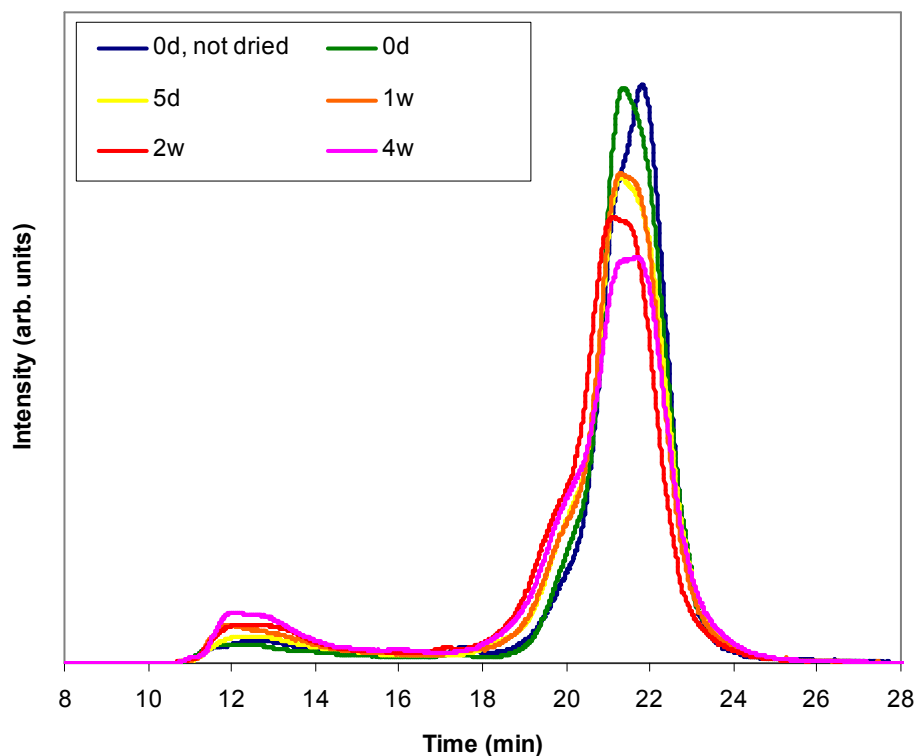


Fig. 5.64 – GPC chromatograms of second oil, methanol dried, from SW. Pyrolysis temperature: 500 °C; storage: ambient temperature

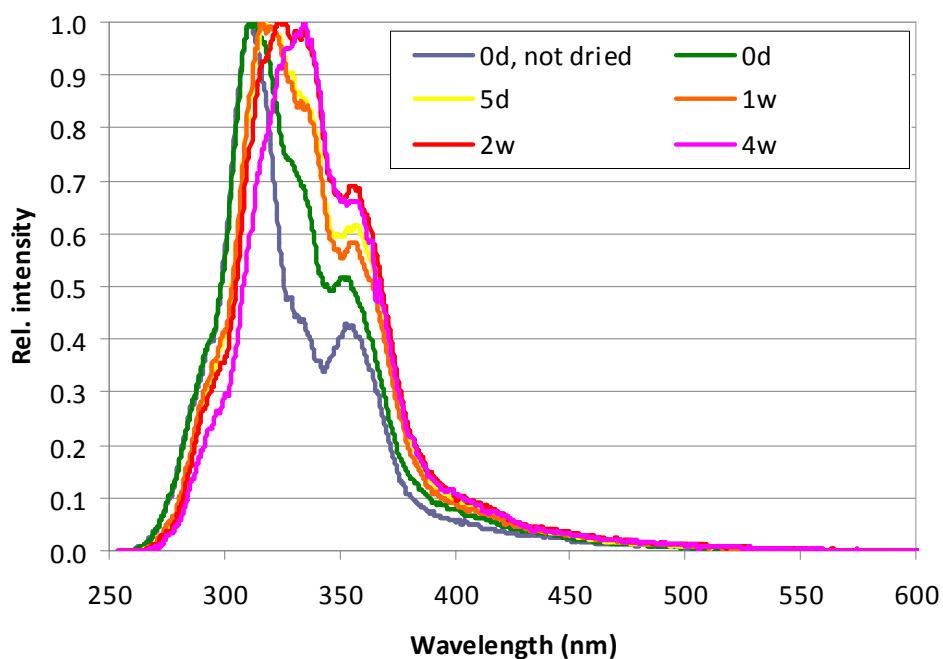


Fig. 5.65 – UVF spectra of second oil, methanol dried, from SW. Pyrolysis temperature: 500 °C; storage: ambient temperature

Unlike second oil from SO, GPC and UVF data show that second oil from SW appears quite reactive. This outcome may indicate a higher reactivity for bio-oils originated from SW.

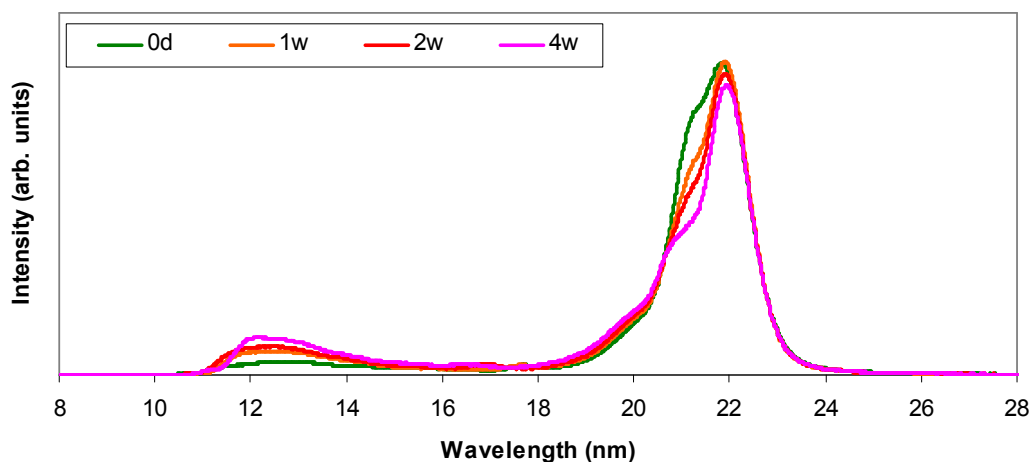


Fig. 5.66 – GPC chromatograms of first oil from SW mixed with methanol. Methanol concentration: 10%; pyrolysis temperature: 500 °C; storage: ambient temperature

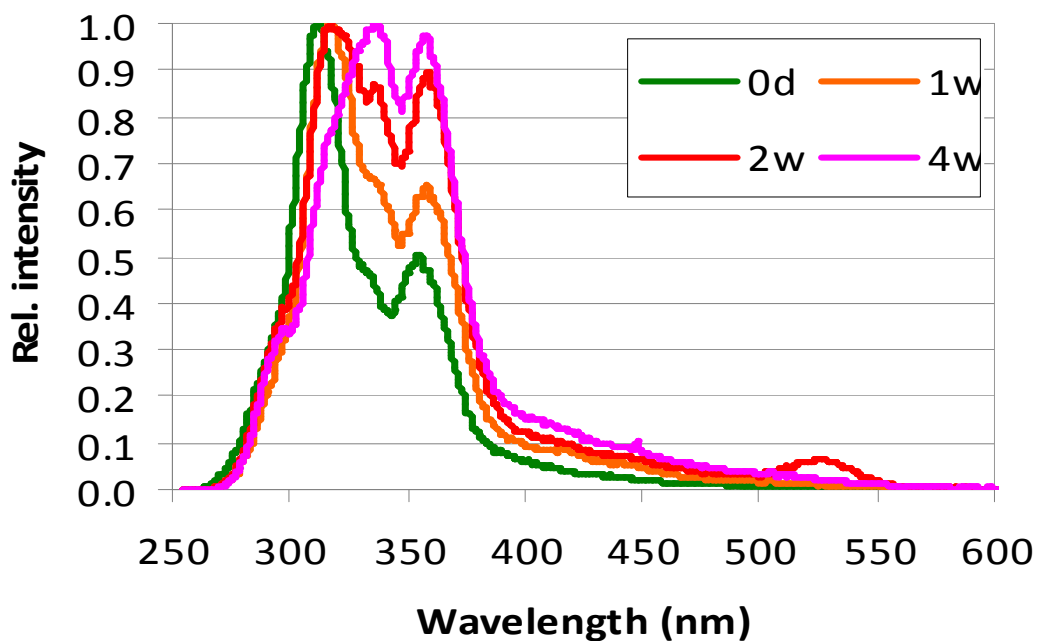


Fig. 5.67 – UVF spectra of first oil from SW mixed with methanol. Methanol concentration: 10%; pyrolysis temperature: 500 °C; storage: ambient temperature

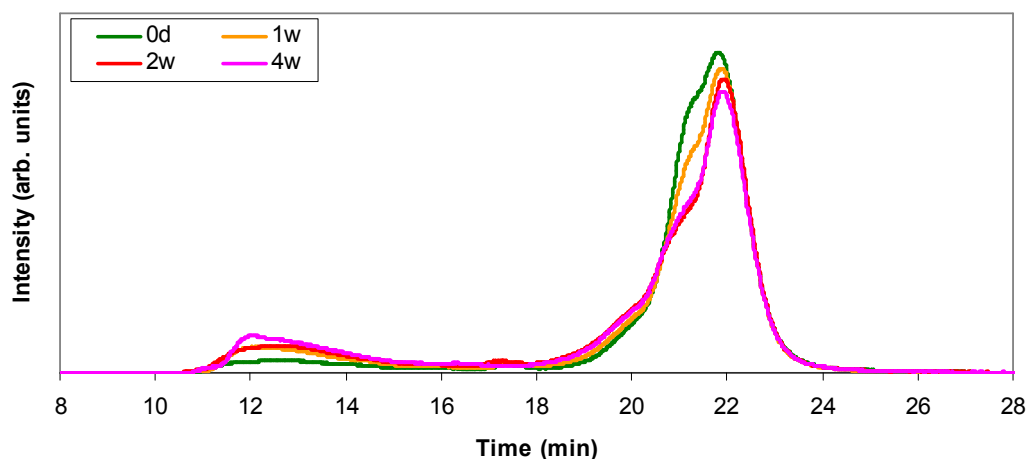


Fig. 5.68 – GPC chromatograms of first oil from SW mixed with methanol. Methanol concentration: 25%; pyrolysis temperature: 500 °C; storage: ambient temperature

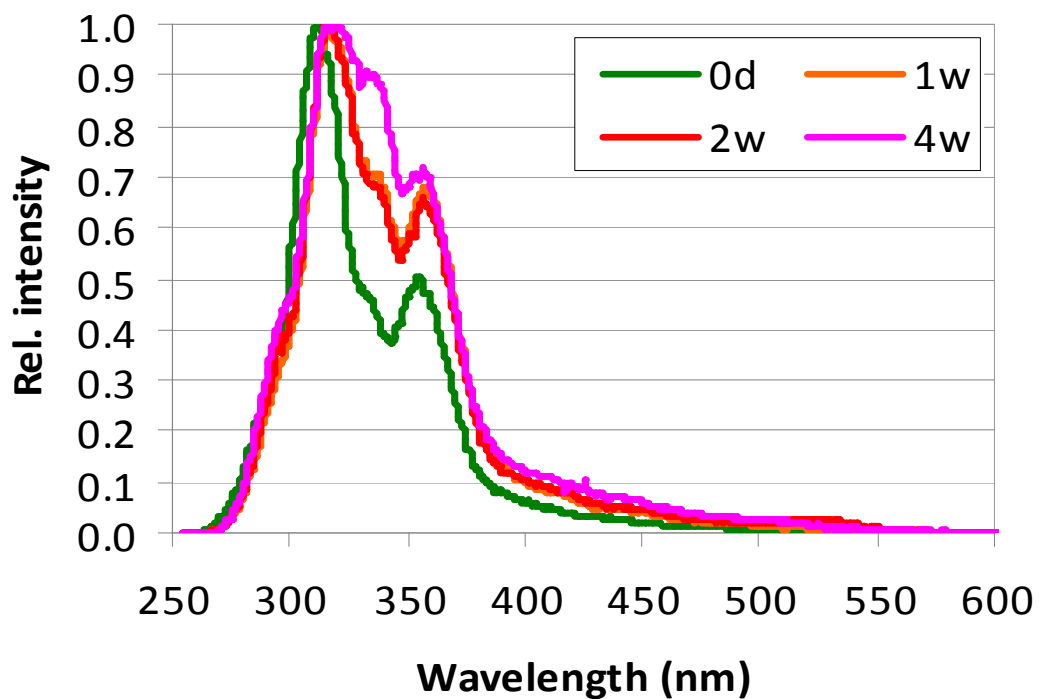


Fig. 5.69 – UVF spectra of first oil from SW mixed with methanol. Methanol concentration: 25%; pyrolysis temperature: 500 °C; storage: ambient temperature

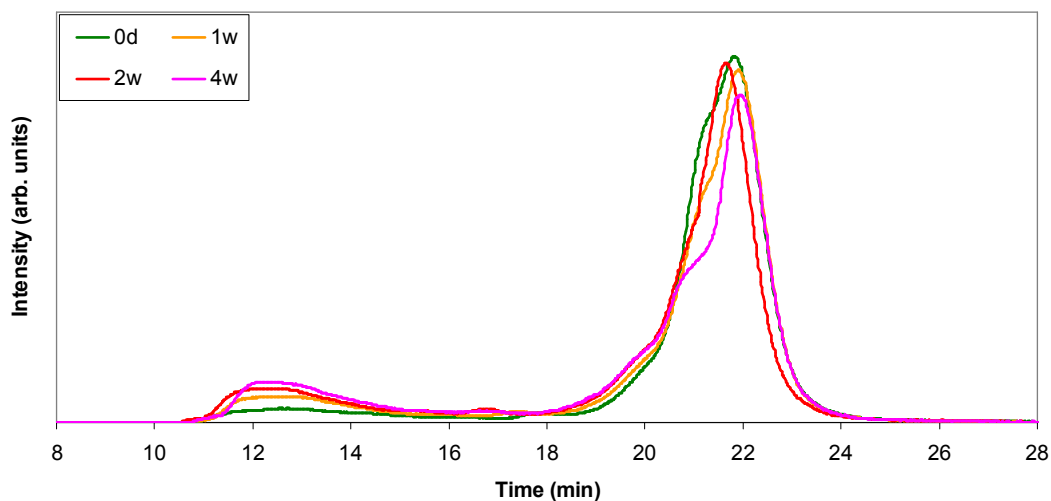


Fig. 5.70 – GPC chromatograms of first oil from SW mixed with acetone. Acetone concentration: 10%; pyrolysis temperature: 500 °C; storage: ambient temperature

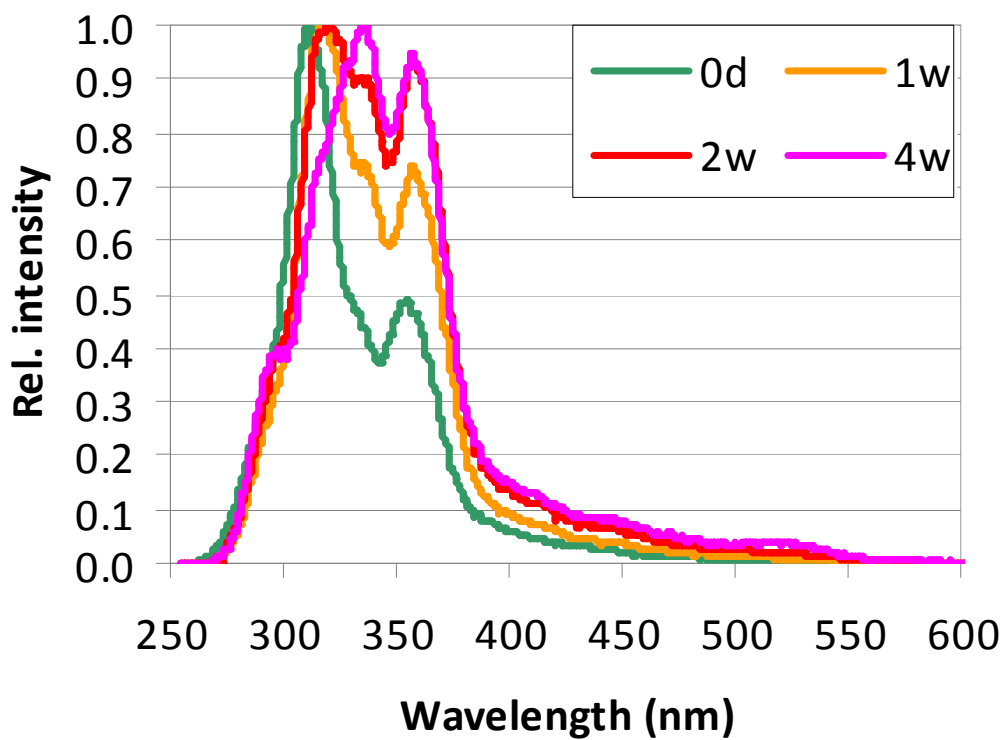


Fig. 5.71 – UVF spectra of first oil from SW mixed with acetone. Acetone concentration: 10%; pyrolysis temperature: 500 °C; storage: ambient temperature

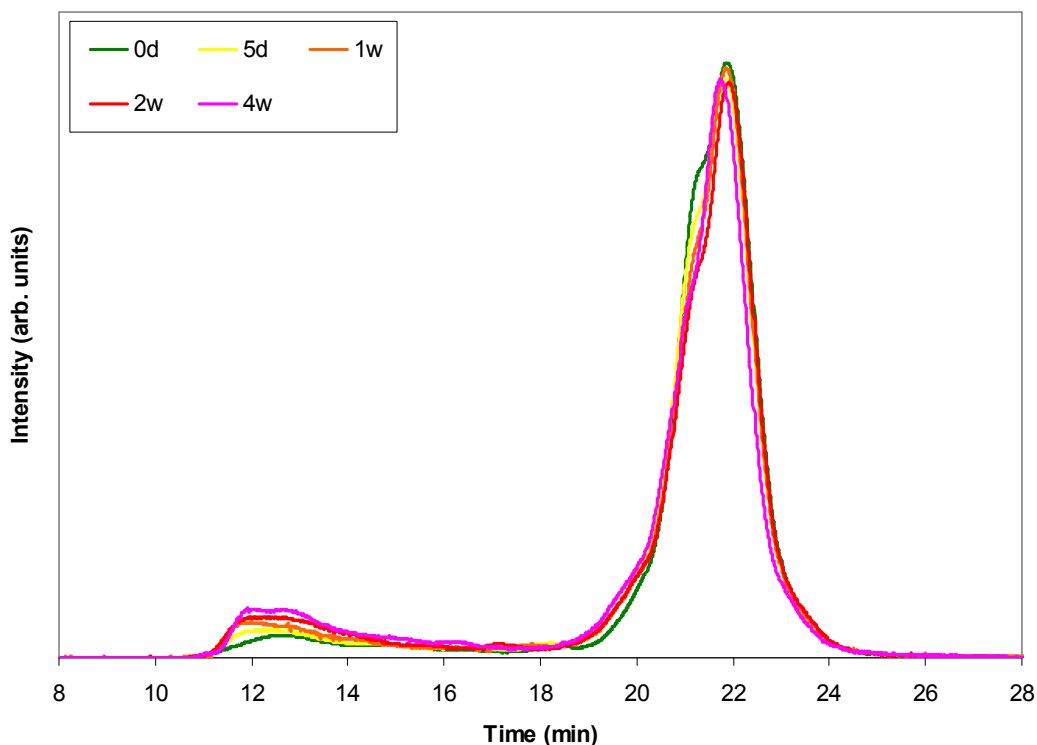


Fig. 5.72 – GPC chromatograms of first oil from SW mixed with acetone. Acetone concentration: 25%; pyrolysis temperature: 500 °C; storage: ambient temperature

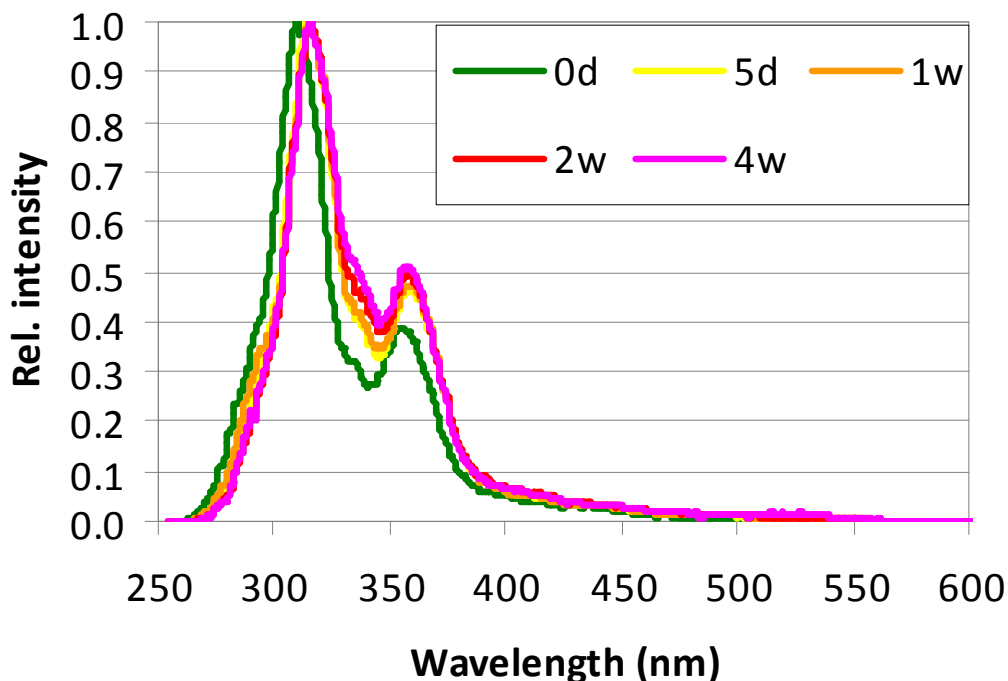


Fig. 5.73 – UVF spectra of first oil from SW mixed with acetone. Acetone concentration: 25%; pyrolysis temperature: 500 °C; storage: ambient temperature

No matter the solvent used, previous plots suggest that a 10% concentration in solvent slows down ageing, but reactivity results to be still strong. More positive effects can be obtained only with solutions at the 25% of solvent, even if the extent of recombination reactions when methanol was used appeared still significant if

compared with SO. A good stabilisation was instead obtained with acetone. This supports the possibilities that oils from SW are more reactive than oils from SO and that acetone may have a better effectiveness, in comparison with methanol, in the prevention of the ageing effects.

Analysis on first oil from CS is reported in figure 5.74 and in figure 5.75. Further analysis concerned with first oil from CS mixed with methanol (figures 5.76, 5.77, 5.78, 5.79) and with acetone (figures 5.80, 5.81). 10% and 25% solvent concentration were tested.

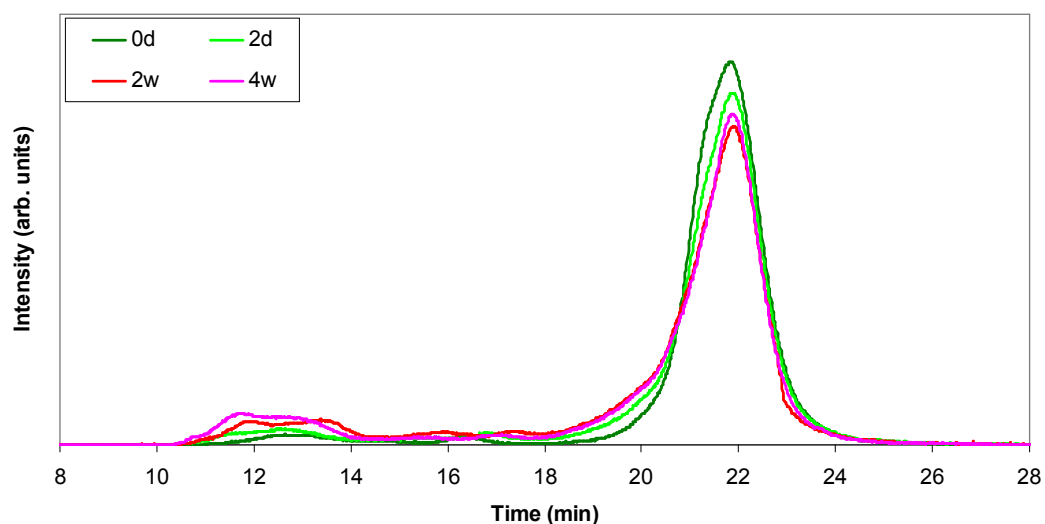


Fig. 5.74 – GPC chromatograms of first oil from CS. Pyrolysis temperature: 500 °C; storage: ambient temperature

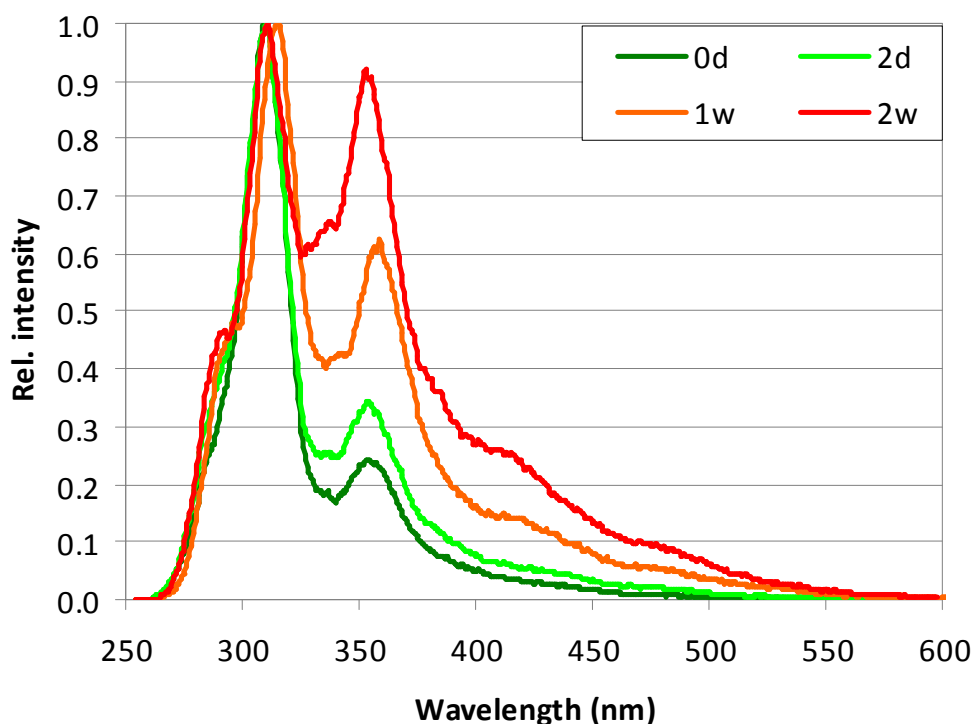


Fig. 5.75 – UVF spectra of first oil from CS. Pyrolysis temperature: 500 °C; storage: ambient temperature

Shapes of chromatograms and spectra from CS first oil resulted to be similar to the ones obtained with SO and to change equally on time. No points of stabilisation were reached during the study, nevertheless, curves suggest that CS first oil may be slightly less reactive than the other oils investigated.

Ageing was slowed down in sample containing the 10% of methanol but significant effects of time were still apparent. A 25% concentration of methanol instead led to more beneficial effects. Recombination reactions appeared to have occurred with less intensity in this sample if compared with the same from SO. Acetone seems to work with the same effectiveness of methanol in the CS oil samples.

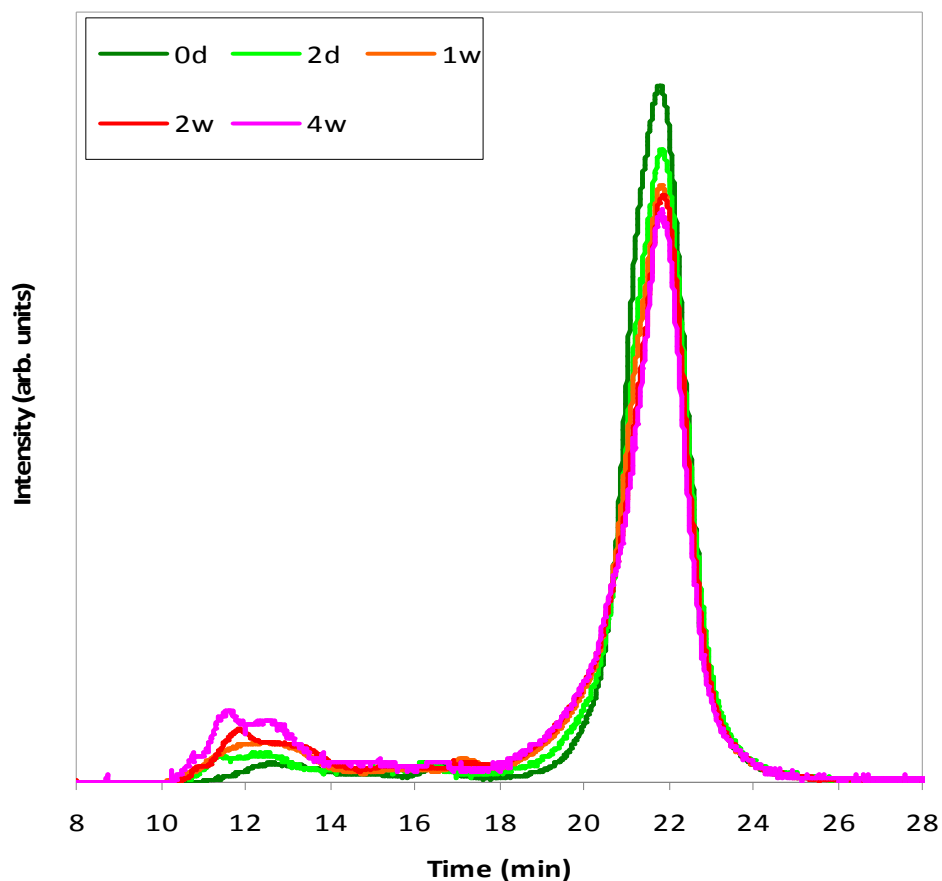


Fig. 5.76 – GPC chromatograms of first oil from CS mixed with methanol. Methanol concentration: 10%; pyrolysis temperature: 500 °C; storage: ambient temperature

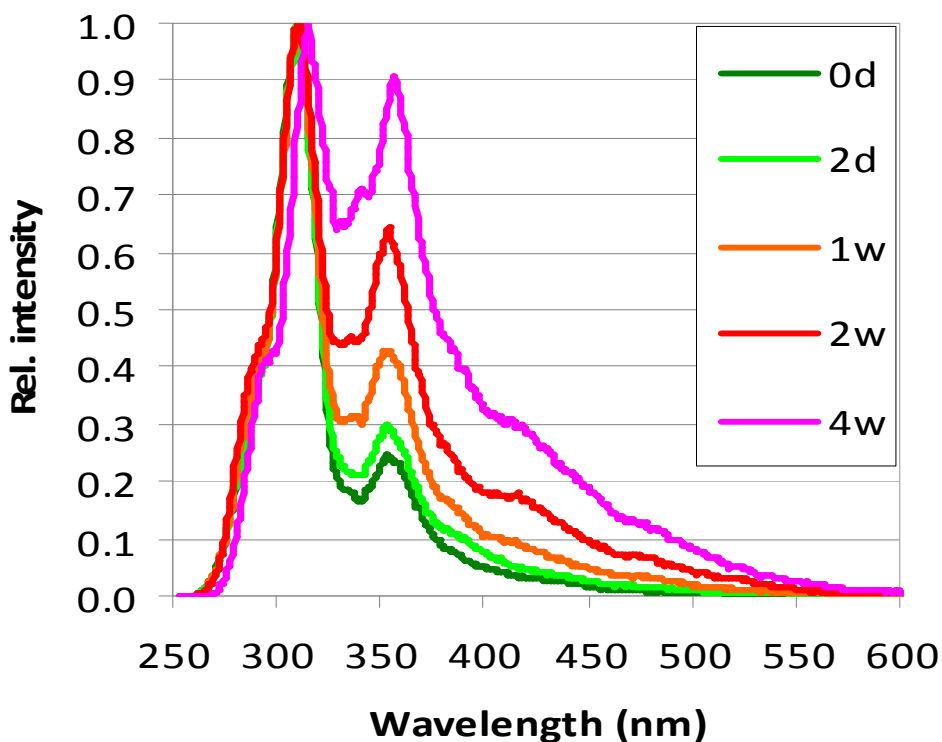


Fig. 5.77 – UVF spectra of first oil from CS mixed with methanol. Methanol concentration: 10%; pyrolysis temperature: 500 °C; storage: ambient temperature

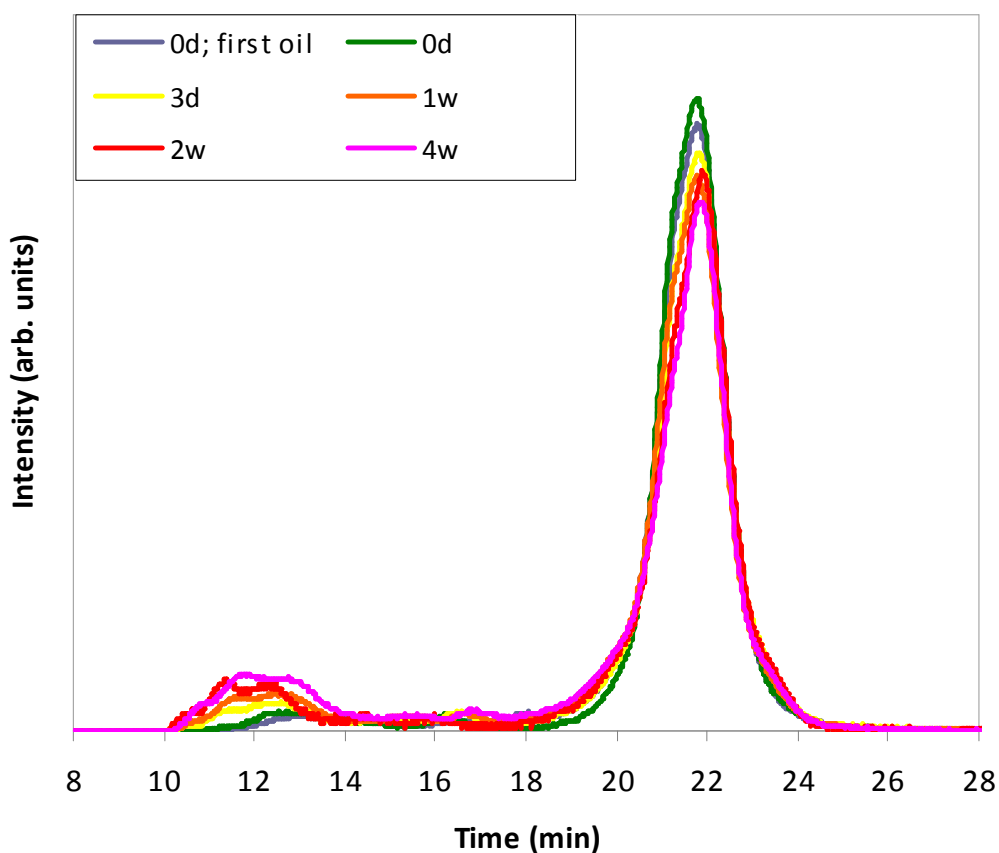


Fig. 5.78 – GPC chromatograms of first oil from CS mixed with methanol. Methanol concentration: 25%; pyrolysis temperature: 500 °C; storage: ambient temperature

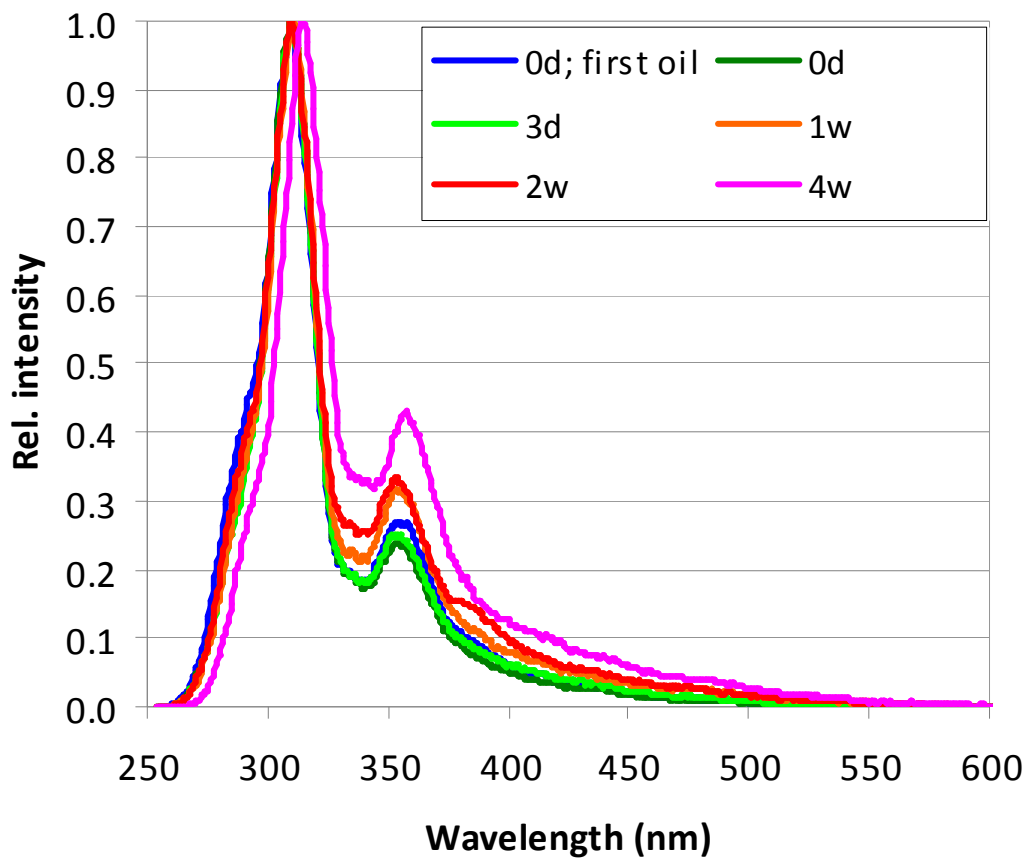


Fig. 5.79 – UVF spectra of first oil from CS mixed with methanol. Methanol concentration: 25%; pyrolysis temperature: 500 °C; storage: ambient temperature

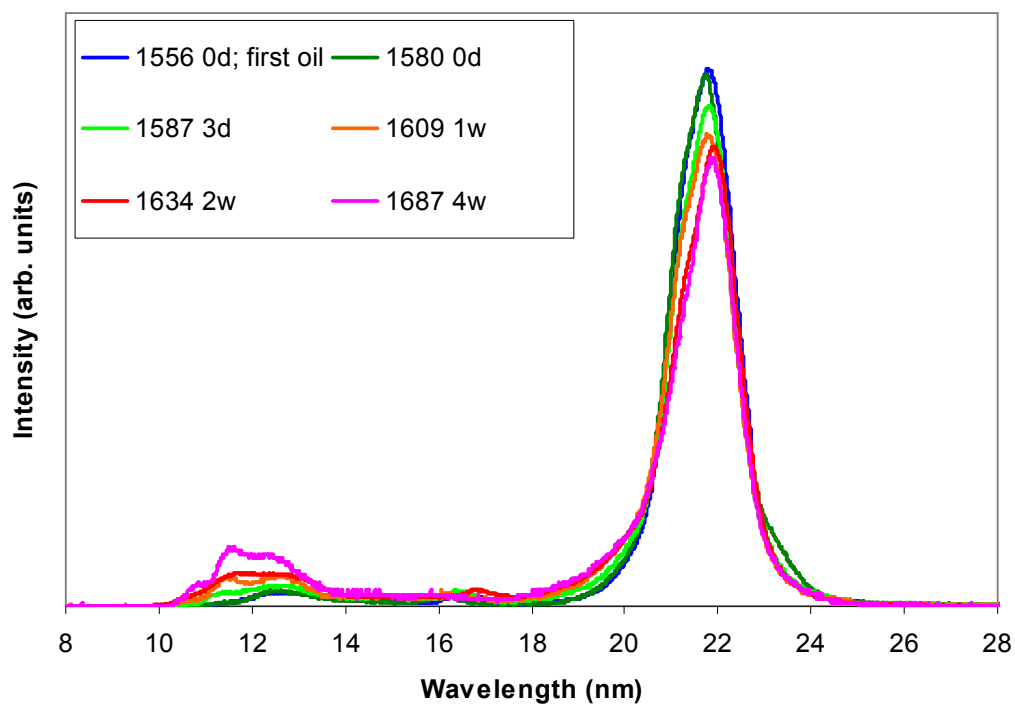


Fig. 5.80 – GPC chromatograms of first oil from CS mixed with acetone. Acetone concentration: 25%; pyrolysis temperature: 500 °C; storage: ambient temperature

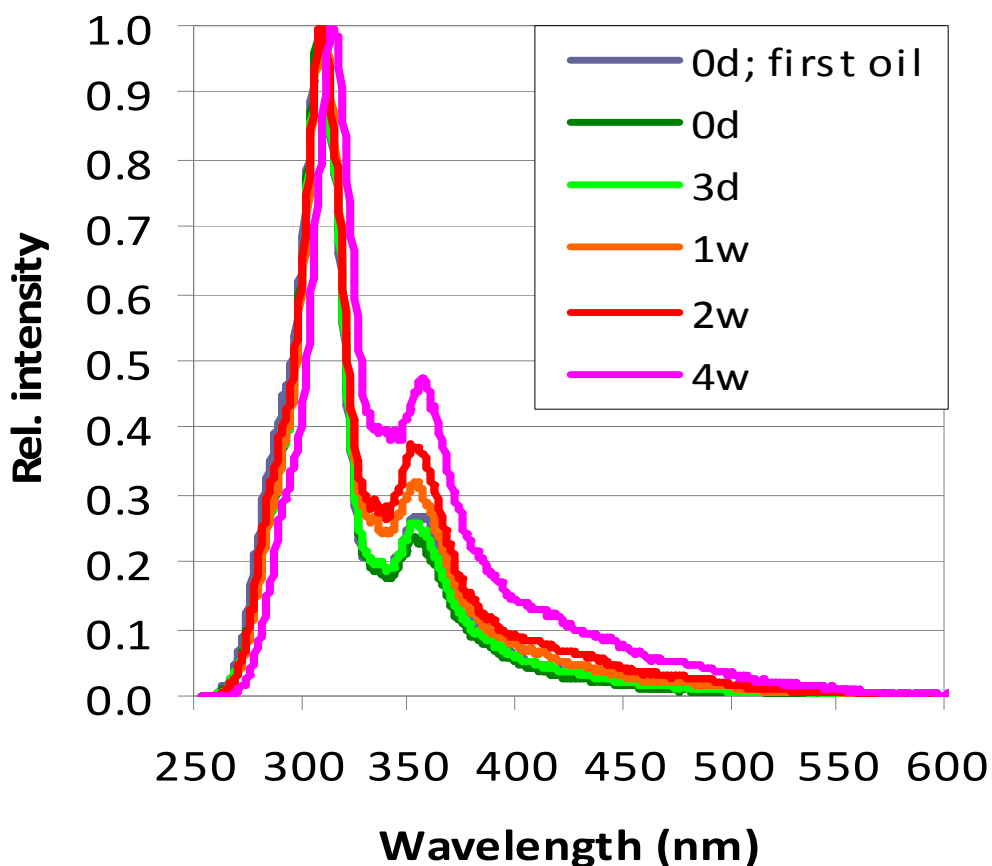


Fig. 5.81 – UVF spectra of first oil from CS mixed with acetone. Acetone concentration: 25%; pyrolysis temperature: 500 °C; storage: ambient temperature

Other marginal investigations

The effect of oil filtration was investigated with GPC and UVF on a sample of first oil produced from pyrolysis of SO at 500 °C. Results of the analysis are shown in figure 5.82 and in figure 5.83.

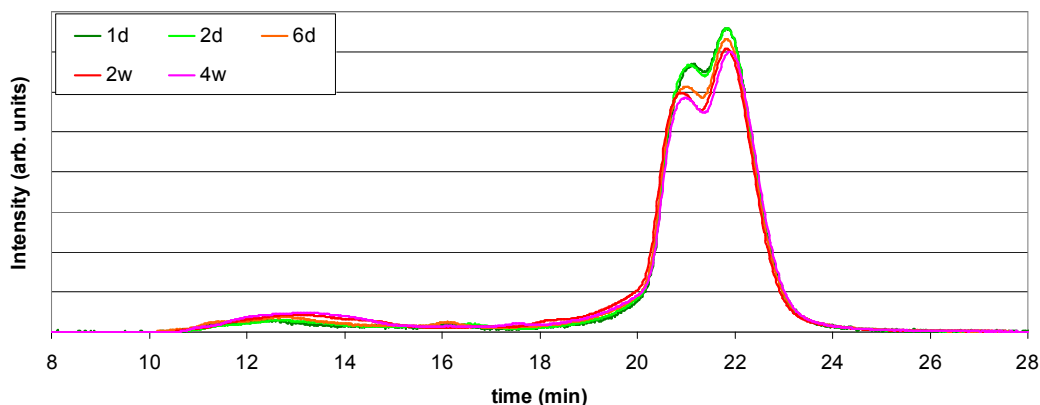


Fig. 5.82 – GPC analysis of unfiltered first oil from pyrolysis of SO at 500 °C

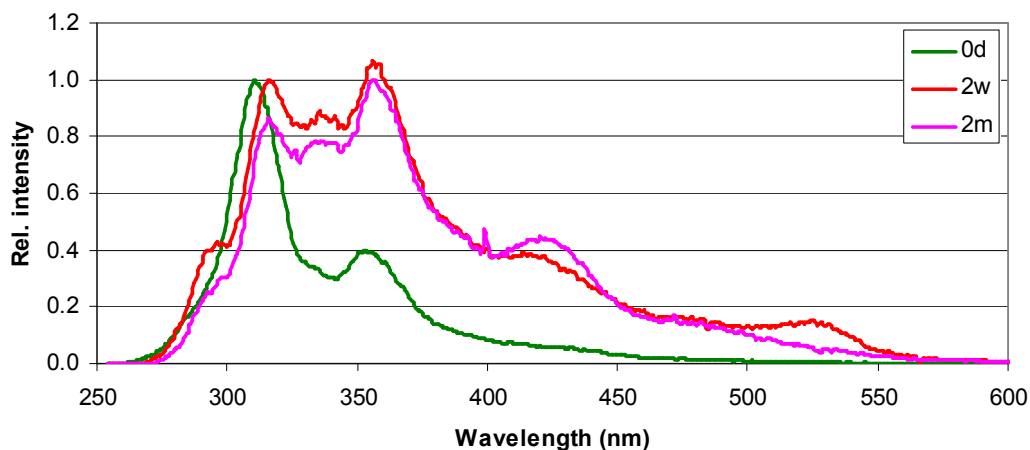


Fig. 5.83 – UVF analysis of unfiltered first oil from pyrolysis of SO at 500 °C

Eventual presence of char particles would have been supposed to increase the extent of polymerisation reactions but no significant differences were detected between the samples filtered and not filtered. This may mean that char particles were not present in the oil or, if present, their microscopic scale was not enough effective to catalyse polymerisation reactions with high intensity.

Further GPC and UVF analysis involved:

- the oil fraction trapped in the filter, named “exit oil” and roughly accounting for the 10% of the total oil;
- the oil fraction collected in the retort, named “retort oil” and roughly accounting for the 10% of the total oil.

Oil was produced from pyrolysis of SO at 500 °C and collected with a not measured amount of methanol and analysed without drying. Figure 5.84 and figure 5.85 present chromatograms and spectra obtained.

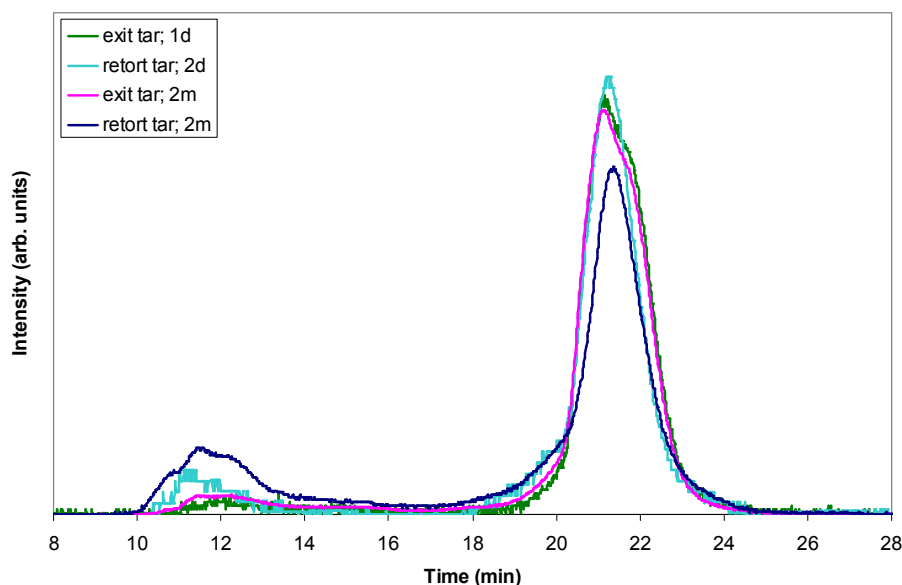


Fig. 5.84 – GPC analysis of marginal oil fractions from pyrolysis of SO at 500 °C

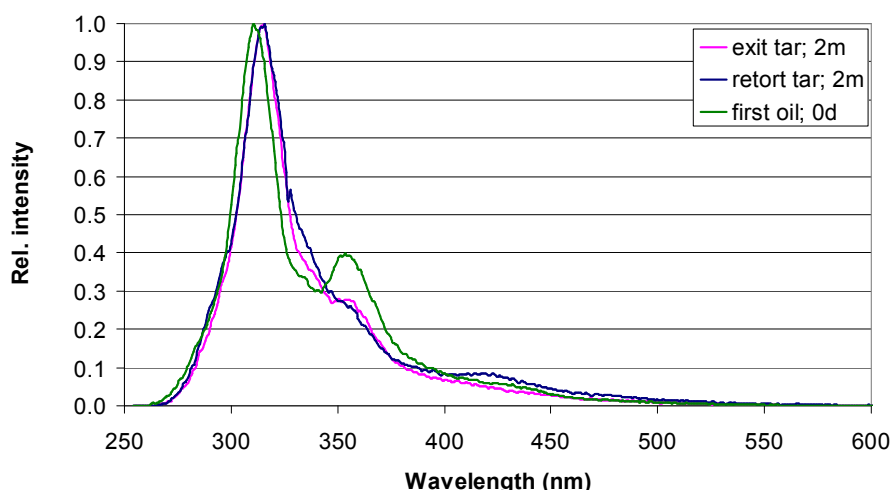


Fig. 5.85 – UVF analysis of marginal oil fractions from pyrolysis of SO at 500 °C

From the analysis of the GPC results, exit oil seemed to be stable over time, even if this may be due to the effect of the methanol dissolved. On the contrary, retort oil was characterised by the presence of reactions leading to polymerisation and molecular weight increase also in presence of methanol. On the other side, exit oil and retort oil presented the same UVF spectra after 2 months of ambient temperature storage. UVF spectra suggest the presence of lighter aromatic structures in these oil fractions in comparison with first and second oils from pyrolysis of SO.

5.4.4 Conclusions

Quick structural changes were highlighted in the bio-oil samples analysed by mean of GPC and UVF analytical techniques. Main structural changes seem to occur with characteristic times of hours and days. Ageing reactions should lead to polymerisation of the compounds contained in the oils, polymerisation which is supposed to involve aromatic and oxygenated compounds.

IR spectra can be consistent with the ageing mechanism proposed by [Diebold, 2000] but the available experimental technique did not allow the discovery of new information on the ageing mechanism.

Results of the analysis confirmed the positive effects on bio-oil stabilisation due to:

- addition of a solvent (i.e. methanol or acetone);
- low storage temperatures (i.e. 5 °C).

Solvents as methanol and acetone are supposed not only to dilute the bio-oil but also to shift the equilibrium composition to a mixture with lower molecular weight compounds. Low storage temperature should instead influence kinetics of the ageing reactions, decreasing reaction kinetics up to the apparent repression of the occurrence of recombination reactions.

With regard to the solvents tested, no particular differences were found between methanol and acetone, even if they resulted to completely stop the ageing process in concentrations higher than 10%. It is however obvious that a high solvent application would be not sustainable. Lower solvent concentration (i.e. 10%) were able only to slow down the structural changes occurring during the ageing process. Nevertheless, parameters like viscosity or water content should be also monitored in order to draw more accurate conclusions.

On the contrary, aqueous phase of bio-oils was found to play a negative role on the mixture stability, as confirmed by [Boucher et al., 2000]. Residual polymeric material sticking in the walls of the condensing system may instead contain material that is more stable or, anyway, stabilised in a very short time.

No particular differences in bio-oil reactivity were depending on the pyrolysis peak temperatures, even if a slightly increase in reactivity was detected at higher temperatures. Effects due to the biomass feedstock seem to be more significant: structural differences were found in bio-oils from SW, when compared with oil samples produced from SO and from CS. As a probable consequence of the original biomass composition, oils from SW seems indeed characterized by a larger amount of clusters and a lower stability which may affect negatively their industrial application.

5.5 Assessment of the hazards due to the pyro-oil compounds

5.5.1 Introduction

Production, storage and delivery of pyro-oils can be affected by several hazards due to the presence of a wide set of classes of compounds [Diebold 2000; Garcia-Perez et al., 2007; Giudicianni, 2006; Nakai et al., 2007; Oasmaa and Peacocke, 2001]. Some of these compounds are potentially harmful to human beings and ecosystems. It is thus apparent that, in addition to fires and explosions, bio-oil hazard may be related also to the undesired release of toxic substances on the environment, whose effects on humans and ecosystems have to be quantified. Reports on the hazardous properties of liquids from biomass pyrolysis are available in literature and some material safety data sheets have also been proposed [Cirad, 2006; Oasmaa and Peacocke, 2001] but they usually describe bio-oil properties without an assessment of the hazards is fully addressed. The actual understanding of the inherent hazards due to bio-oils should be a core issue in sustainability assessment of bio-energy processes and it would be also consistent with the European REACH system [Regolamento CE n. 1907/2006 del Parlamento Europeo e del Consiglio], aimed to the improvement of the protection of human health and the environment through a better and earlier identification of the inherent properties of chemical substances.

A quantitative assessment of the physical-chemical and toxicological hazards connected to the use of bio-oils produced from biomass pyrolysis was thus performed on the basis of the methodological approach developed in this thesis and described in chapter 4. Because of the large number of bio-oil components, an assessment approach based on representative macro-components was also tested. A simplified comparison among different renewable fuels (i.e. bio-oils, biodiesel and ethanol) and a conventional fuel (i.e. a model regular gasoline) is also addressed.

5.5.2 Materials and methods

The assessment procedure is based on the experimental identification of the components contained in the pyro-oils and on the further quantification of their inherent hazard properties. A scheme of the procedure is shown in figure 5.86.

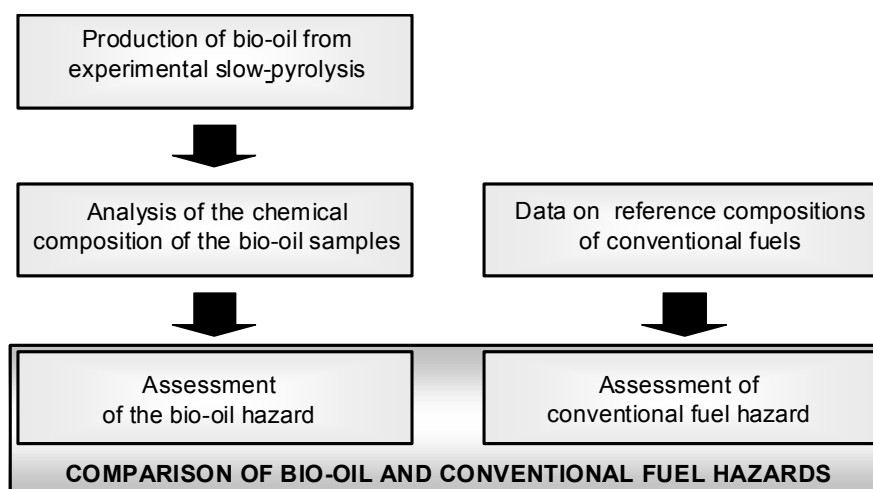


Fig. 5.86 – Assessment methodology flow chart

Pyro-oil samples were produced from pyrolysis of CS, PO and SW in the TR (see section 5.2). Pyro-oil was collected as far as possible as a pure phase and acetone used to wash the traps and to collect the residual material sticking on the trap walls. This mixture was left to concentrate overnight under fume cupboard. Oil samples were stocked in glass vials at ambient temperature (i.e. 25 °C) for some weeks before to be sent to the Faculty of Environmental Science of the University of Bologna, which performed the chemical characterization of the bio-oils.

Chemical analysis of bio-oils was based on GC-MS [Adlard and Handley, 2001; Mc Ewen et al, 1996] and solvent fractionation. Conventional experimental protocols [Oasmaa and Kuoppala, 2008] were used in combination with new characterization techniques developed by the environmental scientists of the University of Bologna. Pure phase and acetone dissolved phase of bio-oils were analyzed separately and the resulting data merged in an integral result.

Table 5.7 summarize the analytical methods used for the analysis of different compounds and the classification used for subsequent hazard evaluations:

- A. compounds directly detectable in the GC-MS were found after an isothermal at 50°C for five minutes followed by a ramp to 310°C at 5°C/min and then by an isothermal at 310°C for three minutes;
- B. silylated samples were analysed in the GC-MS system with the following thermal profile: isothermal at 50°C for five minutes, then ramp to 310°C at 10°C/min;
- C. PAHs were analysed in the GC-MS system with the following thermal profile: ramp from 50°C to 100°C at 20°C/min followed by a ramp from 100°C to 300°C at 5°C/min and then an isothermal at 300°C for 2.50;
- D. the water insoluble phase (i.e. pyrolytic lignin) was detected with solvent fractionation;
- E. sugar content was measured with a Brix refractometer after the subtraction of the sugar-like substances (e.g. hydroxyacetaldehyde and levoglucosan) quantified with the GC-MS.

Tab. 5.7: Summary of the components analysed in the bio-oils

<i>Nr.</i>	<i>Analytical Method</i>	<i>Retention Time (min)</i>	<i>Q_{ion} (m/z)</i>	<i>Compound name</i>	<i>Classification</i>
1	A	2.500	31	Hydroxyacetaldehyde	aldehydes
2	A	2.715	60	Acetic acid	carboxylic acids
3	A	2.898	43	Hydroxyacetone	ketons and alcohols
4	A	4.213	57	1-hydroxy-butanone	ketons and alcohols
5	A	4.269	43	Acetoxy-acetaldehyde	aldehydes
6	A	4.519	58	Butanedial	aldehydes
7	A	4.881	84	(2H)-furan-3-one	ketons and alcohols
8	A	5.881	96	Furfural	furans
9	A	6.563	98	Fufurilic alcohol	furans
10	A	8.436	86	4-hydroxy-butanoic acid	carboxylic acids
11	A	8.789	98	1,2-cyclopentanedione	ketons and alcohols
12	A	10.160	110	5-methyl-fufural	furans
13	A	10.836	94	Phenol	phenols
14	A	11.316	114	4-hydroxy-5,6-dihydro-(2H)-pyranone	ketons and alcohols
15	A	12.316	112	2-hydroxy-3-methyl-2-Cyclopenten-1-one	ketons and alcohols
16	A	13.266	108	2-methyl-phenol	Phenols

Continued on next page

Tab. 5.7 (Continued)

Nr.	Analytical Method	Retention Time (min)	Q_{ion} (m/z)	Name	Classification
17	A	13.928	107	4-methyl-phenol	Phenols
18	A	14.369	109	Guaiacol	Phenols
19	A	15.072	126	Maltol	ketons and alcohols
20	A	15.298	126	3-ethyl-2-hydroxy-2-Cyclopenten-1-one	ketons and alcohols
21	A	16.769	107	4-ethyl-phenol	ketons and alcohols
22	A	17.327	69	di-anidro-isosaccarino- δ -lactone	ketons and alcohols
23	A	17.571	138	4-methyl-guaiacol	Phenols
24	A	17.718	110	Catechol	Phenols
25	A	18.011	69	3,6-Dianhydro-a-glucopyranose	Phenols
26	A	18.288	120	Vinyl-phenol	Phenols
27	A	18.571	97	5-hydroxymethyl-2-fufural	Furans
28	A	19.523	140	Methoxycatechol (<i>o,m,p</i>)	Phenols
29	A	20.063	137	4-ethyl-guaiacol	Phenols
30	A	22.814	123	4-vinyl-guaiacol	Phenols
31	A	22.017	154	Syringol	Phenols
32	A	23.124	121	Eugenol	Phenols
33	A	22.814	123	etil catechol	Phenols
34	A	23.263	151	Vanillin	Phenols
35	A	24.490	168	4-methyl-siringol	Phenols
36	A	24.566	164	<i>trans</i> -iso-eugenol	Phenols
37	A	26.452	168	Ethyl-syringol	Phenols
38	A	28.260	194	<i>cis</i> -2-metoxy-isoeugenol	Phenols
39	A	30.449	194	<i>trans</i> -2-methoxy-isoeugenol	Phenols
40	A	31.151	181	acetosyringone	Phenols
41	A	31.969	167	1-syringil-2-propanone	Phenols
42	B	20.050	TIC	Levoglucosan	Anhydrosugar
43	D	-	-	Pyrolytic lignin (WP)	Polymer
44	E	-	-	Sugar polymers and oligomers	Polymer
45	C	7.127	128	Naphthalene	PAHs
46	C	12.590	152	Acenaphthylene	PAHs
47	C	13.368	153	Acenaphthene	PAHs
48	C	15.519	166	Fluorine	PAHs
49	C	19.701	178	Phenanthrene	PAHs
50	C	19.902	178	Anthracene	PAHs
51	C	25.175	202	Fluoranten	PAHs
52	C	26.133	202	Pyrene	PAHs
53	C	31.838	228	Crysene	PAHs
54	C	32.013	228	benzo[a]anthracene	PAHs
55	C	36.586	252	benzo[b]fluoranten	PAHs
56	C	36.688	252	benzo[k]fluoranten	PAHs

Continued on next page

Tab. 5.7 (Continued)

Nr.	Analytical Method	Retention Time (min)	Q_{ion} (m/z)	Name	Classification
57	C	37.825	252	Benzo[a]pyrene	PAHs
58	C	41.981	276	Dibenzo[a,h]anthracene	PAHs
59	C	42.146	278	benzo[ghi]perylene	PAHs
60	C	42.795	276	Indeno(1,2,3-cd)pyrene	PAHs

The assessment of the inherent hazards was then based on the parametric approach developed in the present thesis and fully described in chapter 4. Due to the lack of information about the bio-oil as a whole, hazard parameters and impact indices were calculated for each bio-oil component and then mass weighted in order to obtain the Integral Hazard Profile (IHP) of the samples analysed.

Two IHPs were found because the analytical methods did not allow for the characterisation of a residual fraction, supposed to be basically composed of water. A higher IHP (h-IHP) was conservatively obtained considering that the characterised matrix is representative for all the bio-oil. A lower IHP (l-IHP) instead resulted from the consideration of the actual concentration of the detected compounds in the bio-oil, after the assignment of a negligible hazard profile to the missing fraction.

Overall hazard indices obtained after normalisation to Toluene were also considered in the analysis and a macro component approach was tested.

5.5.3 Results and discussion

Chemical analysis

Compositions of the analyzed fraction of bio-oils are shown in fig 5.87.

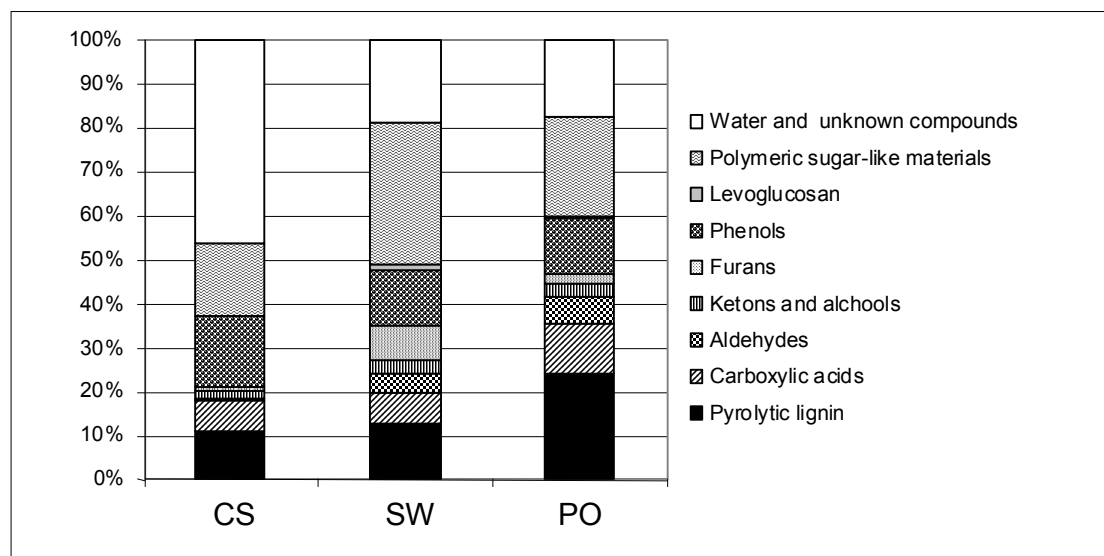


Fig. 5.87 – Bio-oil main constituent evaluated by GC-MS analysis and solvent fractionation scheme

Oil from PO resulted to be mainly composed of a high amount of hydroxyacetaldehyde, pyrolytic lignin, carboxylic acids and phenolic compounds; a large amount of water soluble heavy material (32 % w/w of not GC detectable “sugar-

like” material) and furans (7.6% w/w) were found in the oil from SW; while oil from CS consisted in a completely biphasic structure mainly composed of a large amount of water, phenols (16%) and very low aldehydes content (0.13%). This latter outcome could indicate a large ageing of the matrix [Oasmaa and Kuoppala, 2003]. Pyrolytic lignin content in the oil from PO was quite higher (22%) than the amount contained in the oils from CS and from SW (12% and 13% respectively), likely as a consequence of a higher lignin content in the original biomass feedstock.

Table 5.8 shows the detailed composition of the three samples analysed.

Tab. 5.8 – Composition of the bio-oils analysed

Compound name	CS (% by weight)	PO (% by weight)	SW (% by weight)
1 <i>Hydroxyacetaldehyde</i>	-	5.5	3.1
2 <i>Acetic acid</i>	6.2	10	6.2
3 <i>Hydroxyacetone</i>	1.0	2.0	1.7
4 <i>1-hydroxy-butanone</i>	0.35	0.55	0.56
5 <i>Acetoxy-acetaldehyde</i>	0.10	0.30	0.49
6 <i>Butanedial</i>	0.029	0.17	0.77
7 <i>(2H)-furan-3-one</i>	0.011	0.014	0.017
8 <i>Furfural</i>	0.38	1.3	3.4
9 <i>Fufurilic alcool</i>	0.53	0.53	3.2
10 <i>4-hydroxy-butanoic acid</i>	0.77	1.2	0.74
11 <i>1,2-cyclopentanedione</i>	0.011	0.057	0.30
12 <i>5-methyl-furfural</i>	0.092	0.20	0.52
13 <i>Phenol</i>	2.9	4.7	1.6
14 <i>4-hydroxy-5,6-dihydro-(2H)-pyranone</i>	-	0.004	0.020
15 <i>2-hydroxy-3-methyl-2-cyclopenten-1-one</i>	0.27	0.38	0.35
16 <i>2-methyl-phenol</i>	1.2	1.0	0.66
17 <i>4-methyl-phenol</i>	2.0	1.1	1.4
18 <i>Guaiacol</i>	0.075	0.35	0.52
19 <i>Maltol</i>	0.020	0.041	0.046
20 <i>3-ethyl-2-hydroxy-2-Cyclopenten-1-one</i>	0.053	0.054	0.056
21 <i>4-ethyl-phenol</i>	3.3	0.18	2.5
22 <i>Dianhydro-isosaccarino-δ-lactone</i>	0.022	0.012	0.059
23 <i>4-methyl-guaiacol</i>	0.030	0.18	0.31
24 <i>Catechol</i>	0.75	1.7	0.77

Continued on next page

In all the samples the main compound identified was acetic acid with yields from CS, SW and PO respectively of 6.2%, 6.2% and 10% by weight. For PO and SW, hydroxyacetaldehyde was the second most abundant compounds, with 5.5% and 3.1%. Hydroxyacetaldehyde was not detected in the bio-oil obtained from CS pyrolysis.

Regarding semi-volatile pyrolysis products from carbohydrates (in this case mainly cellulose and hemicellulose): bio-oil from SW was characterized by a high furan derivatives content (3.4% furfural, 3.2% fufurilic alcool 0.52% methylfurfural and 0.48% hydroxymethylfurfural), the highest content in cellulose alkali catalyzed pyrolysis products like 2-hydroxy-3-methyl-2-Cyclopenten-1-one (0.35%) and cyclopentanedione (0.30%) and the highest levels of levoglucosan (1.5%), mainly

produced from the non catalytic pyrolysis of cellulose and which may indicate a general higher glucan content in the feedstock.

Tab. 5.8 (Continued)

Compound name	CS (% by weight)	PO (% by weight)	SW (% by weight)
25 3,6-Dianhydro- α -glucopyranose	0.074	0.085	0.11
26 Vinyl-phenol	5.4	-	2.7
27 5-hydroxymethyl-2-fufural	0.036	0.085	0.48
28 Methoxycatechol (<i>o m p</i>)	0.0039	0.32	0.086
29 4-ethyl-guaiacol	0.014	0.11	0.34
30 4-vinyl-guaiacol	0.027	0.47	0.20
31 Syringol	0.025	0.45	0.24
32 Eugenol	0.0012	0.019	0.038
33 4-Ethyl-catechol	0.027	0.46	0.21
34 Vanillin	0.013	0.067	0.13
35 4-methyl-siringol	0.020	0.61	0.26
36 <i>trans</i> -iso-eugenol	0.0074	0.15	0.13
37 ethyl-syringol	0.0023	0.025	0.035
38 <i>cis</i> -2-metoxy-isoegenol	-	0.052	0.024
39 <i>trans</i> -2-methoxy-isoegenol	0.0060	0.19	0.019
40 Acetosyringone	0.011	0.089	0.049
41 1-syringil-2-propanone	0.011	0.10	0.34
42 Levoglucosan	0.015	0.97	1.5
43 pyrolytic lignin (WP)	11	24	13
44 Sugar polymers and oligomers	17	22	32

Concerning with lignin pyrolysis derivatives, oils from CS and SW were characterized by the highest vinyl-phenol (respectively 5.4% and 5.7%) and ethyl-phenol (respectively 2.9%, 1.6%) content, that are typical products from pyrolysis of herbaceous biomass [Ralph and Hatfield, 1991]. On the other hand, oil from PO was dominated by phenol (4.7%), methyl-phenols (2.1%) and catechol (1.7%).

Results from the analysis of PAHs are shown in table 5.9. A higher amount of PAHs was found in bio-oil from PO (4.8 mg/kg, expressed as benzo[a]pyrene equivalent), while a lower content was observed for SW (2.1 mg_{BaP}/kg) and CS (1.0 mg_{BaP}/kg).

An 82% and an 81% of the samples resulted respectively analysed for oils from PO and from SW, while the coverage for the oil from CS was 64%. The undetected fraction of bio-oils is supposed to be composed by water and sugar polymers.

Hazard assessment of the bio-oil samples

The hazard assessment of the bio-oils was performed from the results of the chemical analysis.

Properties of each component identified were quantified and hazard parameter scores assigned after the consultation of several sources: scientific literature [Lewis, 1992], databases [ESIS; RTECS; SCORECARD; SIRI; TOXNET], material safety data sheets [Chemexper], and predictive models (e.g. group contribution methods and structure activity relationships as those reported by [Allen and Shonnard, 2002]).

Tab. 5.9 – PAH content in the bio-oils analysed

Compound name	CS (mg/kg)	PO (mg/kg)	SW (mg/kg)
45 Naphthalene	3.4	40	12
46 Acenaphthylene	3.0	11	3.5
47 Acenaphthene	1.9	8.3	3.9
48 Fluorine	7.0	36	18
49 Phenanthrene	4.6	34	16
50 Anthracene	2.2	17	5.6
51 Fluoranten	1.3	9.5	4.5
52 Pyrene	1.4	11	5.0
53 Crysene	0.9	6.0	1.9
54 benzo[a]anthracene	0.4	2.5	2.1
55 benzo[b]fluoranten	0.3	1.5	0.7
56 benzo[k]fluoranten	0.1	0.4	0.4
57 Benzo[a]pyrene	0.6	2.8	1.1
58 Dibenzo[a,h]anthracene	0.2	1.0	0.5
59 benzo[ghi]perylene	0.5	1.9	0.6
60 Indeno(1,2,3-cd)pyrene	0.1	0.6	0.03

Hazard parameter scores of compounds presenting a significant level of hazard are presented in table 5.10.

Tab. 5.10 – Hazard parameters of the most relevant compounds detected in the bio-oil

Compound	1a	1b	1c	1d	2a	2b	2c	2d	3a	4a	5a	5b	5d
2	1	1	1	0	3	1	2	3	1	2	3	1	2
8	2	1	2	1	3	2	1	3	1	1	3	0	2
9	2	2	1	1	3	1	1	3	1	1	3	0	2
13	3	2	2	1	3	1	1	3	1	2	3	0	1
16	2	2	2	1	2	2	1	3	1	2	3	0	3
17	2	2	2	1	2	2	1	3	1	2	3	0	1
23	0	2	1	0	2	1	1	3	1	2	3	0	1
25	1	2	2	1	2	1	1	3	1	2	3	0	1
26	0	2	1	0	2	1	1	3	1	2	3	0	1
45	1	2	3	1	2	2	1	2	1	2	3	0	1
46	1	2	1	0	2	2	1	2	2	2	3	0	1
47	0	3	2	1	2	2	1	2	2	2	3	0	1
48	0	2	2	1	2	2	1	2	2	2	3	0	1
49	1	3	1	1	2	2	1	2	3	2	3	0	1
50	1	3	2	1	2	2	1	1	3	2	3	0	1
51	0	3	2	1	2	2	1	1	3	2	3	0	1
52	0	3	2	1	2	2	1	1	3	2	3	0	1
53	1	3	0	1	2	2	1	1	3	3	3	0	1
54	0	3	0	2	2	2	1	1	3	3	3	0	1
55	0	3	0	2	2	1	1	1	3	3	3	0	1
56	0	3	0	2	2	1	1	1	3	3	3	0	1
57	0	3	3	2	2	1	1	1	3	3	3	0	1
59	0	3	1	2	2	1	1	1	3	3	3	0	1
60	0	3	0	2	2	1	1	1	3	3	3	0	1
Min	0	0	0	0	2	1	1	1	1	1	3	0	1
Max	3	3	3	2	3	2	2	3	3	3	3	1	3

The selected compounds account for 24 of the 59 chemicals identified and show that substances with very different properties can be contained in bio-oils. With reference to the physical-chemical properties of the bio-oil components, most of them present high molecular weight and solubility in water, low-medium potential to volatilize and to persist in environment and low lipophylicity (i.e. low K_{ow}). Moreover, some of the components present also significant scores for the hazard properties directly affecting the endpoints considered by the method (i.e. acute and chronic toxicity for humans, ecotoxicity, carcinogenicity, flammability). Several components (i.e. 2 = acetic acid; 8, 9 = furans; 13, 16, 17, 23, 25, 26 = phenols and methyl phenols; PAHs) appear to be toxic to human for long term exposure and ecosystems. Some components moreover are particularly toxic also for acute inhalation or ingestion (i.e. 2 = acetic acid; 8, 9 = furans; 13, 16, 17 = phenol and methyl phenols) or show carcinogenic potential (i.e. 8, 9 = furans; 13, 16, 17, 24 = phenols and methyl phenols; PAHs). Finally, acid acetic appeared the only flammable compound present in significant concentration in bio-oils.

Impact indices were quantified from the hazard parameters and also reported in table 5.11, from which the most hazardous components of bio-oils can be screened with respect to the different endpoints considered by the method.

Tab. 5.11 – Impact indices of the most relevant compounds detected in the bio-oil

Compound	ATI	ETI	CTI	CI	FHI	OHI
2	4.5	6	2	0	6	2.5
8	9	3	2	1	0	2.9
9	6	6	1	1	0	2.5
13	9	12	4	2	0	5.0
16	0	12	4	2	0	3.5
17	0	12	4	2	0	3.5
23	0	12	2	0	0	2.0
25	0	12	4	2	0	3.5
26	0	12	2	0	0	2.0
45	0	8	6	2	0	3.5
46	0	8	4	0	0	2.0
47	0	12	8	4	0	5.5
48	0	8	8	4	0	5.0
49	0	12	6	6	0	6.0
50	0	6	12	6	0	6.8
51	0	6	12	6	0	6.8
52	0	6	12	6	0	6.8
53	0	9	0	9	0	5.6
54	0	9	0	18	0	10.1
55	0	9	0	18	0	10.1
56	0	9	0	18	0	10.1
57	0	9	27	18	0	16.9
59	0	9	9	18	0	12.4
60	4.5	6	2	0	6	2.5
<i>Min</i>	0	0	0	0	0	0.0
<i>Max</i>	9	12	27	18	6	16.9

Indices reveal again the presence of many components which can affect strongly ecosystems and human health, due to chronic toxicity in the latter case. Moreover,

some components can be a problem for human health also due to acute toxicity and to carcinogenicity. Fire hazard is instead appreciable only for acetic acid and indeno(1,2,3-cd)pyrene.

Obviously, the extent of the inherent hazardousness of bio-oils is affected by the concentration of its compounds. Integral hazard profiles (IHPs) were obtained for each bio-oil sample as the mass weighted average of the hazard profiles corresponding to each different components. Due to the partial chemical characterisation of the bio-oils, only the compounds contained in the bio-oil matrix could be analysed. Nevertheless, the undetected fraction of bio-oils is supposed to contain material (i.e. water and sugar polymers) whose inherent hazard can be considered negligible in the present approach. Two mixtures profiles were obtained for each sample:

- a higher IHP (h-IHP), considering that the matrix is representative for all the bio-oil;
- a lower IHP (l-IHP), taking into account for the actual presence of material with negligible inherent hazard in the bio-oil.

Due to its polymeric nature and to the lack of hazard data, a negligible hazard profile was assigned to lignin, sugar polymers and oligomers, which were thus excluded from the calculation of the h-IHP. It is evident that the higher IHP and the lower IHP outlines a range inside which the inherent hazard of the bio-oil samples should be included. The resulting integral profiles are reported on table 5.12 (the hazard parameters) and on table 5.13 (the impact indices). Data are also shown on figure 5.88 and on figure 5.89 in order to enhance the comparison among the hazard parameters and the impact indices of the different bio-oils samples.

Tab. 5.12 –Integral Hazard Profiles: hazard parameters of bio-oil samples and comparison with other fuels

Fuel	1a	1b	1c	1d	2a	2b	2c	2d	3a	4°	5a	5b	5d
<i>CS, l-IHP</i>	0.2	0.4	0.3	0.1	2.1	1.1	1.1	1.5	1.0	1.2	3.0	0.1	1.1
<i>CS, h-IHP</i>	0.9	1.5	1.2	0.3	2.5	1.2	1.3	3.0	1.0	1.9	3.0	0.2	1.4
<i>PO, l-IHP</i>	0.4	0.4	0.3	0.1	2.3	1.1	1.2	1.7	1.0	1.3	3.0	0.1	1.1
<i>PO, h-IHP</i>	1.2	1.2	0.9	0.3	2.7	1.2	1.5	3.0	1.0	1.9	3.0	0.3	1.4
<i>SW, l-IHP</i>	0.3	0.5	0.3	0.1	2.2	1.1	1.1	1.7	1.0	1.3	3.0	0.1	1.1
<i>SW, h-IHP</i>	1.0	1.3	0.9	0.4	2.6	1.3	1.4	3.0	1.0	1.8	3.0	0.2	1.4
<i>CS, l-IHP macro</i>	0.6	0.4	0.4	0.2	2.3	1.0	1.1	1.5	1.0	1.2	3.0	0.1	1.1
<i>CS, h-IHP macro</i>	2.2	1.5	1.6	0.7	3.0	1.1	1.3	3.0	1.0	2.0	3.0	0.3	1.3
<i>PO, l-IHP macro</i>	0.6	0.4	0.4	0.1	2.4	1.7	1.2	1.7	1.0	1.3	3.0	0.1	1.1
<i>PO, h-IHP macro</i>	1.7	1.3	1.2	0.4	3.0	1.2	1.6	3.0	1.0	1.9	3.0	0.3	1.4
<i>SW, l-IHP macro</i>	0.6	0.4	0.4	0.2	2.3	1.8	1.1	1.6	1.0	1.3	3.0	0.1	1.1
<i>SW, h-IHP macro</i>	1.8	1.3	1.3	0.5	3.0	1.2	1.5	3.0	1.0	1.9	3.0	0.2	1.4
<i>Ref. bio-oil, IHP</i>	0.8	0.8	1.0	0.3	2.9	1.9	2.3	3.0	1.0	2.1	2.4	1.0	1.5
<i>Biodiesel, IHP</i>	0.0	3.0	0.0	0.6	2.0	3.0	1.0	1.0	3.0	2.0	3.0	0.0	1.0
<i>Bio-ethanol</i>	0	0	1	1	3	2	2	3	1	2	3	3	2
<i>Gasoline, IHP</i>	0.2	2.5	1.0	0.2	2.2	2.8	1.9	1.8	1.9	1.6	3.0	2.5	2.2

Tab. 5.13 –Integral Hazard Profiles: impact indices of bio-oil samples and comparison with other fuels

Fuel	ATI	ETI	CTI	CI	FHI	OHI
CS, l-IHP	0.6	2.3	0.6	0.2	0.4	0.7
CS, h-IHP	2.4	9.0	2.3	0.6	1.5	2.5
PO, l-IHP	1.0	2.4	0.6	0.2	0.6	0.8
PO, h-IHP	2.9	6.8	1.7	0.6	1.8	2.2
SW, l-IHP	0.9	2.4	0.5	0.2	0.4	0.7
SW, h-IHP	2.7	6.8	1.5	0.5	1.1	2.0
CS, l-IHP macro	1.8	2.4	0.8	0.3	0.4	1.0
CS, h-IHP macro	7.1	9.2	3.1	1.3	1.6	3.9
PO, l-IHP macro	1.8	2.6	0.8	0.3	0.7	1.0
PO, h-IHP macro	5.2	7.4	2.2	0.8	2.0	2.9
SW, l-IHP macro	1.8	2.3	0.7	0.3	0.4	1.0
SW, h-IHP	5.8	7.4	2.3	0.9	1.3	3.1
Macro						
Ref. bio-oil, IHP	2.7	3.8	1.5	0.4	7.0	2.1
Biodiesel, IHP	0.0	6.0	0.0	3.5	0.0	2.5
Bio-ethanol	0	0	2	2	12	2.5
Gasoline, IHP	0.8	7.6	2.6	0.4	15.8	3.2

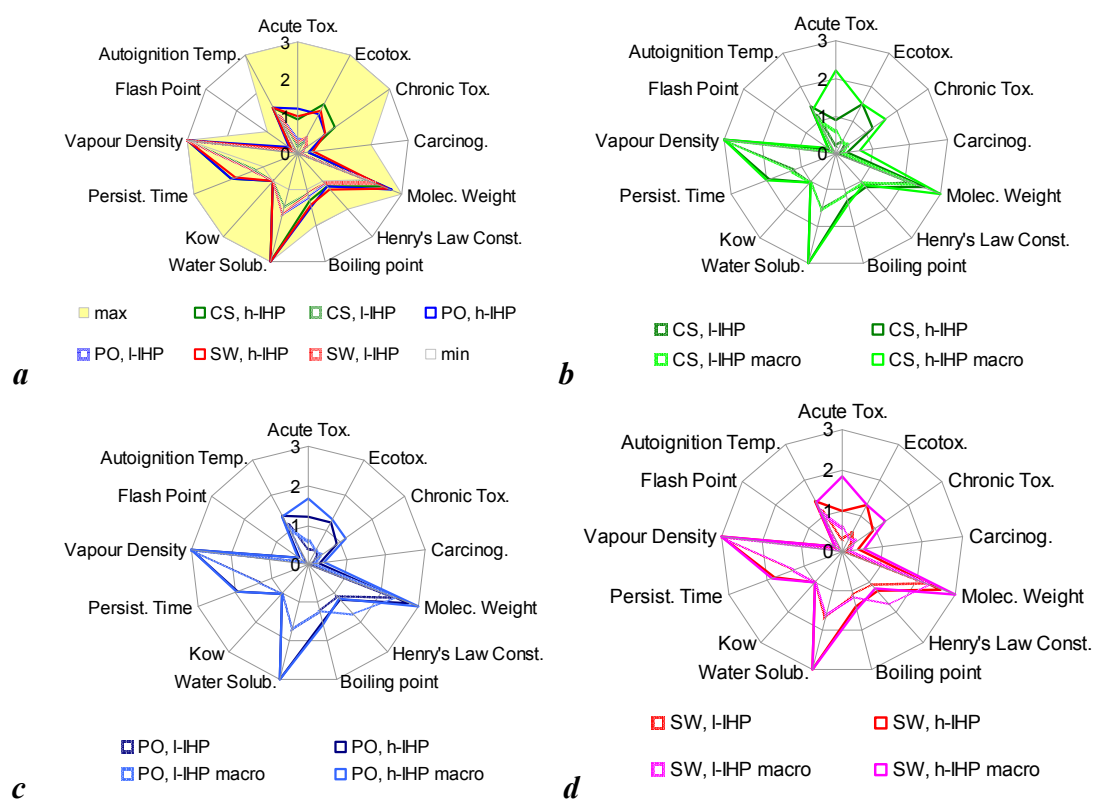


Fig. 5.88 – Hazard footprints of the three bio-oils: comparison between h-IHPs and l-IHPs (a) and between standard and family compounds-based procedure (b = CS; c = PO; d = SW)

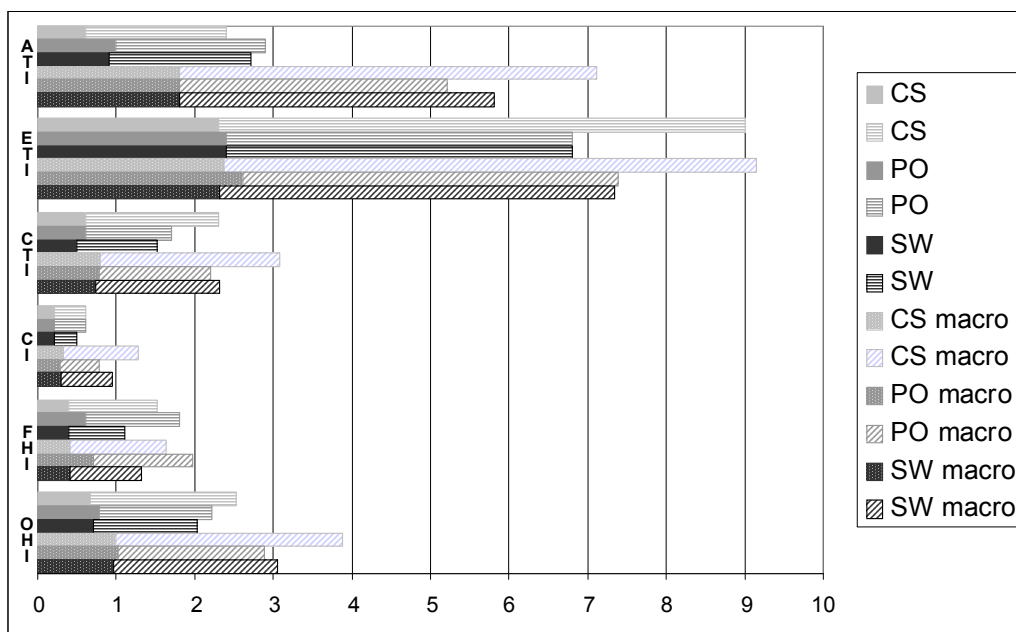


Fig. 5.89 – Impact bar chart of the three bio-oils: comparison between h-IHPs and l-IHPs (a) in the standard and in the family compounds-based procedure

The three matrixes of bio-oils yielded very similar h-IHPs, as figure 5.88 (a) and 5.89 point out. Bio-oil samples seem to have the potential to affect all the endpoints considered by the hazard assessment method, water ecosystems in particular. Ecotoxicity and chronic toxicity associated to the bio-oil sample from CS were slightly higher due to its resulting matrix composition. As a consequence, higher ETI and CTI were yielded for CS. This sample also presented slightly higher scores for FHI and, thus, OHI. When a negligible hazard was assigned to the water-polymeric fraction which was not characterised, the l-IHP of the samples resulted significantly lower and homogeneous.

Family compounds based hazard assessment

The identification of the bio-oil components is often a resource-consuming procedure. A lower level of detail may be useful to understand the major sources of hazard due to bio-oils. The assessment of the hazard due to the bio-oil samples was thus repeated resorting to a streamlined approach based on the identification of macro-categories of compounds and on the assignment of a representative compound to each “family”. The chemical families identified in the bio-oil samples are reported in figure 5.87 with their cumulative content in the mixtures. The representative compounds assigned to each families are listed in table 5.14, while the scores of parameters and indices resulting from this simplified family compound-based assessment are shown in table 5.12 and in table 5.13.

From the vision of tables 5.12 and 5.13 it is apparent that the bio-oil samples strikes all the endpoints considered in the assessment method also with the simplified approach. With exclusion of the toxic inhalation parameter, whose hazard level resulted increased, IHPs were quite similar to the ones previously yielded with the standard procedure, as shown on figure 5.88 (b,c,d) and on figure 5.89. The discordance for the toxic inhalation parameter and for the corresponding index (i.e. the ATI) is mainly due to the macro-compound selected for the phenol family (i.e. phenol). Many compounds were indeed included in this family but only phenols and

methyl phenols are actually harmful to humans for acute toxicity by inhalation. A higher OHI also resulted as a consequence of the higher ATI registered for the phenols family. On the whole, the streamlined assessment indicates that a simplified procedure can be a good and straightforward method for the obtainment of useful pieces of information about the bio-oil hazard without a too much detailed chemical analysis is requested.

Tab. 5.14 – Chemical families identified in bio-oils and representative compounds.

Macro category of compounds	Representative compound
Levoglucozan	Levoglucozan
Carboxylic acids	Acetic acid
Aldehydes	Hydroxyacetaldehyde
Ketons and alcohols	Hydroxyacetone
Furans	Furaldeyde
Phenols	Phenol
PAHs	Anthracene

Assessment of different liquid fuels

The methodology outlined in chapter 4 was also applied to the hazard assessment of different fuels:

- a reference bio-oil, whose model composition was taken from literature [Iojoiu et al., 2007];
- bio-ethanol and biodiesel [Cardone et al., 2003; Lima et al., 2004], which are currently playing a significant role in the renewable energy market, and
- a model composition for a regular unleaded gasoline [Marathon Petroleum Company LCC].

This allowed for a vertical comparison between bio-oils and different bio-fuels and a horizontal comparison with a conventional fuel.

A pure ethanol content in bio-ethanol obtained from biomass fermentation was considered. Compositions of reference bio-oil, biodiesel (from palm oil trans-esterification) and regular gasoline are reported on table 5.15. Further details about the modelling can be found in [Cordella et al., 2008a; Cordella et al., 2008b].

Tab. 5.15 – Model compositions considered in the assessment of the liquid fuels. Content of the compounds by weight is reported in brackets

Reference bio-oil	Bio-diesel	Regular gasoline
Acetic acid (20%)	Oleic acid, methyl ester (43.3%)	2,2,4-trimethylpentane (25%)
Pentanoic acid (2%)	Palmitic acid, methyl ester (34.4%)	2,4-dimethylpentane (15%)
Propanoic acid (3%)	Linoleic acid, methyl ester (14.7%)	n-octane (12%)
Methylformate (2%)	Stearic acid, methyl ester (5.9%)	n-eptane (10%)
Butyrolactone (1%)	Glycerides (1%)	n-decano (6%)
Methanol (2,5%)	Oleic acid (0.3%)	n-pentane (4%)
Ethanol (1,5%)	Palmitic acid (0.2%)	n-esane (1%)
Ethylenglycol (2%)	Linoleic acid (0.1%)	cycloesane (1%)
Acetone (3%)	Stearic acid (0.0%)	2,3-dimethyl-2-butene (6%)
Butanone (1%)	Methanol (0.1%)	Toluene (8%)
Acetaldehyde (11%)	Glycerol (0.0%)	Xylene (6%)
Pentanal (1%)		1,2,4-trimethylbenzene (3%)
Ethanedial (5%)		Benzene (1.5%)
Phenol (4%)		Ethylbenzene (1.2%)
Dimethylphenol (1%)		Naphtalene (0.3%)
Ethylphenol (2%)		
Dihydroxybenzene (3%)		
Furan (6%)		
Water (29%)		

IHPs resulting from the assessment of these fuels are reported in table 5.12 and in table 5.13 and they are also plotted on figure FHF and FIBC. The l-IHP of the bio-oil from CS is also reported for the sake of comparison. The lower IHP was selected as a reference basis rather than the higher IHP in order to take into account for all the material contained in bio-oils. A more consistent comparison, indeed, seemed to be yielded when water and polymers, whose impact can be considered negligible in the present approach, were included in the assessment.

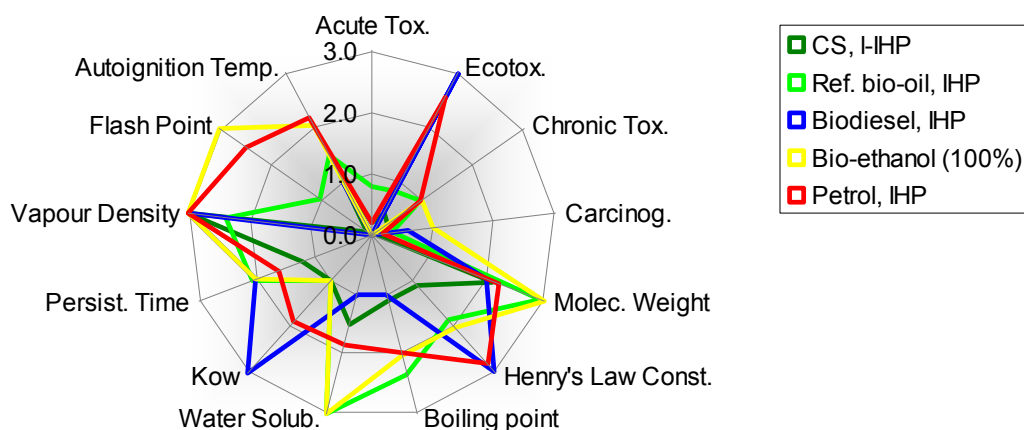


Fig. 5.90 – Hazard footprints of the different fuels assessed and comparison with the lower IHP of bio-oil from CS

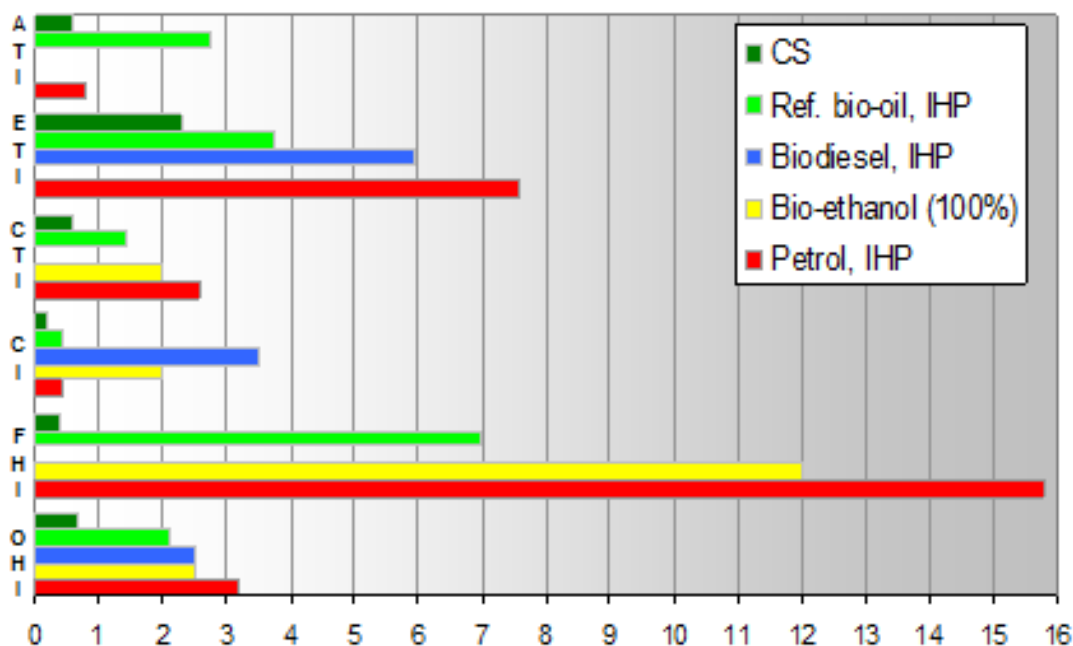


Fig 5.91 – Impact indices of the different fuels assessed and comparison with the lower IHP of bio-oil from CS

Even if the composition of the reference bio-oil differed from the oil samples previously characterized, the analysis highlighted again the presence of a wide set of hazardous components, which can impact all the endpoints considered by the method. The hazard profile of the reference bio-oil is qualitatively similar to the ones of the bio-oil samples but it resulted to be closer to the h-IMP than to the l-IMP. Two apparent differences were in particular registered in the reference bio-oil: the larger

presence of toxic compounds, e.g. acetic acid and furans, and a higher fire hazard, with the latter mainly due to a larger content of acetic acid (20%) and acetaldehyde (11%). As a consequence, the OHI score of the reference bio-oil resulted more than doubled in comparison with the corresponding index of the CS bio-oil.

A significantly higher extent of fire hazard resulted to be associated also to bio-ethanol, in addition to toxic and possible carcinogen effects under significant and chronic intakes [SCORECARD; SIRI]. The analysis of the biodiesel instead mainly evidence the presence of methyl esters, which are highly toxic for ecosystems and suspected to be carcinogen according to [SCORECARD; SIRI]. Moreover, the possible presence in the biodiesel of compounds (i.e. methanol and glycerol) which are toxic for human beings and highly flammable/explosive is to be considered, while suspect carcinogenic effects and a high tendency to bioaccumulation are highlighted for the residual fatty acids contained in the biodiesel. As a consequence, two endpoints are affected by biodiesel: ecosystem toxicity and human carcinogenicity (mainly due to the inherent properties of the methyl esters). It's worthy noticing the absence of fire hazard for biodiesel in this assessment, due to the high flash point that the biodiesel components score in this assessment. An additional consideration concerns methyl esters and fatty acids. Because the chemicals belonging to these two classes of compounds show homogenous properties, support is given to the possibility of an assessment based only a limited number of representative macro-components. As a consequence of index scores, higher OHI scores were registered for bio-diesel and bio-ethanol if compared with the bio-oil from CS and the reference bio-oil.

About the model gasoline, all the endpoints considered by the assessment method resulted to be affected by this fuel, even if with a higher extent than bio-oils. Consequently, the highest OHI score was registered for gasoline. Gasoline in fact contains many components whose concentration can be variable but which are toxic for humans and ecosystems and which show a significant high fire hazard. Moreover, the trend of the hazard parameters inside categories of similar compounds is very homogenous, supporting again the possibility to assess the hazard profile of a fuel based on a limited set of representative compounds.

With reference to the single indices, the highest presence of compounds hazardous for their acute toxicity by inhalation was registered in the reference bio-oil, followed by gasoline and bio-oil from CS. Apart from biodiesel, for which no significant presence of toxic compounds for humans was detected, chronic toxic effects may be possible in gasoline, bio-ethanol and bio-oils. All the fuels analysed seem moreover to have carcinogenic potential, with the highest potentials associated with bio-diesel and bio-ethanol. Nevertheless, the extent of the inherent hazard for humans is sensitively lower than ecotoxicity and fire hazard. Gasoline yielded the highest ETI, followed by biodiesel and bio-oils, while gasoline was followed by bio-ethanol, reference bio-oil and bio-oil samples in the fire hazard fuel ranking. No ecotoxic effects and fire hazard were respectively registered for bio-ethanol and biodiesel.

It is apparent that significant differences exist between the set of fuels assessed and no fuels can be considered universally better than others with reference to all the end points considered in the hazard assessment. When indices were recombined to an overall index, differences between the fuels were noticeably flattened and a hierarchy of fuels tracked: gasoline appeared as the worst fuel followed by biodiesel, bioethanol, reference bio-oil and bio-oil samples. It is moreover worthy noticing that the inherent hazards due to the bio-oil samples are significantly lower because of the inclusion of water and of polymers in the hazard characterisation. Bio-oils can be considered as raw fuels and thus it is possible that a similar hazard profile can

correspond to crude oil or heavy oil. On the contrary, a worse hazard ranking may be expected for fuels derived from bio-oils, as suggested by the reference bio-oil, whose model composition, indeed, did not take into account for any polymeric materials as supposed in upgraded fuel products.

5.5.4 Conclusions

An approach to the assessment of the hazards due to chemical substances was applied to liquids obtained from slow-pyrolysis of biomass feedstock. No significant differences were detected among the different samples of bio-oil analysed, which presented, with different extent, several hazardous compounds affecting all the end-points considered by the assessment procedure. Production, storage and use of bio-oils may thus involve, under accidental conditions, to the emission of compounds which are toxic for human beings and the environment and which are possible precursors of fires.

Due to the large number of compounds contained in bio-oils, a streamlined approach based on the selection of a limited number of macro-compounds was tested. The simplified procedure yielded results which were consistent with the standard procedure and can lead to an effective and faster screening of the targets affected by potential accidental scenarios.

The hazard performance of bio-oils were also compared with that of other conventional fuels: a reference bio-oil, bio-ethanol, bio-diesel and a model gasoline. The comparison highlighted that inherent hazardous properties are associated not only to fossil fuels but also to several components contained in the fuels produced from the biomass. Different fuels were interested by different kinds and levels of hazard and a hazard ranking was difficult to be tracked since fuels which were less hazardous with reference to an end-point resulted worse for other hazardous properties. Nevertheless, the hazard due to bio-oil resulted to be lower than those due to refined products like bio-ethanol, bio-diesel and gasoline, with the latter one which appeared to be the worst fuel among the ones compared.

In conclusion, the present approach appears to be a valid tool for the identification of the hazard scenarios which may concern with productive plants and warehouse of bio-oils and other fuel liquids. The tracking of the hazards due to chemicals is indeed one of the major issue claimed in the UE REACh system and also a robust sustainability assessment of bio-fuel trade should focus on this topic, in connection with the prevention and control of the potential negative effects due to a fuel.

CHAPTER 6

ECONOMICAL ASSESSMENT OF AN ENERGY SUPPLY CHAIN BASED ON BIOMASS SLOW PYROLYSIS

6.1 Introduction

Slow pyrolysis is one of the processes which can be implemented in supply chains aimed at the exploitation of the energy potential offered by biomass. With reference to the world energy scenarios, attention on the biomass pyrolysis process is due to the possible production of solid (i.e. char) and liquid (i.e. pyro-oil) renewable fuels. Due to the higher energy density of the pyro-products in comparison with the original feedstock, pyrolysis can be considered a thermo-chemical densification process. As a consequence, potential benefits in the transport and in the storage stages of a bio-energy supply chain may be obtained. Nevertheless, industrial success of the pyrolysis process is still restricted due to an approach not often oriented to the life cycle thinking (i.e. to the consideration of the main economic, environmental and societal issues associated with all the stages interested by the supply chain) and also by the existence of inherent limits in the process (as also confirmed by the analysis described in chapter 5).

An evaluation model was built in order to screen the economic feasibility of a power supply chain based on the biomass slow pyrolysis process. Pyrolysis products were supposed to be co-fired with coal in existing large power plants (i.e. with a capacity higher than 200 MW_{el}). Co-combustion with coal is one of the most efficient systems already available in order to exploit the energy contained in biomass [Moncada Lo Giudice, 2006] and in biomass derived fuels. This is in particular due to:

- the small modifications required for the conversion of a conventional coal combustion power plant into a co-combustion plant with no significant efficiency loss (until the coal-combustion ratio is lower than 80% [Moncada Lo Giudice, 2006]);
- the fossil fuel saved and the fossil CO₂ emission avoided during the combustion as a consequence of the substitution of coal with a renewable source of energy;
- the large percentage of electricity worldwide produced from coal (i.e. 38% in OECD [EIA, 2004]; 11.5% in Italy [Terna, 2008 a]);
- the flexibility of the option (coal power plants can be fed with a wide range of fuels).

Territory availability was considered the limiting factor for the implementation of the densification process. As a consequence, the model focused on the electricity which can be produced from single slow pyrolysis plants working at fixed capacities and regardless of the power capacity installed at the co-combustion plant. Power plant adaptation to co-combustion was however assessed. Supply chains based on four crops of strategic interest for Italy were evaluated: CS, PO, SO, SW. 8280 operational hours per year and different feeding rates were considered for the pyrolysis process, i.e. from 0.036 to 5.4 t/h (at the highest capacity this can be approximately equivalent up to 37 km²/yr of land demand, depending on the biomass feedstock). The effects due to the industrial scale of the biomass pyrolysis process were thus investigated in a life cycle perspective.

All the stages of the bio-power supply chains were modelled in order to quantify the cash flows occurring from the biomass production to the power generation. This

required the calculation of mass and energy balances and the collection of economic data. The Net Present Value (NPV) analysis method (see chapter 4) was then applied to the supply chain model. A differential (costs) analysis was performed: credits due to coal substitution were thus included. According to the European Emission Trading System (ETS) [European Commission, 2009], the credits due to the CO₂ emission avoided during the combustion were also considered. The key performance indicator (KPI) selected in order to monitor the overall economic performance of the supply chains is the Electricity Surcharge Indicator (ESI). ESI is measured in €/kWh_e and it is defined as the electricity surcharge that results in a NPV equal to zero. The output of the assessment can thus express the incremental cost due to the implementation of biomass pyrolysis processes in a supply chain formerly based on coal.

The incidence of the key parameters of the model on the outcome of the economic assessment was also tested with sensitivity analysis and the performances of public support systems promoted by UE assessed.

Useful pieces of information can be gained from the analysis in order to understand the feasibility of power supply chains based on the biomass slow pyrolysis.

6.2 Description of the economic model

The economic model considered the full evolution of the energy system: from the biomass production to the power generation through co-combustion of the biomass pyrolysis products with coal. The following sub-systems, which correspond to the single stages of the supply chain (see figure 6.1), were identified and modelled:

1. Biomass production, i.e. the farm activities involved in the biomass growing and harvesting;
2. Collection of the biomass, i.e. the loading and delivery of the raw material from the field to the pyrolysis plant;
3. Densification process, i.e. the slow pyrolysis process, pre-treatment processes for the biomass conditioning included;
4. Transport of the pyrolysis products, i.e. the loading and delivery of char and pyro-oil to the power plant;
5. Power generation, i.e. the co-combustion of the biomass pyrolysis products with coal.

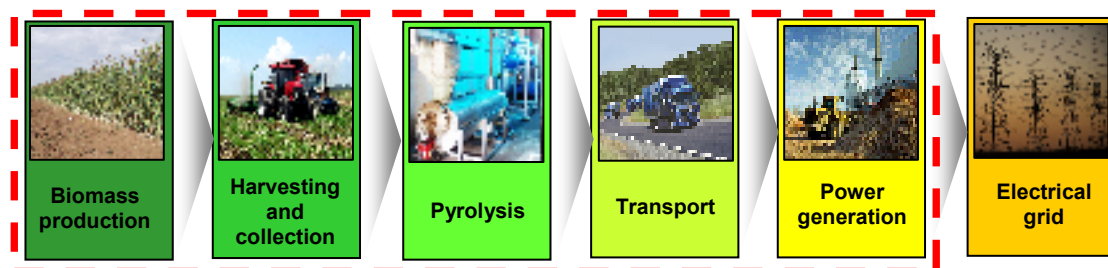


Fig. 6.1 – Stages of the biomass-to-power supply chains modelled

The supply chain modelling was aimed at the quantification of mass, energy and economic balances, which was possible only after the collection of many pieces of information (e.g. experimental pyrolysis yields and engineering, thermodynamic and economic data) and the formulation of convenient assumptions (e.g. hypothesis related to territory and logistics). Cross disciplinary competences were thus required in the modelling. A detailed description of each sub-system is reported in the following with particular reference to the main assumptions effected in the modelling.

A sensitivity analysis was also performed in order to understand the most sensitive parameters of the model and the potential effectiveness of some public support systems.

6.2.1 General methodological assumptions

General methodological assumptions of the model are reported on table 6.1.

According to the NPV analysis methodology, all the cash flows occurring in the supply chain were referred discounted to their present value based on a Return on Equity index (ROE) and on the inflation rate. ROE and inflation rate were respectively selected from average values typical for the thermoelectric industry [New York University] and from national statistics on the energy sector [ISTAT]. A 10 years economic life span and an annual operative capacity equal to 8280 hours were considered. An additional year was considered for the planning, implementation and start-up of the pyrolysis process.

All the cash flows quantified in the modelling are expressed with reference to the second semester of 2008 in Italy. Cash flows referred to a different space-temporal context were updated based on specific coefficients (e.g. Marshall & Swift Equipment Cost Index [Peters et al., 2003], ISTAT data [ISTAT], OECD Comparative Price Levels [OECD]).

Loan capital was considered equal to 35 % of the total investment, in accordance with the typical value considered in the chemical industry [Perry and Green, 1997]. A 10 years amortization schedule, a fixed interest rate (i.e. 4.68% on an annual basis [OECD]) and constant mortgage repayments were supposed for the loan capital.

Tab. 6.1 – Main methodological parameters of the model

Parameter	Value
Currency reference	€
Regional reference	Italy
Temporal reference	2008, II semester
Planning, implementation and start-up (y)	1
Fiscal years (y)	10
Annual operational hours (h)	8280
Tax rate (%)	40
Inflation rate (%)	3.51
ROE (%)	11.4
Capital loan (% of total capital investment)	35
Interest rate on loan (%)	4.68

6.2.2 Biomass production

Supply chains based on different ligno-cellulosic biomass species were modelled. A wide range of energy crops was considered, including both annual crops, i.e. CS and SO, and perennial crops, i.e. PO and SW. Annual crops are planted and harvested during the same production season while perennial crops do not need to be replanted after each harvest. Foremost characteristics of the biomass feedstock investigated are given in table 6.2 with reference to yields, energy content, harvest system and moisture content of the biomass. In particular, different harvest systems and specific

bulk density were considered depending on the single biomass species: baling for CS and SW; chipping for PO and chopping for SO. Relevant effects on logistic are due to the harvesting system implemented (see paragraph 6.2.3). Biomass was supposed to be dried on the field for two months to a final 25% moisture content. 1% dry material loss was monthly considered as a consequence of natural drying [Rentizelas et al., 2009]. Further agronomic details about the crops investigated can be found in [ARSIA, 2004; Gelletti et al., 2006; Venturi et al., 2008].

Tab. 6.2 – Biomass feedstock characteristics

Biomass	Harvest^(a)	Yield^(a) (t_{db}·ha⁻¹·yr⁻¹)	LHV^(a) (GJ·t_{db}⁻¹)	Moisture^(b) (%) by weight, w.b.)	Bulk density^(c) (kg/m³)
CS (*)	Bales	8	16.8	40-60	130
PO	Chips	17	17.7	40-50	240
SO	Chopped	22	17.1	50-70	100
SW	Bales	12	17.4	40-50	130

(*) corn grains (co-product): 10 t_{db}·ha⁻¹(a)

a [DiSTA, Venturi et al., 2008]

b [ARSIA, 2004; Gelletti et al., 2006; Thornley et al., 2009]

c [Scurlock]

Costs of biomass production are reported in table 6.3. They were obtained from [DiSTA] and include all the agricultural expenses due to:

- tools and machinery (mortgage, maintenance, assurance);
- workforce;
- operative costs (the cost of the fuels included);
- raw materials;
- other generic costs incurred (estimated equal to the 15% of the costs due to tools and machinery).

Rent and profitability of land were excluded from the model due to high uncertainty. CS costs were calculated assigning a credit (150 €/t) to the corn grains (i.e. the other co-product in the corn farming); while sowing costs were allocated over 15 years for perennial species.

Tab. 6.3 – Biomass production costs

Biomass	[€/ha]	[€/t_{db}]
CS (*)	193	24.1
PO	710	41.8
SO	1002	45.5
SW	380	31.7

(*) a credit due to the sale of corn grain was included (150 €/t)

6.2.3 Transport of the biomass to the pyrolysis plant

Pyrolysis plant was supposed to be placed in the centre of a circular area of production and harvest of the biomass (see figure 6.2).

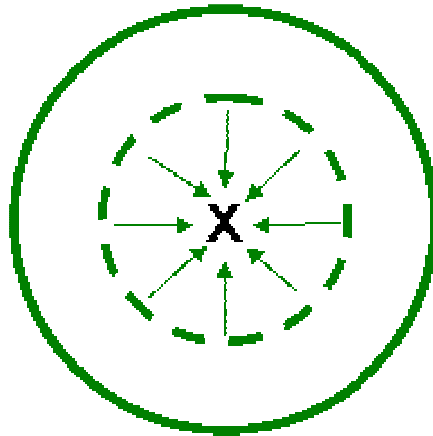


Fig. 6.2 – Territorial modelling

The area yearly required in order to supply the slow pyrolysis process was calculated as the product of the feeding rate of the pyrolysis plant (ranging from 0.036 to 5.4 t/h) and the annual operational time (i.e. 8280 h) divided by the biomass yield and a correction factor expressing the land effectively involved in biomass production, assumed equal to 40.8% of the territory [ISTAT, 2007]. The distance of concentration was calculated, according to equation 7.1, as the area-weighted average radius of the collection area, multiplied by a tortuosity factor:

$$DC = TF \cdot \int_0^R \frac{2\pi r^2 dr}{\pi R^2} = \frac{2}{3} R \quad (7.1)$$

Where:

DC = distance of concentration;

R = collection area radius;

TF = tortuosity factor (considered to be 1.6, corresponding to secondary rural roads [Thornley et al., 2009]).

A small truck was supposed to be used for the biomass transport. A gross weight of 14 t and a payload of 8.5 t were considered, equivalent to a diesel consumption of 0.225 L/km with empty trips and 0.275 L/km with full loads. A linear distribution was considered for intermediate load factors. Data were obtained from [Volvo Truck Corporation, 2008]. An arbitrary volume of 25 m³ was considered. Specific load factors were calculated based on material densities and truck volume. A return back empty trip was also considered. Results of the logistic modelling are shown in table 6.4 with reference to a 25% moisture content.

Tab. 6.4 – Biomass transportation modelling

Parameter	Bales	Chips	Chopped
Load factor (%)	38.2	70.6	29.4
Fuel consumption – with load (L/100 km)	24.4	26.0	24.0
Fuel consumption – empty (L/100km)	22.5	22.5	22.5
Return back total consumption (L/100 km)	46.9	48.5	46.5
Return back total consumption (L·t _{daf} ⁻¹ ·km ⁻¹)	0.192	0.108	0.248

The transport process was supposed to be contracted out. Costs due to truck purchase, use and maintenance were included as well as lorry driver salary. A life span equal to 600'000 km was considered [CSST, 2007] for an overall kilometric cost of 1.82 €/km.

Kilometric cost was then adjusted in order to take into account for the load factor, depending on the bulk density of the transported material (see table 6.2).

6.2.4 Biomass pyrolysis

In the slow pyrolysis process biomass is converted to solid and liquid fuels (i.e. char and bio-oil) under the application of thermal energy, which is supposed to be supplied by the gaseous product of pyrolysis. Biomass was considered to be fed with a 7% moisture content, a particle size equal to few millimetres and then to be processed at 650 °C. The main building blocks of the pyrolysis process (i.e. biomass feeding, pyrolysis reaction, char and bio-oil collection, pyrolysis gas burning and flue gas treatment) were modelled, as well as the processes requested in order to condition biomass to the specifications required by the pyrolysis process (i.e. drying and grinding).

Pre-treatment processes

The modelling of the biomass conditioning considered:

- drying of the raw biomass to 7 % moisture content in a co-current rotary drum dryer;
- grinding of the dried biomass to few millimetres in a hammer mill.

Immobilized capital was assessed as well as costs associated with workforce, maintenance, energy, licences & patents and indirect costs.

The assessment of the immobilized capital was based on the method of Miller [Perry and Green, 1997]. A preliminary sizing of the equipments used in biomass conditioning was requested. Equipments were dimensioned based on the feeding rate of the pyrolysis process (i.e. 0.036 - 5.4 t/h). FOB costs were then found in [Matche] and the installed costs estimated. Installed costs considered: battery limits, storage and handlings, utilities and services. Results of the estimation are reported in table 6.5.

Tab. 6.5 –Pre-treatment processes, immobilised capital

Slow pyrolysis feeding rate (t/h)	Immobilised Capital (k€)
0.036	69.7
0.090	135.1
0.180	209.6
0.270	261.8
0.360	324.9
0.900	513.3
1.800	863.6
2.700	1170.8
3.600	1453.0
4.500	1718.0
5.400	1970.0

Workforce cost estimation was based on the calculation of the hours required to process a raw material mass unit (i.e. the operational hours), in accordance with the correlation of Wessel [Perry and Green, 1997]. Two operational units were considered. The number of operators requested in the pre-treatment processes was obtained considering a total amount of 1740 working hours per year (equivalent to 8

working hours per day, 245.5 days per year), i.e. the typical value in the chemical industry [FILCEM-CGIL]. Depending on the feeding rate of the pyrolysis plant, the number of operators ranged from 5 to 14. The cost was finally determined assuming a gross annual salary equal to 23796 € [FILCEM-CGIL].

Maintenance costs were estimated equal to the 6% of the annual depreciation charge [Perry and Green, 1997].

Energy costs are due to fuel consumed during drying and to electricity. Fuel consumption was calculated from the thermal energy required to dry the biomass to 7% moisture content. Combustion of no. 2 fuel oil (thermal efficiency: 85%) was considered; the cost of the fuel estimated according to the methodology described in [Ulrich and Vasudevant, 2006]. Power consumption of dryer and of mill was estimated from technical data on existing equipments operating in similar process conditions. Cost of power was calculated according to [Ulrich and Vasudevant, 2006]. Results of the calculation are reported in table 6.6.

Tab. 6.6 – Pre-treatment processes, energy costs

Slow pyrolysis feeding rate (t/h)	Drying		Grinding
	Fuel [c€/kg _{water}]	Electricity [c€/kg _{water}]	Electricity [c€/kg _{biomass}]
0.036	0.81	0.07	0.003
0.090	0.81	0.09	0.008
0.180	0.81	0.11	0.016
0.270	0.81	0.13	0.023
0.360	0.81	0.14	0.031
0.900	0.81	0.17	0.078
1.800	0.81	0.21	0.155
2.700	0.81	0.23	0.233
3.600	0.81	0.25	0.310
4.500	0.81	0.27	0.388
5.400	0.81	0.28	0.466

Costs of licenses and patents and indirect product costs were estimated in accordance with the scheme provided in [Perry and Green, 1997]: costs of licences and patents and indirect costs were respectively considered proportional to the sum of product partial costs (i.e. the costs of production less the costs of patents and licenses) and to the cost of labour. Specific coefficients were used [Perry and Green, 1997]:

- 2.5% for costs of patents and licenses;
- 10% for costs due to quality control;
- 15% for costs due to auxiliary services.

Indirect period costs were instead considered negligible.

Pyrolysis process

Immobilized and circulating capitals associated with the slow pyrolysis process were estimated as well as workforce, maintenance, utilities, licences & patents and indirect costs. The modelling required the identification of the main equipment involved in the process and the further quantification of mass, energy and cash balances. This was possible after the design of the process, whose layout is reported in figure 6.3, and a preliminary sizing of the equipments. Biomass is stored in vertical tanks and then fed

to a screw reactor by mean of a conveyor belt and of a hopper. A pyrolysis temperature equal to 650 °C is set-up. Char is separated from the pyrolysis products and collected in a storage tank; oil is instead condensed from the volatile products of pyrolysis with an organic scrubber operating with a bio-oil-water mixture (temperature: 5 °C). Oil is separated from water in a decanter and then collected in a storage tank. Light products of pyrolysis are supposed to be burnt in order to supply the thermal energy requested in the slow pyrolysis process. Flue gases are finally treated with active carbons before they are released in atmosphere. Further details on the slow pyrolysis process can be found in [Bertocchi, 2008]

The sizing of the equipments and the application of mass and energy balances required physical-chemical and thermodynamic data [e.g. Perry and Green, 1997] related to the biomass slow pyrolysis process and the gain of pieces of information from experimental activities (see chapter 5). Techno-economic literature [Perry and Green, 1997; Matche] was instead consulted for further quantification of the cash flows.

Slow pyrolysis yields are the core issue in the process modelling and they were obtained from the experimental activities outlined in chapter 5. Yields are reported in table 6.7, referred to 650 °C pyrolysis temperature and 7% moisture content in the biomass feedstock (under the hypothesis that all the moisture of the biomass is collected with the bio-oil and that pyrolysis water is not affected by the biomass moisture content). Characteristics of char and bio-oil, requested for the modelling of this and of the following sub-systems, were taken from scientific literature and reported in table 6.8.

Tab. 6.7 - Experimental slow pyrolysis yields (biomass moisture reference: 7% w.b.)

	Biomass	Char	Bio-oil	Light Products
CS		26.7	36.4	36.9
PO		20.7	39.9	39.4
SO		24.8	38.1	37.1
SW		21.2	41.5	37.3

Tab. 6.8 – Characteristics of char and bio-oil

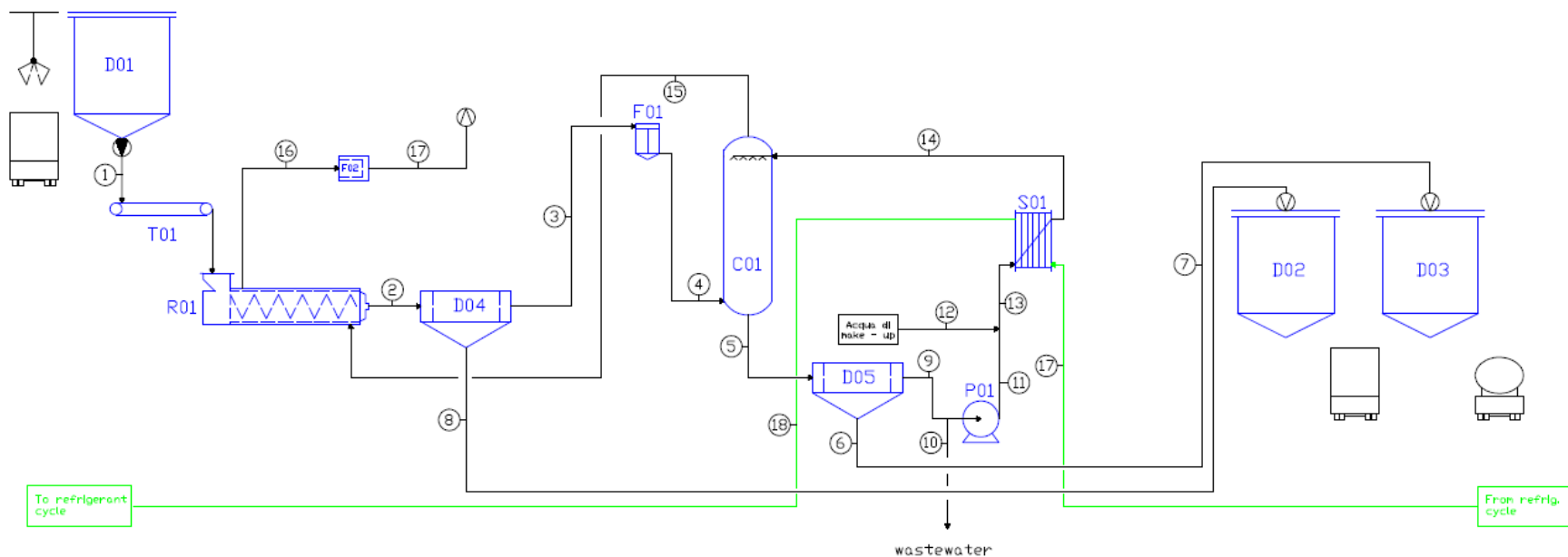
Product	LHV (MJ/kg) ^d			Density (kg/m ³)	Water (%)		
	Min	Average	Max		Min	Average	Max
Char	26 ^a	29.6 ^a	34.1 ^a	300 ^b	-	-	-
Bio-oil ^c	18	20	22	1150-1250	20	25	30

a [Phyllis Database]

b [Scurlock]

c [Oasmaa and Czernik, 1999]

d char: MJ/kg_{d.a.f.}; bio-oil: MJ/kg_{d.b.}



Block	Equipments	Block	Equipments
Raw biomass storage	D01 – Biomass storage tank	Bio-oil condensation system	C01 – Spray tower
Feeding	T01 – Conveyor Belt		D05 – Decanter
Pyrolysis reactor	R01 – Screw reactor		P01 – Centrifugal pump
Char separation	D04 – Gravitational separator		S01 – Heat exchanger
Char filter	F01 – Ceramic filter	Char storage	D02 – Char storage tank
Flue gas treatment	F02 – Active carbons	Bio-oil storage	D03 – Oil storage tank

Fig. 6.3 – Biomass slow pyrolysis layout

Average figures were considered for heating value, density and water content. LHV of bio-oil and char was corrected in order to take into account for water and ash content. No ash content was considered for bio-oil and no water content for char. Biomass ash content was measured during the experimental analysis described in chapter 5 so that different figures were obtained. Results are shown in table 6.9.

Tab. 6.9 – LHVs of char and bio-oils produced from different biomass species

Biomass	LHV	
	Char (MJ/kg _{d.b.})	Bio-oil (MJ/kg _{w.b.})
CS	24.5	
PO	25.9	14.4
SO	25.0	
SW	25.7	

The pyrolysis products yielded from 1 kg of wet biomass (moisture content: 7%) can thus produce approximately 10.4–10.7 MJ_{th}, depending on the species considered.

Thermal energy required in the process was calculated and compared with the energy which can be produced from the pyro-gas in order to check the thermal independence of the process. The following gases were included in the energy balance: CH₄, CO, CO₂, H₂. Two model compositions were found from [Falyushin et al., 2009] resulting in a pyro-gas LHV ranging from 6.30 to 16.9 MJ/kg. With reference to 100 kg of wet biomass, 175-188 MJ of thermal energy were requested in order to heat the process streams, which resulted lower than the energy obtainable from the pyro-gas (232-665 MJ) even when pyrolysis heat reaction was estimated and included.

The assessment of the immobilized capital was based on the method of Miller [Perry and Green, 1997]. All the basic equipments involved in the pyrolysis process were sized with reference to the feeding rate range of the pyrolysis process (i.e. 0.036 – 5.4 t/h). FOB costs were then found in [Matche] and the installed costs estimated. Due to bio-oil acidity and corrosion problems, a correction factor was applied to the equipments requiring stainless steel (i.e. pyrolysis reactor, decanter, char filters, oil condensing system, and storage tanks). A conservative sizing was realized in order to guarantee plant functionality regardless the biomass feedstock processed. Capital investment on the biomass storage tanks was directly calculated from the installed cost of the equipment. The installed costs of the plant considered: battery limits, storage and handlings, utilities and services. Results of the estimation are reported in table 6.10.

The costs breakdown of the immobilised capital is shown in table 6.11, where the preponderant contribution due to the battery limits area is apparent for all the plant capacities considered. Relative incidence to the costs due to storage and handlings facilities results to increase with the plant capacity at the expense of battery limits and utilities. Contribution of the process blocks to the FOB costs of the battery limits area is instead reported in table 6.12, from which a significant amount of capital results invested in storage tanks.

Workforce cost estimation was based on the calculation of the hours required to process a raw material mass unit (i.e. the operational hours), in accordance with the correlation of Wessel [Perry and Green, 1997]. Three operational units were considered: reaction unit, separation unit and storage unit. The number of operators requested in the pre-treatment processes was obtained considering a total amount of 1740 working hours per year (equivalent to 8 working hours per day, 245.5 days per

year), typical value in the chemical industry [FILCEM-CGIL]. Depending on the feeding rate of the pyrolysis plant, the number of operators ranged from 7.16 to 21.23. The cost was finally determined assuming a gross annual salary equal to 23796 € [FILCEM-CGIL].

Tab. 6.10 – Slow pyrolysis plant, immobilised capital

Biomass pyrolysis feeding rate (t/h)	Immobilised capital (k€)
0.036	732.7
0.090	1196.4
0.180	1840.7
0.270	2265.4
0.360	2509.7
0.900	4006.4
1.800	6008.0
2.700	7980.3
3.600	9781.3
4.500	11453.0
5.400	13036.9

Tab. 6.11 – Slow pyrolysis plant, costs division of the immobilised capital

Biomass pyrolysis feeding rate (t/h)	Battery limits	Storage and Handlings	Utilities	Services	Indirect costs
0.036	42.85	13.48	10.71	8.72	24.24
0.090	42.29	14.17	10.57	8.72	24.24
0.180	42.18	14.31	10.55	8.72	24.24
0.270	41.86	14.72	10.46	8.72	24.24
0.360	41.32	15.39	10.33	8.72	24.24
0.900	40.43	16.51	10.11	8.72	24.24
1.800	40.08	16.94	10.02	8.72	24.24
2.700	40.24	16.74	10.06	8.72	24.24
3.600	40.37	16.59	10.09	8.72	24.24
4.500	40.46	16.47	10.12	8.72	24.24
5.400	40.54	16.37	10.14	8.72	24.24

Tab. 6.12 – Slow pyrolysis plant, contributions to the FOB costs

Biomass pyrolysis feeding rate (t/h)	Storage tanks (%)	Reactor (%)	Condensation System (%)
0.036	43.25	29.32	27.43
0.090	45.23	28.74	26.03
0.180	45.79	28.33	25.88
0.270	45.95	28.34	25.71
0.360	45.95	28.43	25.62
0.900	45.39	28.81	25.80
1.800	44.62	29.44	25.94
2.700	44.02	29.91	26.07
3.600	43.53	30.30	26.17
4.500	43.17	30.64	26.19
5.400	42.85	30.94	26.21

Maintenance costs were estimated equal to 6% of the annual depreciation charge [Perry and Green, 1997].

Costs of the following utilities were included and calculated according to [Ulrich and Vasudevant, 2006]:

- electricity;
- make-up of demineralised water;
- treatment of the water purge from the oil condensation system;
- flue gas treatment;
- solid particles removal from the char filter.

Costs were estimated for different feeding rates of the slow pyrolysis plant. Make-up water and water purge stream were calculated from mass and energy balanced applied to the condensation system of the pyrolysis plant. Purge was considered equal to 5% of the refrigerant fluid flowing in the condenser. A complete recycle of refrigerant fluid is possible in 24 hours with this amount of make-up/purge and it should avoid the occurrence of corrosive phenomena and bio-oil aging. Solid and gaseous waste flows were also calculated from mass balance. No fuel consumption in the process was considered since all the thermal energy demand of the process was supposed to be supplied with the pyrolysis gas. Power consumption of basic equipments was calculated from technical data and head losses assessed for the centrifugal pump. 85.3% efficiency was considered in the electric equipments in which power engines were used [JRC-CEMEP, 2003]; while the coefficient of performance (COP) of the refrigeration loop was considered equal to 4.5 (average value of the industrial range: 3-6). Specific utilities costs are summarised in table 6.13 for different feeding rates of the slow pyrolysis plant.

Tab. 6.13 – Specific costs for utilities

Feeding rate (t/h)	Electricity (c€/kWh)	Make-up water (€/m ³)	Waste treatment		
			Solid (€/kg)	Liquid (€/m ³)	Gas (€/Nm ³)
0.036	12.42	1.273	0.1334	151.1	0.02169
0.090	12.42	0.7561	0.1334	60.56	0.02009
0.180	12.42	0.5162	0.1334	30.37	0.01909
0.270	12.42	0.4157	0.1334	20.30	0.01857
0.360	12.42	0.3579	0.1334	15.27	0.01823
0.900	12.42	0.2281	0.1334	6.214	0.01729
1.800	12.42	0.1679	0.1334	3.195	0.01670
2.700	12.42	0.1427	0.1334	2.188	0.01639
3.600	12.42	0.1281	0.1334	1.685	0.01619
4.500	12.42	0.1185	0.1334	1.383	0.01605
5.400	12.42	0.1115	0.1334	1.182	0.01593

Costs of licenses and patents and indirect product costs were estimated in accordance with the scheme provided in [Perry and Green, 1997]: costs of licences and patents and indirect costs were respectively considered proportional to the sum of product partial costs (i.e. the costs of production less the costs of patents and licenses) and to the cost of labour. Specific coefficients were used [Perry and Green, 1997]:

- 2.5% for the cost of patents and licenses;
- 10% for the cost due to quality control;
- 50% for the cost due to auxiliary services.

Indirect period costs were considered negligible, while circulating capital was assessed as sum of the costs associated with:

- the amount of raw materials requested for 3 months of production;
- the combustion of the pyrolysis products after 1 month of production;
- 1 month of credit toward clients.

Semi-finished products and bank deposit were not considered.

6.2.5 Transport of the pyrolysis products

The distance between pyrolysis plant and power station was considered equal to 60 km. A truck was supposed to be used for the biomass transport. A gross weight of 24 t and a payload of 14 t were considered, equivalent to a diesel consumption of 0.275 L/km with empty trips and 0.35 L/km with full loads. A linear distribution was considered for intermediate load factors. Data were obtained from [Volvo Truck Corporation, 2008]. An arbitrary volume of 40 m³ was considered for char. Specific load factors were calculated based on material densities and truck volume. A return back empty trip was also considered. Results of the logistic modelling are shown in table 6.14.

Tab. 6.14 – Pyrolysis products transportation modelling

	Char	Bio-oil
Load factor (%)	85.7	100
Fuel consumption – With load (L/100 km)	33.9	35
Fuel consumption – empty (L/100km)	27.5	27.5
Return back total consumption (L/100 km)	61.4	62.5
Return back total Consumption (L·t _{daf} ⁻¹ ·km ⁻¹)	0.0512	0.048

The transport process was supposed to be contracted out to a logistic company. Costs due to truck purchase, use and maintenance were included as well as lorry driver salary. A life span equal to 600'000 km was considered [CSST, 2007] for a kilometric cost of 1.82 €/km. Kilometric cost was then adjusted in order to take into account for the load factor, depending on the bulk density of the transported material (see table 6.2).

6.2.6 Co-combustion of the pyrolysis products with coal

Cash flows associated with the adaptation of a large power plant to co-combustion were finally assessed. Power conversion efficiency equal to 39% was considered for the co-combustion of the pyrolysis products with coal. No efficiency loss should be expected when the co-firing ratio of bio-fuels is lower than 15-20% by energy [Moncada et al., 2006]. The economic and environmental credits resulting from the coal substitution with char and oil were included in the modelling. LHV and cost of coal were respectively considered equal to 33.1 MJ/kg (typical of lithanthrax, [Enel]) and 178.7 €/t. C.I.F. cost was considered for coal under the assumption that final transport contribution was negligible. The value was obtained as average of the “Europe-ARA” quotations from April to October 2008, weighted by the volume of

coal traded [e-coal.com consultancy]. Consequent credits due to carbon dioxide emission units [European Commission, 2009] saving was calculated assuming that 82.5% of coal is composed of fossil carbon [Enel]. The price of one emission unit (i.e. 1 t CO₂eq.) was considered equal to 21.47 €/t, evaluated as the average of the Blue Next [BlueNext] (spot exchange market) and ECX [European Climate Exchange] (futures exchange market) quotations in the year 2008, weighted by the volume of quotas traded [GME].

Installation of additional tanks for the collection of char and bio-oil at the power plant was considered. The capital investment was evaluated according to the Miller method [Perry and Green, 1997]. Tanks were sized with reference to the products obtained from a single pyrolysis unit and 7 days of storage. Results of the estimation are reported in table 6.15.

Tab. 6.15 – Immobilised capital estimated for the co-combustion

Biomass pyrolysis feeding rate (t/h)	Immobilised capital (k€)
0.036	88.59
0.090	93.14
0.180	98.07
0.270	101.9
0.360	104.9
0.900	118.7
1.800	135.7
2.700	158.5
3.600	191.1
4.500	231.7
5.400	273.7

No further costs were considered under the assumptions that additional request for workforce, utilities or technology adaptation due to co-combustion can be neglected if compared with combustion of pure coal.

6.3 Results and discussion

6.3.1 Costs analysis

Immobilised capital

As a consequence of the implementation of the pyrolysis process in a Biomass-to-Power supply chain, capital investment is requested in the pre-treatment unit, in the pyrolysis facility and in the power plant. Trends of installed costs are plotted in figure 6.3 versus the feeding rate of the slow pyrolysis process. Apparent scale effects can be detected; the analysis moreover shows that immobilised capital investment is mainly due to the slow pyrolysis facility. Since contribution of pre-treatment processes and of the storage area is sensitively lower, they may be considered an addition to the battery limits of the pyrolysis plant.

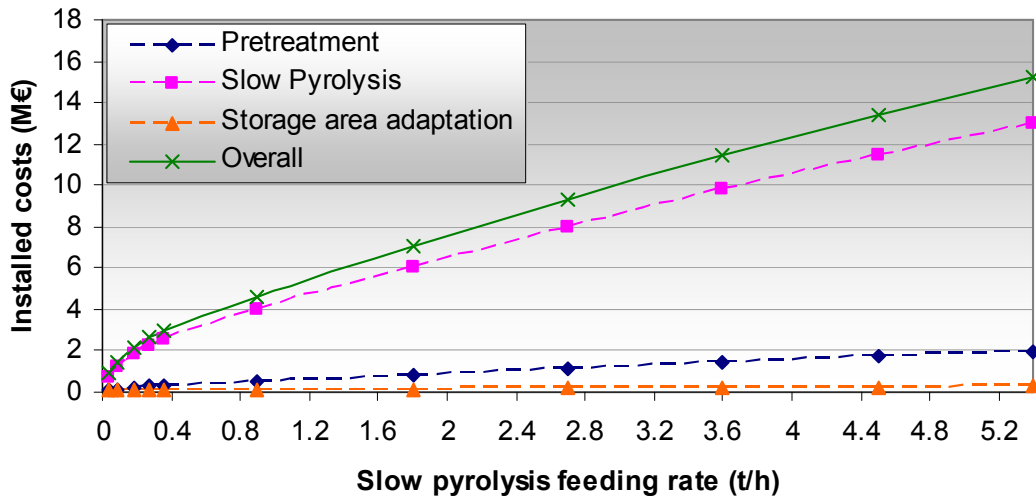


Fig. 6.3 – Trend of installed costs as a function of the slow pyrolysis feeding rate

Product costs

Product costs are reported in table 6.16, calculated at different feeding rates of the slow pyrolysis process and expressed with reference to all the biomass species investigated. A marginal difference was found between the biomasses, mainly due to the biomass specific production costs. Product costs moreover stabilises when the pyrolysis feeding rate is higher than 1.8 t/h. Magnitude order of the costs affected by scale effects (e.g. workforce) become indeed much lower at this capacity if compared with costs not depending on the industrial scale (e.g. raw material costs).

Tab. 6.16 – Product costs (€/kg_{biomass}) as a function of the slow pyrolysis feeding rate

Biomass	Slow pyrolysis feeding rate [t/h]										
	0.036	0.09	0.18	0.27	0.36	0.9	1.8	2.7	3.6	4.5	5.4
CS	1.80	0.93	0.59	0.45	0.38	0.23	0.17	0.15	0.14	0.13	0.13
PO	1.83	0.96	0.61	0.47	0.40	0.25	0.19	0.17	0.15	0.15	0.14
SO	1.83	0.96	0.61	0.47	0.40	0.25	0.19	0.17	0.16	0.15	0.15
SW	1.82	0.95	0.60	0.46	0.39	0.24	0.18	0.16	0.15	0.14	0.13

Product costs breakdown is shown on figure 6.4. It is worthy noticing that transport costs are negligible, suggesting that logistics burdens due the implementation of the slow pyrolysis process in a local market (i.e. with a transport distance lower than 60 km) should not be the most critic issue.

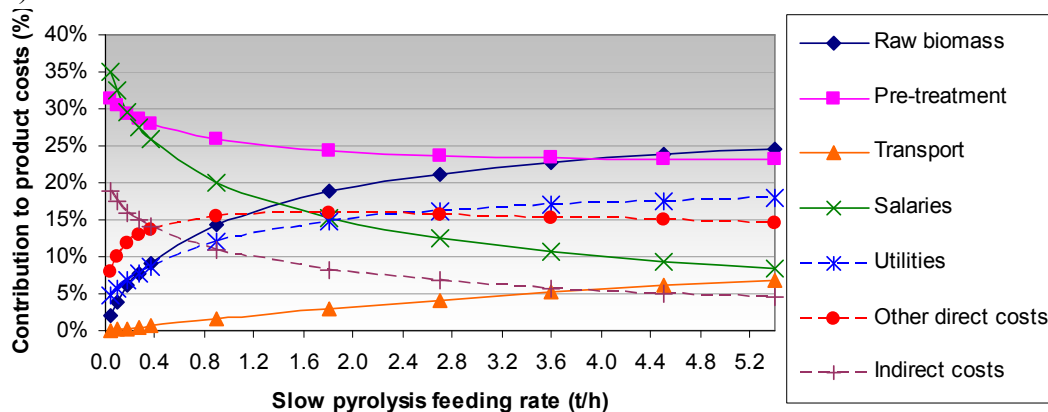


Fig. 6.4 – Product costs analysis (average values of the different biomass species)

On the other hand, pre-treatment costs are the primary voice of cost, as well as costs associated with biomass production, when the pyrolysis feeding rate increases. Utilities are instead the third voice of cost, mainly due to the bio-oil condensation system.

Avoided costs due to coal and emission units saving

The combustion of the biomass pyrolysis products allows coal to be saved and fossil carbon dioxide to be avoided. Economical credits are yielded from the coal not purchased and from the emission units which can be traded in the carbon market [BlueNext, European Climate Exchange]. Credits are reported in table 6.17, the credits due to coal saving, and in table 6.18, the credits obtained from emission units trading. Credits were quantified at different slow pyrolysis feeding rates with reference to 8280 operational hours per year and to the specific costs reported on section 6.2.6, i.e. 178.7 €/t_{coal} and 21.47 €/t_{emission unit}.

Tab. 6.17 – Credits due to coal saving (k€/yr)

Biomass pyrolysis feeding rate (t/h)	CS	PO	SO	SW
0.036	19.21	17.60	18.84	18.18
0.090	48.03	44.01	47.10	45.44
0.180	96.07	88.02	94.21	90.88
0.270	144.1	132.0	141.3	136.3
0.360	192.1	176.0	188.4	181.8
0.900	480.4	440.1	471.0	454.4
1.800	960.7	880.2	942.1	908.9
2.700	1441	1320	1413	1363
3.600	1921	1760	1884	1818
4.500	2402	2201	2355	2272
5.400	2882	2641	2826	2727

Tab. 6.18 – Credits due to unit emission saving (k€/yr)

Biomass pyrolysis feeding rate (t/h)	CS	PO	SO	SW
0.036	6.979	6.395	6.844	6.603
0.090	17.45	15.99	17.11	16.51
0.180	34.90	31.97	34.22	33.01
0.270	52.35	47.96	51.33	49.52
0.360	69.80	63.95	68.44	66.03
0.900	174.5	159.9	171.11	165.1
1.800	349.0	319.8	342.2	330.2
2.700	523.5	479.6	513.3	495.2
3.600	698.0	639.5	684.5	660.3
4.500	872.5	799.4	855.6	825.4
5.400	1047	959.3	1026	990.5

Credits due to coal saving are about the triple than the cash flows generated with the trading of the emission units. Figures depends on the biomass char/oil specific yields: higher credits result in general to be associated with biomass species characterised by

a higher char yield because of a higher LHV of char in comparison with bio-oil. The economic performance should thus be improved if char yield is maximised (and light products are also produced in order to supply the thermal energy required by the process).

6.3.2 Electricity Surcharge Indicator

The supply chain modelling of the cash flows described in the previous sections allowed the application of the Net Present Value analysis method and the calculation of the Electricity Surcharge Indicators (ESI). The indicator is measured in €/kWh_{el} and it is defined as the electricity surcharge that results in a NPV equal to zero. ESIs are plotted in figure 6.5 for all the biomass species and the slow pyrolysis feeding rates investigated in the analysis. Figures refer to the amount of electricity generated from renewable source of energy.

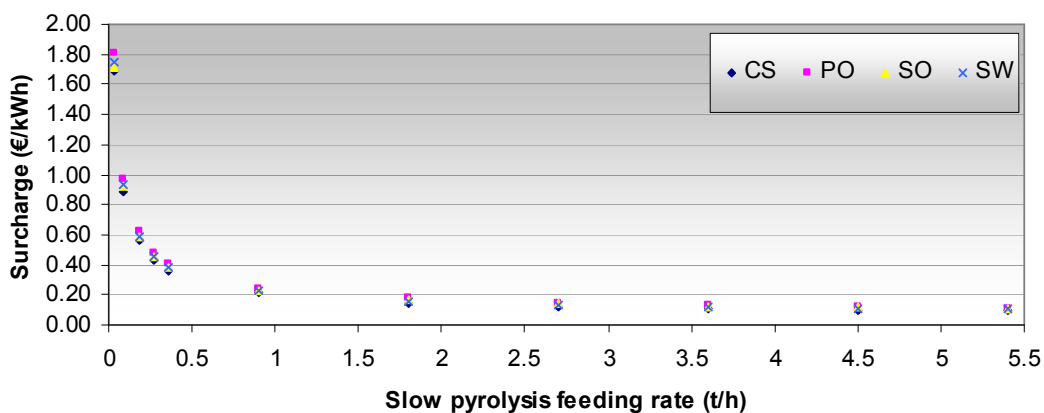


Fig. 6.5 – Electricity Surcharge Indicators calculated at different pyrolysis feeding rates and for different biomass species (figures refer to the amount of electricity generated from renewable source of energy)

Since positive ESIs resulted for all the cases analysed in the study, the implementation of the pyrolysis process is expected to increase significantly the price of the electricity produced from renewable sources of energy. Scale effects were found: surcharge decreases as the pyrolysis feeding rate increases until a stabilisation point is reached when the feeding rate is equal to 1.8-3.6 t/h. The same trend is observed with all the biomass species investigated. Original values of ESI are reported in table 6.19.

No matter the biomass analysed, the surcharge stabilises on values close to the electricity selling price in Italy in 2008 (i.e. 0.1242 €). Nevertheless, overprice is feedstock depending: CS was the biomass with the best performance, roughly 20% better than PO (i.e. the worst) when stabilisation was reached. Cash flow analysis revealed the primary influence on the output of the model of the pyrolysis yields: a bigger amount of products can be indeed obtained from biomasses with high yields in char and in oil (e.g. CS, SO, SW). Economic performance is in particular favoured by high char yields. If compared with char, lower energy content and higher collection and treatment costs are indeed associated with pyro-oil. A preferable destination for bio-oil may thus be the production of high quality products in bio-refineries.

Tab. 6.19 – ESI values for different pyrolysis feeding rates and biomass species (figures refer to the amount of electricity generated from renewable energy source)

Biomass pyrolysis Feeding rate (t/h)	CS	PO	SO	SW
0.036	1.684	1.811	1.716	1.754
0.09	0.8914	0.9672	0.9167	0.9315
0.18	0.5637	0.6186	0.5863	0.5922
0.27	0.4355	0.4823	0.4571	0.4595
0.36	0.3645	0.4067	0.3855	0.3860
0.9	0.2131	0.2452	0.2328	0.2294
1.8	0.1473	0.1745	0.1663	0.1612
2.7	0.1210	0.1459	0.1397	0.1339
3.6	0.1065	0.1300	0.12490	0.1187
4.5	0.09721	0.1197	0.1155	0.1090
5.4	0.09081	0.1125	0.1089	0.1023

Surcharges takes into account for the coal substitution with biomass pyrolysis products. In addition to the higher costs of electricity production, a complete coal substitution in a power plant would decrease the energy conversion efficiency and it would require further plant adaptation and an extensive land demand. These kinds of problems are avoided when the co-combustion ratio of pyrolysis products is lower than 20% by energy. If the surcharge due to the production of electricity from renewable source of energy is allocated to the overall power generation from co-combustion, a smaller increase of the cost of electricity is obtained. The effect is visibly much more pronounced as the co-combustion ratio of the pyrolysis products decreases. Table 6.20 shows the results obtained considering a 200 MW_{el} power plant, 10% by energy fed with SO pyrolysis products. SO was chosen because of the lowest land demand between the biomass assessed.

Tab. 6.20 – ESI allocation to co-combustion of SO pyrolysis products with coal (overall capacity: 200 MW_{el}; co-combustion ratio of pyrolysis products: 10% by en.)

Biomass pyrolysis feeding rate (t/h)	€/kWh_{renewable}	€/kWh_e	kW_{el} from a single pyrolysis unit	Pyrolysis units requested for 20 MW_{el} (nr)
0.036	1.716	0.172	46	439
0.09	0.917	0.092	114	176
0.18	0.586	0.059	228	88
0.27	0.457	0.046	342	59
0.36	0.386	0.039	456	44
0.9	0.233	0.023	1139	18
1.8	0.166	0.017	2279	9
2.7	0.14	0.014	3418	6
3.6	0.125	0.012	4558	5
4.5	0.115	0.012	5697	4
5.4	0.109	0.011	6837	3

On the basis of the results presented, larger pyrolysis plants (i.e. with feeding rates higher than 1.8 t/h) should be preferred. The pyrolysis process and the crop choice should be moreover aimed at the maximisation of the char production and at the minimisation of the land demand. Regarding to the power production process, high

overall capacity and small co-combustion ratio of biomass pyrolysis products are the additional conditions which can sustain the supply chains economy without resorting to public support systems.

6.3.3 Market saturation analysis

The implementation of a project based on biomass pyrolysis can supply renewable electricity and yield emission unit credits in change of land demand. The annual saturation of the Italian markets due to the production of 165.6 GWh of electricity (i.e. equivalent to 20 MW_{el} capacity and 8280 hours of annual production) from biomass pyrolysis products is given in table 6.21.

Tab. 6.21 – Electricity, farm lands and unit emissions Italian market saturation due to the production of 156.6 GWhe from biomass pyrolysis products

	CS	PO	SO	SW
Power production (GWh/y)		165.6		
Power consumption in Italy, 2008 (GWh/y) ^a		359 163		
Quota from biomass pyrolysis (%)		0.04611		
Land use (ha·y)	18 900	8 342	6 746	11 510
Land occupation as farm in Italy, 2005 (ha·y) ^b		12 707 846		
Quota from biomass pyrolysis (%)	0.1025	0.0420	0.03613	0.06051
Emission units saved (t/y)	141 497	137 533	139 900	138 061
Emission units assigned to the thermochemical sector in Italy, 2008-2012 (t/y) ^c		100 660 000		
Quota from biomass pyrolysis (%)	0.1406	0.1366	0.1390	0.1372

a [Terna, 2008 b]

b [Annuario SEAT, 2005]

c [Ministero dell'Ambiente e della Tutela del Territorio e del Mare e Ministero dello Sviluppo Economico, 2006]

The amount of power produced would satisfy 0.04611% of the electricity consumed in Italy in 2008. Land use demand would be marginal on a national scale – it ranges from 0.03613% (SO) to 0.1025% (CS) of the Italian farmlands – but extensive surfaces are requested on a local basis. Nevertheless, it should be observed that land requested in order to harvest CS is also functional to the production of corn grains. Farm sub-products may thus be materials effectively available in order to feed bio-energy supply chains. Emission units saving would be more intensive, from 0.053085% (SO) to 0.1487% (CS) if compared with the quotas assigned to the Italian thermo-chemical sector.

Since electricity production from biomass is strongly related to land use and to decrease of the CO₂ combustion emissions, the previous figures allows a preliminary insight of the consequences due to the production of a certain amount of electricity, the energy use of a fixed amount of land or the obtainment of carbon credits. For instance, the production of 1% of the electricity consumed in Italy in 2008 with

pyrolysis products would have the potential to save roughly 3% of the emission units assigned to the thermo-chemical sector but larger amount of land would be requested, i.e. from 1.151% of the Italian farmlands for SO to 3.225% for CS.

6.3.4 Sensitivity analysis

The most significant input parameters were changed in the supply chain based on SO in order to understand the intensity of the perturbations induced on the outcome of the model, i.e. the Electricity Surcharge Indicator. Perturbations were measured through a Specific Variation Index (SVI), defined according to equation 6.2:

$$SVI = \frac{\left| \frac{ESI' - ESI^o}{ESI^o} \right|}{\left| \frac{P' - P^o}{P^o} \right|} \quad (6.2)$$

Where:

- ESI' is the electricity surcharge after the perturbation;
- ESI^o is the electricity surcharge before the perturbation;
- P' is the parameter perturbed;
- P^o is the original parameter considered in the modelling.

Table 6.22 lists the parameters on which sensitivity analysis was performed and the uncertainty range considered for the analysis. The highest scores of the Specific Variation Indices resulting from the single perturbation of one parameter at several pyrolysis feeding rates are reported on table 6.23.

Tab. 6.22 – Parameters perturbed and perturbation intensities.

Area	Parameter	Perturbation intensity
Market	Raw biomass production costs	± 10%
	Transport costs	± 10%
	Coal cost	± 10%
	Emission unit cost	± 10%
	Interest rate on loan	± 50%
Logistics	Pyro-products transport distance	Min. - 50%; Max. + 100%
Business	Capital loan	Min. 0%; Max. 100%
	ROE	Min. 0.0432; Max. 0.15
Technical	Char LHV	± 15%
	Bio-oil LHV	± 15%
	Char yield	± 5%
	Bio-oil yield	Min. - 5%; Max. +45%
	Coal LHV	± 5%

As a general rule, the influence of the parameters on the output of the model increases with the pyrolysis plant feeding rate, meaning that sources of uncertainty should be reduced, especially when larger plants are analysed. From the analysis of the single SVIs, the ranking of the most sensitive parameters can be drawn:

1. Coal LHV;
2. Char and bio-oil yields;
3. Bio-oil and char LHV;
4. Coal cost.

Lower sensitivity was instead found for biomass production costs, capital loan, emission unit cost, ROE and pyro-products transport distance, while transport costs and interest rate on loan variations did not affected the results significantly.

Tab. 6.23 – Specific Variation Indices obtained from the single perturbation of one parameter (figures refer to the highest scores calculated for each parameter)

	Biomass pyrolysis feeding rate (t/h)					
	0.036	0.180	0.360	1.800	3.600	5.400
Coal LHV	0.2131	0.6239	0.9488	2.200	2.929	3.359
Char yield	0.6344	0.8069	0.9432	1.468	1.774	1.955
Bio-oil yield	0.5507	0.6855	0.7921	1.203	1.442	1.583
Bio-oil LHV	0.5363	0.5964	0.6440	0.8273	0.9341	0.9972
Coal cost	0.0488	0.1429	0.2172	0.5028	0.6687	0.7663
Char LHV	0.5849	0.6012	0.6141	0.6633	0.6915	0.7080
Raw biomass production costs	0.0310	0.0907	0.1380	0.3199	0.4260	0.4885
Capital loan	0.0502	0.0800	0.1021	0.2157	0.3334	0.4186
Emission unit cost	0.0223	0.0652	0.0990	0.2289	0.3041	0.3481
ROE	0.1127	0.1624	0.1907	0.2640	0.2917	0.3033
Pyro-products Transport distance	0.0097	0.0283	0.0430	0.0996	0.1325	0.1519
Transport costs	0.0012	0.0034	0.0052	0.0120	0.0159	0.0182
Interest rate on loan	0.0079	0.0126	0.0160	0.0339	0.0524	0.0658

The sensitivity analysis thus confirmed the importance of the availability of experimental and industrial data for the performance of a consistent assessment. Influence of yields and LHV of char and oil is apparent since all the cash flows are directly depending on them. Parameters referred to coal becomes instead significant in the quantification of the credits due to the fossil fuel saving and to the carbon dioxide emissions avoided. In other words, surcharge is strongly related to the difference between the production costs associated with pyrolysis products and with coal. Coal cost, in particular, fluctuates over time and it is supposed to increase in future due to higher mining costs resulting in a potential decrease in the surcharge. The second credit voice (i.e. the carbon dioxide emissions decrease) is instead less significant and it seems depending more on the coal and the pyrolysis parameters than on its inherent value.

6.3.5 Analysis of the performances of different public support systems

The economic performance of the bio-energy supply chains based on the pyrolysis process may be improved resorting to public support systems promoted by UE in the field of renewable energy [European Commission, 2005; European Parliament and Council, 2001, Wind Energy - The Facts]. Different incentive systems were included in the assessment and compared:

- Investment grants, obtained after tendering procedures placed by the States (e.g. France and Ireland).

- Systems based on tax incentives and soft loans (e.g. Malta, Finland, Cyprus, UK and the Czech Republic).
- Fixed tariffs, characterised by a specific price that must be paid to producers of green electricity (existing in most of the Member States).
- Green certificate systems, market-based instruments in which electricity from renewable energy source (RES-E) is sold at conventional power-market prices. Green certificates are controlled by States but they do not weigh on them.
- The green certificate system currently exists in Sweden, United Kingdom, Italy, Belgium and Poland.

Investment grants, tax incentives, soft loans and fixed tariffs/green certificates were ranked based on the public investment required in order to decrease the surcharge due to the production of electricity from biomass pyrolysis products. Three decrease thresholds were considered: 1%, 5%, and 100%. Surcharges were also compared with the market values of the green certificates in Italy in 2008.

The power supply chain based on SO pyrolysis was considered the reference system of the test and different pyrolysis feeding rates were analysed over a 10 years period. The support schemes were implemented in the economic model based on the following guidelines:

1. all the public incentives are constant and guaranteed over all the reference period (i.e. 10 year);
2. only one support scheme can be implemented and no financial limit exists;
3. investment grants are supposed to be obtained at the initial time and to cover a fraction of the installed costs. The public investment is calculated as difference with the base case (i.e. full surcharge);
4. tax rate is modulated in the tax incentives evaluation. The public investment is calculated as difference between full and decreased duties.
5. interest rate is modulated in the soft loan evaluation. The public investment is calculated as the difference between full and decreased interest charge;
6. the fixed tariff and the green certificates are considered equivalent to the surcharge. The capital required is proportional to the electricity produced.

Results obtained with the surcharge decrease threshold set up at 1%, 5% and 100% are respectively shown on figure 6.6, figure 6.7 and figure 6.8.

All the public schemes were able to support the 1% decrease in the electricity surcharge, even if with different public investment requests. Investment grants resulted to be the most affordable public scheme while fixed tariffs the most onerous. A similar same performance was yielded from soft loan and tax incentives. Nevertheless, it should be observed that an immediate amount of money is to be financed in case of grant incentives; while the other systems allow for a more distributed public funding whose implementation may be simpler on practice. A partial solution may be the partitioning of the investment grant on more fiscal years, even if the economic performance would be worse.

The 5% surcharge decrease was not possible with soft loan. Investment grants are still the best scheme, while tax incentives and fixed tariffs obtained very similar performances. The 100% surcharge decrease seemed instead possible only resorting to fixed tariff. Investment grants failed even considering a complete funding of the installed capital (they usually cover 40%-50% of the investment).

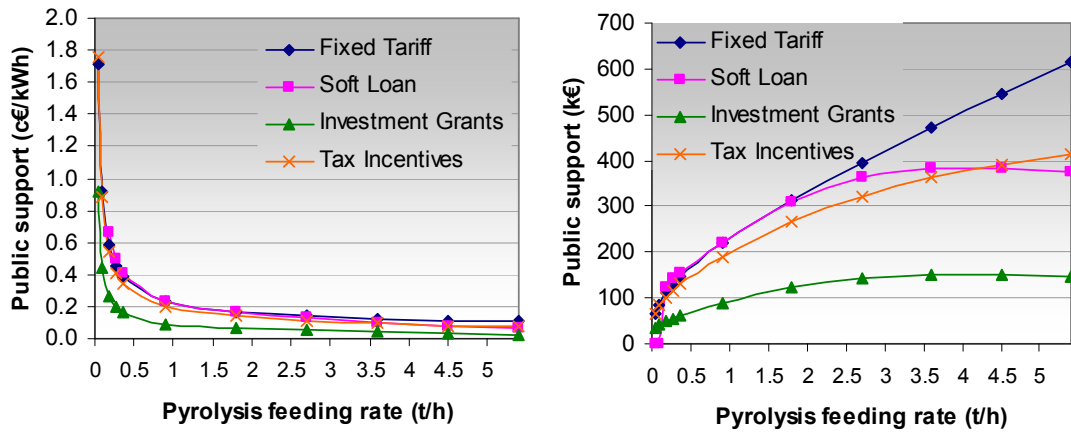


Fig. 6.6 – Public supports extent in order to obtain 1% decrease in ESI

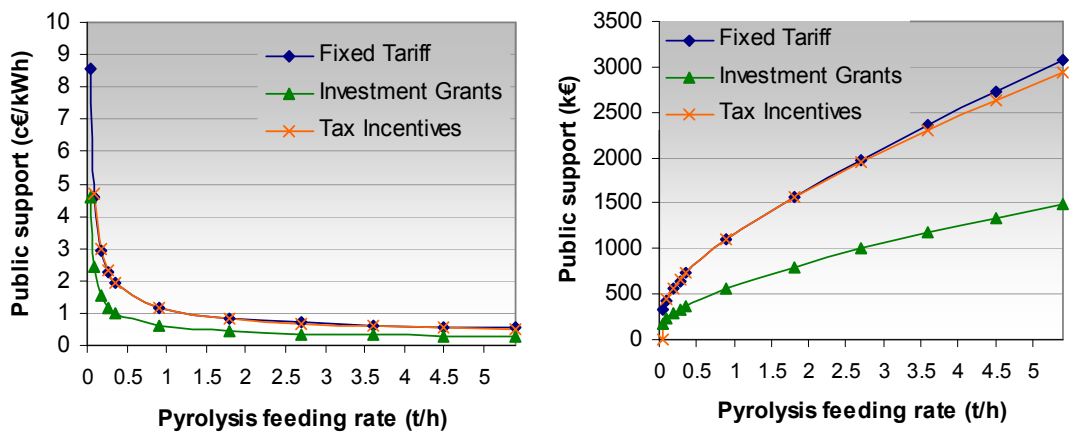


Fig. 6.7 – Public supports extent in order to obtain 5% decrease in ESI

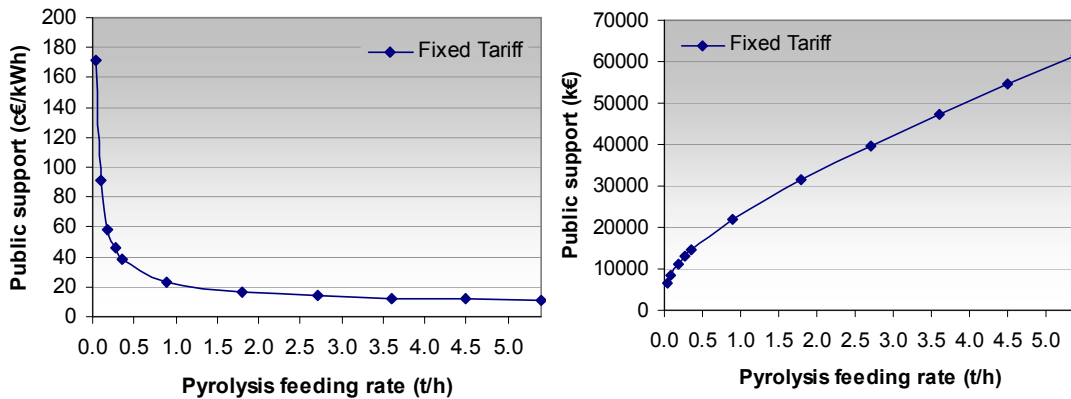


Fig. 6.8 – Public supports extent in order to obtain 100% decrease in ESI

Surcharge decreases were compared in table 6.24 with the average values of the green certificates in Italy in 2008. From the comparison it is possible to observe that green certificates are an effective scheme for the decrease of the surcharge, especially when the pyrolysis feeding rate increases. Nevertheless, the 100% surcharge decrease is possible only for values higher than the Italian average price in 2008, but quite close at high pyrolysis feeding rates.

Tab. 6.24 - Ratios of the electricity surcharge decrease to the average value of the green certificates in 2008 in Italy (103.5 €/MWh).

Biomass pyrolysis feeding rate (t/h)	ESI decrease threshold		
	1%	5%	100%
0.036	0.1659	0.8293	16.58
0.09	0.0886	0.4429	8.86
0.18	0.0567	0.2833	5.665
0.27	0.0442	0.2209	4.417
0.36	0.0373	0.1863	3.725
0.9	0.0225	0.1125	2.250
1.8	0.0161	0.0803	1.607
2.7	0.0135	0.0675	1.349
3.6	0.0121	0.0603	1.207
4.5	0.0112	0.0558	1.116
5.4	0.0105	0.0526	1.052

Supply chain economic performance can be improved resorting to public incentive systems. Even if fixed tariff and green certificates did not resulted the most efficient support systems, they are the only schemes which showed the potential to cover the full surcharge. Moreover, the funding is distributed over time and proportional to the electricity effectively transmitted at the grid so that the actual production from renewable energy source can be controlled. Investment grants, tax incentives and soft loan systems seem instead more efficient if a partial surcharge decrease is to be reached.

It should be finally observed that no surcharge allocation due to co-combustion was considered, this would have significantly decreased the public incentive extents; however, the relative performance of the schemes should remain qualitatively unchanged.

6.3.6 Conclusions

A model for the assessment of the economic performance due to power supply chains based on the co-combustion of biomass slow pyrolysis products with coal was developed. Four biomass species were analysed: CS, PO, SO, SW. The assessment was based on the economic modelling of the supply chains and on the application of the NPV analysis tool. The surcharge due to the implementation of the pyrolysis process was calculated. Apparent scale effects were highlighted; the surcharge stabilised at the value of the kWh price in 2008 in Italy (i.e. 0.1242 €); a 20% variation range was found between the worst and the best biomass investigated (i.e. PO and CS). As a consequence, pyrolysis plants with a feeding rates higher than 1-2 t/h (i.e. equivalent to 13-38 km²·yr) should be considered in industrial applications aimed at co-combustion of the pyrolysis products in large power plants and with small co-combustion ratio. This could allow the economic sustainability of the supply chains without resorting to public incentives. The pyrolysis process should be moreover aimed at the maximisation of the char production. The importance of the availability of experimental and industrial data and the positive effects of public support systems was moreover pointed out with sensitivity analysis. The model thus proved to be a flexible and effective analysis tool in the feasibility study of power supply chains based on the biomass slow pyrolysis.

CHAPTER 7

LIFE CYCLE ASSESSMENT OF ALTERNATIVE BIO-ENERGY SUPPLY CHAINS

7.1 Goal and scope definition

Different aspects concerning with the sustainability of the biomass pyrolysis process were analysed in the previous chapters. The feasibility of a bio-energy supply chain based on the slow pyrolysis process was pointed out by an economical assessment (see chapter 6); however, experimental work confirmed the presence of some critical issues associated with the industrial use of the pyrolysis products which still need to be solved (see chapter 5). Moreover, according to the three objectives of sustainability (i.e. economical growth, environment protection and social progress) [IUCN, 2006], environmental compatibility of the supply chain should be also investigated before it is implemented on an industrial scale.

Due to the higher energy density of the pyrolysis products, the inclusion of a densification process in a bio-energy supply chain is supposed to decrease the environmental burdens due to the transport of the biomass from the field of production of the feedstock to the energy conversion plant. Nevertheless, practical guidelines can be drawn only in a life cycle perspective (see chapter 4).

Energy from biomass is a current topic in many LCA studies present in literature. Applications concern both with direct combustion of biomass and issues related to logistics [see for example Boukis et al., 2009; Heller et al., 2004; Mann and Spath, 2001; Qin et al., 2006; Rentizelas et al., 2009; Thornley et al., 2009] and with production and use of bio-fuels for transports [see for all Cherubini et al., 2009; Cherubini and Ulgiati, 2010; Cordella et al., 2009; RENEW; Tilman et al., 2006; Van Vliet et al., 2009] while only marginal investigations [Di Maria and Fantozzi, 2004; Khoo, 2009; Manyele, 2007] focused on energy systems based on pyrolysis.

A Life Cycle Assessment study (LCA) was performed in order to assess topical environmental burdens associated with potential biomass-to-power (BtP) supply chains based on the combustion of char-oil slurries obtained from slow pyrolysis of biomass. Direct combustion of the biomass feedstock was considered the reference scenario for a direct comparison with alternative renewable based energy supply chains.

A metric composed by three key performance indicators was set up for the assessment: non-renewable Cumulative Energy Demand (CED), emissions of Green-House Gases (GHGs) and Land Occupation (LO) were monitored along the supply chains examined. Further details about the indicators are given in section 7.2.

The performances were assessed on the basis of 1 kWh_{el} produced from biomass feedstock (i.e. the Functional Unit). Power plant capacity was considered a core parameter in order to outline the impacts due to the electricity production on a yearly basis. According to the Functional Unit (FU) of the study, the investigation of the bio-energy supply chains presented a “cradle-to-grid” extension, i.e. from the production of the biomass feedstock to the power generation.

The base scenario considered power production from biomass derived fuels in co-combustion (CO) with coal. A 200 MW_{el} power plant was assumed, operating 8280 hours per year with a coal co-combustion ratio equal to 90% on an energy basis. 20

MWel thus resulted to be fed with renewable energy sources. Slow pyrolysis plants were supposed to process 5.4 t/h of biomass and to be placed at 60 km from the power plant. The same transport distance was considered also when the preliminary step of energy densification was excluded from the analysis.

Supply chains based on four biomass species (i.e. CS, PO, SO, SW) were compared in order to select a reference biomass. All the species investigated in the assessment can play a significant role in the Italian bio-energy scenarios (Italy) and they were also the object of the analysis performed in the previous chapters of the thesis, i.e. economic assessment (chapter 6) and experimental activities (chapter 6), from which fundamental pieces of information for the LCA study were collected.

Burdens due to power generation from coal in Italy [Ecoinvent Database] were also used as a comparative basis in order to weight the performances of supply chains based on renewable/fossil sources of energy.

A sensitivity analysis was then performed in order to analyse the effects on the life cycle performances due to a change in:

- transport distance to the power plant;
- power plant capacity from renewable sources of energy;
- power plant technology, i.e. Co-combustion (CO), Thermal Power Station (TPS) and Integrated Gasification Combined Cycle (IGCC), fixed the capacity from renewable source of energy;
- pyro-oil yield.

Consequences due to the presence of a mechanical densification process (i.e. pelletizing) in place of the thermo-chemical process of slow pyrolysis were also investigated. Further details about the supply chain modelling are given in section 7.3. Useful indications to the lifecycle stakeholders can be drawn from the present LCA study for the identification of the potential application ranges of bioelectricity supply chains. The results of the analysis can be also a robust basis for further environmental investigation of life cycles based on the biomass pyrolysis process and, more in general, on the biomass feedstock.

7.2 Key Performance Indicators

The Life Cycle Impact Assessment (LCIA) is based on the input/output data collected during the supply chain modelling and which composes the Life Cycle Inventory (LCI).

Several environmental impact categories can be characterized. The choice of the impact categories is not unambiguous but depending on several factors, such as: the targets of the study, the public perception of the environmental issues, the analyst sensitivity. A comprehensive set of indicators should be included in an impact assessment metric in order to obtain a consistent evaluation scenario.

Two main categories of indicators can be generally used: midpoint indicators and endpoint indicators, according to the intensity in the modelling of the cause-effect chain [Bare et al., 2000]. Midpoint modelling is on the middle of the environmental mechanism chain and it aims to quantify environmental impacts on the basis of equivalence factors between the items present in the LCI. A deeper modelling characterizes endpoint indicators, which are thus closer to the representation of the physical effects on society. Perception and interpretation of endpoints indicators is easier but at the expense of an increase in uncertainty.

As a consequence of the current concern on climate change and on world demand for energy, attention in LCA is often paid on single indicators related with these issues

[see for all Dornburg and Faaij, 2005; Tilman et al., 2006; Van Vliet et al., 2009]. It is moreover apparent that another hot-spot connected with biomass based systems is the request for land. Three key performance indicators were considered in the present LCA study on a midpoint dimension: non-renewable Cumulative Energy Demand (CED), emission of greenhouse gases (GHGs) and Land Occupation (LO). A partial but significant footprint of some potential impacts due to the supply chains was yielded with this metric.

7.2.1 Non-renewable Cumulative Energy Demand

The Cumulative Energy Demand (CED) [Frischknecht et al., 2007] of a supply chain takes into account for the overall amount of energy (MJ eq.) consumed under a life cycle perspective. Energy is generally calculated as the sum of feedstock energy (i.e. the energy contained in raw materials which are directly converted to energy), process energy (i.e. the energy requested by all the processes involved in the life cycle) and embedded energy (i.e. the net energy needed for the production, transportation and disposal after use of products and materials consumed along the supply chain). While feedstock energy is an internal flow of energy, the other typologies of energy can be considered external flows.

The original indicator was modified in order to take into account for non-renewable flows of energy in the supply chains and for all the external flows of energy. Biomass energy content, used to feed the power supply chains, was thus excluded from the calculation.

7.2.2 Carbon footprint

This indicator considers the overall amount of green house gases (GHGs), expressed as kg CO_{2eq.}, emitted along the supply chains, a.k.a. “carbon footprint” [Carbon Trust]. Carbon footprints were calculated according to the IPCC’s Global Warming Potential (GWP₁₀₀) [IPCC, 2007] with few modifications.

Carbon dioxide fixed by the biomass during the photosynthesis process and the emission of biogenic carbon oxides (i.e. CO and CO₂) were neglected. Moreover, the GWP₁₀₀ assigned to biogenic methane was considered equal to the difference between the one corresponding to the fossil methane (i.e. 23) and the mass of CO₂ which would be emitted if the carbon contained in the CH₄ were oxidized to CO₂ (i.e. 44/16). Finally, emissions due to land use change were not included under the hypothesis that land use destination was kept unchanged for a long period of time.

7.2.3 Land Occupation

Land Occupation (LO) takes into account for the spatial and temporal requests of land in all the processes involved by the supply chains. It is measured as m²·yr and it is a significant indicator for the assessment of the territorial sustainability.

7.3 Supply chain modelling

The input/output data needed for the analysis were obtained at the end of a detailed modelling process, which required cross-disciplinary competences (e.g. environmental, logistic, technical, territorial) due to the nature of the bio-energy topic.

The first step of the modelling was aimed at the definition of the stages involved by the bio-energy supply chains. According to the Functional Unit (FU) of the study, the System Boundaries (SB) of the supply chains included five sub-systems:

1. production of the biomass;
2. transport of the biomass to collection points;
3. potential application of a densification process;
4. transport of the bio-fuel (i.e. raw biomass or the densification products) to the power plant;
5. power generation.

Energy consumption, GHGs emissions and land use were then quantified for each stages based on:

- the collection of a great extent of data (e.g. experimental pyrolysis yields, technical and thermodynamic data);
- the calculation of mass and energy balances;
- the consultation of literature data and specific databases, e.g. Ecoinvent [Ecoinvent Database].

An effort was made in order to match the spatial and temporal dimension and the technology level involved by the life cycles. In particular, due to the relative novelty of the investigated supply chains, it is important to remark that the modelling was coupled with experimental activities, mainly aimed at the collection of biomass specific pyrolysis yields.

A “third order” analysis [Goedkoop et al., 2007] performed in the present application: all the processes involved by the life cycles and the foremost materials and energy streams connected to each sub-system were included together with an estimation of the environmental burdens embedded in the materials used for the construction of the capital goods.

In presence of co-products, land, mass and energy streams were allocated on the basis of appropriate physical or economic criteria.

7.3.1 Production of the biomass

Supply chains based on different lignocellulosic biomass species were modelled. Four different lignocellulosic biomass species were analysed in the study: CS, PO, SO and SW. The foremost characteristics of the crops, which were investigated in the previous chapters of the thesis, are given in the section 6.2.2. Yields, energy content, harvest system and moisture content of the biomass feedstock were indeed reported in table 6.2. In particular, different harvest systems and specific bulk density were considered depending on the single biomass species: baling for CS and SW; chipping for PO and chopping for SO. Baling option was considered also for SO in order to investigate the effects of the harvest system. Significant effects on logistics are indeed due to the harvest system (see the section 7.3.2). Biomass was supposed to be left on the field to dry for two months to a final 25% moisture content. 1% dry material loss was monthly considered as a consequence of natural drying [Rentizelas et al., 2009]. Further agronomic details about the crops investigated can be found in [ARSIA, 2004; Gelleti et al., 2006; Venturi et al., 2008].

Basic input data concerning with the production of the biomass species were provided by [DiSTA] and are reported on table 7.1 with reference to 1 ha of production. Data includes consumption of raw materials (i.e. rhizomes, seeds, fertilisers, pesticides) and energy (i.e. the diesel used by tools and machinery) in the process. The amount of tools and machinery allocated to 1 ha of production was also provided.

Tab. 7.1 – Inputs in the production of the crops considered in the study
(reference basis: 1 ha) [DiSTA]

Sowing	CS Bales (*)	PO Chips	SO Bales	SO Chopped	SW, Bales
Diesel (L)	0	175	0	0	128
Triple superphosphate (48% P ₂ O ₅) (kg)	0	288	0	0	240
Rhizomes (kg)	0	8	0	0	8
Gliphosate (33%) (kg)	0	1.65	0	0	1.65
Tools and machinery (kg)	0	8.9	0	0	7.375
Production	CS Bales (*)	PO Chips	SO Bales	SO Chopped	SW Bales
Diesel (L)	237	8	138	138	31
Triple superphosphate (48% P ₂ O ₅) (kg)	96	0	67.2	67.2	96
Urea (46% N) (kg)	207	128.8	115	115	92
Seeds (kg)	25	0	6	6	0
Gliphosate (33%) (kg)	1.65	0	1.65	1.65	0
Tools and machinery (kg)	47.76	0.4	8.96	8.96	2.65
Harvesting	CS Bales (*)	PO Chips	SO Bales	SO Chopped	SW Bales
Diesel (L)	20	25	20	40	20
Tools and machinery (kg)	2.7	16	2.7	11.55	2.7

(*) corn grains are the other co-product of the crop

Biomass sowing was allocated over 15 years of production in case of perennial crops. Two co-products are yielded from corn farming, i.e. CS and corn grains, so that an allocation of the input data is required. Different allocation criteria were tested, even if an energy basis should be considered the most appropriate basis in the current application. Table 7.2 reports specific yields and allocation factors resulting from different allocation procedures.

Tab. 7.2 – Yields and allocation factors for CS and corn grains,
co-products of corn farming

	CS	Corn grains
Yield (t/ha)	8	10
LHV (GJ/t)	16.8	15.8
Economic value (€/t)	55	150
Mass basis (%)	44.4	55.6
Energy basis (%)	46	54
Economic basis (%)	22.7	77.3

Environmental information of concern for the study (i.e. energy demand, GHG emissions and land occupation) were obtained coupling the data reported on the previous tables with specific characterisation factors found in literature [Ecoinvent Database]. Characterisation factors are shown in table 7.3.

Tab. 7.3 – Characterisation factors for the processes involved in the biomass cultivation [Ecoinvent Database]

Process (FU)	MJ_{eq.}	kg CO₂ eq	m²·yr
Diesel (1 L)	45.1	3.03	0.00778
Triple superphosphate (48% P ₂ O ₅) (1 kg)	26.8	2.07	0.092
Urea (46% N) (1 kg)	63.6	3.37	0.0623
Glyphosate (33%) (1 kg)	322	15.9	0.237
Rizoms (1 kg)	18.7	2.06	0
Seeds (1 kg)	13.1	2.03	4.35
Steel (1 kg)	62	3.7	0.163

Further modelling included GHGs emissions due to biomass decomposition (i.e. CO₂ and CH₄), occurring during natural drying, and to nitrogen fertilizers application in the soil (i.e. N₂O).

Both aerobic and anaerobic processes of decomposition were considered for biomass. 90% of the decomposed biomass is supposed to be involved with aerobic processes and to yield 1.67 kg CO₂ per kilogram of biomass decomposed. Anaerobic pathway of degradation interests the remaining 10% and yields 0.0667 kg CH₄ per kilogram of biomass decomposed [Mann and Spath, 2001].

N₂O emissions from nitrogen fertilisers (i.e. urea, in the present application) were modelled with the parameters given by [De Klein et al., 2006], which include leaching, run/off, atmospheric deposition and contribution to the emission due to the interaction of fertilisers with soil. As a result of the estimate, an emission of 4.87 kg/ha was considered for CS, 2.94 kg/ha for PO, 3.13 kg/ha for SO and 2.10 kg/ha for SW.

7.3.2 Transport of the biomass to concentration points

Due to logistic reasons, biomass was supposed to be concentrated in collection points where the potential application of the densification process can occur. The collection area of a single unit was supposed circular and based on a yearly production of 44'712 t of biomass (moisture content: 7 %), equivalent to a 5.4 t/h pyrolysis plant working 8280 hours per year. A correction factor was applied to the area in order to account for the land effectively used in biomass production (40.8% of the land [ISTAT, 2007]). The number of units needed to feed yearly the BtP supply chains was considered.

The distance of concentration was calculated, according to equation 7.1, as the area-weighted average radius of the collection area, multiplied by a tortuosity factor:

$$DC = TF \cdot \int_0^R \frac{2\pi r^2 dr}{\pi R^2} = \frac{2}{3} R \quad (7.1)$$

Where:

DC = distance of concentration;

R = collection area radius;

TF = tortuosity factor (considered to be 1.6, corresponding to secondary rural roads [Thornley et al., 2009]).

A small truck was supposed to be used for the biomass transport. A gross weight of 14 t and a payload of 8.5 t were considered, equivalent to a diesel consumption of

0.225 L/km with empty trips and 0.275 L/km with full loads. A linear distribution was considered for intermediate load factors. Emission of 2.6 kg CO₂ was associated to 1 L of diesel consumed. Data were obtained from [Volvo Truck Corporation, 2008]. An arbitrary volume of 25 m³ was considered. Specific load factors were calculated based on material densities and truck volume. A return back empty trip was also considered. Results of the modelling are shown in table 6.4 with reference to 25% moisture content (see section 6.2.3).

Low sulphur diesel was the transportation fuel considered; burdens due to infrastructures were then added from the Ecoinvent process “Transport, lorry 3.5-16 t, fleet average/RER U” [Ecoinvent Database], which presented a 0.355 load factor to be corrected. Characterisation factors for these processes were obtained from Ecoinvent and they are reported on table 7.4.

*Tab. 7.4 – Characterisation factors
for the transportation processes [Ecoinvent Database]*

Process (FU)	MJ_{eq.}	kg CO_{2 eq}	m²·yr
Diesel low sulphur (1 L)	45.3	0.437	0.00782
Infrastructure, load factor = 0.355 (1 t·km)	1.1	0.0517	0.00747

7.3.3 Potential application of a densification process

A densification process can be applied at the concentration point in order to increase the energy density of the fuel to be fed to the power plant.

The densification process examined in the present work is the slow pyrolysis process, in which biomass is converted to solid and liquid fuels (i.e. char and bio-oil) under the application of thermal energy, which can be theoretically supplied by the gaseous product of pyrolysis. Environmental modelling of slow pyrolysis has to take into account for energy consumptions, GHGs emission and land occupation associated with the building blocks of the process. The process layout is the same considered in the economic assessment (see section 6.2.4). Biomass is supposed to be dried to 7% moisture content, grinded to a particle size equal to few millimetres and then processed at 650 °C. Modelling included also biomass conditioning (i.e. storage, drying and grinding) required in order to fulfil the pyrolysis specifications.

Biomass pre-treatment

Biomass is stored, dried to 7% moisture content and grinded to fine particles (i.e. 1 mm size) before the densification process.

The following burdens were associated to 1 m³ of biomass stored: 0.0304 MJ_{eq.}; 0.00127 kg CO_{2eq.}; 0.0442 m²·yr. Data refers to a non ventilated warehouse present in [Ecoinvent Database].

Thermal and electric energy are consumed in the drying and in the grinding process. Moisture content of the biomass was supposed to change from 25% to 7% during drying. From mass balance, 240 kg of water are evaporated per 1000 kg of biomass leaving the drying process, for a consequent request of 661 MJ of thermal energy from light fuel oil (85% energy conversion efficiency is considered). Consumption of 0.138 kWh (see section 6.2.4) and 25 kWh [Van Loo and Koppejan, 2008] of electricity were also assigned to the drying and the grinding of 1000 kg of biomass

material. Specific environmental loads due to energy and machinery production were taken from [Ecoinvent Database] and reported in table 7.5.

Tab. 7.5 – Burdens associated with energy processes and machinery production [Ecoinvent Database]

Process (FU)	MJ_{eq.}	kg CO₂_{eq}	m²·yr
Electricity from oil (1 kWh)	12.2	0.879	0.00196
Thermal energy from light fuel oil burned in 1 MW industrial furnace (1 MJ)	1.29	0.0866	0.000207
Drying (1kg of water evaporated)	0.0415	0.00247	0.0475
Grinding (1 kg of input biomass)	0.00491	0.000319	0.0000132

The slow pyrolysis process

Material and energy flows involved in the slow pyrolysis were calculated from mass and energy balances, which required a preliminary design of the process and experimental, technical and thermodynamic data (see section 6.2.4).

Pyrolysis products (i.e. char and bio-oil) are supposed to be transported in a power plant and burned for the production of electricity. Yields in char and bio-oil are the core element of the modelling and they were obtained from the experimental activities outlined in chapter 5. Characteristics of the biomass based fuels were taken from literature [Oasmaa and Czernik, 1999; Phyllis Database; Scurlock] and reported in section 6.2.4 in table 6.8. Yields are also reported in section 6.2.4 in table 6.7 with reference to 650 °C pyrolysis temperature and 7% of moisture content in the biomass feedstock. Average figures were considered for heating value, density and water content. LHV of bio-oil and char was also corrected in order to take into account for water and ash content. No ash content was considered for bio-oil and no water content for char. Biomass ash content was measured during the experimental analysis described in chapter 5 so that different figures were found for the chars examined in the study. Results are shown in section 6.2.4 in table 6.9. Under these assumptions, about 10.4–10.7 MJth can be produced from 1 kg of biomass at 7% of moisture, depending on the species considered.

No thermal energy consumption was considered in accordance with the results of the energy balance of the process (see section 6.2.4). However, process modelling included consumption of electricity and water and the burdens embedded in the equipments (supposed composed of stainless steel and concrete). The following inputs were estimated from the economic modelling (see section 6.2.4) and allocated to 1 kg of biomass processed:

- 0.0720 kWh of electric energy;
- 0.587 L of water demineralised;
- 0.0936 kg of stainless steel;
- 0.000560 kg of concrete.

End-of-pipe treatment processes of flue gas and wastewater were neglected; the overall life time of the pyrolysis plant was considered equal to 124200 hours. Environmental burdens associated with these inputs were found in [Ecoinvent Database] and reported in table 7.6.

Tab. 7.6 – Environmental burdens associated with materials and with the energy required in the slow pyrolysis [Ecoinvent Database]

Process (FU)	MJ _{eq.}	kg CO ₂ _{eq.}	m ² ·yr
Concrete (1 kg)	0.153	0.00891	0.00591
Electricity from oil (1 kWh)	12.2	0.879	0.00196
Steel (1 kg)	62	3.7	0.163
Water (1 L)	0.000301	0.0000248	0.000000115

Modifications of the densification process

Modifications were implemented to the densification step in order to obtain a preliminary comparison with alternative processes.

The first modification interested the pyrolysis process. Pyrolysis yields in liquid product were observed to range significantly during the experimental activities performed, mainly depending on the different cooling system applied. Char yields instead appeared rather constant (see section 5.1). Bio-oil yields were thus increased to 145% of the original values. This may be, for example, representative of a more efficient condensation train or, to a first approximation, of a different pyrolysis system to a first approximation (e.g. fast pyrolysis). An increase in the energy output from the process results from the oil yield increase, however, 656 MJ of additional thermal energy are necessary in order to process 1 t of wet biomass due to the consequent decrease in light products, which supposed to supply the heat required by the process. In accordance with the pre-treatment processes, this amount of energy was supposed to be supplied with light oil.

A streamlined modelling concerned also with an alternative mechanical process: pelletizing. Pelletizing was modelled from literature data under the assumption that slow pyrolysis biomass specifications are required also in the pellet production, so that the same pre-treatment processes were considered. 100 kWh of electricity were associated with the pelletizing of 1 t of dry biomass [Świgoń and Longauer, 2005]. No waste was supposed to be formed during the process. 0.0375 MJ_{eq.}, 0.00215 kg CO₂_{eq.}, 0.00101 m²·yr were allocated to the plant. Burdens were adapted from [Ecoinvent Database]. Life time of the plant, pellets density and moisture content were respectively considered equal to 15 years, to 650 kg/m³ and to 7%.

7.3.4 Transport of the bio-fuel to the power plant

Transport distance from the concentration points to the power plant was calculated according to the equation 7.2:

$$DT = 9.143 \cdot e^{0.0935 \cdot PC} \quad (7.2)$$

where:

DT = distance of transport (km);

PC = power capacity of the plant supplied by biomass derived fuels (MW_e)

Two truck typologies were supposed to be used for the fuel transport:

- A gross weight of 24 t and a payload of 14 t were considered for distances up to 60 km. This is equivalent to a diesel consumption of 0.275 L/km with empty trips and 0.35 L/km with full loads. An arbitrary volume of 40 m³ was moreover assigned to transport in bales, chips or chopped;

- A gross weight of 40 t and a payload of 26 t were considered for distances longer than 60 km. This corresponds to a diesel consumption of 0.235 L/km with empty trips and 0.32 L/km with full loads. An arbitrary volume of 80 m³ was moreover assigned to transport in bales, chips or chopped.

A linear distribution was considered for intermediate load factors. Emission of 2.6 kg CO₂ was associated to 1 L of diesel consumed. Data were obtained from [Volvo Truck Corporation, 2008].

Specific load factors were calculated based on material densities and truck volumes. A return back empty trip was also considered. Results of the modelling are shown in table 7.7 and in table 7.8 with reference to the wet weight of the transported material. Low sulphur diesel was the transportation fuel considered, burdens due to infrastructures were then added from the Ecoinvent process “Transport, lorry 3.5-16 t, fleet average/RER U” [Ecoinvent Database], which presents a 0.355 load factor. Characterisation factors for these processes were obtained from Ecoinvent [Ecoinvent Database] and they are reported in table 7.3.

Tab. 7.7 – Diesel consumption in the transportation stage depending on the modality of transportation of different biomass based fuels (1/2)

Transport distance (km)	Bales		Chips		Chopped	
	< 60	> 60	< 60	> 60	< 60	> 60
Load factor (%)	37.1	40	68.6	73.8	28.6	30.8
Fuel consumption – With load (L/100 km)	30.3	26.9	32.6	29.8	29.6	26.1
Fuel consumption – empty (L/100km)	27.5	23.5	27.5	23.5	27.5	23.5
Return back total consumption (L/100 km)	57.8	50.4	60.1	53.3	57.1	49.6
Return back total Consumption (L·t _{ss} ⁻¹ ·km ⁻¹)	0.148	0.0646	0.0835	0.037	0.1905	0.0827

Tab. 7.8 – Diesel consumption in the transportation stage depending on the modality of transportation of different biomass based fuels (2/2)

Transport distance (km)	Char		Bio-oil		Pellet	
	< 60	> 60	< 60	> 60	< 60	> 60
Load factor (%)	85.7	92.3	100	100	100	100
Fuel consumption – with load (L/100 km)	33.9	31.3	35	32	35	32
Fuel consumption – empty (L/100km)	27.5	23.5	27.5	23.5	27.5	23.5
Return back total consumption (L/100 km)	61.4	54.8	62.5	55.5	62.5	55.5
Return back total consumption (L·t _{ss} ⁻¹ ·km ⁻¹)	0.0512	0.0229	0.048	0.0213	0.0446	0.0213

7.3.5 Power generation

Three different typologies of power production were modelled: Co-combustion (CO), Thermal Power Station (TPS) and Integrated Gasification Combined Cycle (IGCC).

Co-combustion

Biomass based fuels are co-fired with coal in an entrained bed power plant. Power efficiency was calculated according to the equation 7.3, obtained through curve fitting in the range 1-600 MWe of industrial data referred to co-combustion power plants.

$$PE = 0.51 \cdot \ln(PC) + 36.73 \quad (7.3)$$

Where,

PE = power conversion efficiency (%)

PC = power capacity of the plant (MWe)

Co-firing ratio of renewable sources was assumed lower than 20% by energy (10%). As a consequence, no efficiency loss due to co-firing was considered [Moncada Lo Giudice et al., 2006].

Char was supposed to be pulverised before the co-combustion of the slow pyrolysis products. A consequent electricity demand of 40 kWh per ton of material fired results from pulverisation [Van Loo and Koppejan, 2008]. The burdens associated with the production of machinery used during grinding were also included.

In the direct co-combustion of baled, chipped or chopped biomass material, the same sequence of pre-treatment processes applied before the densification step (i.e. storage, drying to a 7% moisture content, grinding) are considered at the power plant, where also pulverisation occurs.

Embedded burdens associated with the power plant adaptation to co-combustion were also included. Construction materials required for the installation of additional storage tanks were considered. 0.00000566 kg of steel and 0.000393 kg of concrete per kg of material fed to co-combustion were estimated from the economic modelling and included in the analysis. The environmental loads reported in table 7.6 were then assigned to the construction materials.

No credit was assigned to potential coal substitution under the hypothesis that the same benefit can be obtained with all the typologies of power plant. This may represent an energy scenario in which additional energy production is considered.

Thermal Power Station

TPS efficiency was calculated according to the equation 7.5, obtained through curve fitting in the range 1-250 MWe of data referred to power plants.

$$PE = 5.1 \cdot \ln(PC) + 11.1 \quad (7.5)$$

Where,

PE = power conversion efficiency (%)

PC = power capacity of the plant (MWe)

In the direct co-combustion of baled, chipped or chopped biomass material, the same sequence of pre-treatment processes applied before the densification step (i.e. storage, drying to a 7% moisture content, grinding) are considered to occur at the power plant.

Embedded burdens associated with the power plant facility were estimated from [Ecoinvent Database] according to equation 7.6. Parameters of the equation are given in table 7.9.

$$EB = \alpha \cdot TC^\beta \quad (7.6)$$

Where,

EB = embedded burden allocated to 1 kWh_{th}

TC = thermal capacity (MW_{th})

Tab. 7.9 – Parameters for the estimation of the environmental burdens allocated to the thermal power station

Parameter	MJ_{eq.}	CO_{2eq.}	m²·yr
A	0.0142	0.0009	0.0025
B	0.1121	0.1231	-0.536

Integrated Gasification Combined Cycle

IGCC efficiency was calculated according to the equation 7.6, obtained through curve fitting in the range 1-100 MWe of literature data points concerning with power plants.

$$PE = TE \cdot 3.64 \cdot \ln(PC) + 33.4 \quad (7.6)$$

Where,

PE = power efficiency (%);

TE = thermal conversion efficiency at the gasifier (raw biomass: 0.84; char-oil slurry: 0.94), modelled from [Heinrich, 2007];

PC = power capacity of the plant (MWe).

Char was supposed to be pulverised before the gasification of the slow pyrolysis products. A consequent electricity demand of 40 kWh per ton of material fired results from pulverisation [Van Loo and Koppejan, 2008]. The burdens associated with the production of machinery used during grinding were also included.

In the direct co-combustion of baled, chipped or chopped biomass material, the same sequence of pre-treatment processes applied before the densification step (i.e. storage, drying to a 7% moisture content, grinding) are considered at the power plant, where also pulverisation occurs.

No additional contributions due to gas cleaning were included. The same embedded burdens estimated in the TPS facility were finally considered also in the IGCC model.

7.3.6 Power supply chain based on coal

Power production in Italy from coal combustion was considered the reference system for the comparison with a fossil based supply chain. 11.7 MJ_{eq.}; 1.03 kg CO_{2eq.}; 0.024 m²·yr are associated with the production of 1 kWh of electric energy, on the basis of the process “Electricity, hard coal, at power plant/IT”, present in [Ecoinvent Database].

7.4 Results and discussion

7.4.1 Assessment of power supply chains based on different biomass species

Power supply chains based on the slow pyrolysis of biomass were preliminarily investigated. Environmental performances due to CS, PO, SO and SW were screened. Co-combustion (CO) of the biomass slow pyrolysis products with coal in a 200 MWe

power plant operating 8280 hours per year is considered. Pyrolysis products are supposed to be transported 60 km and to be fed with a co-combustion ratio equal to 10% by energy. Results of the comparison are shown in table 7.10 on an intensive and on an extensive basis. Different allocation criteria were in particular applied to CS production.

Tab. 7.10 – Comparison between the environmental performances of power supply chains based on the slow pyrolysis of different biomass feedstock.

Biomass	CS, bales, NO	CS, bales, \$	CS, bales, EN	SO, bales	SO, Chopped	PO, chips	SW, bales
MJ / kWhe	2.388	3.148	3.910	3.065	3.129	3.033	3.238
Kg CO_{2eq} / kWhe	0.148	0.234	0.320	0.246	0.250	0.250	0.265
m²·yr / kWhe	0.015	0.274	0.540	0.421	0.423	0.519	0.710
TJ / yr	395.4	521.4	647.5	507.6	518.1	502.3	536.2
Mt CO_{2eq} / yr	0.02450	0.03868	0.05303	0.04072	0.04140	0.04144	0.04390
km²·yr / yr	2.540	45.45	89.48	69.78	69.99	86.01	117.6

NO = biomass production completely allocated to corn grains

\$ = economic allocation of the burdens due to biomass production

EN = energy allocation of the burdens due to biomass production

Depending on the biomass feedstock considered, the following ranges were found for external energy consumption, GHG emission and land occupation:

- 2.388–3.910 MJ/kWhe;
- 0.148–0.320 kgCO_{2eq}/kWhe;
- 0.015–0.710 m²·yr/kWhe.

CS supply chain performance was particularly affected by the allocation basis considered in the biomass production stage. Apart from land occupation, whose largest value was obtained in the SW system, CS generally resulted both the best and the worst biomass, respectively when all the I/Os of biomass production were allocated to grain corns or when an energy allocation basis was instead considered.

Range of the results becomes narrower if CS is excluded from the comparison, as shown in table 7.11. In particular, no significant differences are observed between the two harvest systems considered for SO (i.e. baling vs. chopping).

Land occupation is instead particularly sensitive to the biomass feedstock. This indicates the strong influence of biomass yields on the life cycle performances, while impacts due to logistics should be marginal. In other words, according to these preliminary results, the biomass yield seems the most important parameter of choice between the different supply chains.

Tab. 7.11 – Comparison between SO, PO and SW based supply chains.

KPI	SO, bales	SO, chopped	PO, chips	SW, Bales
MJ/kWh	-2.05%	Reference	-3.07%	+3.48%
kgCO _{2eq} /kWh	-1.61%	Reference	+0.08%	+5.99%
m ² ·yr/kWh	-0.47%	Reference	+22.70%	+67.85%

7.4.2 Gravity analysis

A gravity analysis, i.e. the analysis of the single sub-systems contributions to the life cycle KPIs, was performed in order to identify the hot-spots of the supply chains.

Cumulative Energy Demand

Figure 7.1 shows the contributions to CED due to the different stages of the supply chains investigated.

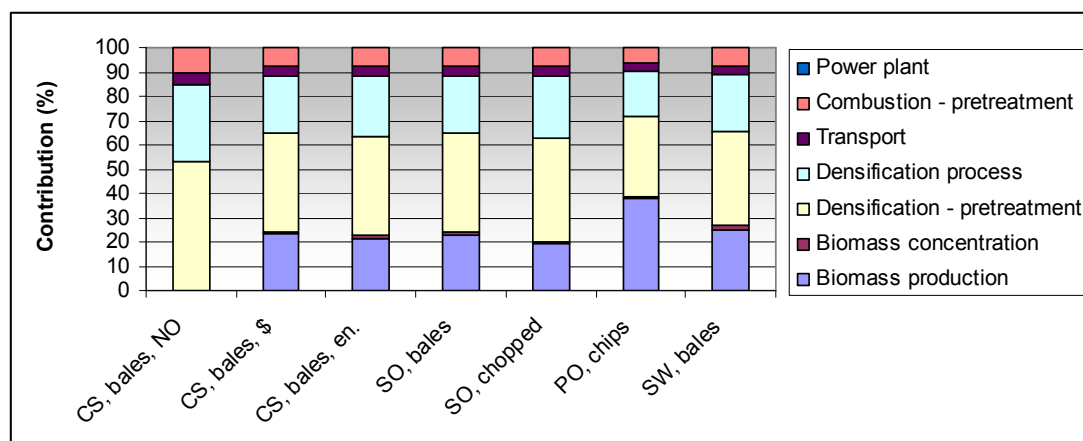


Fig. 7.1 – Contribution to CED due to the different stages of the biomass pyrolysis based power supply chains

The most of the energy is demanded by the pre-treatment processes of the slow pyrolysis process (from 32% for PO to 43% for SO, chopped), followed by biomass production (from 19% for SO, chopped to 38% for PO), and by the slow pyrolysis densification process (from 19% for PO to 25% for SO, chopped). Burdens due to logistics are appreciably lower, below 5%, while contribution due to the pre-treatment at the power plant (i.e. pulverisation) is equal to 8%. It must be in particular observed that the significant contribution of the pre-treatment processes is in strong accordance with the results of the economic assessment (see chapter 6).

Energy requests in the pre-treatment processes are essentially due to heat (58%) and power (41%), while production and supply of fertilisers and pesticides (50-55%, with higher figures corresponding to annual crops) are prevailing in the biomass production stage, followed by diesel consumption (40-42%). Energy consumption in the slow pyrolysis process is instead mainly due to electricity (90%). The energy embodied into equipment materials (10%) may also have a significant contribution.

Carbon Footprint

Figure 7.2 shows the contributions to Carbon Footprint (CF) due to the different stages of the supply chains investigated.

Energy consumption and GHG emissions should follow the same trends when systems based on fossil fuels are investigated, so that similar results should be expected in the CF analysis. Nevertheless, biomass production is the most significant process in this impact assessment category (from 39% for SO chopped to 53% for PO), followed by pre-treatment processes at the pyrolysis plants (from 25% for PO to 33% for SO chopped) and by the densification process (from 14% for PO to 18% for

SO chopped). Logistics and co-combustion pre-treatments nearly account together for 10%, with a similar contribution.

The increase of the relative significance of the biomass production stage in the carbon footprint can be explained by the emissions associated with application of fertilisers into soil and with biomass degradation. Carbon footprint of the production stage is indeed strongly related to the emission of N₂O (from 35% for SO chopped to 44% for PO) and CH₄ (from 19% for SW to 23% for SW). Production and supply of fertilisers and pesticides (21-32%, from perennial to annual crops) followed by diesel consumption (7-11% for perennial crops, 18-20% for annual crops) are the other two main causes of GHG emissions.

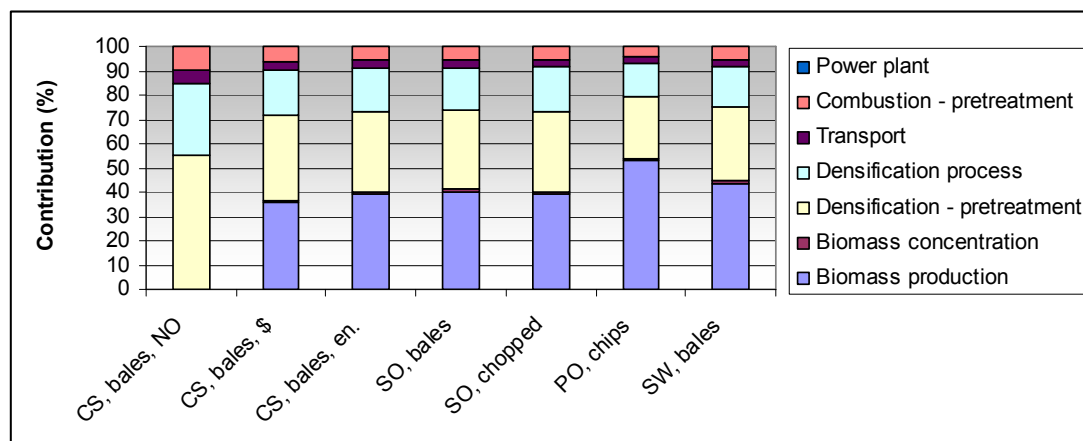


Fig. 7.2 – Contribution to Carbon Footprint due to the different stages of the biomass pyrolysis based power supply chains

Pre-treatment carbon footprint is again due to the thermal and electric energy requests, 61% and 38% respectively, while electricity consumption and equipment materials contribute to slow pyrolysis with the same proportions found in the CED analysis.

Land Occupation

Figure 7.3 shows the contribution to Land Occupation due to the different stages of the supply chains. Land occupation is basically associated with the biomass production stage (roughly 97%). Additional 3% is allocated to the area requested in order to store the biomass.

7.4.3 Comparison with the coal based power supply chain

Supply chains performances were compared with a coal based supply chain (see table 7.12). It is apparent from the comparison that co-combustion of slow pyrolysis products can decrease significantly the life cycle energy demand (-66.6%/-79.6%) and the GHGs emissions (-68.9%/-85.6%). According to the assumptions of the assessment, 1001-1824 TJ/y of primary energy (equivalent to 0.0132%-0.024% of the Italian total primary energy supply in 2003 [IAEA]) may be saved and the emission of 0.9185-1.691 Mt CO_{2eq}/y (equivalent to 0.9125%-1.68% of the emission units assigned yearly to the thermo-chemical sector in Italy in the period 2008-2012 [Ministero dell'Ambiente e della Tutela del Territorio e del Mare e Ministero dello Sviluppo Economico, 2006]) avoided on an extensive basis. On the contrary, a

on direct combustion and on combustion of the pyrolysis products are also indicated in the table.

Tab. 7.13 – Assessment of the environmental performances of power supply chains based on the direct combustion of different biomass feedstock (in brackets: relative difference with reference to the equivalent supply chains based on slow pyrolysis)

Biomass	MJ / kWhe	kg CO_{2eq} / kWhe	m²·yr / kWhe
CS, Bales, NO	1.472 (-38.36%)	0.093 (-37.12%)	0.013 (-17.74%)
CS, bales, \$	1.996 (-36.60%)	0.152 (-34.90%)	0.191 (-30.33%)
CS, bales, EN	1.916 (-37.49%)	0.159 (-35.49%)	0.289 (-31.47%)
SO, bales	2.041 (-34.78%)	0.167 (-33.26%)	0.290 (-31.47%)
SO, chopped	1.668 (-45.02%)	0.144 (-42.32%)	0.334 (-35.61%)
PO, chips	2.521 (-35.52%)	0.212 (-33.87%)	0.374 (-30.69%)
SW, bales	1.998 (-38.28%)	0.169 (-36.37%)	0.477 (-32.89%)

No matter the biomass feedstock considered, a decrease in energy requests, GHGs emissions and land demand is observed when the densification step is excluded. The reasons can be found through gravity analysis, represented on figure 7.4, on figure 7.5 and on figure 7.6.

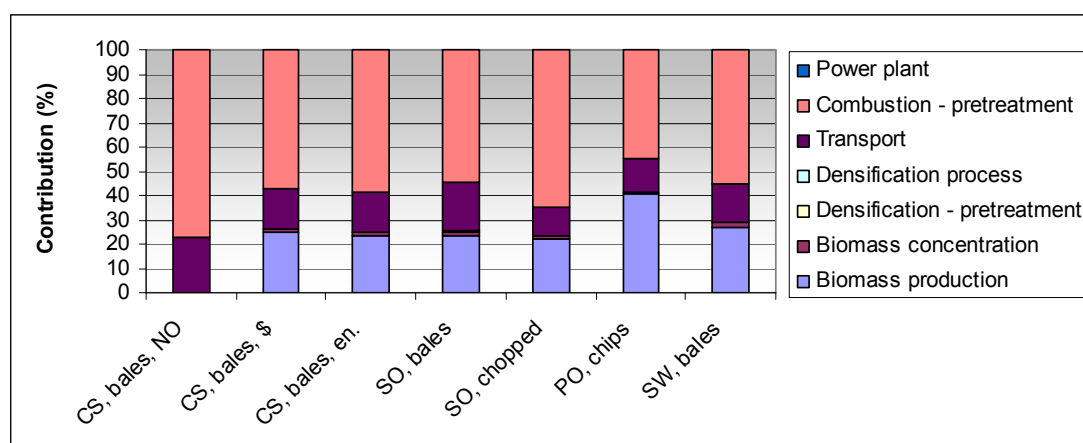


Fig. 7.4 – Contribution to CED due to the different stages of the power supply chains based on direct combustion of the biomass

As a consequence of the densification process exclusion, material with lower energy density, i.e. raw biomass, is to be transported. Burdens due to logistics thus increase, with a factor roughly ranging from 2 to 5, depending on the density of the material transported. Nevertheless, the impact categories assessed in the present work seem to be mainly affected by other stages of the supply chains rather than the transportation process (e.g. pre-treatment processes and biomass production). Higher energy yields by hectare and lower land demands moreover result from the exclusion of the

densification process. This explains the decrease of all the indicators considered in the analysis.

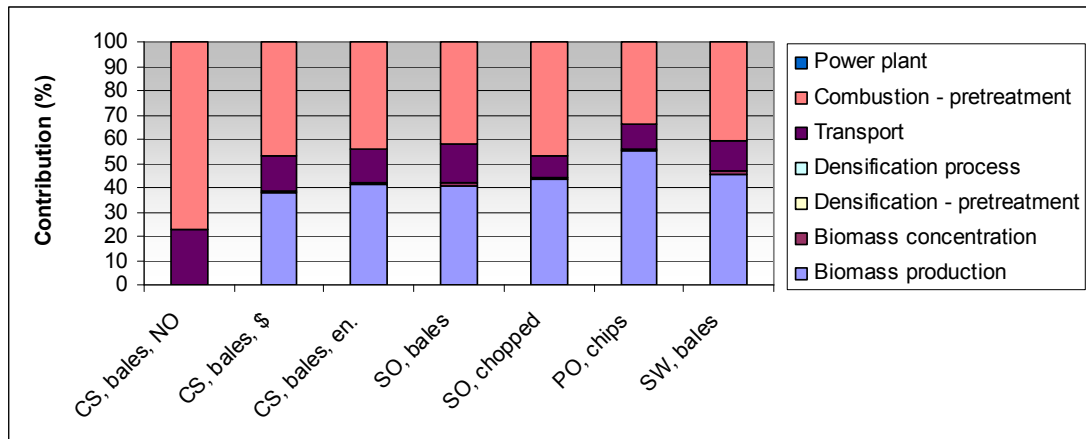


Fig. 7.5 – Contribution to Carbon Footprint due to the different stages of the power supply chains based on direct combustion of the biomass

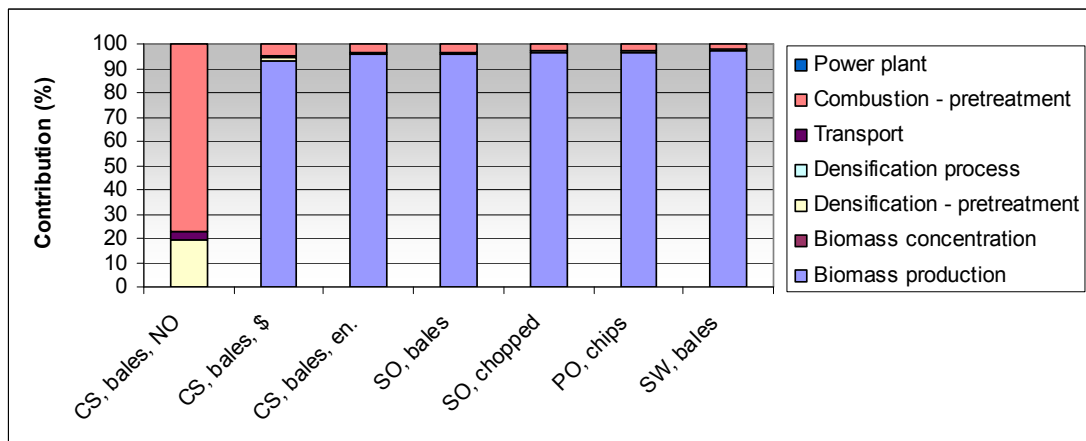


Fig. 7.6 – Contribution to Land Occupation due to the different stages of the power supply chains based on direct combustion of the biomass

Analysis of the effects due to the transport distance variation

If compared with combustion of the biomass pyrolysis products, direct combustion appeared a better option (even if other environmental issues should be investigated, e.g. the emission of pollutants in the environment). It is worthy understanding if conditions exist that supply chains based on the pyrolysis process are favourite.

The pyrolysis process allows for the production of fuels with higher energy density than the original biomass feedstock. Transport distance to the power plant was changed in order to find the length after which the pyrolysis process implementation results in a better bio-power supply chain performance.

Distances at which co-combustion of biomass or slow pyrolysis products yield equivalent burdens (i.e. named “break even distances”) were found both for systems based on chopped SO and on baled SO. Indications on the effects of the transport density can thus be addressed. Results are plotted on figure 7.7, on figure 7.8 and on figure 7.9.

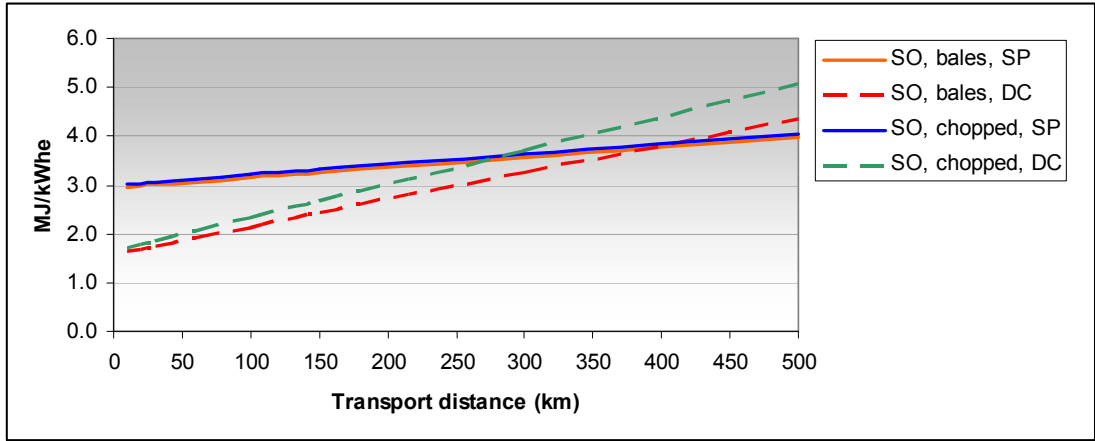


Fig. 7.7 – CED trends as a function of the transport distance (SP = slow pyrolysis products combustion; DC = direct biomass combustion)

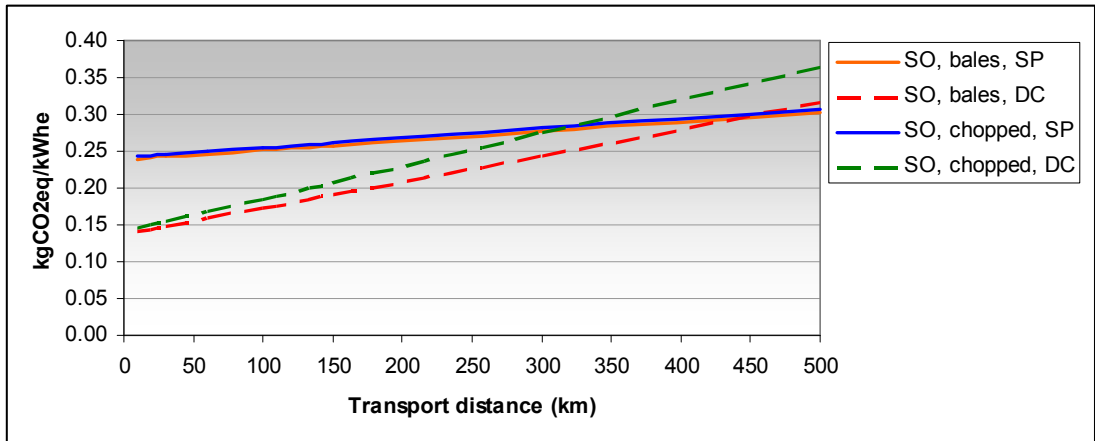


Fig. 7.8 – CF trends as a function of the transport distance (SP = slow pyrolysis products combustion; DC = direct biomass combustion)

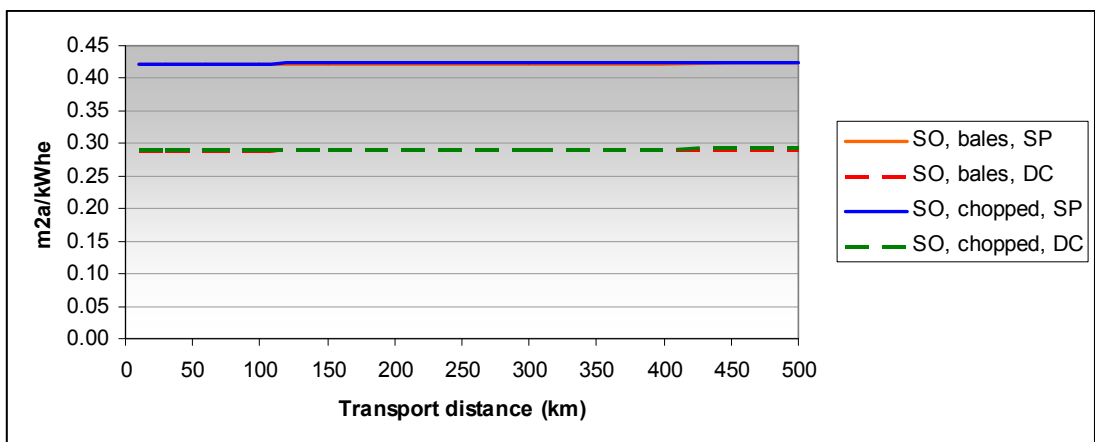


Fig. 7.9 – LO trends as a function of the transport distance (SP = slow pyrolysis products combustion; DC = direct biomass combustion)

Land occupation is not affected by transports (as apparent on figure 7.9), so that it was not possible to find a break even distance.

No matter the biomass transportation modality to the pyrolysis plant (i.e. bales/chopped), nearly the same energy demand and the same GHG emissions are yielded in the supply chains based on the slow pyrolysis of SO (char and bio-oil are transported in both the systems). The different energy densities are instead significant when the supply chains based on direct combustion are considered: the performance difference increases as the transport distance becomes longer.

395 km of transport (CED: 3.777 MJ) are required in order to obtain the same energy demand in both the supply chains based on baled SO; the break even distance decreases to 285 km (CED: 3.599 MJ) for chopped SO, since materials with lower energy density are obviously penalised. CED scores at the break even distance are much lower than the indicator corresponding to coal; they are respectively equal to 32.3% and 30.8% of the coal score.

440 km of transport (CF: 0.295 kgCO_{2eq}) are instead required in order to obtain the same carbon footprint in both the supply chains based on baled SO; the break even distance decreases to 320 km (CF: 0.283 kgCO_{2eq}) for chopped SO, since materials with lower energy density are obviously penalised. CF scores are still much lower than the indicator corresponding to coal; they are respectively equal to 28.6% and 27.5% of the coal score.

Scale-effect analysis

Scale effects due to a change in the power plant size were also investigated. Supply chains based on slow pyrolysis or on direct combustion of SO were compared: the renewable power capacity that results in equivalent burdens (i.e. named break even capacity) was found. Results are plotted on figure 7.10, on figure 7.11 and on figure 7.12 with reference to the renewable power capacity. An exponential dependence of the transport distance on the power capacity was considered in accordance with equation 7.2.

CED and CF plots are very similar: slight increases occur after 10 MWe and they become more and more appreciable as capacity increases, following a nearly exponential trend. The supply chain registering the best performance is inverted between 30 and 40 MWe. Trends are basically due to the presence of two opposite mechanisms in the supply chain model. Efficiency increases up to a stationary value as capacity increases, resulting in smaller amounts of fuel to be transported per kWh. Nevertheless, also longer transport distances results at higher capacities so that they become prevalent on efficiency effects. If compared with the performances of a supply chain based on coal, benefits due to the combustion of a renewable feedstock would disappear when the supply chain scale is equivalent to 60 MWe, in case of DC, or 80 MWe, in case of SP (due to the different energy density of the fuels transported).

LO is instead nearly constant up to 60-70 MWe and then the exponential increase starts, mainly because of effects due to logistics. 90 MWe is the order of magnitude of the break even capacity which was found. Table 7.14 reports the percentage of Italian farm lands (2005 data [Annuario SEAT, 2005]) which would be necessary in order to implement supply chains based on SP or CD of SO at different scales. A power scale lower than 80 MW may present logistic problems to territory on a local scale but it should be on theory practicable.

According to the outcomes of the analysis, when the supply chain scale is included between 0-30 MWe, DC is more energy and carbon efficient than SP. 30-80 MWe is thus the range in which projects based on SP should be preferable placed, taking into

account that the best environmental benefits are obtained at smaller scales. Results are expressed with reference to energy demand, GHG emissions and land occupation; it must be however remarked that also other environmental issues should be addressed (e.g. the emission of pollutants in the environment).

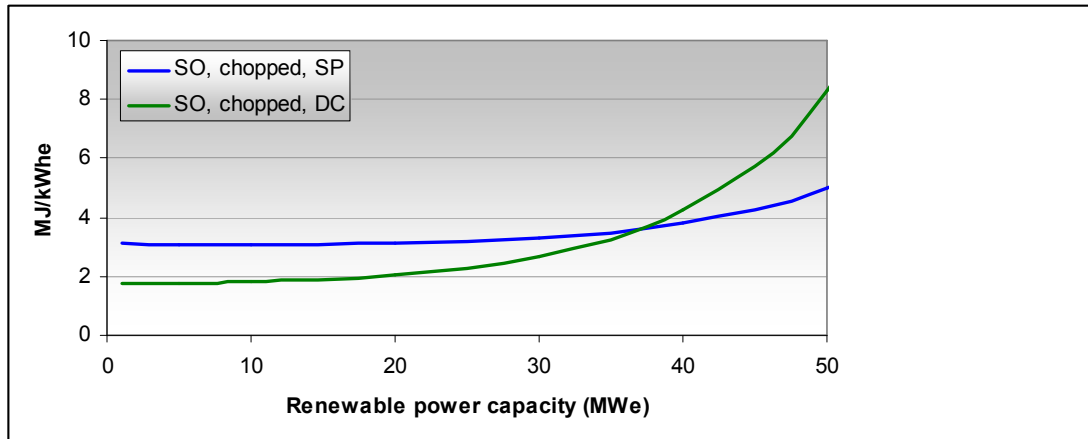


Fig. 7.10 – CED trends as a function of the renewable power capacity (SP = slow pyrolysis products combustion; DC = direct biomass combustion)

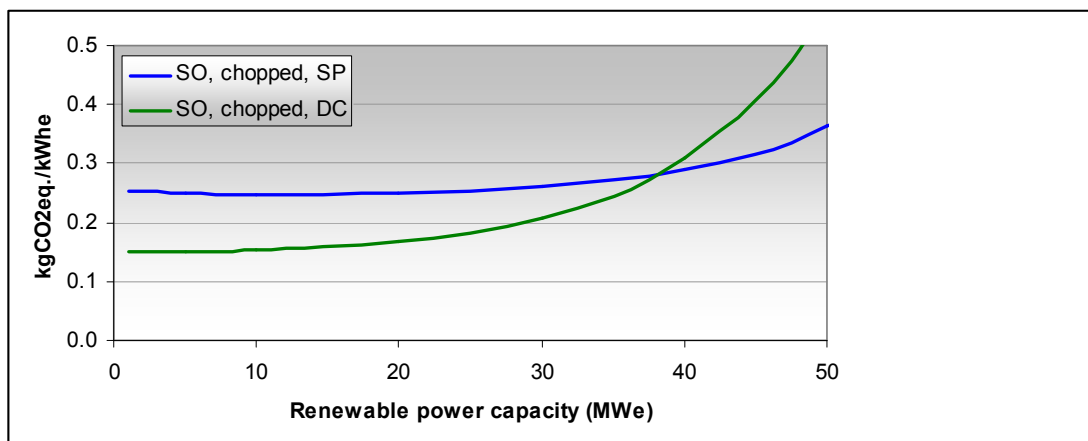


Fig. 7.11 – CF trends as a function of the renewable power capacity (SP = slow pyrolysis products combustion; DC = direct biomass combustion)

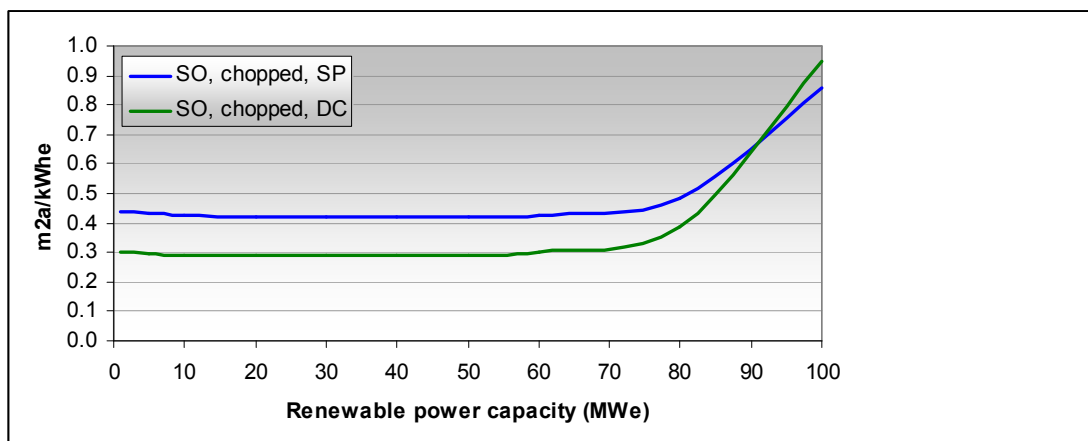


Fig. 7.12 – LO trends as a function of the renewable power capacity (SP = slow pyrolysis products combustion; DC = direct biomass combustion)

Tab. 7.14 – Percentage of Italian farm lands (2005 data [Annuario SEAT, 2005]) which would be necessary in order to implement bio-power supply chains based on slow pyrolysis (SP) or direct combustion (DC) of SO at different scales.

System	Renewable power capacity (MWe)				
	10	20	40	60	80
SP (%)	0.0278	0.0551	0.110	0.167	0.252
DC (%)	0.0190	0.0377	0.0754	0.118	0.202

7.4.5 Comparison between different typologies of power plant and different densification processes

A streamlined assessment was finally completed in order to screen the change in performance due to a different power plant or to a different densification process. Production of 20 MWe from bio-fuels and a transport distance equal to 60 km were considered. The supply chains based on baled SO and on SO chopped were assessed.

Analysis of the effects due to a different power production system

Thermal power station (TPS) and integrated gasification combined cycle (IGCC) were implemented in the model and compared with co-combustion (CO). Outcomes of the analysis are shown in table 7.15.

Tab. 7.15 – comparison between co-combustion (CO), thermal power station (TPS) and integrated gasification combined cycle (IGCC). Renewable capacity: 20 MWe; bio-fuel transport distance: 60 km. (B/SP = biomass/slow pyrolysis products feeding)

Biomass	MJ/kWhe	kg CO _{2eq} /kWhe	M ² ·yr/kWhe
SO, bales, B-CO	1.916	0.159	0.289
	(-38.8%)	(-36.4%)	(-31.7%)
SO, bales, B-IGCC	2.034	0.168	0.303
	(-35.0%)	(-32.8%)	(-28.4%)
SO, chopped, B-CO	2.041	0.167	0.29
	(-34.8%)	(-33.2%)	(-31.4%)
SO, chopped, B-IGCC	2.164	0.177	0.304
	(-30.8%)	(-29.2%)	(-28.1%)
SO, bales, B-TPS	2.479	0.214	0.427
	(-20.8%)	(-14.4%)	(+0.9%)
SO, chopped, B-TPS	2.663	0.226	0.429
	(-14.9%)	(-9.6%)	(+1.4%)
SO, bales, SP-IGCC	2.898	0.232	0.396
	(-7.4%)	(-7.2%)	(-6.4%)
SO, chopped, SP-IGCC	2.957	0.236	0.397
	(-5.5%)	(-5.6%)	(-6.1%)
SO, bales, SP-CO	3.065	0.246	0.421
	(-2.0%)	(-1.6%)	(-0.5%)
SO, chopped, SP-CO	3.129	0.25	0.423
	(-)	(-)	(-)
SO, bales, SP-TPS	4.207	0.344	0.623
	(+34.4%)	(+37.6%)	(+47.3%)
SO, chopped, SP-TPS	4.301	0.351	0.625
	(+37.5%)	(+40.4%)	(+47.8%)

As expected, supply chains based on the slow pyrolysis process appear less efficient (at the power capacity and at the transport distance considered in the analysis) than the equivalent supply chain based on the raw biomass feeding. This is in particular true with all the power plant typologies. Preference of baling harvest systems to chopping is moreover confirmed. TPS always yielded higher burdens than CO and IGCC, due to lower conversion efficiency. It is instead worthy noticing that IGCC improved only the performance of the SP based systems, while co-combustion destination appeared preferable for raw biomass. This is strictly connected to the assumptions effected in the modelling: a higher gasification thermal efficiency was indeed assigned to the char-oil slurry (see section 7.3.5).

Analysis of the effects due to modifications of the densification process

Implementation of alternative densification processes in the supply chains based on co-combustion was then assessed. Slow pyrolysis was compared with pelletizing. Conventional yields were considered as well as higher oil yields (i.e. +45%). The absence of the densification step was also included for sake of comparison. Outcomes of the analysis are shown in table 7.16. The best supply chain performance was obtained with the direct combustion of the raw biomass. As a consequence of the I/O modelling (see section 7.3.3), the environmental burdens associated with pelletizing were lower than in slow pyrolysis even when the oil yield was increased. The performance of the two pyrolysis system is nearly the same: energy demand and GHGs emissions are slightly lower in the conventional slow pyrolysis but the increase in land occupation is appreciable. When oil yield increases, indeed, the energy output of the pyrolysis process increases (so that less land is necessary to supply a certain amount of energy) but benefits are offset by an increase of the process energy demand.

Tab. 7.16 – Comparison between bio-energy systems based on conventional slow-pyrolysis (SP), oil yield increased slow-pyrolysis (SP+), direct combustion of biomass (DC), pelletizing (P). Power plant: co-combustion; renewable capacity: 20 MWe; bio-fuel transport distance: 60 km.

Biomass	MJ / kWhe	kg CO_{2eq} / kWhe	m²·yr / kWhe
SO, bales, DC	1.916 (-38.8%)	0.159 (-36.4%)	0.289 (-31.7%)
SO, chopped, DC	2.041 (-34.8%)	0.167 (-33.2%)	0.29 (-31.4%)
SO, bales, P	2.326 (-25.7%)	0.182 (-27.2%)	0.288 (-31.9%)
SO, chopped, P	2.369 (-24.3%)	0.184 (-26.4%)	0.288 (-31.9%)
SO, bales, SP	3.065 (-2.0%)	0.246 (-1.6%)	0.421 (-0.5%)
SO, chopped, SP	3.129 (-)	0.25 (-)	0.423 (-)
SO, bales, FP	3.162 (+1.1%)	0.244 (-2.4%)	0.343 (-18.9%)
SO, chopped, FP	3.214 (+2.7%)	0.248 (-0.8%)	0.344 (-18.7%)

It should be however observed that, due to the streamlined nature of the comparison, results of this section can only provide general indications, which should be broadened with further and more specific analysis.

7.5 Conclusions

Power supply chains based on the biomass slow pyrolysis of different biomass species (i.e. CS, PO, SO, SW) were investigated according to the Life Cycle Assessment approach. Co-combustion of the biomass pyrolysis products with coal was considered as reference scenario. Supply chains were modelled and compared with alternative options, i.e. direct combustion of the raw biomass and power production from coal. A hard effort was required in the modelling for the collection of experimental (i.e. biomass specific pyrolysis yields), technical, territorial, logistic, thermodynamic and environmental pieces of information. Energy demand, GHG emissions and land occupations were monitored along the supply chains: overall performances were assessed and the most critical elements identified.

Results show that, if compared with power generation from coal, life cycle non renewable energy demand and GHG emissions can decrease significantly. On the contrary, larger extensions of territory are demanded. The implementation of bio-energy supply chains could be however possible on a local scale without it affects significantly the land demand for food, especially if farm sub-products are used in energy production.

Annual crops (i.e. CS and SO) have the potential to yield higher amounts of pyrolysis products if compared with perennial crops (see chapter 5). Nevertheless, inputs of fertilisers and energy requested during the biomass growing seem to offset this inherent benefit so that no significant differences are observed between crops. Only land occupation is particularly sensitive to the biomass feedstock. This indicates the importance of biomass yields as parameter of choice between different crops.

Pyrolysis based supply chain performance resulted strongly depending on the pre-treatment processes, in accordance with the outcomes of the economic assessment (see chapter 6). Biomass production was another critical stage of the supply chains, followed by the pyrolysis process. Contribution to environmental loads due to logistics instead appeared negligible (still in accordance with the economic assessment).

Performances were improved when the densification process was excluded. The lower energy density of the biomass was indeed offset by higher energy yields by hectare. With reference to energy demand and carbon footprint, biomass slow pyrolysis is favourite at long transport distances (order of magnitude: 300-400 km depending on the density of the biomass material transported) and at large supply chain scales (30-80 MWe). Large capacities should be on theory feasible but they may force logistics pressure (i.e. traffic) and offset the environmental benefits which are obtained at smaller scales. Performance of the pyrolysis based supply chain may be moreover improved resorting to an integrated gasification combined cycle (IGCC).

A detailed technical examination should involve the investigation of the effects due to a different fuel destination and to the implementation of a different densification process (e.g. pelletizing). Moreover, although energy demand, climate change and land occupation are dramatic societal topics, other environmental aspects should be also addressed (e.g. the emission of pollutants).

The LCA methodology appears an effective tool in the investigation of bio-energy systems under a life cycle perspective and in the identification of the most critical

stages of the supply chains. Useful indications to the potential implementation of bioelectricity supply chains can be drawn to the lifecycle stakeholders from the present study. The results of the analysis can be also a robust basis for further environmental investigation of life cycles based on the biomass pyrolysis process and, more in general, on the biomass feedstock.

CONCLUSIONS

The present work was aimed at the analysis of issues related to the sustainability of power supply chains based on the biomass slow pyrolysis process, i.e. the thermal decomposition of organic material in liquid (i.e. oil), solid (i.e. char) and gaseous products. The following aspects were in particular addressed:

- inherent hazards and some practical limitations in the use of the pyrolysis products;
- economical feasibility of the pyrolysis process implementation;
- life cycle assessment (LCA) of energy consumptions, greenhouse gases (GHG) emissions and land occupation associated with alternative bio-power supply chains based (or not) on the pyrolysis process.

The assessment was complicated by the lack of industrial and commercial references. The analysis was thus performed coupling experimental activities with assessment tools applied on a life cycle scale. Two groups of activities were developed: experimental investigations on the biomass pyrolysis process (G1) and supply chain sustainability assessment (G2).

G1 activities allowed the obtainment of useful pieces of information on the biomass pyrolysis process, to be used also in the subsequent sustainability assessment.

Different species (i.e. corn stalks, poplar, sorghum, switchgrass) were processed in a fixed bed reactor (i.e. the Gray King reactor) and the pyrolysis yields registered. Significant differences were found between species, suggesting that some biomass can be more functional than others depending on the specific application of the products (e.g. char combustion, bio-slurry combustion or gasification, processing of the pyro-oil in bio-refinery). Asymptotic trends were moreover found when the pyrolysis peak temperature was increased up to 650 °C.

Thermal decomposition profiles of biomass and solid residue of pyrolysis (i.e. char) were analysed with a TGA apparatus. Consistent results were obtained with Gray King reactor and with TGA. Biomass contains a large amount of volatiles and the more the volatile material of the biomass the more the oil yielded. Char analysis moreover showed that larger amounts are yielded at low pyrolysis temperatures but its quality (measured as decrease of the volatile material content) is improved when the temperature is higher than 500 °C.

Some limitations in the use of the liquid product of pyrolysis were also found. Quick structural changes in bio-oil samples were indeed observed with GPC and with UVF analytical techniques. Main structural changes lead to polymerisation of the oxygenated compounds contained in the bio-oil with consequent increase of viscosity and they seem to occur with characteristic times of hours and days. This process is called aging. Positive effects on bio-oil stabilisation were confirmed when a solvent (i.e. methanol or acetone) was added or when bio-oil was stored at low temperatures (i.e. 5 °C). High solvent concentrations (more than 10%) were necessary in order to stop the aging process almost completely, which would be not sustainable first of all for safety reasons. Lower solvent concentration were however able to slow down the structural changes. On the contrary, aqueous phase contained in bio-oils was confirmed to play a negative role on the mixture stability. No particular differences in bio-oil reactivity were instead found with a change in the pyrolysis peak temperature,

even if a slightly increase in reactivity was detected at higher temperatures. Effects due to the biomass feedstock seem to be more significant.

On the basis of the results obtained, 650 °C was selected as reference temperature of the pyrolysis process and pyrolysis yields obtained with a tubular fixed bed reactor. Pyrolysis yields were considered the key parameters for the economic and environmental modelling and assessment of the bio-energy supply chains.

An approach to the identification of the inherent hazards due to mixtures of chemical substances was finally developed and applied to the assessment of liquids obtained from biomass slow-pyrolysis. Under accidental conditions, production, storage and use of bio-oils may be affected by the emission of compounds which are toxic for human beings and the environment and which are precursors of fires. No significant differences were detected between different bio-oil samples. Due to the large number of compounds contained in bio-oils, a streamlined approach based on the selection of a limited number of macro-compounds was tested. The simplified procedure yielded consistent outcomes and the approach resulted to be an effective screening tool. The inherent hazards of bio-oils were also compared with those of other conventional fuels: a reference bio-oil, bio-ethanol, bio-diesel and a model gasoline. It was worth noticing that also biomass derived fuels contain hazardous components similarly to fossil fuels. Nevertheless, different fuels were interested by different kinds and levels of hazard and a ranking was difficult to be tracked.

G2 addressed the assessment of the economic and environmental sustainability of power supply chains based on the biomass slow pyrolysis process. The reference scenario considered co-combustion of coal with oil and char produced from the pyrolysis of the biomass species previously investigated.

An evaluation supply chain model was firstly developed. Cross disciplinary competences were required in order to face with the agro-industrial dimension of the biomass system. The collection of the pieces of information requested was extensive and involved both literature data (i.e. territorial, logistics, engineering, economical and environmental data) and experimental data (i.e. experimental pyrolysis yields) due to the lack of industrial and commercial references. Conventional analysis tools, i.e. Net Present Value and Life Cycle Assessment methodology were then applied in a life cycle perspective in order to track the economical and environmental performance of the supply chains.

The key performance indicator of the economic assessment was the electricity surcharge which results in a NPV equal to zero. The incremental cost due to the implementation of biomass pyrolysis processes in a supply chain formerly based on coal combustion was calculated with reference to different scales of the pyrolysis process. The electricity surcharge per kWh generated from biomass pyrolysis products decreases as the feeding rate of the pyrolysis process increases and it nearly approaches to the Italian market price of electricity in 2008 when the feeding rate is higher than 1-2 t/h, which is roughly equivalent to 10-40 km²·yr. A 20% variation range was found between the worst and the best performing biomass (i.e. poplar and corn stalks). The pyrolysis process resulted economically feasible without resorting to any public support scheme when the pyrolysis products are produced in large capacity plants and co-fired in large power plants with small co-combustion ratios. The pyrolysis process should be moreover aimed at the maximisation of the char production if power generation is the final destination of the pyrolysis products. The importance of the availability of experimental and industrial data and the positive effects of public support systems was moreover pointed out.

The metric of indicators considered in the LCA was composed of: non renewable energy demand, greenhouse gases emissions and land occupation. Co-firing of biomass slow pyrolysis products with coal can decrease significantly the non renewable energy demand (i.e. -66.6% / -79.6%) and the greenhouse gases emissions (i.e. -68.9% / -85.6%) of the power supply chain. On the contrary, larger extensions of territory are demanded (17.5 - 28.6 times the land occupation required by coal combustion). The implementation of bio-energy supply chains could be possible on a local scale without it affects significantly the land demand for food, especially if farm sub-products are used in energy production. Annual crops (i.e. corn stalks and sorghum) have the potential to yield higher amounts of pyrolysis products if compared with perennial crops. Nevertheless, inputs of fertilisers and energy requested during the biomass growing seem to offset this inherent benefit so that no significant differences are observed between crops. Only land occupation is particularly sensitive to the biomass feedstock. This indicates the importance of biomass yields as parameter of choice between different crops. The largest contributions to the environmental burdens of the biomass pyrolysis based supply chains were often associated with the pre-treatment processes (i.e. biomass drying and milling), in accordance with the economical assessment. Significant contributions were also due to biomass production and, to a lesser extent, to the pyrolysis process. Contribution due to logistics instead appeared negligible. Co-combustion of the pyrolysis products with coal was compared with alternative energy routes. Environmental performances were improved when the densification process was excluded from the supply chains, i.e. in case of direct biomass combustion. The lower energy density of the biomass was indeed offset by higher energy yields by hectare. With reference to energy demand and carbon footprint, biomass slow pyrolysis should be favoured when the transport distances are long (order of magnitude: 300-400 km) or when a large production of electricity from bio-fuels is required (i.e. 30-80 MWe). Large capacities should be on theory feasible but they may force logistics pressure (i.e. traffic) and offset the environmental benefits which are obtained at smaller scales. Performance of the pyrolysis based supply chain may be moreover improved resorting to an integrated gasification combined cycle. Models and methods introduced in G2 resulted to be effective and flexible analytical tools in the critical assessment of the sustainability of bio-energy supply chains under a life cycle perspective.

In conclusion, useful indications for the potential implementation of bio-electricity supply chains can be drawn to the lifecycle stakeholders. Slow pyrolysis is a relatively original concept in the bio-energy portfolio and several technical issues are still to be solved before the process can be implemented on a commercial scale, e.g. oil aging and corrosiveness. Competition with alternative biomass-to-energy routes is moreover another factor to be considered. If compared with direct combustion, for instance, i.e. with the simplest technique available in order to exploit the energy content of biomass, the pyrolysis process seemed to add technological complications which can yields some potential benefits only when transport distance and dimension of the supply chain increase significantly. A detailed technical examination should involve different fuel destination and alternative densification processes (e.g. pelletizing). Moreover, although energy demand, climate change and land occupation are dramatic societal topics, other environmental aspects should be also addressed (e.g. emission of pollutants). In this context, the results of the analysis can be a reliable basis for further investigations.

LIST OF REFERENCES

Adlard, E.R. and Handley, A.J. (2001). Gas chromatographic techniques and applications. London: Sheffield Academic

AEBIOM – European Biomass Association. <http://www.aebiom.org/>

Allen, J.; Browne, M.; Hunter, A.; Boyd, J. and Palmer, H. (1998) Logistics management and costs of biomass fuel supply. *International Journal of Physical Distribution & Logistics Management*, 28 (6), 463-477

Allen, D.T. and Shonnard, D.R. (2002). Green engineering . Prentice Hall PTR, Upper Saddle River (NJ, USA)

Annuario SEAT (2005) Agricoltura e floricoltura
http://www.annuarioseat.it/scetendenze/agroalimentare/agricoltura_e_floricoltura.pdf

Antal, M.J. and Grønli, M. (2003). The Art, Science, and Technology of Charcoal production. *Ind. Eng. Chem. Res*, 42, 1619-1640

ARSIA (2004) Le colture dedicate ad uso energetico: il progetto Bioenergy Farm. Quaderno ARSIA 6/2004. www.avanzi.unipi.it

Bare, J.C; Hofstetter, P.; Pennington, D.W. and Udo de Haes, H.A. (2000) Midpoints versus endpoints: The sacrifices and benefits. *Int. J. LCA*, 5 (6), 319-326

Beer, L.L.; Boyd, E.S.; Peters, J.W. and Posewitz, M.C. (2009) Engineering algae for biohydrogen and biofuel production. *Current Opinion in Biotechnology*, 20(3), 264-271.

Begon, V.; Megaritis, A.; Lazaro, M.J.; Herod, A.A.; Dugwell, D.R. and Kandiyoti, R. (1998). Changes in sample reactivity and catalyst deactivation during early stages of the hydrocracking of a coal extract, *FUEL*, 77, 1261-1272

Begon, V.; Suelves, I.; Herod, A.A.; Dugwell, D.R. and Kandiyoti, R. (2000). Structural effects of sample ageing in hydrocracked coal liquefaction extracts. *Fuel*, 79, 1423-1429

Benkhedda, Z. and Landais, P. (1992). Spectroscopic Analyses of Aromatic Hydrocarbons Extracted from Naturally and Artificially Matured Coals. *Energy & Fuels*, 6, 166-172

Berndes, G.; Hoogwijk, M. and Van den Broek, R. (2003) The contribution of biomass in the future global energy supply: a review of 17 studies. *Biomass and Bioenergy*, 25(1), 1-28.

Bertocchi, M. (2008) Analisi di una filiera per la valorizzazione energetica di biomassa basata su un processo di densificazione pirolitica. Ms.Eng. thesis in Chemical Engineering. Alma Mater Studiorum – Università di Bologna

Biomass Energy Centre. <http://www.biomassenergycentre.org.uk>

BlueNext, <http://www.bluenext.fr/>

Boucher, M.E. ; Chaala, A.; Pakdel, H. and Roy, C. (2000). Bio-oils obtained by vacuum pyrolysis of softwood bark as a liquid fuel for gas turbines. Part II: Stability and ageing of bio-oil and its blends with methanol and a pyrolytic aqueous phase. *Biomass and Bioenergy*, 19, 351-361

Boukis, I.; Vassilakos, N.; Karellas, S. and Kakaras, E. (2009) Techno-economic analysis of the energy exploitation of biomass residues in Heraklion Prefecture—Crete. *Renewable and Sustainable Energy Reviews*, 13, 362–377

Bridgwater, A.V. (1999). Principles and practice of biomass fast pyrolysis processes for liquids. *J Anal Appl Pyrol*; 5(1–2), 3–22.

Bridgwater, A.V. and Peacocke G.V.C. (2000). Fast pyrolysis processes for biomass, *Renewable Sustainable Energy Rev.*, 4, 1–73.

Bridgwater, A.V. (2003) Renewable fuels and chemicals by thermal processing of biomass. *Chemical Engineering Journal*, 91, 87–102

British Standards Institution (1991). BS 1016-107.2 – Methods for analysis and testing of coal and coke. Caking and swelling properties of coal. Assessment of caking power by Gray-King coke test.

Brossard Perez, L.E. and Cortez, L.A.B. (1997). Potential for the use of pyrolytic tar from bagasse in industry. *Biomass and Bioenergy*, 12 (5),363-366

Calemma, V.; Iwanski, P.; Nali, M.; Scotti, R. and Montanari, L. (1995). Structural Characterization of Asphaltenes of Different Origins *Energy & Fuels*, 9, 225-230

Carbon Trust, <http://www.carbontrust.co.uk/Pages/Default.aspx>

Cardone, M.; Mazzoncini, M.; Menini, S.; Rocco, V.; Senatore, A.; Reggiani, M. and Vitolo, S. (2003). Brassica carinata as an alternative oil crop for the production of biodiesel in Italy: agronomic evaluation, fuel production by transesterification and characterization, *Biomass and Bioenergy*, 25, 623–636

Chaala, A.; Ba, Y.; Pérez, M.G. and Roy, C. (2004). Colloidal properties of bio-oils obtained by vacuum pyrolysis of softwood bark: ageing and thermal stability. *Energy Fuel*, 18, 1535–1542

Chemexper. Catalog of chemicals suppliers, physical characteristics and search engine. <http://www.chemexper.com>

Cherubini, F.; Birda, N.D.; Cowieb, A.; Jungmeiera, G.; Schlamadingerc, B. and Woess-Gallascha, S. (2009) Energy- and greenhouse gas-based LCA of biofuel and bioenergy systems: Key issues, ranges and recommendations. *Resources, Conservation and Recycling*, 53, 434–447

Cherubini, F. and Ulgiati, S. (2010) Crop residues as raw materials for biorefinery systems – A LCA case study. *Applied Energy*, 87, 47–57

Cirad (2006). Bio-oil from wood hydro-pyrolyzed – Material Safety Data Sheet. <http://www.Cirad.fr>

Coates, J. (2000). Interpretation of Infrared Spectra, A Practical Approach. In *Encyclopedia of Analytical Chemistry*, John Wiley & Sons Ltd, Chichester (UK)

Commission Green Paper of 29 November 2000 Towards a European strategy for the security of energy supply. Document 52000DC0769

Cordella, M. (2006) Metodologia LCA applicata alla produzione di una birra. Ms.Eng. thesis in Environmental Engineering. Alma Mater Studiorum – Università di Bologna

Cordella, M.; Barontini, F. and Cozzani, V. (2008). Pyrolysis processes for bio-oil production: analysis of the hazards of the reaction products. Proceeding of the XVII Congresso Nazionale della Divisione di Chimica Industriale, Società Chimica Italiana, Genoa (I), 109

Cordella, M.; Barontini, F.; Santarelli, F. and Cozzani, V. (2008) Valutazione del rischio associato alla produzione ed allo stoccaggio di combustibili derivanti da biomasse. Proceedings of the VI Convegno Nazionale Valutazione e Gestione del Rischio negli Insediamenti Civili ed Industriali, DIMNP, Pisa (I), p. 93

Cordella, M.; Stramigioli, C.; Santarelli, F. and Fazio, S. (2009) Analisi degli impatti ambientali legati ad una filiera per la produzione di biodiesel di seconda generazione. Proceedings of Ecomondo 2009, Maggioli Editore, Rimini (I), 922-927

Cordella, M.; Tugnoli, A.; Morra, P.; Barontini, F.; Spadoni, G. and Cozzani, V. (2008) Assessment of the hazard footprint of substances formed in the loss of control of chemical systems. Chemical Engineering Greetings to Prof. Eliseo Ranzi, AIDIC – Elioticinese Service Point, Milan (I), 151-160

Cordella, M.; Tugnoli, A.; Barontini, F.; Spadoni, G. and Cozzani, V. (2009) Inherent safety of substances: Identification of accidental scenarios due to decomposition products. *Journal of Loss Prevention in the Process Industries*, 22, 455–462

Cozzani, V., Smeder, M. and Zanelli, S. (1998). Formation of hazardous compounds by unwanted reactions in industrial accidents. *Journal of Hazardous Materials*, 63, 131–142.

Cozzani, V. and Zanelli, S. (1997). EUCLID: A study on the emission of unwanted compounds linked to industrial disasters. EUR 17351 EN. European Commission.

Cozzani, V. and Zanelli, S. (1999). Precursors of dangerous substances formed in the loss of control of chemical systems. *Journal of Hazardous Materials*, 65, 93–108.

CSST – Centro Studi sui Sistemi di Trasporto (2007) Aggiornamento al 01.01.2008 dei costi delle imprese italiane di autotrasporto di cose per conto di terzi raffrontati con quelli di analoghe imprese appartenenti a Germania, Francia, Spagna, Austria, Slovenia, Ungheria, Polonia e Romania. Rapporto per il Ministero dei Trasporti e della Navigazione della Repubblica Italiana – Comitato Centrale per l’Albo degli Autotrasportatori di cose per conto terzi.

Dale, V.; Garten, C.; Leiby, P.; Perla, D.; Smith, B. and Storey, J. (2009) Sustainability of Bioenergy Systems: Cradle to Grave - A Workshop for Oak Ridge National Laboratory, the US Environmental Protection Agency, and their collaborators. September 10 – 11, 2009, in Oak Ridge, Tennessee (USA)

Das, P.; Ganesh, A. and Wangikar, P. (2004). Influence of pretreatment for deashing of sugarcane bagasse on pyrolysis products. *Biomass and Bioenergy*, 27, 445–457

De Klein, C.; Novoa, R.S.A; Ogle, S.; Smith K.A.; Rochette, P.; Wirth, T.C.; McConkey, B.G.; Mosier, A.; Rypdal, K.; Walsh, M. and Williams, S.A. (2006) N₂O Emissions from Managed Soils, and CO₂ Emissions from Lime and Urea Application, Ch. 11 in the 2006 IPCC Guidelines for National Greenhouse Gas Inventories. <http://www.ipcc-nggip.iges.or.jp/public/2006gl/index.html>

Demirbas, A. (2001) Biomass resource facilities and biomass conversion processing for fuels and chemicals. *Energy Conversion and Management*, 42 (11), 1357-1378

Dewulf, J. and Van Langenhove, H. (2006) *Renewables-Based Technology: Sustainability Assessment*. John Wiley & Sons

Di Maria, F. and Fantozzi, F. (2004) Life cycle assessment of waste to energy micro-pyrolysis system: Case study for an Italian town. *Int. J. Energy Res.*, 28, 449–461

Diebold, J.P. and Czernik, S. (1997). Additives To Lower and Stabilize the Viscosity of Pyrolysis Oils during Storage. *Energy & Fuels*, 11, 1081-1091

Diebold, J.P. (2000). A Review of the Chemical and Physical Mechanisms of the Storage Stability of Fast Pyrolysis Bio-Oils. NREL/SR-570-27613, Golden (Colorado), <http://www.doe.gov/bridge>

Directive 2001/77/EC of the European Parliament and of the Council of 27 September 2001 on the promotion of electricity produced from renewable energy sources in the internal electricity market. *Official Journal of the European Communities* L 283/33

Directive 2003/87/EC Of the European Parliament and of the Council of 13 October 2003 establishing a scheme for greenhouse gas emission allowance trading within the Community and amending Council Directive 96/61/EC. *OJ L 275*, 25.10.2003

Directive 2009/28/EC of the European Parliament and of the Council of 23 April 2009 on the promotion of the use of energy from renewable sources and amending and subsequently repealing Directives 2001/77/EC and 2003/30/EC. Official Journal L 140 , 05/06/2009 P. 0016 - 0062

DiSTA, Department of Agro-Environmental Science and Technology of the University of Bologna (Italy), <http://www.dista.unibo.it/grici/>

Dornburg V. and Faaij A.P.C. (2005) Cost and CO₂ emission reduction of biomass cascading: methodological aspects and case study of SRF poplar. *Climatic Change*, 71, 373–408

Doshi, V.A.; Vuthaluru, H.B. and Bastow, T. (2005) Investigations into the control of odour and viscosity of biomass oil derived from pyrolysis of sewage sludge. *Fuel Processing Technology*, 86, 885– 897

e-coal.com consultancy. <http://www.e-coal.com/consultancy.htm>

Ecoinvent Database (v. 2.0), www.ecoinvent.ch

EIA – Energy Information Administration (2009) International Energy Outlook 2009. EIA, U.S. Department of Energy – Office of Integrated Analysis and Forecasting, Washington, DC (USA). DOE/EIA-0484(2009)

Enel. Proprietà chimiche e fisiche (composizione) dei principali carboni fossili. http://www.enel.it/attivita/ambiente/carbone/doc/tab_proprieta_carboni_fossili.pdf

EPA (2006) Life Cycle Assessment: Principles and Practice. EPA/600/R-06/060 document. <http://www.epa.gov/NRMRL/lcaccess/pdfs/600r06060.pdf>

EPRI and U.S. Department of Energy (1997) Renewable Energy Technology Characterizations. TR-109496

European Climate Exchange, <http://www.ecx.eu/>

European Commission (2001). Commission Directive 2001/59/EC of 6 August 2001 adapting to technical progress for the 28th time Council Directive 67/548/EEC on the approximation of the laws, regulations and administrative provisions relating to the classification, packaging and labelling of dangerous substances, Official Journal of the European Communities, L 225 , 21.08.2001

European Commission (2005) Communication from the commission: The support of electricity from renewable energy sources. Brussels, 7.12.2005, COM(2005) 627 final.

European Commission (2006) Integrated Pollution Prevention and Control Reference Document on Best Available Techniques for Large Combustion Plants.

European Commission (2009) Emission Trading System (EU ETS). http://ec.europa.eu/environment/climat/emission/index_en.htm

European Parliament and Council (2001) Directive 2001/77/EC of the European Parliament and of the Council of 27 September 2001 on the promotion of electricity produced from renewable energy sources in the internal electricity market. Official Journal of the European Communities, L 283/33

European Patent Office (1996). EP0718392A1 – Method of upgrading biomass pyrolysis liquids for use as fuels and as a source of chemicals by reaction with alcohols. European Patent Application number 95309400.0

ESIS. European chemical Substances Information System.
<http://ecb.jrc.ec.europa.eu/esis>

Faaij, A. (2006) Modern Biomass Conversion Technologies. Mitigation and Adaptation Strategies for Global Change, 11, 343–375

Fahmi, R.; Bridgwater, A.V.; Donnison, I.; Yates, N. and Jones, J.M. (2007). The effect of lignin and inorganic species in biomass on pyrolysis oil yields, quality and stability. Fuel, 87, 1230–1240

Falyushin, P.L.; Zhuravskii, G.I.; Bratishko, R.F.; Kozhurin, V.N.; Anufrieva, E.V. (2009) Qualitative characteristics of the fuel gas obtained as a result of the thermochemical processing of plant biomass by the pyrolysis method. Journal of Engineering Physics and Thermophysics, 82 (3), 442-447

FAO – Forest Industries Division (1987). Simple technologies for charcoal making. FAO Forestry Paper 41, Rome, <http://www.fao.org/docrep/x5328e/x5328e00.htm>

Fava, J.A. (2002) Int J LCA, Life Cycle Initiative: A Joint UNEP/SETAC Partnership to Advance the Life-Cycle Economy. 7 (4), 196-198

FILCEM–CGIL (Federazione Italiana Lavoratori Chimica Energia Manifatture)
<http://www.filcemcgil.it/>

Frischknecht R., Jungbluth N., Althaus H.-J., Bauer C., Doka G., Dones R., Hischer R., Hellweg, S., Humbert S., Köllner T., Loerincik Y., Margni M. and Nemecek T. (2007) Implementation of Life Cycle Impact Assessment Methods. ecoinvent report No. 3, v2.0. Swiss Centre for Life Cycle Inventories, Dübendorf (CH)

Gagnon, N.; Hall, C.A.S and Brinker, L. (2009) A Preliminary Investigation of Energy Return on Energy Investment for Global Oil and Gas Production. Energies, 2, 490-503

Garcia-Perez, M.; Chaala, A.; Pakdel, H.; Kretschmer, D. and Roy, C. (2007). Characterization of bio-oils in chemical families, Biomass and Bioenergy, 31, 222–242

Garcia-Perez, M.; Chaala, A. and Roy, C. (2002). Vacuum pyrolysis of sugarcane bagasse. Journal of Analytical and Applied Pyrolysis, 65, 111–136

Gauglitz, G. and Vo-Dinh, T. (2003).. Handbook of spectroscopy. Wiley-VCH, Verlag (Germany)

Gelleti, R.; Jodice, R.; Mauro, G.; Migliardi, D.; Picco, D.; Pin, M.; Tomasinsig, E.; Tommasoni, L.; Chinese, D.; Monaco, B.; Nardin, G. and Simeoni, P. (2006) Energia dalle biomasse - Le tecnologie, i vantaggi per i processi produttivi, i valori economici e ambientali. AREA Science Park, www.aria.trieste.it

Giudicianni, P. (2006). Composizione chimica e caratteristiche di combustione dei liquidi derivati da pirolisi di biomasse. Tesi di Dottorato di Ricerca in Ingegneria Chimica (XVII ciclo), Università degli studi di Napoli "Federico II", Napoli (I)

GME – Gestore Mercati Elettrici, <http://www.mercatoelettrico.org/En/Default.aspx>

Goedkoop, M.; De Schryver, A. and Oele, M. (2007) SimaPro 7 Introduction to LCA with SimaPro 7 (v. 4.2). www.pre.nl

Gómez Diaz, C.J. (2006). Understanding Biomass Pyrolysis Kinetics: Improved modeling Based on Comprehensive Thermokinetic Analysis, Ph.D Thesis, Universitat Politècnica de Catalunya, Barcelona (Spain)

Goyal, H.B.; Seal, D. and Saxena, R.C (2008) Bio-fuels from thermochemical conversion of renewable resources: A review. Renewable and Sustainable Energy Reviews, 12, 504–517

Green Power Market Development Group: Advancing Green Power for a Sustainable Energy Future - A project of the Climate, Energy and Pollution Program. World Resource Institute. <http://www.thegreenpowergroup.org/>

Heinimöa, J. and Jungingerb, M. (2000) Production and trading of biomass for energy – An overview of the global status. Biomass and Bioenergy, 33(9), 1310-1320

Heinrich, E. (2007) The status of the FZK concept of biomass gasification. Learning material of the 2nd European Summer School on Renewable Motor Fuels, Warsaw (PL)

Heller, M.C.; Keoleiana, G.A.; Mann, M.K. and Volk T.A. (2004) Life cycle energy and environmental benefits of generating electricity from willow biomass. Renewable Energy, 29, 1023–1042

Herbohn, J.L. and Harrison, S.R. (2002) Introduction to Discounted Cash Flow Analysis and Financial Functions in Excel. In: Harrison, S.R., Herbohn, J.L., Mangaoang, E.O. and Vanclay, J.K. Socio-Economic Research Methods in Forestry: A Training Manual, Leyte State University, ViSCA, Baybay, The Philippines, (109-118). 4-10 February, 2002.

Higman, C. and Van der Burgt, M. (2003) Gasification. Gulf Professional Publishing (Elsevier Science), Burlington, MA (USA)

IAEA – International Atomic Energy Agency. Energy and Environment Data Reference Bank (EEDRB) – Italy, <http://www.iaea.org/inisnkm/nkm/aws/eedrb/data/IT-tpes.html>

IEA – International Energy Agency (2007) Bioenergy Project Development & Biomass Supply. IEA GUIDELINES, Paris (F)

IEA – International Energy Agency (2004) World Energy Outlook 2004

IEA – International Energy Agency (2008) World Energy Outlook 2008

Iojoiu, E.E.; Domine, M.E.; Davidian, T.; Guilhaume, N. and Mirodatos, C. (2007). Hydrogen production by sequential cracking of biomass-derived pyrolysis oil over noble metal catalysts supported on ceria-zirconia. *Applied Catalysis A: General*, 323, 147-161

IPCC – Intergovernmental Panel on Climate Change. <http://www.ipcc.ch/>

IPCC (2007) IPCC Fourth Assessment Report. The Physical Science Basis. <http://www.ipcc.ch/ipccreports/ar4-wg1.htm>

ISO 14040 (2006) Environmental management - Life cycle assessment - Principles and framework, International Organisation for Standardisation (ISO), Geneva

ISO 14044 (2006) Environmental management - Life cycle assessment - Requirements and guidelines, International Organisation for Standardisation (ISO), Geneva

ISTAT – Istituto nazionale di statistica, <http://www.istat.it/>

ISTAT (2007) Aziende e relativa superficie per forma di utilizzazione dei terreni, classe di superficie totale e classe di superficie agricola utilizzata (SAU). http://www.istat.it/dati/dataset/20090120_01/indexnp.html

IUCN – The World Conservation Union (2006). The Future of Sustainability: Rethinking Environment and Development in the Twenty-first Century. Report of the IUCN Renowned Thinkers Meeting, 29-31 January 2006, www.iucn.org

JRC-CEMEEP (2003) Efficienza dei motori elettrici per risparmiare energie proteggere l'ambiente. <http://sunbird.jrc.it/energyefficiency/motorchallenge/pdf/italiano.pdf>

Kandiyoti, R.; Herod, A.A. and Bartle, K.D. (2006). Solid Fuels and Heavy Hydrocarbon Liquids: Thermal Characterization and Analysis, Elsevier, Amsterdam, ISBN: 0-0804-4486-5

Karekezi, S. and Kithyoma, W. (2006) Bioenergy and Agriculture: Promises and Challenges. Bioenergy and the Poor. In: 2020 Vision for Food, Agriculture, and the Environment. International Food Policy Research Institute, Washington DC, USA.

- Khoo, H.H. (2009) Life cycle impact assessment of various waste conversion technologies. *Waste Management*, 29, 1892–1900
- Klare, M.T. (2004) *Blood and Oil: The Dangers and Consequences of America's Growing Dependency on Imported Petroleum*. Henry Holt, New York (NY)
- Kletz, T.A. (1998) *Process Plants: A Handbook for Inherent Safer Design*, 2nd ed. Taylor & Francis, Philadelphia, PA (USA)
- Ladanai, S. and Vinterbäck, J. (2009) *Global Potential of Sustainable Biomass for Energy*. SLU, Institutionen för energi och teknik – Swedish University of Agricultural Sciences, Department of Energy and Technology. Report 013
ISSN 1654-9406, Uppsala (SW)
- Lakowicz, J. (1999). *Principles of Fluorescence Spectroscopy*. Kluwer Academic and Plenum Publishers, New York
- Larson, E.D. (2006) A review of life-cycle analysis studies on liquid biofuel systems for the transport sector. *Energy for Sustainable Development*, X (2)
- Lathe, G.H. and Ruthven, C.R.J. (1956). The Separation of Substance and Estimation of their Relative Molecular Sizes by the use of Columns of Starch in Water. *Biochem J.*, 62, 665–674
- Lee, D.L.; Owens, V.N.; Boe, A.; Jeranyama, P. (2007) *Composition of Herbaceous Biomass Feedstocks*. North Central Sun Grant Center - South Dakota State University, document SGINC1-07
- Lees, F.P. (1996) *Loss prevention in the process industries*. London: Butterworths.
- Lewis, R.J. (1992). *Sax's dangerous properties of industrial materials* (8th ed.). Van Nostrand Reinhold, New York
- Li, C.Z.; Wu, F.; Cai, H.Y and Kandiyoti R. (1994). UV-Fluorescence Spectroscopy of Coal Pyrolysis Tars. *Energy Fuels*, 8, 1039-1048
- Lima, D.G.; Soares, V.C.D.; Ribeiro, E.B.; Carvalho, D.A.; Cardoso, E.C.V.; Rassi, F.C.; Mundim, K.C.; Rubim, J.C. and Suarez, P.A.Z. (2004). Diesel-like fuel obtained by pyrolysis of vegetable oils, *J. Anal. Appl. Pyrolysis*, 71, 987–996
- Mackay, D. (2001) *Multimedia Environmental Models – The Fugacity Approach* (2nd ed.), CRC Press
- Mann, M.K. and Spath, P.L. (2001) A life cycle assessment of biomass cofiring in a coal-fired power plant. *Clean Prod Processes* 3, 81-91
- Manyele, S.V. (2007) Lifecycle assessment of biofuel production from wood pyrolysis technology. *Educational Research and Review*, 2 (6), 141-150

Marathon Petroleum Company LCC. MSDS Number 0127MAR019.
http://www.mapllc.com/MSDS/msds_home.html

Matche, <http://www.matche.com/>

Mc Ewen, C.; Kitson, N.; Fulton G.; Larsen, B.S. (1996). Gas chromatography and mass spectrometry: a practical guide. Boston: Academic Press

Mc Naught A.D. and Wilkinson A. (1997). IUPAC Compendium of Chemical Terminology, 2nd ed. (the "Gold Book"). Blackwell Scientific Publications, Oxford (UK); XML on-line corrected version: <http://goldbook.iupac.org> (2006-) created by Nic, M., Jirat, J., Kosata. B.; updates compiled by Jenkins, A.

Ministero dell'Ambiente e della Tutela del Territorio e del Mare e Ministero dello Sviluppo Economico (2006) Approvazione del Piano nazionale di assegnazione delle quote di CO₂ per il periodo 2008-2012. D.M. 18 dicembre 2006 (2006)

Mitchell, C.P.; Bridgwater, A.V.; Stevens, D.J.; Toft, A.J. and Watters, M.P. (1995) Technoeconomic Assessment of Biomass to Energy. Biomass and Bioenergy, 9 (1-5), 205-226

Moncada Lo Giudice, G.; Costarelli, I. and Giraldi, D. (2006) La co-combustione di biomasse e carbone nelle grandi centrali termoelettriche. La Termotecnica, Settembre 2006, 1-7

Moore, J.C. (1964). Gel permeation chromatography. I. A new method for molecular weight distribution of high polymers. *J. Polym. Sci.*, 2, 835-843

Mousquès, P.; Dirion, J. L. and Grouset, D. (2001) Modeling of solid particles pyrolysis. Journal of Analytical and Applied Pyrolysis, 58-59 (1), 733-745

Munkhtsetseg, S.; Khomich, A.V. ; Poklonskii, N.A. and Davaasambuu, J. (2007). Infrared absorption spectra of coals with different degrees of coalification. Journal of Applied Spectroscopy, 74 (3), 338-343

Nakai, T.;Nami Kartal, S.; Hata, T and Imamura, Y. (2007). Chemical characterization of pyrolysis liquids of wood-based composites and evaluation of their bio-efficiency. Building and Environment, 42, 1236–1241

Nan, L.; Best, G. and Coelho De Carvalho Neto, C. (1994) Integrated energy systems in China - The cold Northeastern region experience. FOOD AND AGRICULTURE ORGANIZATION OF THE UNITED NATIONS, Rome (I)
<http://www.fao.org/docrep/t4470e/t4470e00.htm#Contents>

New York University – Leonard N. Stern School of Business,
<http://www.stern.nyu.edu/>

Oasmaa, A.; Leppämäki, E.; Koponen P.;Levander, J. and Tapola E. (1997). Physical characterisation of biomass-based pyrolysis liquids – Application of standard fuel oil analyses. VTT Publications 306, Espoo (Finland)

- Oasmaa, A. and Czernik, S. (1999). Fuel Oil Quality of Biomass Pyrolysis Oils-State of the Art for the End Users. *Energy & Fuels*, 13, 914-921
- Oasmaa, A. and Peacocke, C. (2001). A guide to physical property characterisation of biomass-derived fast pyrolysis liquids. VTT Publications 450, Espoo (Finland)
- Oasmaa, A. and Kuoppala, E. (2003). Fast Pyrolysis of Forestry Residue. 3. Storage Stability of Liquid Fuel. *Energy & Fuels*, 17, 1075-1084
- Oasmaa, A.; Kuoppala, E.; Selin, J.F.; Gust, S. and Solantausta Y. (2004). Fast Pyrolysis of Forestry Residue and Pine. 4. Improvement of the Product Quality by Solvent Addition. *Energy & Fuels*, 18, 1578-1583
- Oasmaa, A.; and Kuoppala, E. (2008). Solvent Fractionation Method with Brix for Rapid Characterization of Wood Fast Pyrolysis Liquids. *Energy Fuels*, 22 (6), 4245–4248
- OECD – Organisation for Economic Co-operation and Development, http://www.oecd.org/home/0,3305,en_2649_201185_1_1_1_1_1,00.html
- Perry, R.H. and Green, D.W. (1997) Perry's Chemical Engineers' Handbook, Seventh Edition. McGraw-Hills, New York (NY, USA)
- Peters, M.S.; Timmerhaus, K.D. and West, R.E. (2003) Plant Design and Economics for Chemical Engineers, Mc Graw Hil
- Phyllis Database – The composition of biomass and waste. <http://www.ecn.nl/phyllis/defs.asp>
- Pimentel, D.; Marklein, A.; Toth, M.A.; Karpoff, M.N.; Paul, G.S.; Mc Cormack, R.; Kyriazis, J. And Krueger, T. (2009) Food Versus Biofuels: Environmental and Economic Costs. *Hum Ecol*, 37, 1–12
- Pindoria, R.V.; Lim, J.Y.; Hawkes, J.E.; Lazaro, M.J.; Herod, A.A. and Kandiyoti, R. (1997). Structural characterization of biomass pyrolysis tars/oils from eucalyptus wood waste: effect of H-2 pressure and sample configuration, *FUEL*, 76, 1013-1023
- Polymer science learning center. “Infrared spectrometry – Spettrometria infrarossa”, <http://pslc.ws/italian/ir.htm>
- Presidenza del Consiglio dei Ministri della Repubblica Italiana (1989). Decreto del Presidente del Consiglio dei Ministri del 31 marzo 1989 concernente l'applicazione dell'art. 12 del decreto del Presidente della Repubblica 17 maggio 1988, n. 175, concernente rischi rilevanti connessi a determinate attività industriali, Supplemento alla G.U. n. 93 del 21 aprile 1989
- Qi, Z.; Jie, C.; Tiejun, W. and Ying, X. (2007). Review of biomass pyrolysis oil properties and upgrading research. *Energy Conversion and Management*, 48, 87–92

Qiang, L.; Wen-Zhi, L. and Xi-Feng, Z. (2009). Overview of fuel properties of biomass fast pyrolysis oils. *Energy Conversion and Management*, 50, 1376–1383

Qin, X.; Mohan, T.; El-Halwagi, M.; Cornforth, G. and McCarl, B.A. (2006) Switchgrass as an alternate feedstock for power generation: an integrated environmental, energy and economic life-cycle assessment. *Clean Techn Environ Policy*, 8, 233–249

Ralph, J and Hatfield, R.D. (1991). Pyrolysis-GC-MS characterization of forage materials. *J. Agric. Food Chem.*, 39 (8), 1426–1437

Regolamento CE n. 1907/2006 del Parlamento Europeo e del Consiglio del 18 dicembre 2006

Rendell, D. (1987). *Fluorescence and Phosphorescence*. Wiley, Chichester (UK)

RENEW – sustainable energy systems for transport, www.renew-fuel.com/home.php

Rentizelas, A.A.; Tolis, A.J. and Tatsiopoulos, I.P. (2009). Logistics issues of biomass: The storage problem and the multi-biomass supply chain. *Renewable and Sustainable Energy Reviews*, 13, 887–894

RTECS. Registry of toxic effects of chemical substances. <http://www.cdc.gov/niosh/rtecs>

SCORECARD. The pollution information site. <http://www.scorecard.org/>

Scurlock, J. Bioenergy Feedstock Characteristics, <http://bioenergy.ornl.gov/>

SETAC - Society of Environmental Toxicology and Chemistry. www.setac.org

Sharma, A. and Schulman, S.G. (1999). *Introduction to Fluorescence Spectroscopy*. In *Techniques in Analytical Chemistry Series*, Wiley-Interscience (John Wiley and Sons, Inc.), New York

Silveira, S. (2005) *Bioenergy – Realizing the potential*. Elsevier, Oxford (UK)

Sims, R.H.; Hastings, A.; Schlamadinger, B.; Taylor, G. and Smith, P. (2006) Energy crops: current status and future prospects. *Global Change Biology* 12, 2054–2076.

SIRI. Vermont safety information resources, Inc. <http://hazard.com>

Smeets, E.; Faaij, A. and Lewandowski, I. (2004) A quickscan of global bio-energy potentials to 2050: An analysis of the regional availability of biomass resources for export in relation to the underlying factors. Report NWS-E-2004-109, Copernicus Institute - Department of Science, Technology and Society Utrecht University. http://www.eubia.org/fileadmin/template/main/res/pics/about_biomass/Deployment_and_resources/smeetsglobalquickscan2050.pdf

- Spath, P.L. and Dayton, D.C. (2003) Preliminary Screening — Technical and Economic Assessment of Synthesis Gas to Fuels and Chemicals with Emphasis on the Potential for Biomass-Derived Syngas. NREL/TP-510-34929. Golden, CO (USA)
- Stamatov, V; Honnery, D.; Soria, J. (2006). Combustion properties of slow pyrolysis bio-oil produced from indigenous Australian species. *Renewable Energy*, 31, 2108–2121
- Strezov, V.; Patterson, M.; Zymła, V.; Fisher, K.; Evans, T.J. and Nelson, P.F. (2007) Fundamental aspects of biomass carbonisation. *J. Anal. Appl. Pyrolysis*, 79, 91–100
- Świgoń, J. and Longauer, J. (2005) Energy consumption in wood pellets production. Proceedings of the 11th Polish Drying Symposium, Poznań (PL)
- Terna (2008) Bilancio elettrico Italia – 2008. www.terna.it
- Terna (2008) Dati Statistici sull'energia elettrica in Italia – 2008. www.terna.it
- Teske, S.; Zervos, A. and Schäfer, O (2007) Energy [r]evolution – A Sustainable World Energy Outlook. Greenpeace International and European Renewable Energy Council (EREC) publication, PrimaveraQuint, The Netherlands (NL)
- Thermo Nicolet Corporation (2001). Introduction to Fourier Transform Infrared Spectrometry. Madison (Wisconsin, USA), mmrc.caltech.edu/FTIR/FTIRintro.pdf
- Thornley, P.; Upham, P; Huang, Y; Rezvani, S.; Brammerd, J. and Rogers, J. (2009) Integrated assessment of bioelectricity technology options. *Energy Policy*, 37, 890–903
- Tilman, D; Hill, J. and Lehman, C. (2006) Carbon-negative biofuels from low-input high-diversity grassland biomass. *Science*, 314, 1598–1600
- TOXNET. Toxicology data network. <http://toxnet.nlm.nih.gov>
- Trathnigg, B. (1995). Determination of MWD and Chemical Composition of Polymers by Chromatographic Techniques. *Prog. Polym. Sci.*, 20, 615-650
- Ulrich, G.D. and Vasudevant, P.T. (2006) How to Estimate Utility Costs, *CHEMICAL ENGINEERING*, WWW.CHE.COM, APRIL 2006, 66-69
- UNEP - United Nations Environment Programme. Life cycle Impact Assessment Programme of the Life Cycle Initiative. <http://www.unep.org>
- United Nations Department of Economic and Social Affairs / Population Division (2009) World Population Prospects: The 2008 Revision. *POPULATION Newsletter*, June 2009 Number 87
- Van den Broek, R. (2000) Sustainability of biomass electricity systems, an assessments of costs, macro-economics and environmental impacts in Nicaragua, Ireland and the Netherlands. Eburon, Delft (NL)

- Van den Broek, R.; Faaij, A. and Van Wijk, A. (1996) Biomass combustion power generation technologies. *Biomass and Bioenergy*, **11**(4), 271–281
- Van Loo, S. and Koppejan, J. (2002) *The Handbook of Biomass Combustion and Co-firing*, Earthscan, London (UK)
- Van Vliet, O.P.R; Faaij, A.P.C and Turkenburg, W.C. (2009) Fischer–Tropsch diesel production in a well-to-wheel perspective: A carbon, energy flow and cost analysis. *Energy Conversion and Management*, **50**, 855–876
- Venturi, G.; Monti, A. and Fazio, S. (2008) Final report of the project “Network piante ad uso energetico e riciclo di CO₂” promoted by ENI s.p.a. and developed by DiSTA, Department of Agro-Environmental Science and Technology of the University of Bologna (Italy).
- Volvo Truck Corporation (2008) Emissions from Volvo’s trucks. <http://www.volvo.com>
- Wind Energy – The Facts, <http://www.wind-energy-the-facts.org/en/part-3-economics-of-wind-power/chapter-4-prices-and-support-mechanisms/>
- World Bank (2009) World Development Indicators (WDI). WDI Online Databases. Available at <http://web.worldbank.org>
- World Energy Council (2004) *Survey of Energy Resources* (20th Ed.) Elsevier Ltd., Oxford (UK)
- Yang, H.; Yan, R.; Chen, H.; Lee, D.O. and Zheng, C. (2007). Characteristics of hemicellulose, cellulose and lignin pyrolysis. *Fuel*, **86**, 1781–1788
- Yu, F.; Deng, S.; Chen, P.; Liu, Y.; Wan, Y.; Olson, A.; Kittelson and D. Ruan, R. (2007). Physical and Chemical Properties of Bio-Oils From Microwave Pyrolysis of Corn Stover. *Applied Biochemistry and Biotechnology*, Vol. 136–140, 957-970
- Zaror C.A., Hutchings I.S., Pyle D.L., Stiles H.N. and Kandiyoti R. (1985). Secondary char formation in the catalytic pyrolysis of biomass. *Fuel*, **64**, 990-994

APPENDIX A

LIST OF ABBREVIATIONS

A	Ash
A-CFB	Atmospheric pressure Circulating Fluidized Bed
AP	Auto-ignition point
ATI	Acute Toxicity Index
B	Biomass
BaP	Benzo(a)pyrene equivalent
B/C	Benefit to cost
BGCC	Biomass Integrated Gasification/Combined Cycle
B _p	Boiling point
BtP	Biomass-to-Power
CED	Cumulative Energy Demand
CF	Carbon Footprint
CFB	Circulating Fluidized Bed
CHP	Combined Heat and Power
CI	Carcinogenicity Index
CIF	Cost, Insurance, Freight
CO	Co-combustion
CO ₂ eq	CO ₂ equivalent
COP	Coefficient of Performance
CS	Corn stalks
CSF	Cancer Slope Factor
CTI	Chronic Toxicity Index
d.a.f.	dry ash free
d.b.	dry basis
DC	Direct combustion
DCF	Discounted Cash Flow
DEL	Delivered
DME	DiMethylEther
EC	Effective Concentration
ES	Evaluation Score
ESI	Electricity Surcharge Indicator
ETI	Ecotoxicity Index
ETS	Emission Trading System
FC	Fixed Carbon
FOB	Freight on Board / Free on Board
FP	Flash point
FT	Fischer Tropsch
FT-IR	Fourier Transform Infrared
FU	Functional Unit
G	Group of activities
GC	Gas Chromatography
GHGs	Greenhouse gases
GPC	Gel Permeation Chromatography
GKR	Gray-King reactor

GWP	Global Warming Potential
H	Henry's law constant
HF	Hazard Footprint
HHV	Higher Heating Value
HI	Hazard Index
h-IHP	higher Integral Hazard Profile
HP	Hazard Profile
HPs	Hazard Parameters
HV	Hazard Vector
IEO	Internet Energy Outlook
IGCC	Integrated Gasification Combined Cycle
IHP	Integral Hazard Profile
INST	Installed
I/O	Input/Output
IR	Infrared
IRR	Internal Rate of Return
IV	Impact Vector
K _{ow}	Octanol-water partition coefficient
KPI	Key Performance Indicator
LC	Lethal Concentration
LCA	Life Cycle Assessment
LCI	Life Cycle Inventory
LCIA	Life Cycle Impact Assessment
LD	Lethal Dose
LHV	Lower Heating Value
LO	Land Occupation
l-IHP	lower Integral Hazard Profile
MeOH	Methanol
MHP	Mixture Hazard Profile
MJ _{eq.}	MJ equivalent
MS	Mass Spectrometry
MW	Molecular Weight
NFV	Net Future Value
NMP	1-methyl-2-pyrrolidinone
NPV	Net Present Value
OHI	Overall Hazard Index
P	Pelletizing
PAH	Polycyclic Aromatic Hydrocarbon
PHP	Partial Hazard Profiles
PO	Poplar
PP	Payback Period
RES-E	Renewable Energy Source - Electricity
RfC	Reference Cocentration
RfD	Reference Dose
ROE	Return on Equiti
RME	Rapeseed Methyl Ester
SB	System Boundaries
SNG	Synthetic Natural Gas
SO	Sorghum
SP	Slow pyrolysis

SRC	Short Rotation Crop
SVI	Specific Variation Index
SW	Switchgrass
S _w	Solubility in water
TF	Tortuosity Factor
T _o	Overall persistence time
TPS	Thermal Power Station
TR	Tubular reactor
UV	Ultraviolet Fluorescence
VF	Volatile Fraction
w.b.	wet basis

APPENDIX B

LIST OF PUBLICATIONS

a. International journals

M. Cordella, A. Tugnoli, F. Barontini, G. Spadoni, V. Cozzani (2009), “Inherent safety of substances: identification of accidental scenarios due to decomposition products”, *Journal of Loss Prevention in the Process Industries* 22, p. 466–473

M. Cordella, A. Tugnoli, G. Spadoni, F. Santarelli, T. Zangrando (2008): “LCA of an Italian Lager Beer”, *Int J LCA* 13, n. 2, p.133-139

b. Others

M. Cordella, C. Stramigioli, F. Santarelli, S. Fazio (2009): “Analisi degli impatti ambientali legati ad una filiera per la produzione di biodiesel di seconda generazione”, *Proceedings of Ecomondo 2009*, Maggioli Editore, Rimini (I), p. 922-927

D. Castiello, M. Cordella, M. Puccini, M. Seggiani, S. Vitolo (2009), “Tannery wastewater sludge ash for the production of waterproofing membrane: a technical and environmental feasibility study”, *Proceedings of the XXX IULTCS Congress*, Beijing

M. Cordella, A. Tugnoli, F. Santarelli (2009): “A LCA approach to the environmental impact of overweight and obesity”, *Proceedings of the 15th SETAC LCA Case Studies Symposium*, Paris

M. Cordella, F. Santarelli (2008): “Valutazione attraverso la metodologia LCA di impatti impressi da differenti modalità di confezionamento di birra”, *Proceedings of Ecomondo 2008*, vol. II, Maggioli Editore, Rimini (I), p. 460-465.

M. Cordella, F. Barontini, F. Santarelli, V. Cozzani (2008): “Valutazione del rischio associato alla produzione ed allo stoccaggio di combustibili derivanti da biomasse”, *Proceedings of the VI Convegno Nazionale Valutazione e Gestione del Rischio negli Insediamenti Civili ed Industriali*, DIMNP, Pisa (I), p. 93

M. Cordella, A. Tugnoli, P. Morra, F. Barontini, G. Spadoni, V. Cozzani (2008), “Assessment of the hazard footprint of substances formed in the loss of control of chemical systems”, *Chemical Engineering Greetings to Prof. Eliseo Ranzi*, AIDIC – Elioticinese Service Point: Milan (I), p.151-160

M. Cordella, A. Tugnoli, P. Morra, F. Barontini, V. Cozzani (2008): “Accidental scenarios in the loss of control of chemical processes: screening the impact profile of secondary substances”, *Proceedings of the European Safety and Reliability Association Conference*, CRC Press, London (UK), p. 2347-2352

M. Cordella, F. Barontini, V. Cozzani (2008): “Pyrolysis processes for bio-oil production: analysis of the hazards of the reaction products”, *Proceeding of the XVII Congresso Nazionale della Divisione di Chimica Industriale, Società Chimica Italiana*, Genoa (I), p. 109

M. Cordella, A. Tugnoli, P. Morra, F. Barontini, V. Cozzani (2007): “The inherent safety of substances in accidental scenarios: a procedure for the assessment of hazards due to decomposition products”, Proceedings of the 8th International Conference on Chemical and Process Engineering, Chem. Eng. Trans. 11, AIDIC, Milano (I): p. 363-368

A. Tugnoli, F. Barontini, M. Cordella, P. Morra, V. Cozzani., R. Sanchirico, I. Di Somma, R. Andreozzi (2007): “Assessment of the hazards caused by accidental decomposition products” Proceedings of the 12th International Symposium on Loss Prevention and Safety Promotion in the Process Industries, IchemE Symp. Series n. 153, IchemE, Rugby (UK): p.1501-1506

M. Cordella, A. Tugnoli, G. Spadoni, F. Santarelli, T. Zangrando (2007): “Comparison of bottled and kegged beer: the LCA approach”, Proceedings of the 31st International Congress of the European Brewery Convention, Fachverlag Hans Carl, Nu